Contrails

AFFDL-TR-73-151

THE EFFECT OF GROUND PROXIMITY ON THE LATERAL/DIRECTIONAL AERODYNAMIC AND CONTROL CHARACTERISTICS OF A TILT-WING V/STOL AIRCRAFT AT HIGH LIFT COEFFICIENTS

H.C. CURTISS, JR., J.J. TRAYBAR AND W.F. PUTMAN

PRINCETON UNIVERSITY

AMS-TR-1127

Approved for public release; distribution unlimited.

Approved for Public Release

Contrails

FOREWORD

This final technical report was prepared by the Flight Mechanics Laboratory of the Department of Aerospace and Mechanical Sciences, Princeton University, Princeton, New Jersey under U. S. Air Force Contract Number F33615-71-C-1206. The research was initiated by the Air Force Flight Dynamics Laboratory, Air Force Systems Command, Wright-Patterson Air Force Base, Ohio 45433 under Project Number 8219 and was monitored and administered by Mr. H. Woolard (AFFDL/FGC).

This final report covers the work performed from January 1971 to August 1973. The work was supervised by Professor H. C. Curtiss, Jr., Principal Investigator, and aided by Messrs. Joseph J. Traybar, John P. Kukon and William F. Putman of the Research and Technical Staff of the Flight Mechanics Laboratory. For internal control, the Aerospace and Mechanical Sciences Department has designated this work as Technical Report Number 1127. This report was submitted to the sponsors in September 1973.

This technical report has been reviewed and is approved.

C. B. WESTBROOK
Chief, Control Criteria Branch
Flight Control Division
Air Force Flight Dynamics Laboratory

Approved for Public Release

Contrails

ABSTRACT

A series of experiments was performed in the Princeton Dynamic Model Track to determine the lateral/directional stability and control of a V/STOL type aircraft in ground proximity. Of primary interest were the characteristics associated with flight at high lift coefficients and utilizing high wing incidences with large flap deflections as may be encountered during STOL operations in landings and take-offs where the full or maximum effects of ground proximity are encountered. The configurations tested included combinations of wing incidence and flap deflection up to a maximum of 60 degrees.

Static force and moment measurements were made for seven different wing incidence/flap angle combinations using sideslip angle and roll angle as variables. Also, static measurements were made to determine the control effectiveness of ailerons and differential propeller pitch. All configurations were studied at three altitude ratios; one approximating a high altitude (or out-of-ground effect height), another a low altitude (or in-ground-effect height), and the third an intermediate altitude case.

Approved for Public Release

Contrails

TABLE OF CONTENTS

Approved for Public Release

Contrails

LIST OF ILLUSTRATIONS

Approved for Public Release

Contrails

Approved for Public Release

Contrails

Approved for Public Release

Contrails

LIST OF TABLES

Approved for Public Release

Contrails

SYMBOLS AND NOTATION

A	total propeller disc area, ft^2, (7.54)
b	wing span, ft, (6.75)
c	propeller blade chord, ft; also wing chord, ft
$\bar{c}$	wing mean geometric chord, ft, (0.807)
cp	center of pressure
c/R	propeller blade chord ratio, per-cent
$C_{L,s}$	rolling-moment coefficient based on slipstream dynamic pressure, $\frac{\text{Rolling moment}}{q_s S b}$,
$C_{M,s}$	pitching-moment coefficient based on slipstream dynamic pressure, $\frac{\text{Pitching moment}}{q_s S \bar{c}}$,
$C_{N,s}$	yawing-moment coefficient based on slipstream dynamic pressure, $\frac{\text{Yawing moment}}{q_s S b}$,
$C_{T,s}$	thrust coefficient based on slipstream dynamic pressure and disc loading, $\frac{T/A}{q_s}$
C_T	thrust coefficient based on tip speed where propeller rotational speed is in radians per second, $\frac{T}{\rho \pi R^2 (\Omega R)^2}$
$C_{X,s}$	horizontal - force coefficient based on slipstream dynamic pressure, $\frac{\text{X-force}}{q_s S}$
$C_{Y,s}$	side-force coefficient based on slipstream dynamic pressure, $\frac{\text{Y-force}}{q_s S}$
$C_{Z,s}$	vertical-force coefficient based on slipstream dynamic pressure, $\frac{\text{Z-force}}{q_s S}$
FS	fuselage station

Approved for Public Release

Contrails

h	height of fuselage bottom above ground, ft
h_c	height of port or starboard wing at spanwise station zero, ft
h_p or h_s	height of local spanwise station, port or starboard, ft
$h/\bar{c} = \bar{h}$	altitude-ratio (ratio of fuselage height above ground to wing geometric chord)
IGE	in-ground-effect
i_t	horizontal-tail incidence angle, deg (20)
i_w	wing-tilt or wing incidence angle, deg
ℓ_{p_1}	distance from center line to inboard propeller, ft
ℓ_{p_2}	distance from center line to outboard propeller, ft
L	rolling-moment, ft-lb, positive right wing down
M	pitching-moment, ft-lb, positive nose-up
N	yawing-moment, ft-lb, positive nose-right
OGE	out-of-ground effect
q	free-stream dynamic pressure, $\frac{1}{2} \rho V^2$, lb/ft^2
q_s	slipstream dynamic pressure, $q + \frac{T}{A}$, lbs/ft^2
r	distance along propeller radius (measured from axis of rotation), ft
r/R	propeller blade radial station
R	propeller radius, ft, (0.775); also resultant wing force, lb
S	wing area, ft^2, (5.34)
t	propeller blade thickness, ft
t/c	propeller blade thickness ratio, per-cent
T	total thrust of all propellers, lb

Approved for Public Release

Contrails

V	free-stream velocity, ft/sec
W	weight of model and internal supports, lb, (46.3)
WL	water line
x	sectional horizontal force on wing/propeller system; lb/ft, positive forward
X	horizontal - force, lb, positive forward
y	spanwise distance, ft
$\tilde{y}$	$\tilde{y} = \frac{y}{b/2}$
Y	side-force, lb, positive right
Z	vertical force, lb, positive downward
β	angle of sideslip, deg, (positive nose-left), also blade twist angle, deg
$\delta_{a,p}$ or $\delta_{a,s}$	aileron control surface deflection angle, deg (initial position or zero position is streamlined with flap deflection, positive direction is aileron trailing edge forward or down)
δ_a	average aileron control input, deg $\frac{\delta_{a,p} - \delta_{a,s}}{2}$
δ_f	flap deflection angle, deg
θ	propeller blade total pitch angle, deg, $\theta_o + \Delta\theta$
θ_o	nominal propeller blade pitch angle, deg (12)
θ_p or θ_s	propeller blade pitch angle; port or starboard, deg
$\Delta\theta$	average propeller blade differential pitch control input, deg, $\frac{\theta_s - \theta_p}{2}$
μ_x	tip speed ratio, $V/\Omega R$
ρ	mass density of air, slugs/ft^3
σ	solidity ratio (0.153)

Approved for Public Release

Contrails

ϕ	bank (roll)-angle, deg, positive is right roll
Ω	propeller angluar velocity or RPM, rad/sec or rev/min
$(\ )_P$	port side
$(\ )_S$	starboard side
$\Delta(\ )$	increment in quantity

Approved for Public Release

Contrails

SUMMARY

A series of experiments was performed in the Princeton Dynamic Model Track (PDMT) to determine the lateral/directional stability and control of a tilt-wing V/STOL aircraft in ground proximity. Of primary interest were the characteristics associated with flight at large values of lift coefficients and the use of high wing incidences with large flap deflections as may be encountered during STOL operations in landings and take-offs where the full or maximum effects of ground proximity are encountered. The configurations tested included combinations of wing incidence and and flap deflection up to a maximum of 60 degrees and lift coefficients (based on free stream dynamic pressure) ranging from about 12 to 36.

Static force and moment measurements were made for seven different wing incidence/flap angle combinations using sideslip angle and roll angle as variables. Also, static measurements were made to determine the control effectiveness of ailerons and differential propeller pitch. All configurations were studied at three altitude ratios; one approximating a high altitude (or out-of-ground effect height), another a low altitude (or in-ground-effect height), and the third an intermediate altitude case.

The nature of the data makes it difficult to draw any simple conclusions regarding the general trends. The aerodynamic effects of the presence of the ground appear quite complex and are dependent on the configuration geometry of the aircraft as well as the value of the thrust coefficient. At large values of lift coefficients (greater than about two), the presence of the ground causes significant variations in rolling and yawing moment with aircraft bank angle. Also, the aileron control effectiveness of a tilt-wing configuration decreases markedly as the ground is approached. Static trim considerations indicate that large control deflections are required to counteract roll angle near the ground in all wing/flap combinations except those where flap deflections are approaching the maximum value of 60°. However, for the extreme cases utilizing large wing incidence/flap deflection combinations (especially when flap deflection is 60°), there are indications that flow recirculation rather than static trim problems may be the most significant phenomena causing control difficulties.

There appear to be significant differences in the data acquired by the moving model technique of testing and the moving belt/wind tunnel technique of testing for ground effects. The moving model testing technique as used by PDMT yields somewhat smaller and more rapid onset of the ground effects noticed during flight at the larger values of lift coefficient whereas, by comparison, the moving belt/standard wind tunnel testing techniques show greater and more gradual buildup of ground effects as altitude changes.

Approved for Public Release

Contrails

INTRODUCTION

Experiences with different VTOL aircraft have indicated that the changes in the aerodynamic characteristics of an aircraft as the ground is approached become accentuated as the lift coefficient of the aircraft increases.

Various of the V/STOL prototypes constructed and flown in the past have experienced numerous ground effect problems. One vehicle in particular experienced severe problems under certain ground effect flight conditions. During early flight tests, the XC-142A tilt-wing aircraft experienced random lateral/directional disturbances in ground proximity at the higher wing incidence conditions particularly when attempting to land at air speeds below roughly 45 knots. Other flight tests with several different prototypes of V/STOL aircraft have all revealed problems with vehicle generated disturbances.

The XC-142A, configured at the 45° wing incidence and 60° flap deflection, experienced motions requiring full application of directional and roll controls in order to minimize directional departures and attempt to maintain wings level at the lowest altitudes during descent to landing. During these maneuvers, it has been stated that the transition from satisfactory flying qualities to unacceptable flying qualities was "sharp and without warning" (Reference 1). There were indications that suggested that this phenomena is encountered when the downward deflected wake contacts the ground and some portion of it is then deflected forward and upstream of the aircraft so that it recirculates through and around the propeller/wing system. Other indications suggest that this recirculating flow may be only a contributing factor and that much of this problem may be due to the steady state changes in aerodynamics that occur as a result of ground effect.

The increasing impact of ground effects coupled with increasing interest in various STOL as well as V/STOL concepts requires further experimental data to define clearly the influence of the ground on the aerodynamics of aircraft (References 2 through 22).

Considering ground effect in further detail, flying close to the ground at very high vehicle lift coefficients can be considered as giving rise to two types of phenomena. The first, mentioned above, is the possible presence of a recirculating flow field -- a phenomenon which is difficult to describe quantitatively. The second, and more classical influence is a steady state change in the forces and moments which may be estimated from "image methods". The image method indicates that as the lift coefficient of the aircraft is increased, the lift and the drag of the aircraft are changed as the ground is approached. The drag (or net horizontal force) of the vehicle will steadily decrease (develop a forward component) as the ground is approached. The rate of decrease

Approved for Public Release

Contrails

will increase as the out-of-ground effect lift coefficient becomes larger. The variation in the lift coefficient with approach to the ground depends upon the magnitude of the out-of-ground effect lift coefficient. At low lift coefficients, roughly less than about two, the lift coefficient tends to increase as the ground is approached and the change in lift coefficient may be viewed as arising from an increase in the lift curve slope of the aircraft (Reference 23). As the out-of-ground effect lift coefficient is increased this effect changes sign. There is an out-of-ground effect lift coefficient at which there is essentially no change in lift coefficient with approach to the ground. As the out-of-ground effect lift coefficient is further increased, the lift coefficient will tend to decrease as the ground is approached. The rate of change of lift coefficient with height above the ground will increase as the out-of-ground effect lift coefficient becomes larger.

The source of these changes may be seen by examining the influence of the "image" lifting system. First, consider a two-dimensional thin airfoil. Reference 22 presents the results of the theoretical solution to this problem. Results are shown in Figure 1a where it can be seen that as the out-of-ground effect lift coefficient is increased, the percentage decrease in lift becomes larger. The predominate effect here of the image is that the bound vortex induces a reduction in velocity at the airfoil. This effect becomes increasingly significant at high lift coefficients. The slight increase in lift shown at the lowest lift coefficient at small height to chord ratio is a result of inclusion of the effects of finite chord and the resulting effect of the image in causing an apparent increase in camber. This effect is only important at low lift coefficients and small height to chord ratios and therefore one would expect that generally the effect of the bound vortex is to produce a lift decrease. The lift decrease is generally proportional to lift coefficient.

In the three-dimensional case, the influence of the trailing vortex must also be included. Assuming that the trailing vortex is undeflected as shown in Figure 1b, the trailing vortex image system will produce an upwash at the wing and the bound vortex will produce a decrease in velocity. The magnitude of these velocity changes will be proportional to the lift coefficient of the wing. If the upwash effect is included it will be found that it may be expressed as a reduction in lift curve slope. However, the bound vortex effect, causing a reduction in velocity at the airfoil will become increasingly significant as the lift coefficient increases and is responsible for the lift decrease at high lift coefficients.

Further, at these increased lift coefficients, the wake will be deflected downward resulting in further decreases in horizontal velocity and consequently further decreases in lift. Figure 1c shows the change in velocities induced by the image at the model for zero wake deflection and a wake deflection of 30° as given in Reference 13. The trends given

Approved for Public Release

Contrails

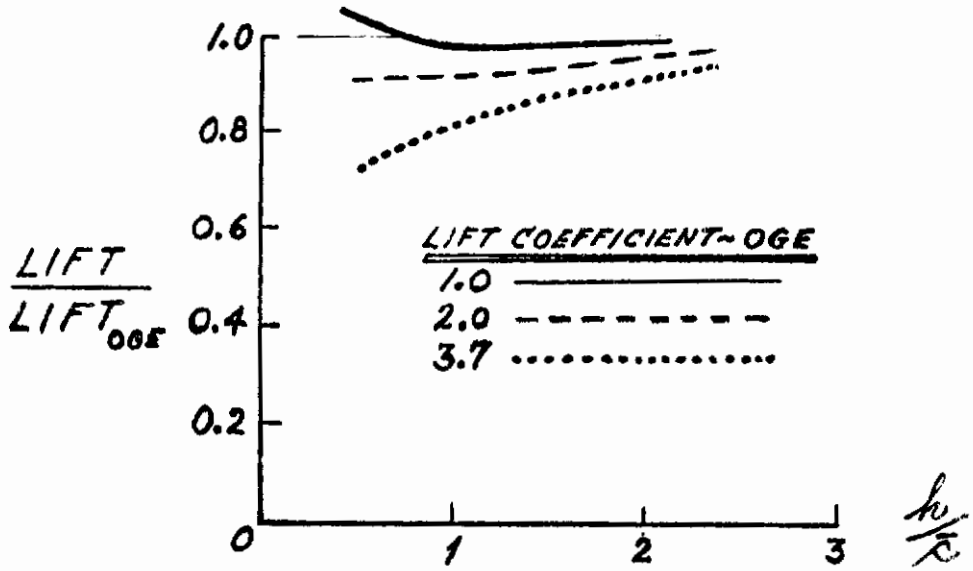

(a). Two-dimensional (Theory).

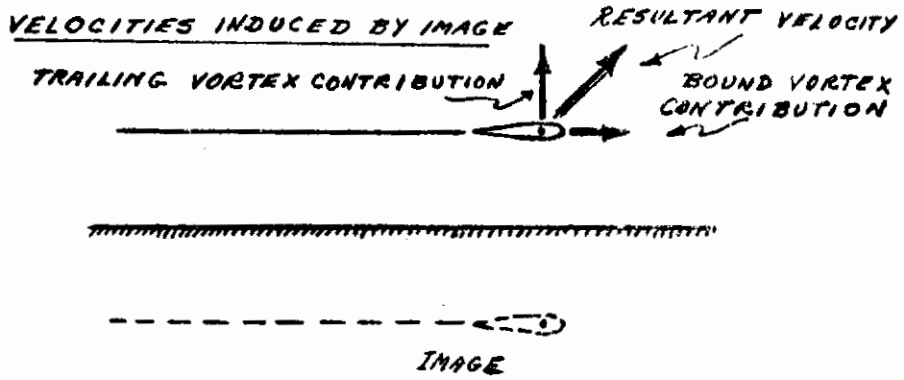

(b). No wake deflection, X = 0

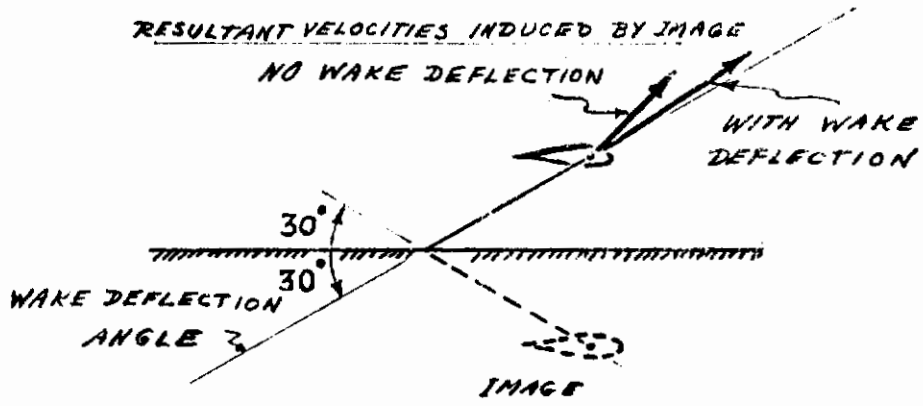

(c). Deflected wake, X = 0

Figure 1. Ground effects on a thin airfoil.

Approved for Public Release

Contrails

by this relatively simple model agree with the results of more detailed theories as found in Reference 2 for example. This elementary image model explains the general trends in variations of lift coefficient and drag coefficient found in the experimental program reported here. The vehicle trim lift coefficient is varied from 12 to 36 in the series of experiments described.

Approved for Public Release

Contrails

FACILITY

The Princeton Dynamic Model Track (PDMT) is a unique model testing facility that incorporates a relatively large test section (30 feet by 30 feet), a powered servo-controlled carriage mounted on a 750 foot monorail and a selection of special booms and mounts for the various applications of interest (Reference 24). The facility was designed primarily for static and dynamic testing of powered vehicles where the need for ease of precise quantitative measurement in the slow speed, high downwash-angle flight-regime, freedom from adverse flow-profiles coupled with correct simulation of ground effects, and accurate control of complex experiments, is essential. In particular, the simulation of aircraft flight in ground effect is more representative in that the model is driven through still air over a fixed ground plane. Thus, simulation errors arising from the presence of a boundary layer, undesirable "free-stream" velocity gradients that might be present in powered model wind tunnel type testing at slower speeds and/or near a tunnel test section ground effect plane, are greatly minimized or eliminated.

For the particular experiments in this investigation, the model was suspended from above on a boom/mount and gimbal system that permitted setting model altitude and attitude. A typical setup for dynamic testing is shown in Figure 2. For this study, the external strain gage and dynamic model control links shown above the model (and labeled as strain-gage-balance) were removed and in its place, a small yaw angle drive system was installed. A six-component, TASK-type, strain gage, incorporating a roll gimbal, was mounted inside the model fuselage.

The servo-controlled carriage is equipped with a variety of instrumentation including an analog computer for carriage (and model) control. This use of the carriage borne computer permits pre-programming specific carriage and model control system behavior. The most efficient utilization of moving model type facilities such as the PDMT dictates that testing be performed in a "quasi-steady" manner. Also, as an aid in interpreting test results, it is convenient to gather the measured data as direct and continuous functions of the important variables. Therefore, in these particular experiments, the testing was performed using very slow pre-programmed variations of four of the five primary model variables; namely, horizontal velocity, yaw angle, aileron deflection and differential propeller pitch. The fifth variable of significance, roll angle, was pre-set at increments of $\pm 4^{\circ}$, $\pm 6^{\circ}$ and $\pm 8^{\circ}$ (ground clearance permitting) to examine the influence of roll angle. The yaw angle was normally varied at these roll angles.

For the $45^{\circ}/60^{\circ}$, $45^{\circ}/40^{\circ}$, $40^{\circ}/60^{\circ}$ and $40^{\circ}/40^{\circ}$, wing/flap angle combinations, runs were made with roll angle setting of $\pm 4^{\circ}$ and $\pm 8^{\circ}$, varying aileron deflection and varying differential propeller pitch to evaluate any nonlinear effects. Thus, many of the curves presented for variations in forces and moments as a function of yaw angle, aileron deflection or differential propeller pitch, are essentially continuous curves. The

Approved for Public Release

Contrails

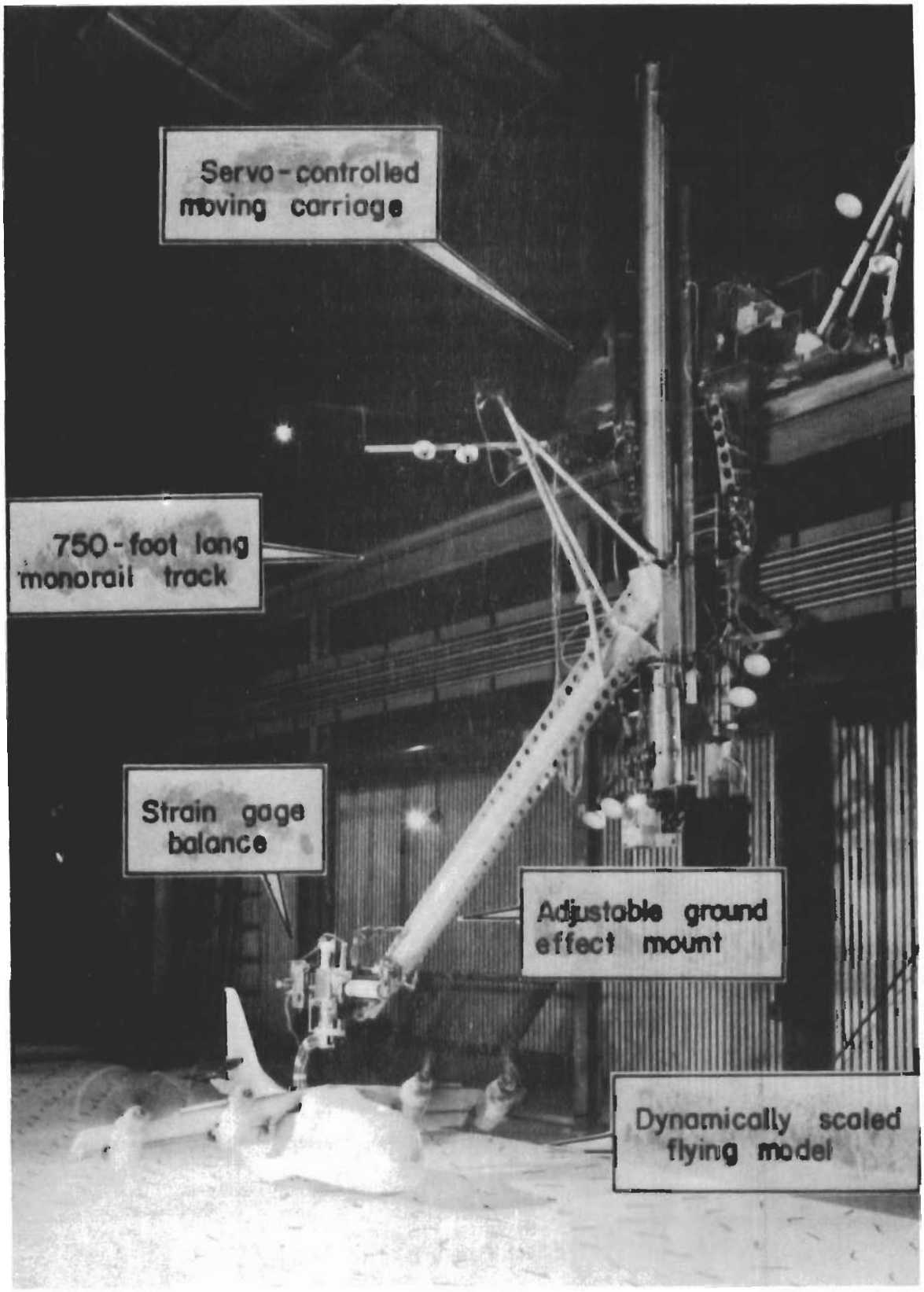

Figure 2. Princeton Dynamic Model Track

Approved for Public Release

Contrails

roll angle curves are not and consist of points at zero ± 4° and ± 8°.

A typical test procedure involved selecting and setting the configuration variables. The tail incidence and average propeller blade pitch were constant throughout the test program. The wing incidence and flap deflection were selected. The model trim velocity was determined by finding the value that corresponded to level flight at the maximum altitude of the experiments. Then the desired variable program was chosen and run about the selected trim condition. The model forward velocity was maintained constant for each wing/flap combination as the altitude was changed.

Approved for Public Release

Contrails

MODEL

A one-tenth scale dynamic model of the XC-142A was utilized in these experiments. A three-view drawing is shown in Figure 3. The wing configuration with pertinent data on the slats, vanes, flaps and ailerons is shown in Figures 4 and 5. The propeller blade characteristics are given in Figure 6.

The fuselage is "sandwich" constructed with an inner and outer Fiberglass skin, vacuum molded and bonded to a Styrofoam core. An aluminum box spar is used for the main structural member of the wing and mohogany ribs with a vacuum molded Fiberglass covering form the external airfoil shape. The double slotted flaps and the ailerons are constructed of low density Styrofoam with Fiberglass coverings. The ailerons are scaled except that the trailing edge cusp of the NACA 63-318 airfoil is retained and a non-conventional aileron-gap-seal, using strips of one-mil plastic sheet, is utilized. In a previous test program, it was found that the unsealed ailerons exhibited poor aerodynamic characteristics which were greatly improved by sealing. More conventional sealing techniques were largely unsatisfactory because of the high friction levels produced.

The leading edge slats were of conventional design and are constructed of a plastic laminate. The slats were located only on the "upgoing blade" side of the wing leading edge. The propeller blades were constructed of Fiberglass by the Hamilton Standard Division of the United Aircraft Corporation. During other test programs and calibrations, it was determined that the starboard side propeller blades have a slightly larger chord than the propeller blades on the port side. The propeller blade pitch angles were set equal on each side and as a consequence with the model in symmetric flight small negative rolling and yawing moments exist. About 0.5 degrees of differential propeller pitch is required to trim this moment. The propeller static thrust characteristics are given in Reference 25.

An electric motor, mounted on a bulkhead in the fuselage, transmitted power from a central transmission to the four propeller gearboxes by means of flexible shafting. A separate power take-off (which was disconnected for these experiments) is provided to drive the tail rotor.

Closed-loop, position type, control systems were provided for the ailerons and propeller pitch. Wing angle, flap angle, roll angle and height (altitude-ratio) were manually adjustable. Pre-selected aileron and collective pitch programs were operated by a computer mounted on the main carriage system. In this series of tests, there was no mixing of aileron or collective pitch controls; in near hovering flight (high wing incidences) the ailerons are intended to provide primarily yaw control whereas, in forward or conventional flight (low wing incidences), they would function normally as roll controls. Similarly, at high incidences roll control was provided by differential propeller pitch (collective pitch--port versus starboard propellers), and at the low wing incidences, differential pitch would be phased out and the rudder would be used to

Approved for Public Release

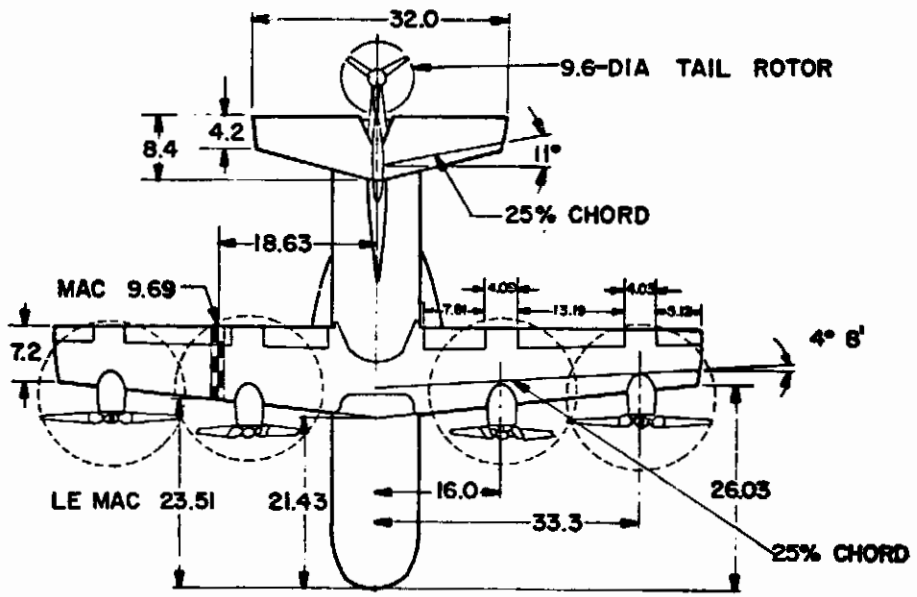

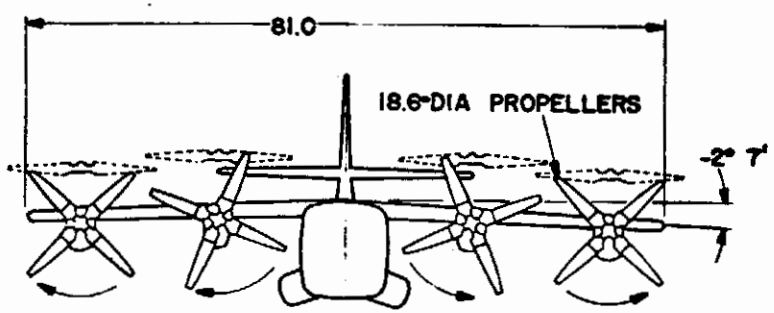

DESIGNATION OF AIRFOIL SECTIONS:

WING	ROOT @ BL 0.0	NACA	63-318
	TIP	NACA	63-318
UNIT HORIZONTAL TAIL	ROOT	NACA	0015
	TIP	NACA	0012
VERTICAL TAIL	ROOT	NACA	0018
	WL 215	NACA	0012
	TIP	NACA	0012

NOTE: ALL DIMENSIONS GIVEN IN MODEL SCALE (IN INCHES)

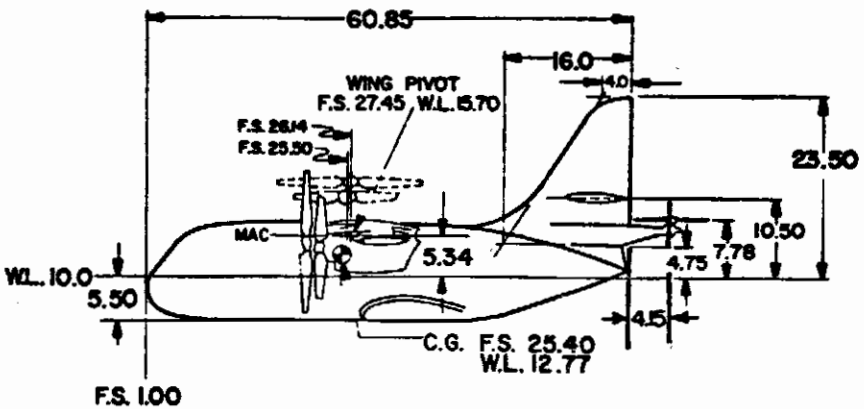

Figure 3. Three view of XC-142A one-tenth scale model.

Approved for Public Release

Approved for Public Release

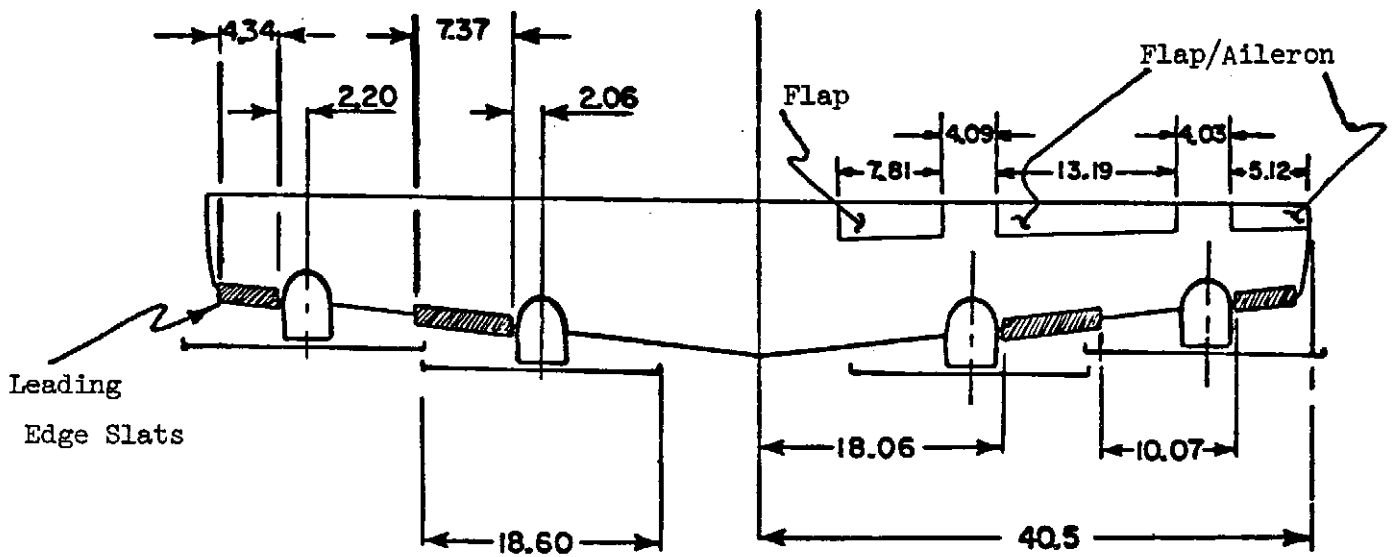

Note: All Dimensions are in inches

Figure 4. Model wing plan arrangement showing spanwise slat, flap and flap/aileron locations.

Confidential

Approved for Public Release

Confidential

Note: Wing Airfoil Section NACA 63-318
Angular Travel of Vane = 1.075 x Angular Travel at Flap
All Dimensions Given in Percent Chord at Any Wing Station

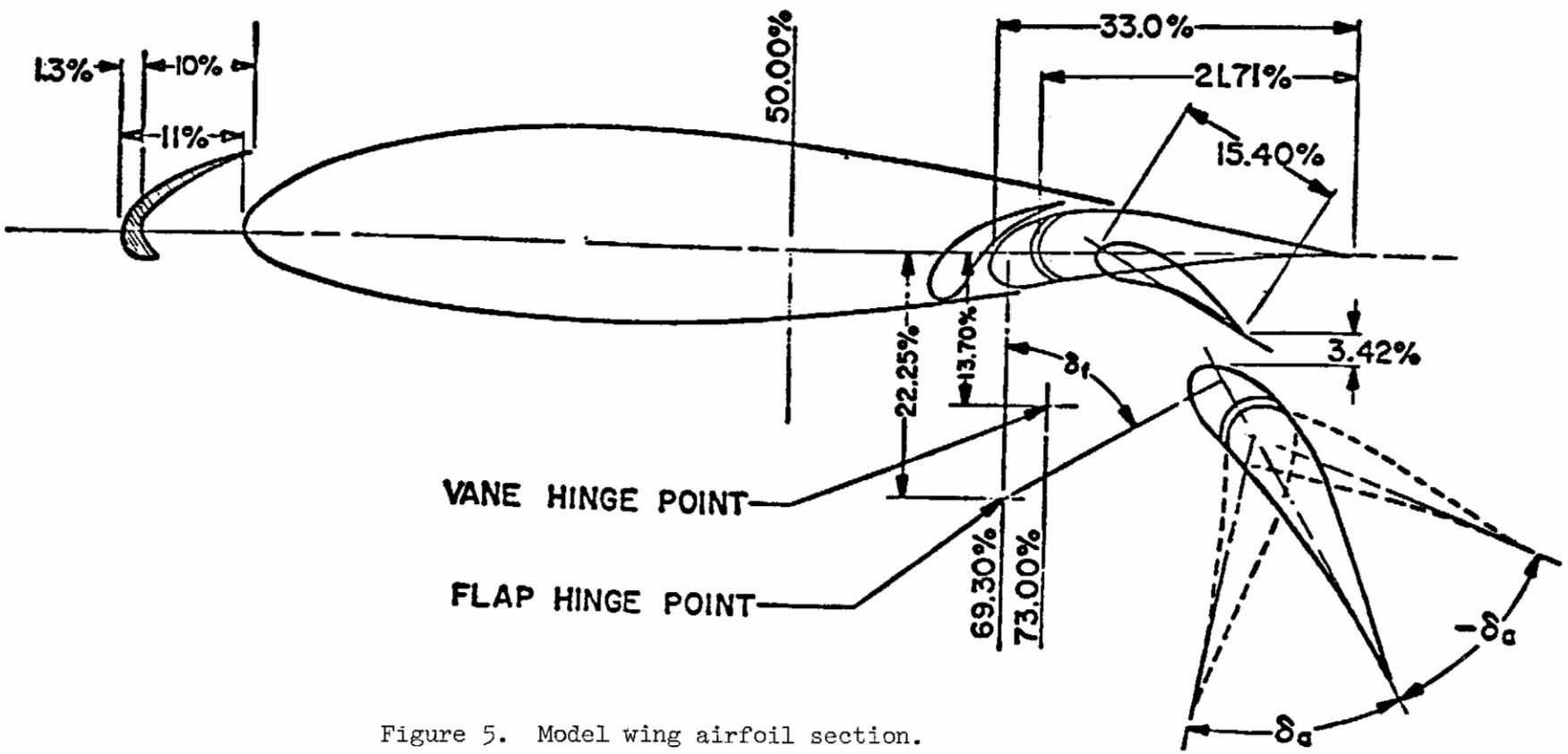

Figure 5. Model wing airfoil section.

Contrails

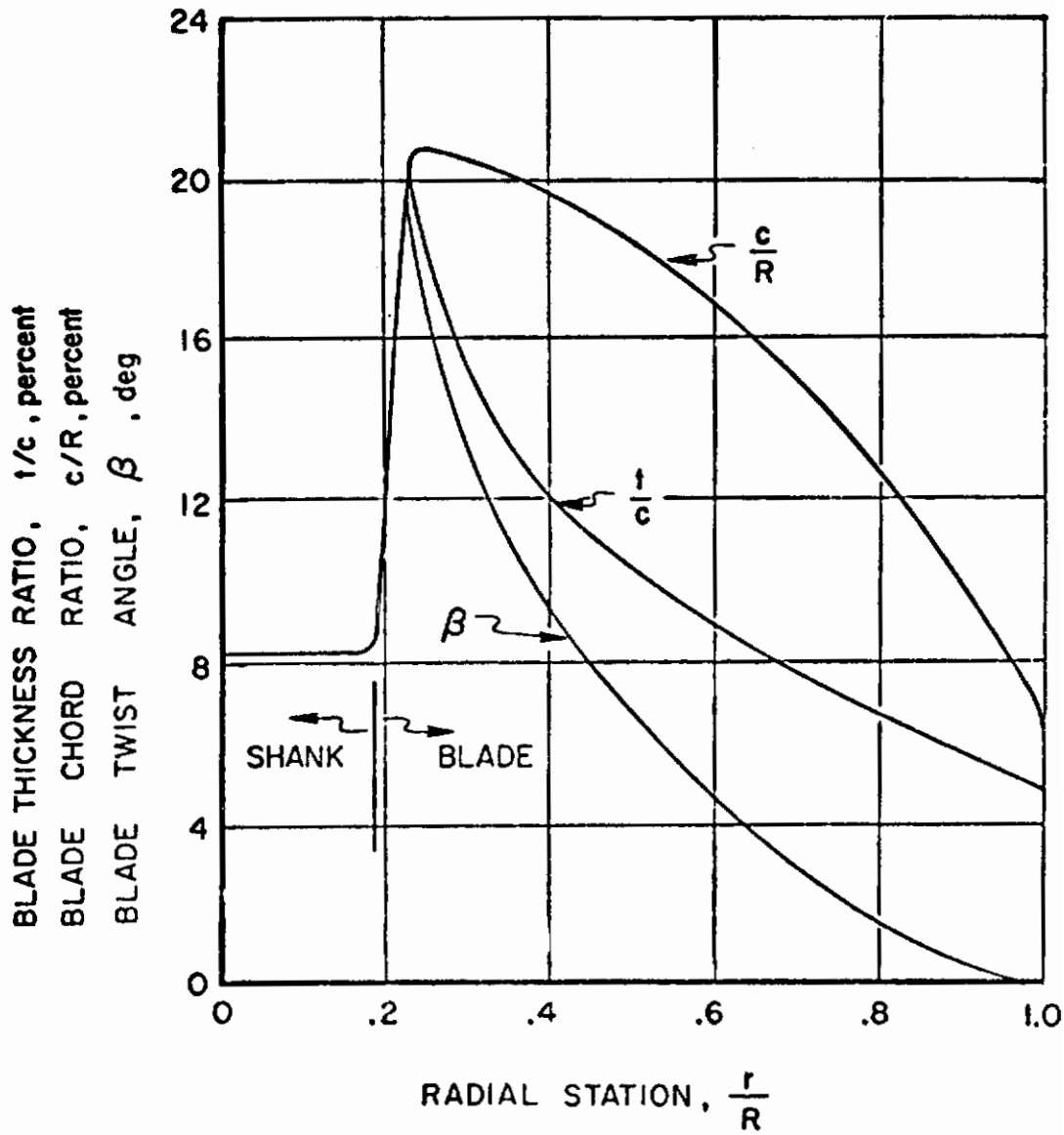

Figure 6. Averaged model propeller blade characteristics.

Approved for Public Release

Contrails

provide conventional yawing or aerodynamic forces. Since the main interest in this test program centered on high wing incidences and low speed flight, the vertical fin had no rudder feature.

The model was originally designed to be used in dynamic as well as static stability and control experiments. It is a precisely built, one-tenth scale, light weight model designed to the scaling laws for dynamic similitude. In this program, the mounts and gimbals were designed to accommodate a body-fixed, six-component, TASK-type internal strain gage balance. The internal mounting attachments were modified to permit initial condition, body-fixed, roll angles to be set. Although maximum settings of roll angle up to about ten degrees were capable, the roll angle limits had to be reduced due to main boom-mount stiffness and wing tip aileron-ground contact problems at the lowest altitudes at the higher wing/flap settings.

At the lowest altitude ($h/\bar{c} = 0.4$) for $i_w = 0^\circ$ and $\delta_f = 0^\circ$, the outboard propeller tips intercept the ground plane at about six degrees of roll angle. At $i_w = 90^\circ$ and $\delta_f = 0^\circ$, the wing tips (ailerons) intercept the ground at about twelve degrees. Of the cases examined in this program, the $i_w = 45^\circ$ and $\delta_f = 60^\circ$ case is the wing/flap combination that permits the smallest excursions in bank angle with reference to wing tip-ground contact problems. For this $45^\circ/60^\circ$ case, wing tip (aileron) ground contact occurs at about eleven degrees. At the lowest altitude ratios ($h/\bar{c} = 0.40$, model fuselage bottom height from floor equal to 3.9 inches), the maximum bank angles permitted were in the four to six degree range for the $45^\circ/60^\circ$ case. Roll angles in excess of these amounts occasionally caused inadvertent ground contact with the outboard ailerons.

The model mount also included a small external assembly containing a programmable yaw angle drive system. This assembly was fixed to the mounting boom just above the model and yaw angle excursions of plus 10° to minus 20° were available. The yaw axis was perpendicular to the floor and space-fixed.

Approved for Public Release

Contrails

AXIS SYSTEM

The axis systems and notation used in the report are shown in Figure 7. The model was supported on a six-component strain gage balance mounted inside the fuselage at the plane of symmetry. The model fuselage pitch attitude was zero degrees for the entire investigation, so that the fuselage bottom was parallel to the ground at zero roll angle. The X axis of the strain gage was aligned along a fuselage reference line parallel to the ground and the Z axis was perpendicular to the ground. Note, since the model fuselage was held level throughout the tests, occasional use is made in this report of the term lift coefficient (synonymously with Z force coefficient) to denote the vertical force component acting on the aircraft. The precise definition and nondimensionalization of all coefficients can be determined by referring to the section on notation.

The strain gage balance center was located at a position equivalent to the full scale coordinates of WL 130.5 and FS 371.2. All data presented in this report were transferred to a center of gravity position equivalent to WL 122.8 and FS 268.8 on the full scale vehicle. This location corresponds to the center of gravity position of the eleventh scale XC-142 model of Reference 3.

The internal strain gage balance mount included a body-axis oriented roll gimbal (axis of strain gage rolls with the aircraft) that permitted various roll angle settings for different flight conditions.

The yaw axis assembly was mounted above the model and yaw angle displacements occurred about a spaced fixed axis system perpendicular to the floor. Since the yaw axis was space fixed and the roll axis was body-fixed, then for small roll angle displacements ($\phi < 10^{\circ}$), the yaw angle of the aircraft is approximately equal to the yaw angle displacement measured at the drive assembly.

Approved for Public Release

Contrails

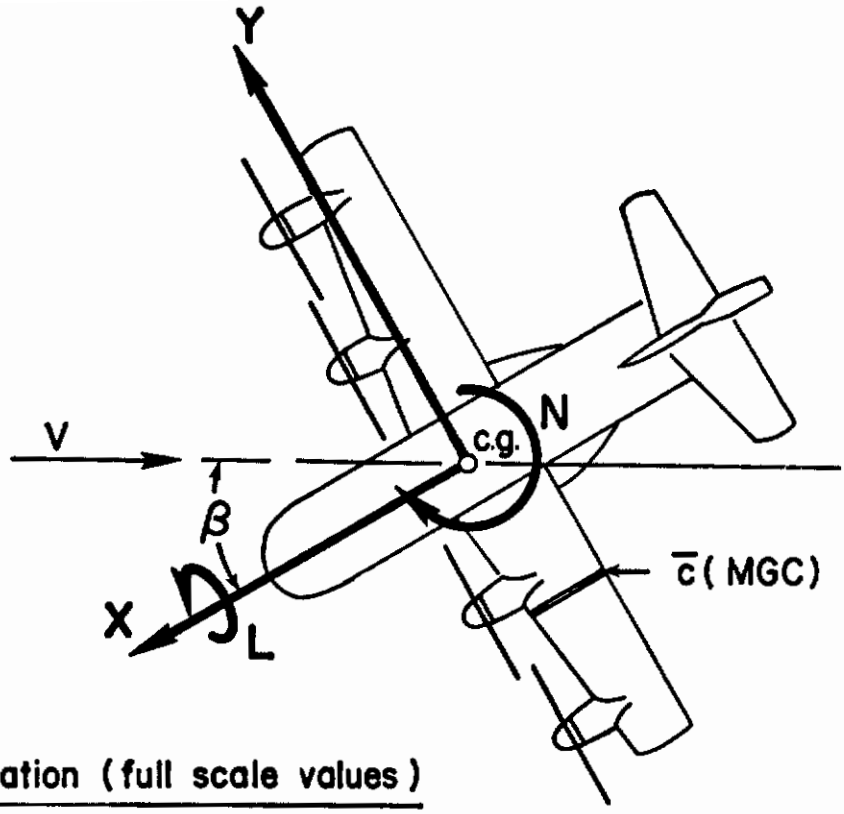

c.g. location (full scale values)

F.S. 268.8"
W.L. 122.8"

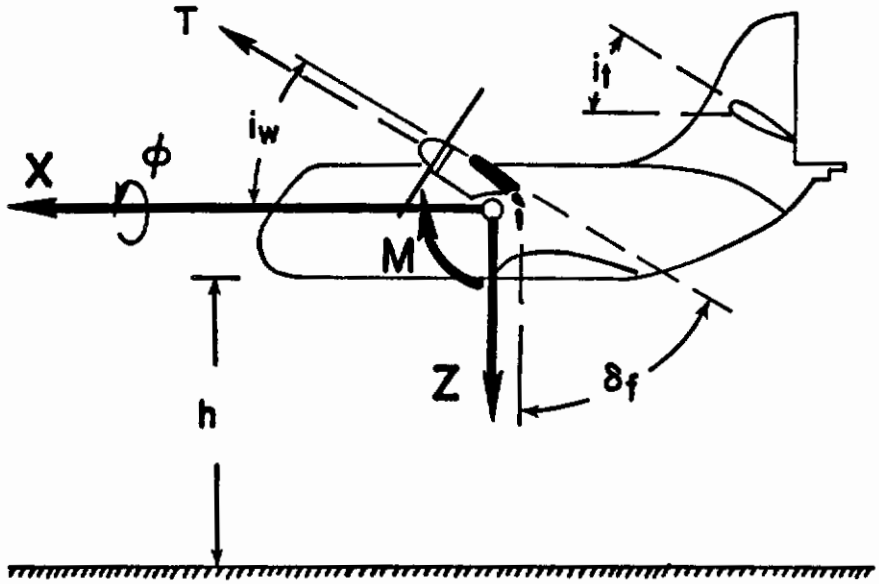

Figure 7. Model axis system and notation.

Approved for Public Release

Contrails

INSTRUMENTATION AND DATA ACQUISITION

The moving carriage contains a telemeter system that transmits time-shared data to a ground station in the control room at a rate of 900 samples per second. The following information is continuously monitored during the course of a run and simultaneously recorded on digital and analog tape recorders for further processing:

A. Six Strain-Gage Quantities

1. Longitudinal Force (Horizontal Force)
2. Side Force
3. Vertical Force
4. Rolling Moment
5. Pitching Moment
6. Yawing Moment

B. Control Positions (Measured by Potentiometers)

1. Port Collective Pitch (Average of Both Port Propellers)
2. Starboard Collective Pitch (Average of Both Starboard Propellers)
3. Port Aileron Deflection
4. Starboard Aileron Deflection

C. Additional Monitored Test Quantities

1. Model Yaw Angle (Potentiometer)
2. Model Propeller RPM (D. C. Tachometer)
3. Model/Carriage Velocity (D. C. Tachometer on carriage and photo-cell actuated electronic timming clocks)

Several other quantities were measured or pre-set prior to the run and coded to the digital tape.

1. Wing Incidence Angle
2. Flap Deflection Angle
3. Tail Incidence Angle
4. Fuselage Pitch Attitude
5. Model Roll Attitude
6. Altitude

All primary variables and other vital monitored data were recorded on-line on Sanborn paper charts. Digital data tapes were processed using a digital program to convert all raw data to dimensional form. A second digital program was utilized to convert all dimensional data to nondimensional form and to perform desired axis transfers. All data were presented on IBM type print-out sheets and selected data were printer plotted. Only selected portions of the data are presented in this report for reasons discussed.

Approved for Public Release

Contrails

EXPERIMENTAL PROGRAM AND TEST CONDITIONS

The experimental program undertaken to examine the various ground effect phenomena of interest was as follows.

The model was tested at seven different combinations of wing tilt angle and flap deflection. During the tests, the average propeller blade angle was set at 12° (measured at three quarters radius) and the propeller RPM was set at 4,000 RPM. The forward speed for each wing incidence/flap setting was then determined such that the strain gage data indicated that the model was at or very near to level flight trim ($X \cong 0$) at the maximum altitude investigated ($\frac{h}{c} = 4.2$). Then variations in the variables pertinent to the experiment were commanded and the forces and moments measured.

Particular interest in these experiments centered about the influence of the presence of the ground on the lateral/directional characteristics of tilt-wing aircraft and, in particular, to make new measurements on the influence of roll angle on the lateral/directional characteristics. Therefore, the following measurements were made about an initial wing level attitude at three height to chord ratios

a.) Yaw Angle
b.) Aileron Deflection
c.) Differential Propeller Pitch

These three experiments involved continuous slow variations of these quantities about the initial condition. The model velocity was held constant at the value determined for equilibrium level flight at the highest altitude. In addition, the roll angle was varied $\pm 4^{\circ}$, $\pm 6^{\circ}$ and $\pm 8^{\circ}$ about wing level attitude. Further, to examine the possible effects of nonlinearities due to roll angle, some of the above variations were also examined at constant roll angles. For example, with the model at a fixed roll angle of four degrees, the yaw angle was varied to examine the effect of a finite roll angle on the sideslip derivatives. Thus, the emphasis of the experimental program was related to the static effects of the presence of the ground. New data are presented showing the importance of the roll angle on the forces and moments in ground effect.

Approved for Public Release

Contrails

DISCUSSION

1. GENERAL

The results and analyses of the experimental data are detailed in this section. First, the influence of the proximity of the ground on the longitudinal characteristics of the various tilt-wing configurations is examined. These results present further longitudinal data on the configurations in ground effect and complement those presently found in the literature cited in this report. In particular, additional longitudinal data, using a moving model test technique, are presented that can be compared to existing results obtained by using fixed models mounted over moving ground planes installed in a conventional type wind tunnels. The general trends shown by the data acquired in this investigation are discussed in detail in the following sub-sections.

With respect to the two different STOL testing techniques, it is interesting to note that although the general trends measured are quite similar using each testing technique (a moving model over a fixed ground plane -- PDMT, versus a fixed model over a moving ground plane mounted in a wind tunnel), significant quantitative differences are detected when comparing specific data. For example, when comparing the trends and influences of the proximity of the ground on certain measured data, it appears that data acquired by the moving model technique (PDMT) compares generally with the data obtained by the fixed model technique -- for the lowest altitude ratio ($h/\bar{c} = 0.40$). However, at the intermediate height ($h/\bar{c} = 1.08$), the moving model technique indicates a lesser influence of the presence of the ground (as compared to the wind tunnel technique) and consequently a sharper change or more rapid onset of the ground effects for changes in height (from the intermediate altitude ratio to the lowest altitude ratio).

A second set of data is presented which details the lateral/directional characteristics of tilt-wing configurations in ground effect. The discussions and analyses are divided into four sub-sections; namely, sideslip characteristics, roll-angle characteristics, differential propeller pitch characteristics and aileron control effectiveness.

Complete data showing continuous measurements through the entire range of sideslip angles are presented because of the various complexities (including nonlinearities) displayed by the sideslip data. Next, the roll angle information is presented and "new" derivatives arising from the variation of the aerodynamic forces and moments with roll angle are discussed. In particular, the most significant aspect of the variations due to roll angle arise from the changes in yawing moment

Approved for Public Release

Contrails

and rolling moment that occur as a result of a bank angle near the ground. In essentially all of the cases investigated, these moment variations were very small or near zero at the greatest height examined ($h/\bar{c} = 4.2$) and became quite significant at the lowest height ($h/\bar{c} = 0.4$). Also, in addition to the aforementioned data, an Appendix considers the possibility of predicting the bank angle effects based only on longitudinal data.

Finally, the variations with ground height found in the two control parameters (differential propeller pitch and aileron input) are discussed. The variations in side force and the moments due to differential propeller pitch are presented. In the case of this differential propeller pitch data, the variation of forces and moments with control input was linear and the only significant changes occurred in rolling moment, yawing moment and side force. Therefore, only the slopes of the propeller differential pitch data are presented as determined from the analysis of the continuous data. There was no measureable influence of roll angle on these data other than an offset of the curves which is explained in more detail in the roll angle discussions. Also, with regard to the aileron effectiveness data, since aileron deflection produced significant changes in the yawing and rolling moments only, the data presented in the later sub-section are restricted to those parameters. Except where specially noted all data are presented in the nondimensional form based on the dynamic pressure of the slipstream as is conventional for tilt-wing aircraft. Also, for additional ease and continuity in reading the analyses of the data, all figures displaying the complete measured data for each variable and other pertinent graphs are compiled together near the end of the report.

2. TRIM CONDITIONS AND NONDIMENSIONALIZATION

The model trim velocity for each wing incidence/flap setting was determined experimentally by finding the velocity at which the resultant X force on the model was zero at the maximum altitude investigated ($h/\bar{c} = 4.2$). The advance ratio determined for all seven cases is listed in Table I. The propeller RPM was essentially constant at 4,000 RPM throughout the experiments so that the advance ratio is representative of forward speed.

Because of the slow forward speeds studied for this particular investigation, it was decided to nondimensionalize the measured forces and moments in the conventional manner most commonly utilized for this envelope of flight conditions. Therefore, except where specifically noted, all coefficients were based on slipstream dynamic pressure where

$$q_s = q + \frac{T}{A} \qquad (1)$$

In order to determine the slipstream dynamic pressure it is necessary to know the propeller thrust as well as the flight velocity. Forward speed

Approved for Public Release

Contrails

TABLE I

FLIGHT CONFIGURATIONS AND CONDITIONS

CASE	i_w/δ_f	μ_{TRIM}*	$C_{T,S}$**	$C_{Z,S}$**	C_Z†	V, knots†† (Full Scale)
I	45°/60°	0.0365	0.960	-1.44	-36.0	23.95
II	40°/60°	0.0535	0.913	-1.59	-18.2	33.68
III	40°/40°	0.0675	0.859	-1.79	-12.7	40.32
IV	45°/40°	0.0555	0.906	-1.67	-17.8	34.06
V	45°/50°	0.0530	0.915	-1.60	-18.8	33.14
VI	50°/30°	0.0580	0.897	-1.70	-16.5	35.38
VII	60°/20°	0.0475	0.932	-1.50	-22.0	30.65

* Model X force $\cong$ 0 at $h/\bar{c}$ = 4.2

** Coefficient based on slipstream dynamic pressure

† Coefficient based on free-stream dynamic pressure

†† Equivalent full scale trim speed where Z/S = 37,400/534 = 70.04 lbs/ft^2 and $C_Z = \frac{Z}{q\,S}$

Approved for Public Release

Contrails

was directly measured by several means but for these experiments it was not possible to provide the instrumentation needed on this particular model to measure the total thrust independently for the other forces. Therefore, the propeller thrust was calculated using the experimental curve given in Figure 8. The data contained in the curves shown in Figure 8 and obtained from References 5 and 25 are published results of measurements made on one propeller operated at the blade angle and rotational velocity identical to that utilized to conduct the experiments reported herein. The T/A curve shown in Figure 8 displays the relationship between model free-stream velocity and the average disc loading characteristic of the propeller. The disc loading curve was approximated by an analytical expression for use in the data reduction program with the digital computer. The numerical expression for the thrust coefficient derived from the T/A curve was

$$C_T = 0.0175 - 0.0219\mu - 0.466\mu^2 \qquad (2)$$

The propeller thrust coefficient based on slipstream velocity is determined from the relationship

$$C_{T,s} = \frac{C_T}{\frac{\mu^2}{2} + C_T} \qquad (3)$$

and the propeller thrust determined from the expression

$$\frac{T}{A} = q\left(\frac{C_{T,s}}{1 - C_{T,s}}\right) \qquad (4)$$

The slipstream dynamic pressure also may be written as

$$q_s = q\left(\frac{1}{1 - C_{T,s}}\right) \qquad (5)$$

All forces and moments were nondimensionalized by q_s as presented here.

Approved for Public Release

Contrails

Coefficients based on freestream velocity may be readily calculated based on the above relationships. That is, for example

$$C_X = C_{X,s} \left(\frac{1}{1 - C_{T,s}} \right) \qquad (6)$$

Similar expressions may be written for all other coefficients. Table I lists the trim advance ratio, the calculated thrust coefficient and the vertical force coefficient based on both freestream and slipstream dynamic pressures for each case. Equivalent flight speeds of the full scale aircraft may be determined by selecting a wing loading for the full scale aircraft and using the measured vertical force coefficient to calculate a full scale dynamic pressure and consequently an airspeed.

3. LONGITUDINAL EFFECTS OF THE PRESENCE OF THE GROUND

The measured variations in the vertical and horizontal force coefficients and the pitching moment coefficient with height above the ground are shown in Figure 9 for all the vehicle configurations examined. The data are presented in nondimensional form based on an estimated propeller thrust coefficient out-of-the-ground effect and therefore, these coefficient variations are proportional to the variations in the dimensional quantities. The value of the horizontal force at the highest altitude is nominally zero since the horizontal velocity of the model was selected on this basis.

The general trends in the measured longitudinal data are those typical of a high lift system operating near the ground. These effects are indicated by previous results on tilt-wing aircraft (References 2, 3, and 5) as well as more recent theoretical work on jet augmented wings, showing a marked increase in horizontal force, a decrease in vertical force and a nose down increment in pitching moment. Two cases do show a departure from these general trends. In Case I ($45^\circ/60^\circ$), there is a small increase in lift as the altitude is changed from the intermediate to lowest height. In Case VII ($60^\circ/20^\circ$), there is a lift increase when

Approved for Public Release

Contrails

moving from the maximum height to the intermediate height. Considering that the resultant force on the aircraft is the sum of the propeller thrust parallel to the shaft and a force produced by the wing (the wing force is approximately normal to the wing chord), the gross trends in these curves primarily indicate that there is a marked reduction in the wing normal force as the ground is approached. In general the changes in vertical force and horizontal force, produced by the presence of the ground, become larger as the lift coefficient of the vehicle based on freestream velocity increases as would be expected from the pervious discussion. The only exception is Case VII ($60^{\circ}/20^{\circ}$), the highest wing incidence examined, which experiences the smallest changes in horizontal and vertical force although the case represents the next to largest lift coefficient.

Note, with regard to the pitching moment data, no attempt was made to trim the model in pitch for these experiments and the tail rotor was not operating so that the pitching moment is not zero at the highest altitude (Figure 9c).

Comparing these data with those of Reference 3, the trends in forces and pitching moments are similar as the ground is approached. However, there is a sizable difference in magnitude of the force changes with approach to the ground. In fact, to the first order and in most of the cases examined, the measured changes in horizontal and vertical force from this program are, at the lowest height ratio ($h/\bar{c} = 0.4$), roughly equal to the data measured at the intermediate height ratio ($h/\bar{c} = 1.08$) of Reference 3. In other words, the effects of the presence of the ground appear much more abrupt from the results of the moving model tests conducted in the PDMT as compared to the wind tunnel tests of Reference 3. A difference in the sharpness of the increase in ground effect, as measured by a moving model as compared to a model in a wind tunnel (without a moving belt), is clearly shown in Reference 26, Figure 9; and also, even with a moving belt (Reference 7, page 443), there is some indication that the variations measured may be more gradual than that obtained with a moving model in the PDMT.

The extremely limited nature of data available for comparisons of this kind makes it difficult to draw more detailed conclusions. The data comparison described above was taken on a jet flap model and may not be directly applicable to a tilt-wing configuration. It is difficult to obtain further confirmation of these differences between a moving model and a moving belt as to which more clearly represents full scale phenomena in flight. However, some evidence is presented in Reference 7 page 62 Figure 10 which reveals that the wind tunnel tests with a moving belt may indicate a somewhat too great a height for the onset of significant ground effects. This leads to the speculation that the moving model tests may give better results.

These differences among the data would appear to be of considerable significance to the consideration of ground effects on any new high lift systems and further experimental research to clarify the differences

Approved for Public Release

Contrails

between a moving model and a model in a wind tunnel with a moving belt system appear highly desirable.

Some of the differences between the data presented here and that of Reference 3 could be accounted for by differences in $C_{T,s}$; however, this does not seem sufficient to explain the large differences when the trends with $C_{T,s}$ are considered (Reference 12). Recall that in the PDMT tests, the thrust of the propeller was not directly measured. However, the propeller blade angle and the aircraft geometry was the same for both series of tests with one exception (where flap deflections of 30° or less were used), the flap vane was removed from the model employed in Reference 3.

4. LATERAL/DIRECTIONAL EFFECTS OF THE PRESENCE OF THE GROUND

A. Sideslip Characteristics

In general, the influence of height as well as roll angle on the aerodynamic force and moment variations with sideslip was found to be quite complex. The general trends measured are in good agreement with Reference 3 including the nature of the nonlinearities in the directional stability. The complete data are presented in Figures 10 through 16. These curves essentially consist of continuous measurements so no points are shown on the curves.

As discussed earlier, small asymmetries in the model result in the fact that the yawing moment and rolling moment of Figures 10 through 16 are not zero when the roll angle and the sideslip angle are zero. This asymmetry is primarily a result of a slightly different propeller blade chord on the starboard propellers compared to the port propellers. It was decided that the experiments should be run with equal collective pitch on both sets of propellers. Approximately 0.5 degrees of differential propeller pitch is required to trim these unbalanced moments. Roll angle of course results in changes in these moments as shown by the curves and discussed in the following text.

The two primary variations with sideslip, the rolling moment and the yawing moment, have been used to determine the directional stability and the dihedral effect at zero roll angle and the results are shown in Figure 17. Care should be taken in interpreting some of these points as there are significant nonlinearities present in some cases. The curves with significant nonlinearities are indicated by the flagged points on the curves. Generally, the directional stability showed nonlinearities at the intermediate height consisting of a marked increase in slope near zero sideslip. The dihedral effect was highly nonlinear in a number of cases at the intermediate and lowest heights.

First, examining the directional stability, it was found to be quite linear out-of-ground effect and comparatively small and similar in magnitude in all the cases examined. Five out of the seven cases indicated a marked increase in directional stability at the intermediate height. In Cases I ($45^{\circ}/60^{\circ}$) and VII ($60^{\circ}/20^{\circ}$), this increase existed

Approved for Public Release

Contrails

over the range of sideslip investigated, while in the other three of the five cases, the increase existed over a range of roughly ± 3° of sideslip and then the slope decreased markedly. At the lowest height ($h/\bar{c} = 0.4$), the directional stability decreased again to a value similar to that at the maximum altitude investigated. In Cases III (40°/40°) and VI (50°/30°), there was a decrease in directional stability as the ground was approached.

The dihedral effect in most of the cases does not vary greatly with height above the ground except in the cases where there are significant nonlinearities present in the curves so that care should be taken in interpreting the larger values. Note particularly the behavior in Case VII (60°/20°), where near zero, an unstable dihedral effect is indicated however, for increased sideslip the slope changes markedly.

The roll angle effects on these derivatives are, in some cases, quite linear; that is, the presence of an initial roll angle does not influence the slopes of the sideslip derivatives but only offsets the curves and in other cases causes significant nonlinearities.

It is difficult to advance any simple reasons for some of the complex trends shown here. One would suspect that as the aircraft approaches the ground, there are marked changes in the manner in which the propeller/wing slipstream interacts with the tail.

The sideslip angle also affects the other forces and moments. The other large effect to be noted is the influence of sideslip on the aircraft pitching moment. The general trend noted here seems to be that the effect of the presence of the ground on pitching moment is considerably reduced by the presence of sideslip. As the altitude is reduced the variation of pitching moment with sideslip becomes an even function with the trend in the variation. When the larger sideslip angles are used, the pitching moments tend to approach the OGE values.

B. Roll Derivatives

As the ground is approached, the rolling moment and yawing moment become significant functions of roll angle. The physical source of this relationship can be seen by considering that the influence of the presence of the ground on the X and Z force of the aircraft arises primarily from the lifting system -- in this case the wing/propeller combination. One method of analysis or approximation suggested in this report and also by other authors, divides the total X and Z force acting on the aircraft into equal halves acting at a point on each wing panel (right versus left). Also note that for the low altitudes where ground effects are detected, significant changes in altitude will occur on each wing panel with aircraft roll angle displacements. Then at a given altitude, a roll angle

Approved for Public Release

Contrails

displacement from level will increase the altitude (decrease the ground effect) of the one wing panel while simultaneously decreasing the altitude (increase the ground effect) on the other wing panel. Therefore, placing one-half of the X and Z force at each wing panel and accounting for the height change of each wign panel due to the geometry of rolling, and analytical connection between X and Z force changes and the yawing and rolling moments can be derived. The interest of this simple analysis and framework in successfully predicting this particular ground effect phenomena based on longitudinal (X and Z force) effects is noted and therefore, an Appendix detailing this approach is included in this report.

Tables II and III list results as determined from the analysis is the Appendix and the measured experimental data. The one column in Table II lists the rolling moment derivative with roll angle as determined from the measured roll angle data shown in Figures 18 through 25 for all cases at three altitude ratios. The other column lists the calculated equivalent value of $\partial C_{Z,s}/\partial h$ (as determined by the analysis in the Appendix) required to produce the same value of rolling moment derivative as measured by experiment. Similarly, Table III lists the measured values of yawing moment derivative with roll angle and the calculated equivalent of $\partial C_{X,s}/\partial h$. It is obvious that variations in vertical force (Z force) will be related to rolling moments and variations in horizontal force (X force) will be related to yawing moments.

In Figures 9a and 9b (discussed in Section 3) the values of $C_{X,s}$ and and $C_{Z,s}$ versus altitude ratio where plotted for all seven cases. The points where simply connected to show the general trends for each case and no attempt was made to draw the actual curves because only three altitude points were available. It was felt that additional altitude intervals were needed before the curves could be drawn with sufficient accuracy so as to be able to evaluate the local slopes at selected altitude ratios to determine $\partial C_{X,s}/\partial h$ and $\partial C_{Z,s}/\partial h$. Also, rather sharp changes occur at the intermediate and lowest altitude ratios making local slope estimation additionally difficult. However, using the theory developed in the Appendix and knowing the measured values of rolling and yawing moment, it is possible to calculate the required values of local slopes for $\partial C_{X,s}/\partial h$ and $\partial C_{Z,s}/\partial h$ to produce the known measured moments. These calculated values of local slopes for $\partial C_{X,s}/\partial h$ and $\partial C_{Z,s}/\partial h$ (listed in Tables II and III) are shown on Figures 26 and 27 as short double-ended arrow lines denoting the local slope calculated for each altitude ratio.

The measured roll angle data obtained by experiments conducted in the Dynamic Model Track are shown in Figures 18 through 24. The data display the changes in force and moments versus roll angle for the three altitude ratios. These particular data were not obtained from continuous

Approved for Public Release

Contrails

TABLE II

Rolling Moment Derivative with Roll Angle

CASE	i_w/δ_f	$h/\bar{c}$	Measured by Experiment $\frac{1}{10}\left(\frac{\partial C_{L,s}}{\partial \phi}\right)$	Calculated Equivalent $\frac{\partial C_{Z,s}}{\partial h}$
I	45°/60°	4.2	0	
		1.08	0.008	0.075
		0.4	0.008	0.075
II	40°/60°	4.2	0	0
		1.08	0.012	0.1126
		0.4	0.014	0.1314
III	40°/40°	4.2	0	0
		1.08	0.0075	0.070
		0.4	0.037	0.34
IV	45°/40°	4.2	0.006	0.056
		1.08	0.016	0.15
		0.4	0.040	0.375
V	45°/50°	4.2	~0	0
		1.08	0.015	0.141
		0.4	0.043	0.403
VI	50°/30°	4.2	~0	0
		1.08	0.010	0.094
		0.4	0.0295	0.277
VII	60°/20°	4.2	~0	0
		1.08	0.022	0.206
		0.4	0.022	0.206

Approved for Public Release

Contrails

TABLE III

Yawing Moment Derivative with Roll Angle

CASE	i_w/δ_f	$h/\bar{c}$	Measured by Experiment $\frac{1}{10}\left(\frac{\partial C_{N,s}}{\partial \phi}\right)$	Calculated Equivalent $\frac{\partial C_{X,s}}{\partial h}$
I	45°/60°	4.2	0	0
		1.08	0	0
		0.4	0	0
II	40°/60°	4.2	0	0
		1.08	-0.025	0.234
		0.4	-0.036	0.338
III	40°/40°	4.2	0	0
		1.08	-0.010	0.094
		0.4	-0.053	0.498
IV	45°/40°	4.2	0	0
		1.08	-0.020	0.188
		0.4	-0.053	0.498
V	45°/50°	4.2	0	0
		1.08	-0.025	0.235
		0.4	-0.048	0.451
VI	50°/30°	4.2	0	0
		1.08	-0.022	0.206
		0.4	-0.056	0.526
VII	60°/20°	4.2	0.002	0
		1.08	-0.033	0.310
		0.4	-0.059	0.554

Approved for Public Release

Contrails

curves but result from faired curves for data taken at fixed roll angle values of 0°, $\pm 4^\circ$, $\pm 6^\circ$ and 8°. Although in a few instances they are generously faired curves, they were developed from all the data taken in the entire test program and represent a best fit curve for a large number of points, particularly for Cases I through IV.

From previous discussions and the Appendix, it can be determined that the sign of C_{L_ϕ} is positive from the fact that the vertical force decreases with height, indicating that an unstable roll spring is produced by the presence of the ground. The sign if C_{N_ϕ} is negative as would be expected from the fact that a forward force is produced by a reduction in height. Consequently rolling to the right tends to cause the nose of the aircraft to yaw left. Figure 25 shows the rolling and yawing moment derivatives (C_{L_ϕ} and C_{N_ϕ}) versus altitude ratio for all seven test cases. Note well that the derivatives C_{L_ϕ} and C_{N_ϕ} are "new" derivatives not normally encountered in more conventional airplanes. At the highest height examined, these derivatives were all zero or very close to zero and rise sharply in value as the ground is approached. Only Case I ($45^\circ/60^\circ$) shows no change in yaw moment with roll angle. The curves were somewhat difficult to interpret in Case I since the data were quite noisy. This noise may very well indicate fluctuating aerodynamics. However, it seems reasonably clear that the slopes are smaller than in all other cases.

Generally, in all cases except Case I ($45^\circ/60^\circ$), the slopes predicted for X force variation from the yawing moment data agree in a quantitative sense with the gross X force trends shown in Figures 9a and 26. The indication is that, if the ground effect on the horizontal force is well defined, it may be possible to obtain an estimate of the variation of yawing moment with roll angle.

In Figure 27, comparisons of the vertical force slopes computed to give agreement with the rolling moment variations with roll angle gives a similar qualitative agreement in most cases with the measured vertical force variation. There does seem to be a tendency for the predicted slopes to be larger than the measured vertical force variation. However, there is a considerable descrepancy between the relative magnitudes. In other words

Approved for Public Release

Contrails

attempting to estimate the rolling moment with the roll angle from the vertical force curves would tend to yield a smaller than measured value and perhaps, at this time, should be considered only qualitative.

The results for Case I ($45^\circ/60^\circ$), are the most difficult to explain as they do not seem to agree at all with the physical model proposed here. Case I shows the largest changes in the vertical force and horizontal force with height and yet has the smallest variations of yawing moment and rolling moment with roll angle. It seems clear that these derivatives have a complex dependence on the details of the configuration. Some of the complexity associated with Case I ($45^\circ/60^\circ$) may be indicated by noting the marked decrease in vertical force coefficient (based on slipstream)contrasted with Cases IV ($45^\circ/40^\circ$) and V ($45^\circ/50^\circ$) at the same wing incidence but smaller flap deflection. This decrease would appear to reveal a marked decrease in wing force indicating perhaps less sensitivity to further changes in other variables. Considering Cases IV ($45^\circ/40^\circ$) and V ($45^\circ/50^\circ$), it is noted that there are only comparatively small differences in the variations being considered. The additional ten degrees of flap deflection from 50° to 60° taken with the consequent change in trim has a significant effect on the influence of the ground.

A similar large difference, at the same wing incidence and comparing 40° and 60° flap deflection, is shown by comparison of the data from Case II ($40^\circ/60^\circ$) and Case III ($40^\circ/40^\circ$). Case III ($40^\circ/40^\circ$) shows quite similar behavior to Cases IV ($45^\circ/40^\circ$) and V ($45^\circ/50^\circ$); and Case II ($40^\circ/60^\circ$) is similar to Case I ($45^\circ/60^\circ$) both with the large flap deflection. Case VI ($50^\circ/30^\circ$), a somewhat higher wing incidence with a smaller flap deflection, shows a reasonable similarity to Cases III, IV, and V. Case VII ($60^\circ/20^\circ$), with a higher incidence and smaller flap deflection shows quite different trends.

Thus, the geometry of the vehicle seems to have considerable inpact on the roll derivatives and in particular the large flap deflection of 60° has considerable impact causing generally a marked reduction in the roll angle effects.

C. Differential Propeller Pitch Characteristics

Owing to the fact that all of the differential propeller pitch data were quite linear and were little influenced by roll angle, only the slopes are presented here. The differential pitch was nominally run through a range from $+1^\circ$ to -1° to determine these slopes. A minus one degree of differential propeller pitch input means that the average blade pitch on the port wing propellers is 13° (one degree above the nominal pitch

Approved for Public Release

Contrails

of 12°) and that on the starboard wing propellers is 11° (one degree less than the nominal blade pitch of 12°). Differential pitch produced significant changes only in rolling moment, yawing moment and side force.

The primary effects of the differential blade pitch control are shown in Figure 28 as slopes of rolling moment coefficient and yawing moment coefficient with differential pitch versus height above ground. The general trend and magnitude of these control effectiveness derivatives are similar for all cases. There is a decrease in the magnitude of the rolling moment coefficient variation with differential pitch as the ground is approached and an increase in the yawing moment coefficient variation with differential pitch. The yawing effect is in a proverse sense, that is, applying differential propeller pitch to attempt to roll left to raise a low right wing (positive differential pitch input), tends to yaw the aircraft nose left. This proverse tendency becomes larger and the primary control effectiveness becomes smaller as the ground is approached. These trends would be expected to aggravate the control problems of the aircraft close to the ground as indicated in a later sub-section.

In general, the data indicated that any nonlinear effects of roll angle on these slopes were quite small; that is, the slopes were essentially independent of roll angle.

The general trend and magnitude of these curves can be seen from a rather simple analytical model of the phenomena. Assuming that the resultant force on the wing ΔR is approximately normal to the propeller thrust line, then the yawing moment and rolling moment are related to the thrust and wing force as follows:

$$N \propto -(\Delta T \cos i_w - \Delta R \sin i_w) \tag{7}$$

$$L \propto -(\Delta T \sin i_w - \Delta R \cos i_w) \tag{8}$$

where ΔT and ΔR are the differences in thrust and wing normal force between the starboard and port wings. Therefore, the derivatives are

$$\frac{\partial N}{\partial(\Delta\theta)} \propto -\frac{\partial T}{\partial\theta}\left(\cos i_w - \frac{\partial(\Delta R)}{\partial(\Delta T)} \sin i_w\right) \tag{9}$$

$$\frac{\partial L}{\partial(\Delta\theta)} \propto -\frac{\partial T}{\partial\theta}\left(\sin i_w + \frac{\partial(\Delta R)}{\partial(\Delta T)} \cos i_w\right) \tag{10}$$

Now assuming that each propeller on the starboard side changes thrust by the same amount per degree and similarly on the port side and neglecting, for the moment, the wing force changes with thrust, the yawing moment and rolling moment coefficients can be expressed as

Approved for Public Release

Contrails

$$\frac{\partial C_{N,s}}{\partial \theta} = - \frac{\rho A(\Omega R)^2 \left(\frac{\partial C_T}{\partial \theta} \cos i_w\right) (2) (\ell_{p_1} + \ell_{p_2})}{q_s \; Sb} \tag{11}$$

$$\frac{\partial C_{L,s}}{\partial \theta} = - \frac{\rho A(\Omega R)^2 \, 2(\ell_{p_1} + \ell_{p_2})}{q_s \; Sb} \frac{\partial C_T}{\partial \theta} \sin i_w \tag{12}$$

where ℓ_{p_1} and ℓ_{p_2} refer to the spanwise location of the two propellers. Placing the geometric characteristics of the aircraft in this expression and using the experimental value of the propeller characteristics $\frac{\partial C_T}{\partial \theta}$ determined in hover at a q_s = 4.2 psf (the nominal slipstream dynamic pressure of the experiments), these expressions become

$$\frac{\partial C_{N,s}}{\partial \theta} = - 0.0385 \cos i_w \quad \text{(per deg)} \tag{13}$$

$$\frac{\partial C_{L,s}}{\partial \theta} = - 0.0385 \sin i_w \quad \text{(per deg)} \tag{14}$$

The hover value of $\frac{\partial C_T}{\partial \theta}$ is a good approximation to the value at these low forward speeds since the advance ratio is small.

These values are shown on the graph (to the right side) of the experimentally measured slopes and the difference between this simple theory and the experimental data is due to the wing force variation with thrust. The general trend with wing force can be sketched from the first expressions taking as a representative value of $\frac{\partial(\Delta R)}{\partial(\Delta T)} \approx 0.4$ (Figure 29).

It can be seen that the general trend of the experimental data indicates a positive $\frac{\partial(\Delta R)}{\partial(\Delta T)}$ as would be expected physically. Also, the trends in the data reveal that as the ground is approached the wing force variation with thrust decreases markedly. This trend would be expected on the basis of the changes in wing force shown by the changes in horizontal force and vertical force which occur as the ground is approached indicating that the wing resultant force decreases markedly.

Approved for Public Release

Contrails

As a rough approximation, the force on the wing

$$R \simeq q_s \, S \, C_R \tag{15}$$

and since

$$q_s = q + \frac{T}{A} \tag{16}$$

$$\frac{\partial R}{\partial T} \approx \frac{S}{A} \, C_R \tag{17}$$

Therefore, as the ground is approached and the wing resultant force coefficient reduces, it would be expected that $\frac{\partial R}{\partial T}$ decreases as shown by the trends in the data. The trend in both the rolling moment and yawing moment derivatives as ground is approached reveals that this derivative $\frac{\partial R}{\partial T}$ is decreasing.

Application of differential pitch also produced a side force as shown in Figure 28a. The trends of $\frac{\partial C_{Y,s}}{\partial \Delta\theta}$ are somewhat more complex. The derivative is rather small and would be expected to arise from lateral force components present due to the negative dihedral of the wings. The sign of the side force is that expected from the small components of wing force acting laterally as the propeller pitch is changed differentially and producing a differential wing force.

Differential pitch did not produce any appreciable change in horizontal force or vertical force and therefore those data are not shown.

Also at the two highest heights ($h/\bar{c} = 4.2$, $h/\bar{c} = 1.08$) there was no change in pitching moment with differential propeller pitch however, at the lowest height ($h/\bar{c} = 0.4$) there was a change in pitching moment. In Cases I ($45^\circ/60^\circ$) through IV ($45^\circ/40^\circ$), in which the nonlinear effects of roll angle on the differential pitch effectiveness were examined, there was a marked increase in the pitching moment change with differential propeller pitch when the aircraft had a roll angle of 4° as shown in Table IV.

The trends and magnitude of the influence of differential propeller pitch generally agree with Reference 3 although it is difficult to make a direct comparison since the differential thrust was obtained from differential RPM in Reference 3 rather than from differential propeller pitch as utilized in this study.

Approved for Public Release

Contrails

TABLE IV

PITCHING MOMENT/COLLECTIVE PITCH DERIVATIVE AS A FUNCTION OF ROLL ANGLE ($h/\bar{c}$ = 0.4)

Case Number and i_w/δ_f	$\frac{\partial C_{M,s}}{\partial(\Delta\theta)}$ (per deg)	
	$\phi = 0^\circ$	$\phi = 4^\circ$
Case II, $40^\circ/60^\circ$	0	0.0095
Case III, $40^\circ/40^\circ$	0	0.006
Case IV, $45^\circ/40^\circ$	0.002	0.004

These changes are small when compared to the total pitching moment change of the aircraft from an $h/\bar{c}$ of 4.2 to 0.4, where the change in pitching moment coefficient is the order of 0.2 indicating that this effect is not very significant.

D. Aileron Control Effectiveness

The primary aileron control effectiveness $\frac{\partial C_{N,s}}{\partial(\delta_a)}$ as a function of height over ground for the various configurations examined is shown in Figure 30. These slopes were obtained from data runs involving continuous aileron deflections. Symmetrical deflections of the ailerons were used in all cases. The complete data for aileron deflection is shown in Figures 31 through 37. In most cases the curves consist of two runs, one with a predominately negative aileron deflection and the other run with a predominately positive aileron deflection. In most cases good agreement at zero deflection was obtained.

The general trend of a decreasing control moment per unit aileron deflection is clearly shown. In addition, the general trend of an increasing aileron effectiveness with decreased flap deflection seems clear. Also, in certain of the test conditions (Cases VII, $40^\circ/40^\circ$, IV, $45^\circ/40^\circ$, and VI, $50^\circ/30^\circ$) a flat spot clearly is present in the data indicating no yawing moment produced by aileron deflection for

Approved for Public Release

Contrails

roughly ± 2.5° of aileron deflection. This is in agreement with the trend shown in Figure 10, of Reference 27, and contributes undoubtedly to the control problems of the aircraft in ground effect.

The rolling moments produced by the aileron were generally small and approximately zero in most of the configurations examined. These trends are shown in Table V where the derivative values are shown per 10° of aileron deflection. Other contributions of the ailerons to the horizontal and vertical forces and pitching moment were small and therefore are not shown.

E. Static Lateral/Directional Control Considerations in Ground Effect

A number of the trends shown by the experimental data taken here imply that there may be significant trimming problems with this aircraft configuration, particularly as a consequence of a bank angle near the ground.

First is the presence of "new" derivatives. Significant rolling moments and yawing moments are produced by roll angle at low heights. In addition, the primary roll control (the differential propeller pitch) tends to be somewhat less powerful as the ground is approached and in most of the cases examined, there is a significant increase in the yawing moment produced by differential pitch. That is, as differential pitch is applied to raise a wing, the yawing due to differential pitch will further increase the yawing tendency of the aircraft which arises from roll angle, adding to the requirements on the aircraft yawing moment control (the ailerons in this case). These two effects coupled with the marked decrease in the aileron control effectiveness as the ground is approached indicate that the aircraft has a marginal control capability near the ground.

The size of these effects can be seen from the following simplified linearized analysis. Consider the balance of yawing and rolling moments if the aircraft rolls as

$$C_{L_{\delta_a}} \delta_a + C_{L_{\Delta\theta}} \Delta\theta = - C_{L_\phi} \phi \qquad (18)$$

$$C_{N_{\delta_a}} \delta_a + C_{N_{\Delta\theta}} \Delta\theta = - C_{N_\phi} \phi \qquad (19)$$

Note, for notation simplicity, the subscript s is deleted in this subsection. Solving for the aileron deflection and differential propeller pitch required per degree of roll angle

$$\frac{\delta_a}{\phi} = \frac{-C_{L_\phi} C_{N_{\Delta\theta}} + C_{N_\phi} C_{L_{\Delta\theta}}}{C_{L_{\delta_a}} C_{N_{\Delta\theta}} - C_{L_{\Delta\theta}} C_{N_{\delta_a}}} \qquad (20)$$

Approved for Public Release

Contrails

TABLE V

Aileron Control Effectiveness Derivatives

CASE	i_w/δ_f	$h/\bar{c}$	$\frac{1}{10}\left(\frac{\partial C_{L,s}}{\partial (\delta_a)}\right)$	$\frac{1}{10}\left(\frac{\partial C_{N,s}}{\partial (\delta_a)}\right)$
I	45°/60°	4.2	0.005	0.01
		1.08	~0	0.01
		0.4	~0	0.007
II	40°/60°	4.2	irreg.	0.009
		1.08	irreg.	0.005
		0.4	irreg.	0.006
III	40°/40°	4.2	-0.005	0.019
		1.08	~0	0.016
		0.4	~0	0.006
IV	45°/40°	4.2	~0	0.016
		1.08	~0	0.013
		0.4	~0	0.006
V	45°/50°	4.2	~0	0.013
		1.08	~0	0.013
		0.4	0.003	0.004
VI	50°/30°	4.2	-0.002	0.023
		1.08	-	0.015
		0.4	-0.001	0.005
VII	60°/20°	4.2	-	0.015
		1.08	-	0.012
		0.4	-	0.002

Approved for Public Release

Contrails

$$\frac{\Delta\theta}{\phi} = \frac{-C_{N_\phi} C_{L_{\delta_a}} + C_{N_{\delta_a}} C_{L_\phi}}{C_{L_{\delta_a}} C_{N_{\Delta\theta}} - C_{L_{\Delta\theta}} C_{N_{\delta_a}}} \qquad (21)$$

In all cases $C_{L_{\delta_a}}$ was quite small and is therefore neglected. Therefore

$$\frac{\Delta\theta}{\phi} = - \frac{C_{L_\phi}}{C_{L_{\Delta\theta}}} \qquad (22)$$

$$\frac{\delta_a}{\phi} = - \frac{1}{C_{N_{\delta_a}}} \left(C_{N_\phi} - \frac{C_{L_\phi} C_{N_{\Delta\theta}}}{C_{L_{\Delta\theta}}} \right) \qquad (23)$$

where C_{N_ϕ} is negative, C_{L_ϕ} is positive and $C_{N_{\Delta\theta}}$ and $C_{L_{\Delta\theta}}$ are negative so that the influence of the yawing moment produced by the differential pitch can be seen to increase the aileron deflection required to counter a bank angle.

Figure 38 shows the aileron deflection required per degree of bank angle to balance a steady roll angle. In Case I ($45^\circ/60^\circ$), the requirement is quite small. Case II ($40^\circ/60^\circ$), is the next largest. Cases III, ($40^\circ/40^\circ$) IV, ($45^\circ/40^\circ$) and V ($45^\circ/50^\circ$) show sharp increases at the lowest height requiring the order of 15 degrees of aileron to counter one degree of bank. The worst case is Case VII ($60^\circ/20^\circ$) which requires 37° of aileron to counter a one degree bank.

The sharpness of the increase is due to the combination of trends described above; namely, the decrease in aileron effectiveness coupled with the increasing roll angle derivatives and the variation in the differential pitch derivatives. The second term in the parenthesis of the above equation ranges from one-third to one-half of the first term.

The large magnitude of these effects seems to indicate that the combination of the various static effects is indeed a significant part of the problem of controlling this aircraft close to the ground.

5. SUMMARY REMARKS

The nature of the data makes it difficult to draw any simple conclusions regarding the general trends. The two basic variables involved are the

Approved for Public Release

Contrails

geometric configuration of the model represented by the wing incidence setting and the flap deflection, and the thrust coefficient. Case II, $(40^{\circ}/60^{\circ})$, IV, $(45^{\circ}/40^{\circ})$, and V, $(45^{\circ}/50^{\circ})$, are at the same thrust coefficient and the general nature of the results indicate that the important stability parameters show a significant sensitivity to the configuration geometry as well as the thrust coefficient as can be seen from the variations in results for Cases II, IV and V.

Similarities between Cases I $(45^{\circ}/60^{\circ})$ and II $(40^{\circ}/60^{\circ})$ and the differences among these cases and the others indicate that there is a marked effect of increasing the flap deflection to 60°. Smaller flap deflections do not seem to have a significant change. The aileron effectiveness, $C_{N_{\delta_a}}$, clearly decreases as the flap deflection increases except in Case VII $(60^{\circ}/20^{\circ})$.

The influence of roll angle on the rolling and yawing moments appears to be largest generally at the lower flap deflections and to be smaller at the higher flap deflections, although any dominant trends are not clear.

Complexities such as these make it difficult to comment on how these results might be extrapolated to other configurations such as a blown flap configuration operating at high lift coefficients.

The vertical and horizontal force variations with height do reveal the importance of bank angle indicating that strong ground effects will give rise to significant lateral/directional effects.

A significant problem associated with the tilt-wing configuration under investigation is related to the changes in control effectiveness, in particular the loss in aileron effectiveness coupled with the effects of the roll angle derivatives.

Approved for Public Release

Contrails

CONCLUSIONS

1. The aerodynamic effects of the presence of the ground appear quite complex and are dependent on the configuration geometry of the aircraft as well as the thrust coefficient.

2. At high aircraft lift coefficients, the presence of the ground causes significant variations in rolling moment and yawing moment with bank angle. These variations are at least qualitatively indicated by the changes in horizontal force and vertical force with altitude. The sign of these effects is such that an unstable roll spring is produced ($C_{L_\phi} > 0$), and a right roll produces a nose left moment.

3. The aileron control effectiveness for a tilt-wing configuration decreases markedly as the ground is approached.

4. Static trim considerations indicate that large aileron deflections are required to balance a roll angle near the ground in all wing incidence/flap angle combinations examined except for those with 60° flap deflections, where the effects were comparatively small. Owing to the fact that control problems of a tilt-wing aircraft were experienced at 60° flap deflection, indications are that recirculation may be most significant in these particular flap combination configurations.

   In a number of different wing/flap combinations the order of 15° aileron deflection was required to counteract 1° of wing bank angle.

5. There is a small decrease in the rolling moment produced by differential propeller pitch as the ground is approached and an increase in the yawing moment produced by differential pitch control input.

6. There appear to be significant differences in the data acquired by the moving model technique of testing and wind tunnel testing with a moving belt. The moving model technique yields somewhat smaller and sharper ground effects at the high lift coefficients of these experiments.

Approved for Public Release

Contrails

RECOMMENDATIONS

1. Further experimental investigations are recommended in order to define carefully the differences in the data when testing vehicles that operate at high lift coefficients with the moving model technique versus the moving belt/wind tunnel techniques.

2. On any aircraft operating at high lift coefficients, the importance of asymmetrical flight conditions in ground effect should be given careful attention.

Approved for Public Release

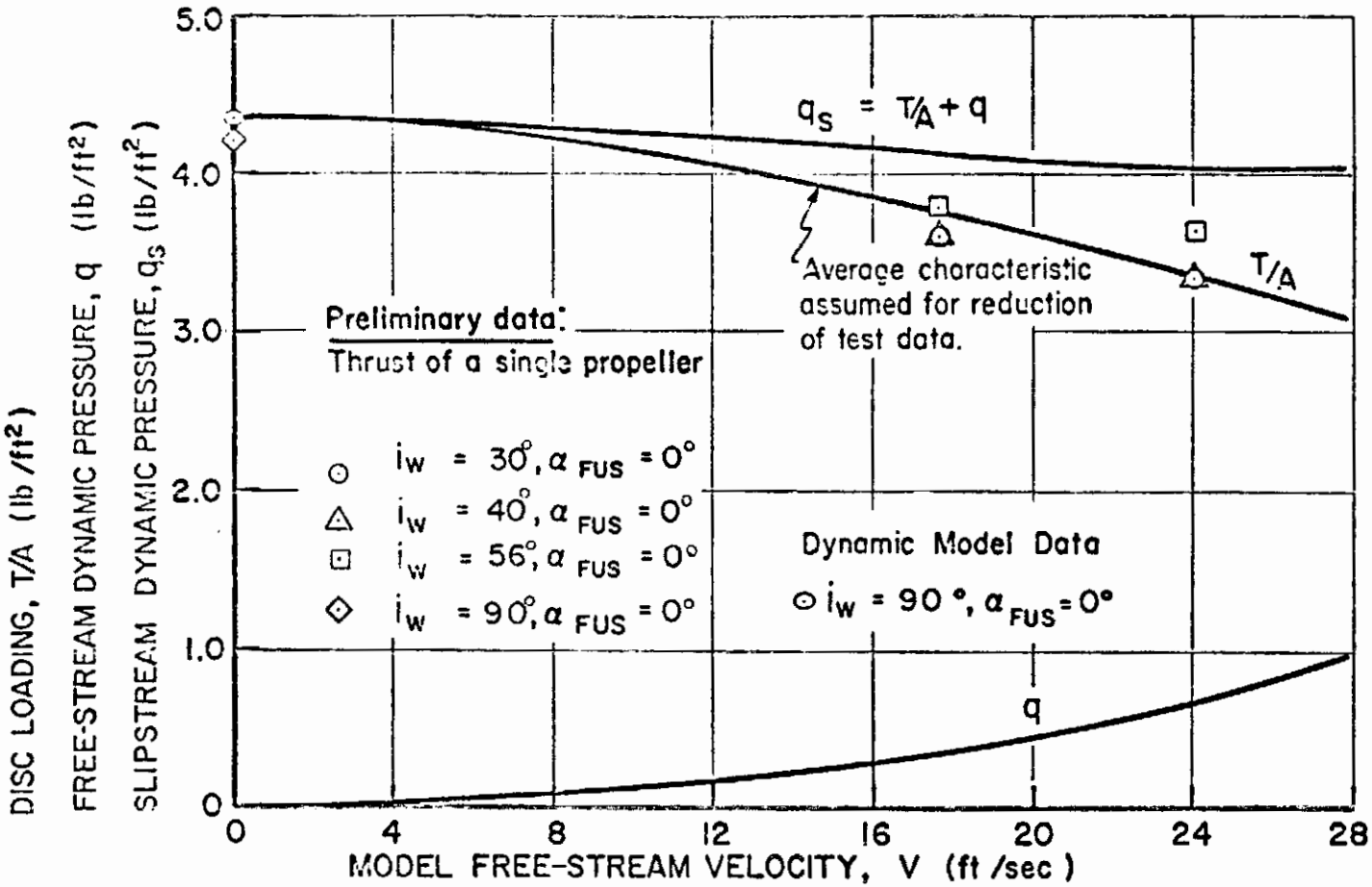

Figure 8. Experimental thrust characteristics of one propeller, Reference 4. (Converted to one-tenth scale and used for reduction of all static data, Reference 5.)

Approved for Public Release

Confidential

Contrails

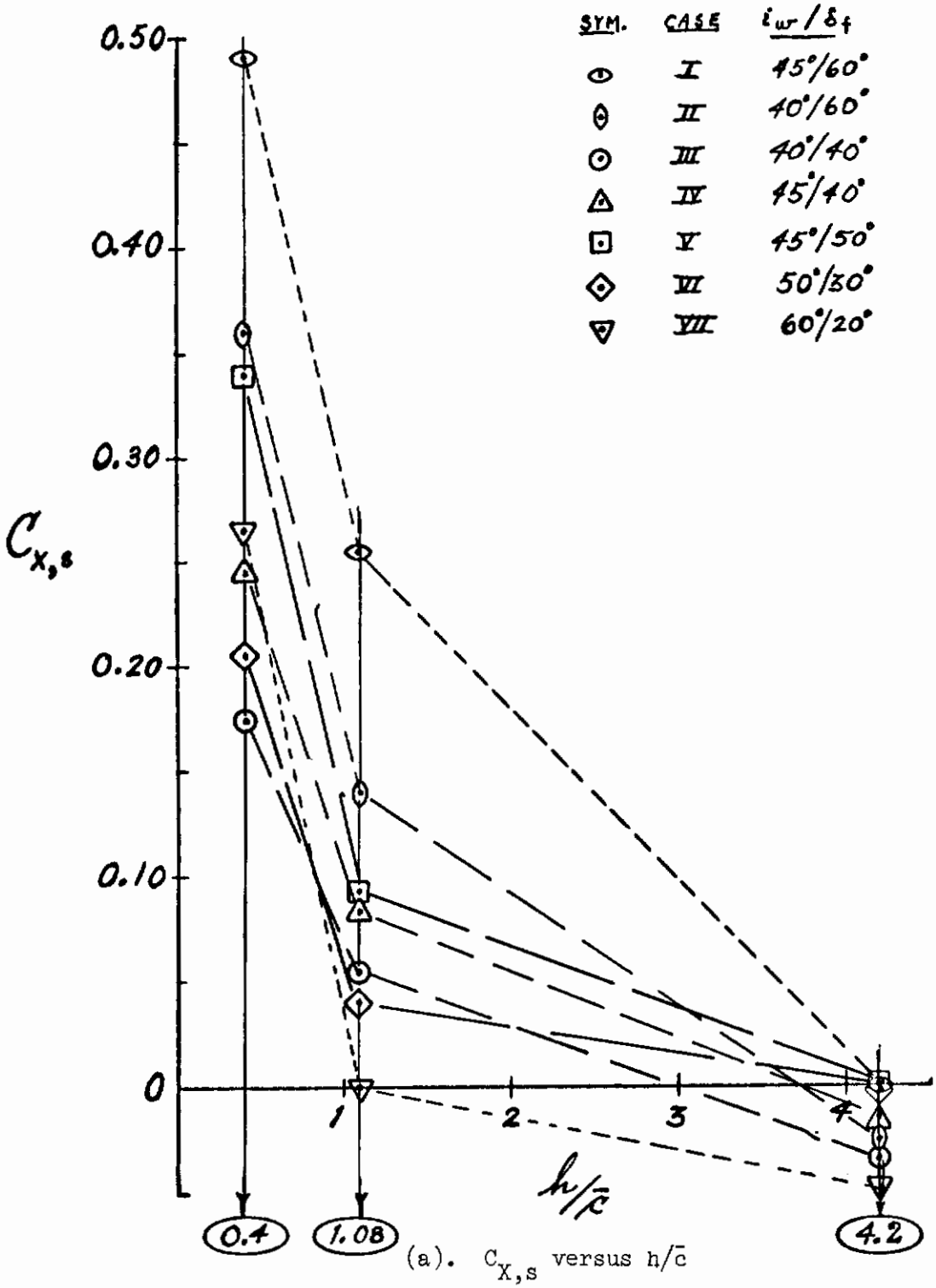

(a). $C_{X,s}$ versus $h/\bar{c}$

Figure 9. Longitudinal ground effect.

Approved for Public Release

Contrails

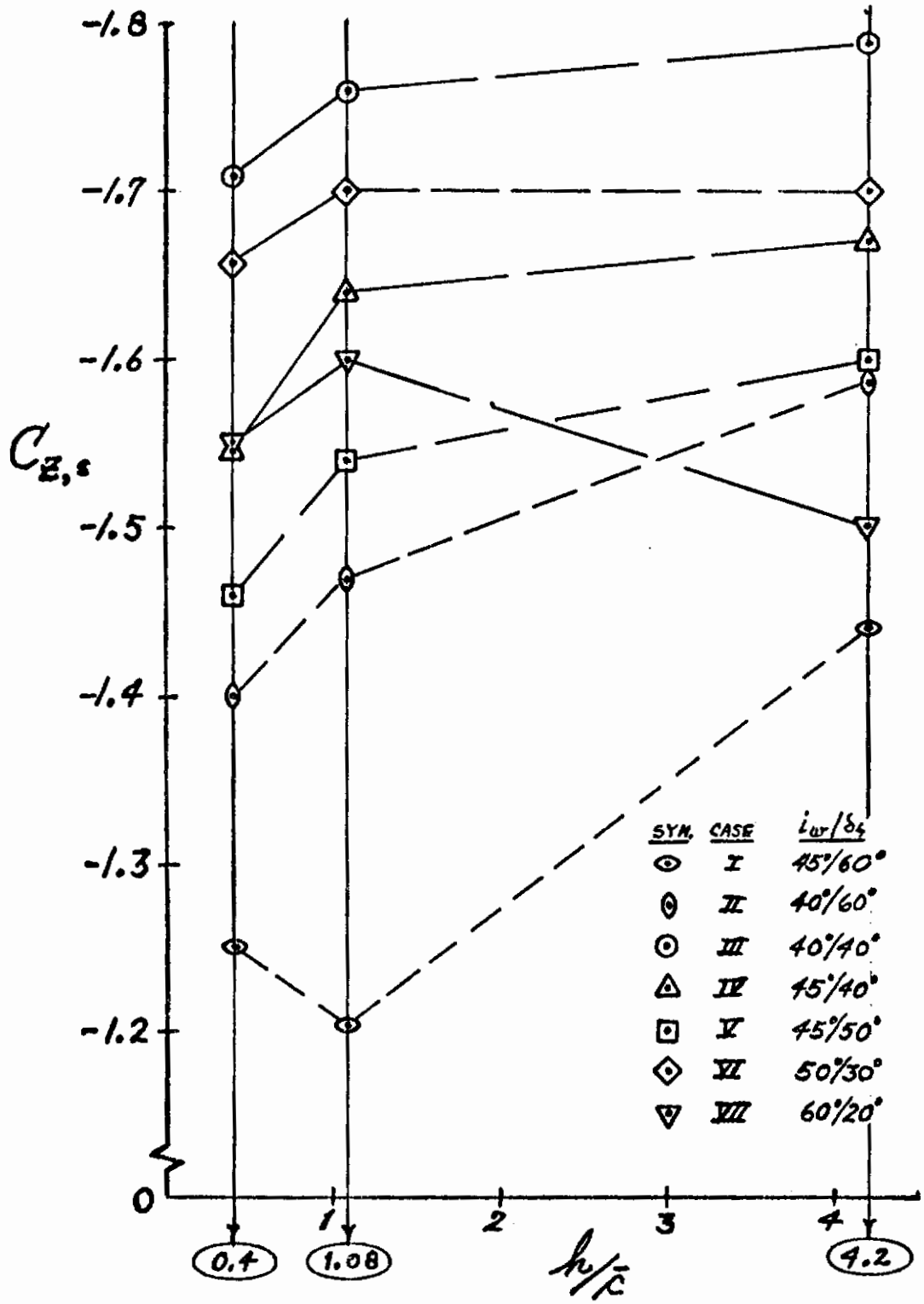

(b). $C_{Z,s}$ versus $h/\bar{c}$

Figure 9. Continued.

Approved for Public Release

Contrails

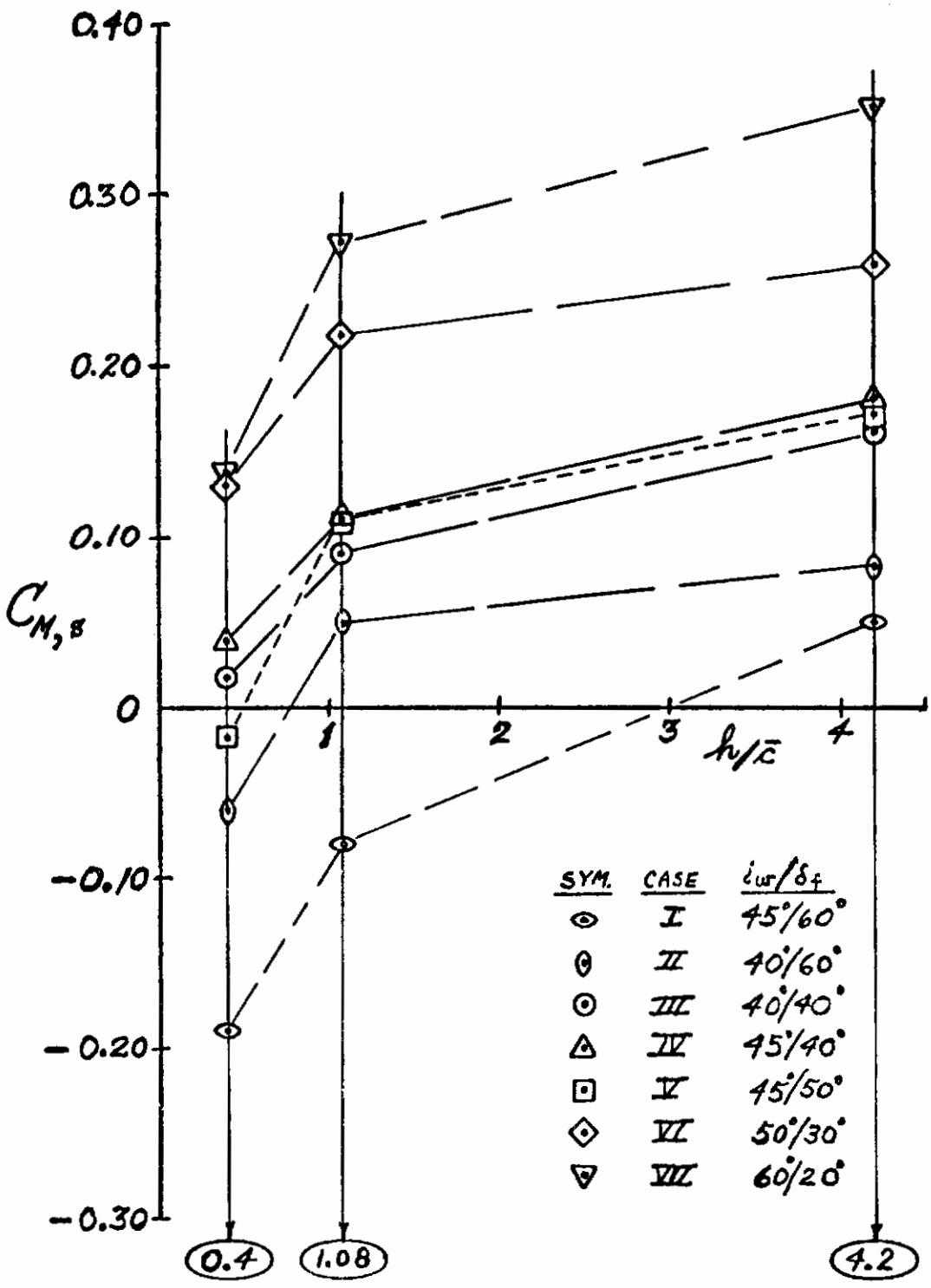

(c). $C_{M,s}$ versus $h/\bar{c}$

Figure 9. Concluded.

Approved for Public Release

Contrails

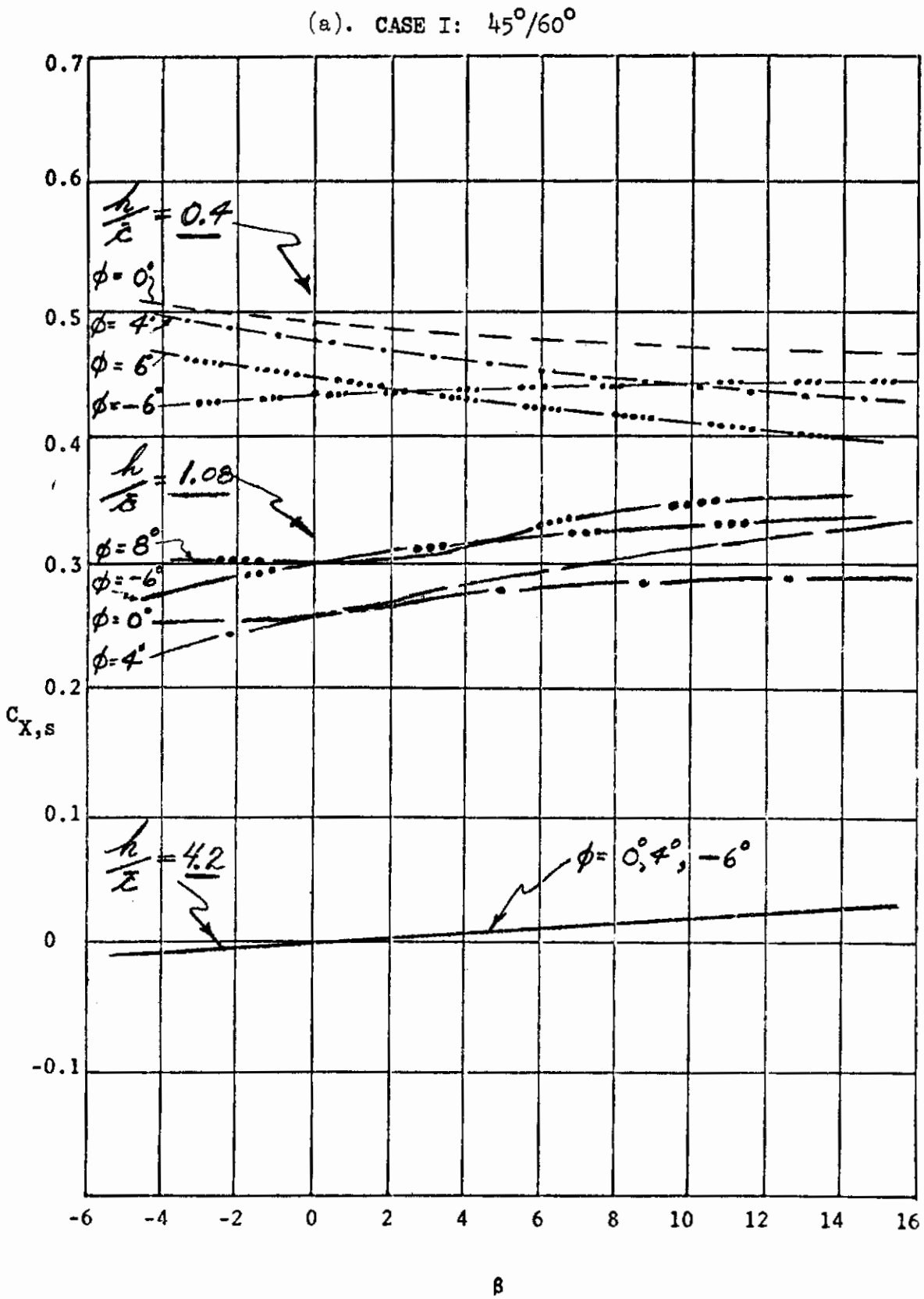

Figure 10. Longitudinal and lateral aerodynamic characteristics versus sideslip angle for various roll angles at three altitude ratios.

Approved for Public Release

Contrails

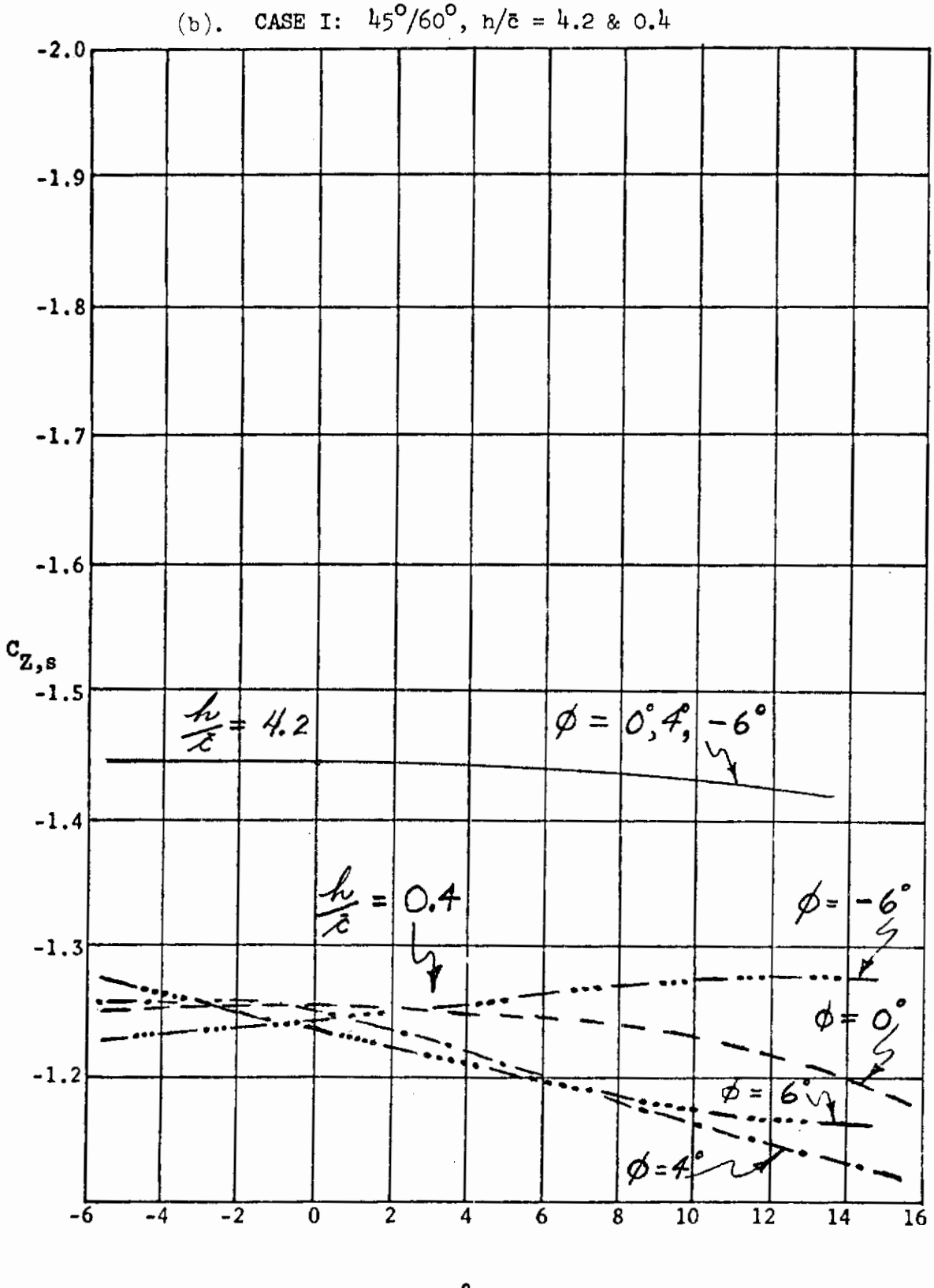

Figure 10. Continued.

Approved for Public Release

Contrails

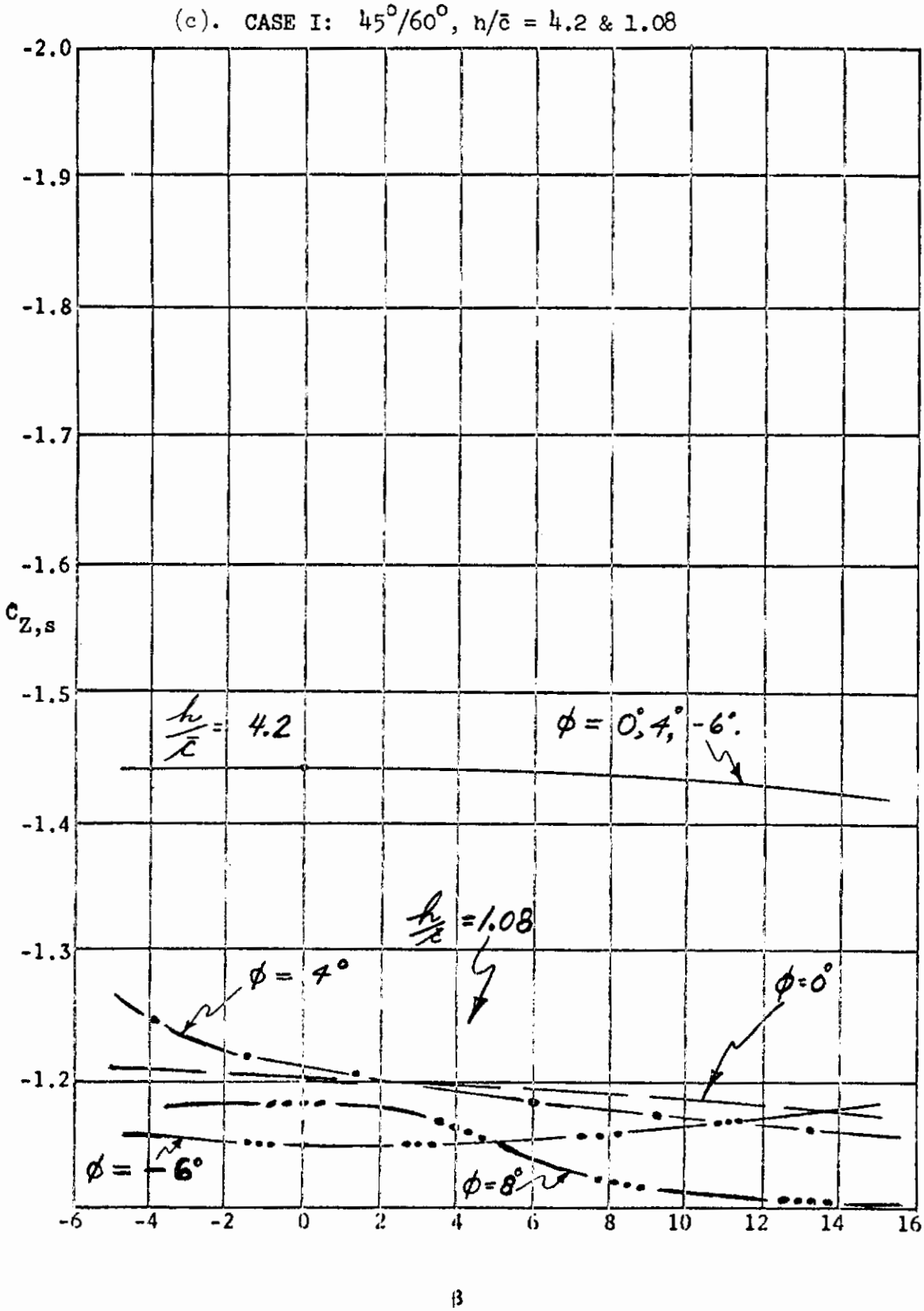

Figure 10. Continued.

Approved for Public Release

Contrails

(d). CASE I: 45°/60°

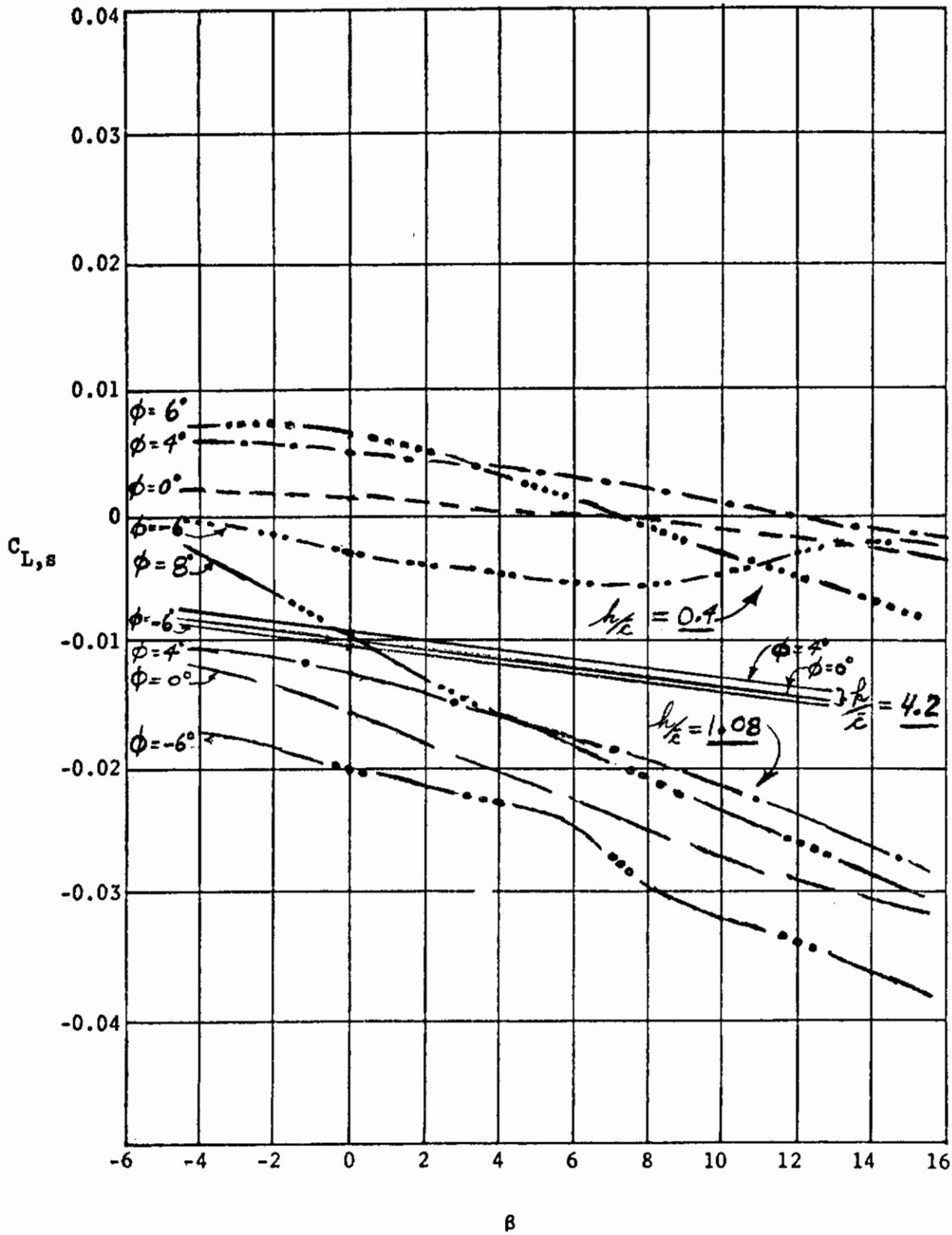

Figure 10. Continued.

Approved for Public Release

Contrails

(e). CASE I: 45°/60°, h/c̄ = 4.2 & 1.08

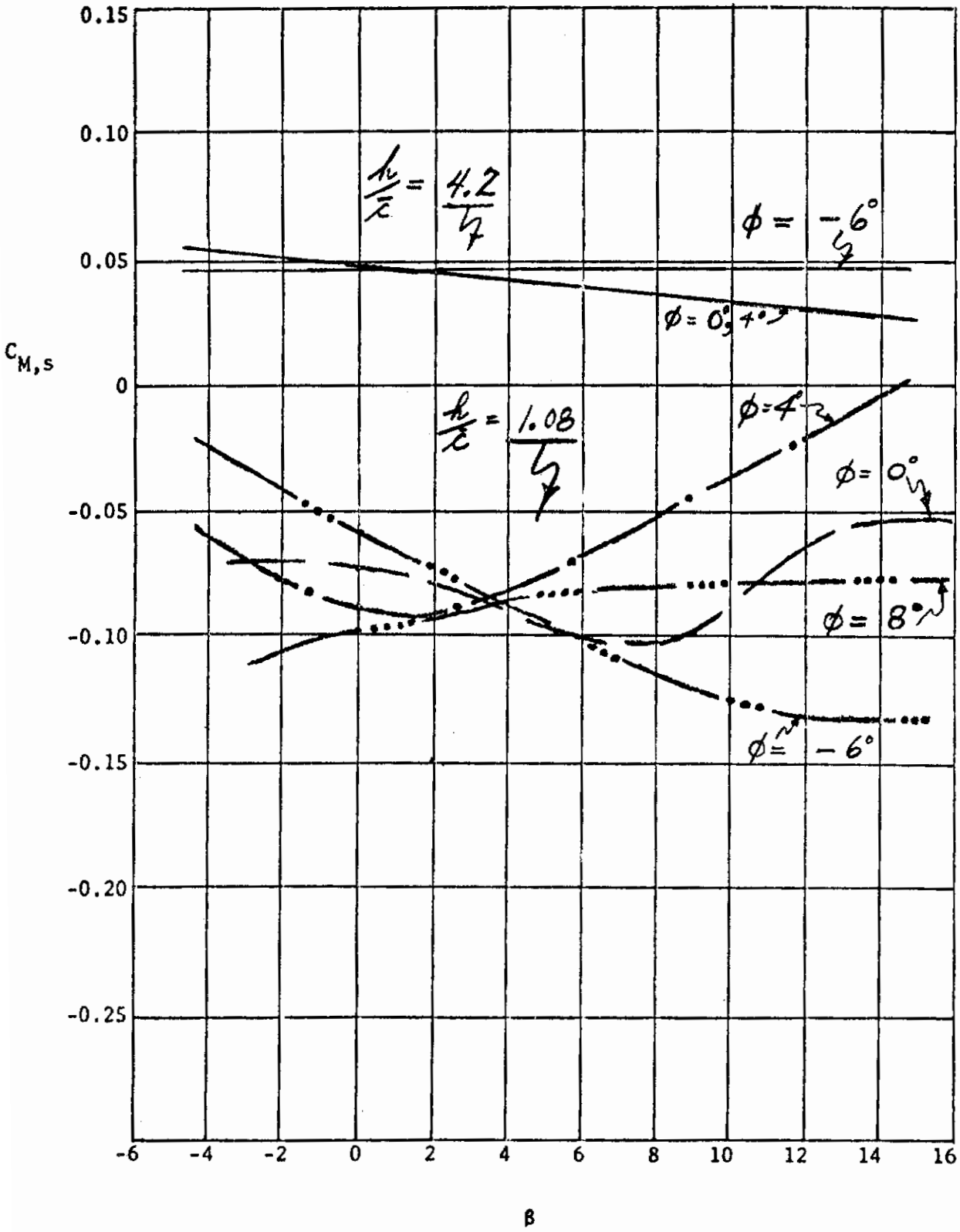

Figure 10. Continued.

Approved for Public Release

Contrails

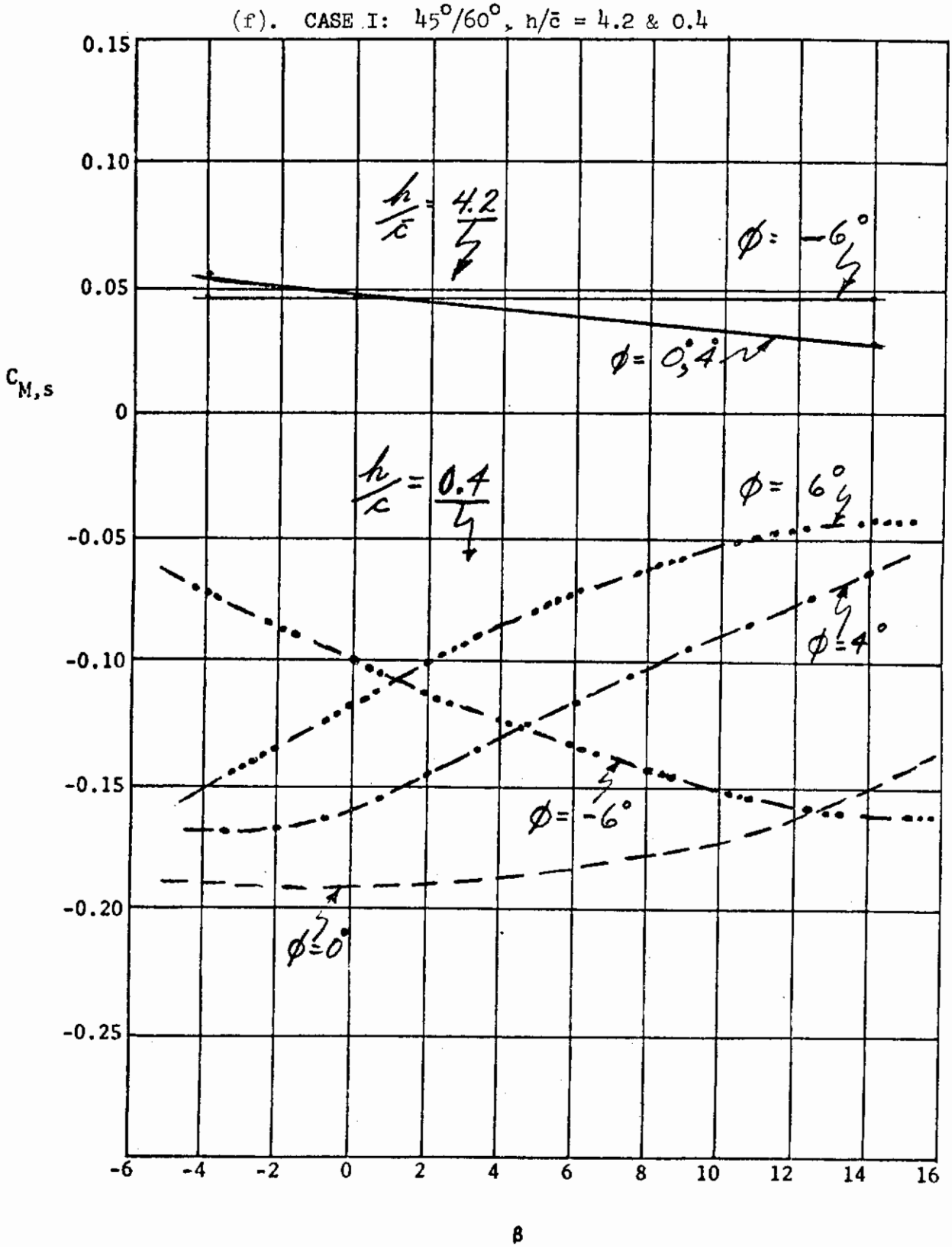

Figure 10. Continued.

Approved for Public Release

Contrails

(g). CASE I: $45^{\circ}/60^{\circ}$, $h/\bar{c} = 4.2$ & 1.08

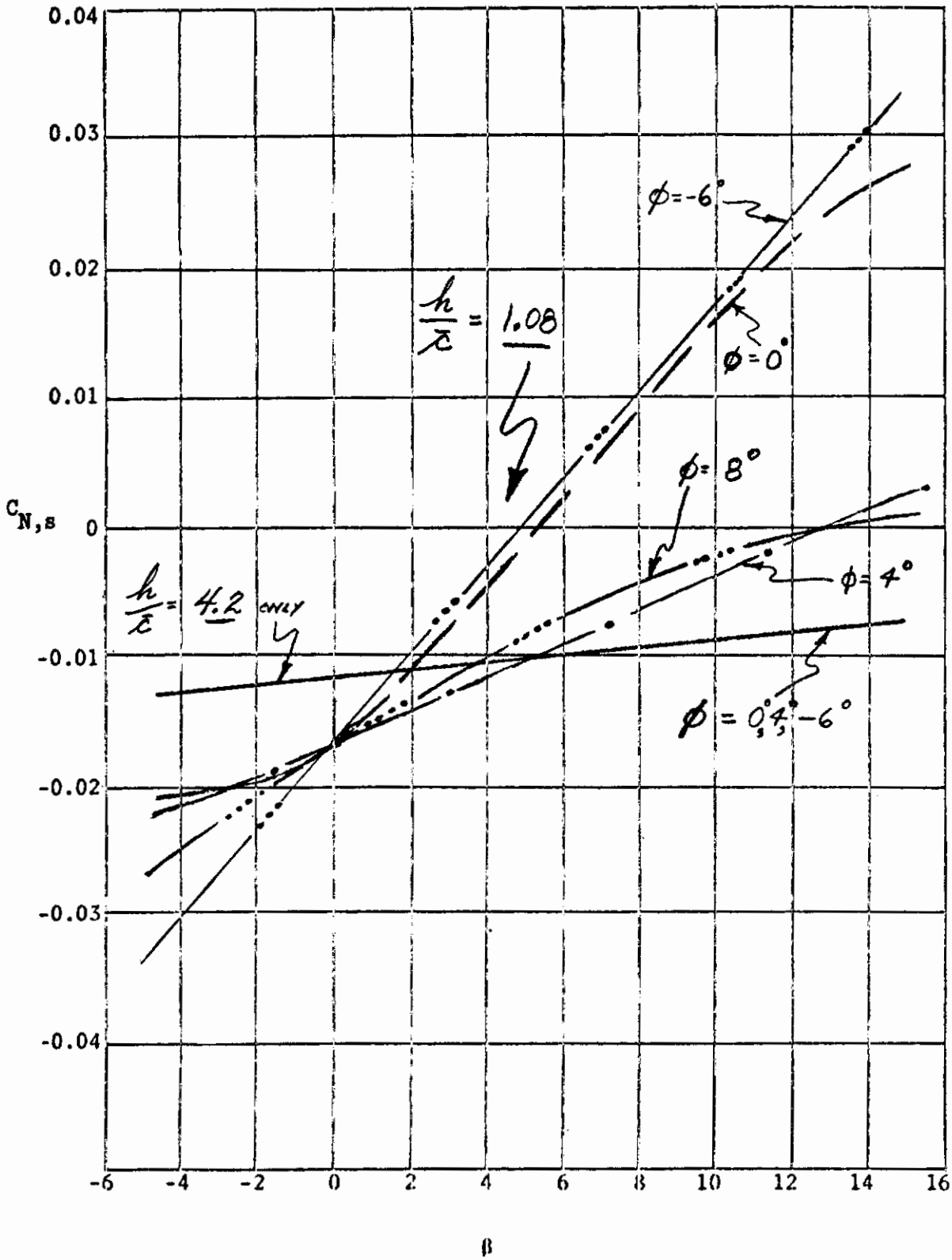

Figure 10. Continued.

Approved for Public Release

Contrails

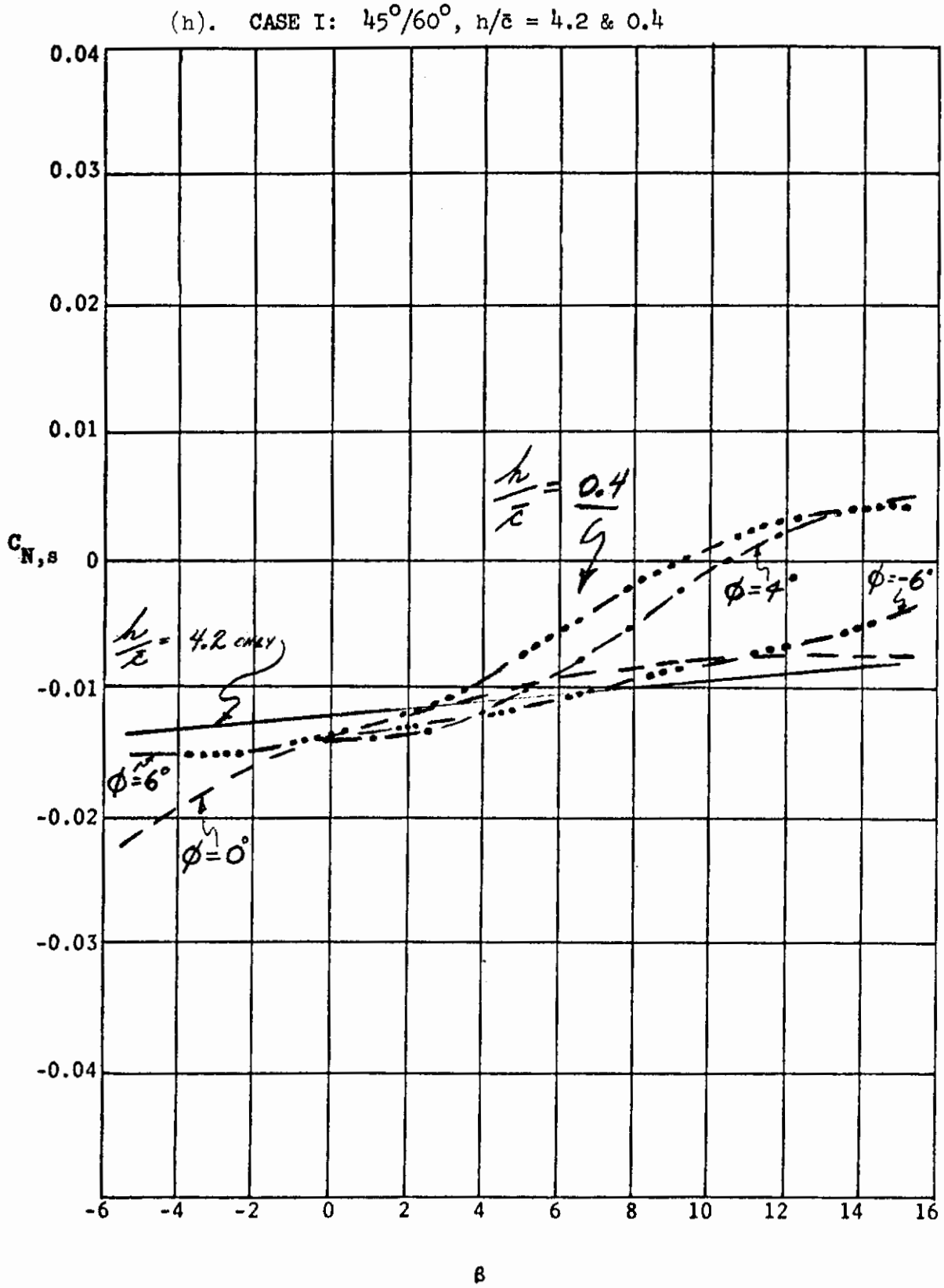

Figure 10. Concluded.

Approved for Public Release

Contrails

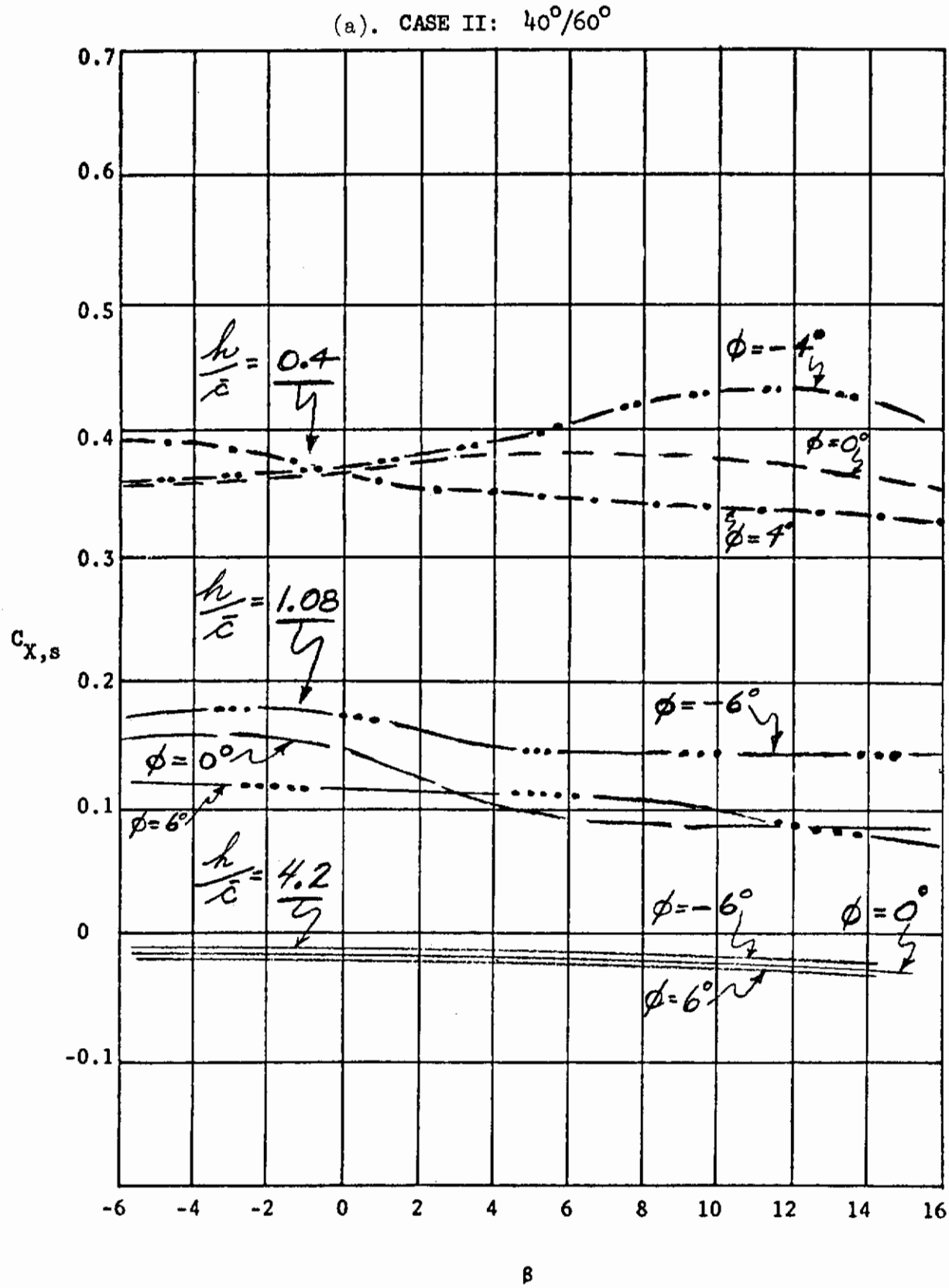

Figure 11. Longitudinal and lateral aerodynamic characteristics versus sideslip angle for various roll angles at three altitude ratios.

Approved for Public Release

Contrails

(b). CASE II: 40°/60°

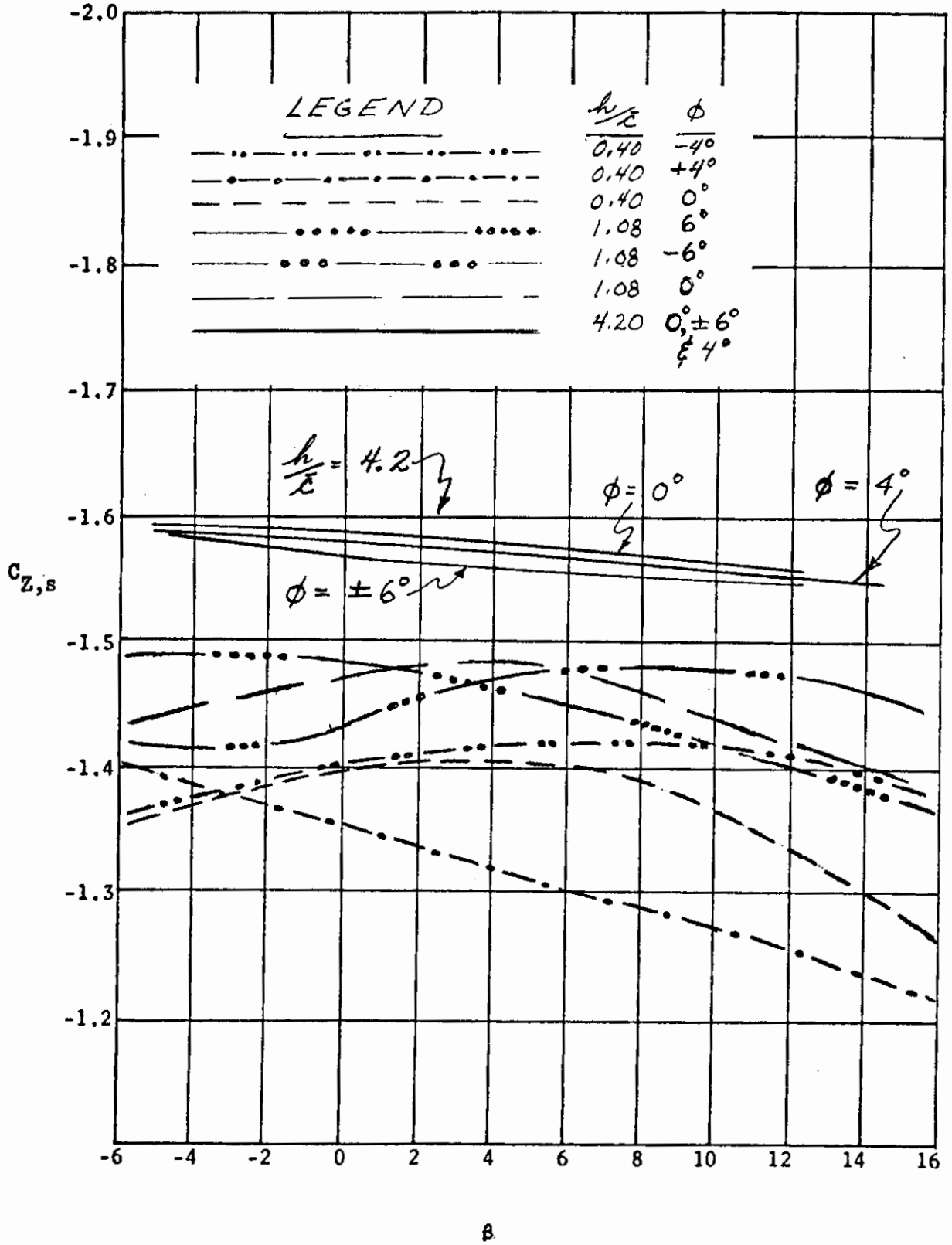

Figure 11. Continued.

Approved for Public Release

Contrails

(c). CASE II: 40°/60°

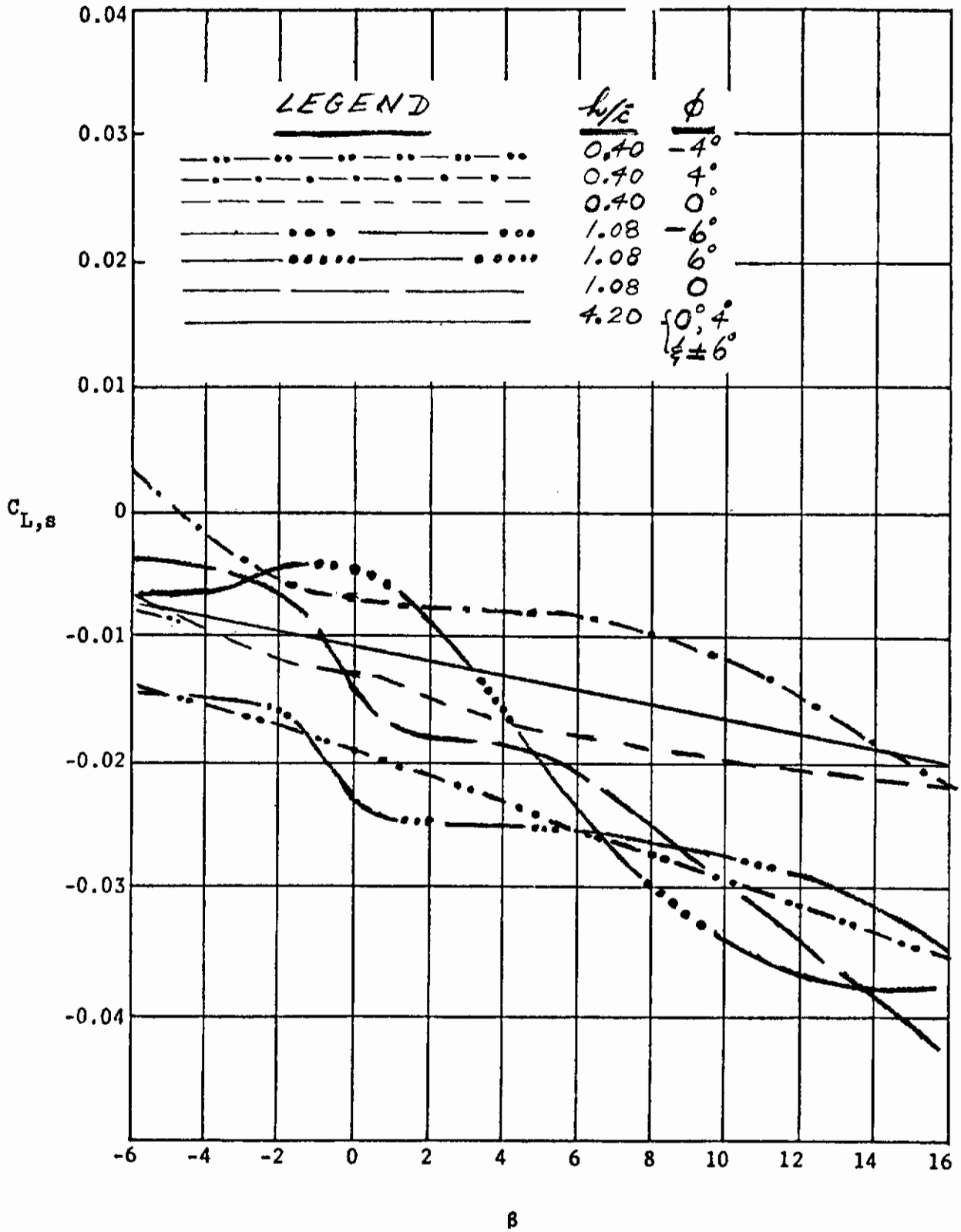

Figure 11. Continued.

Approved for Public Release

Contrails

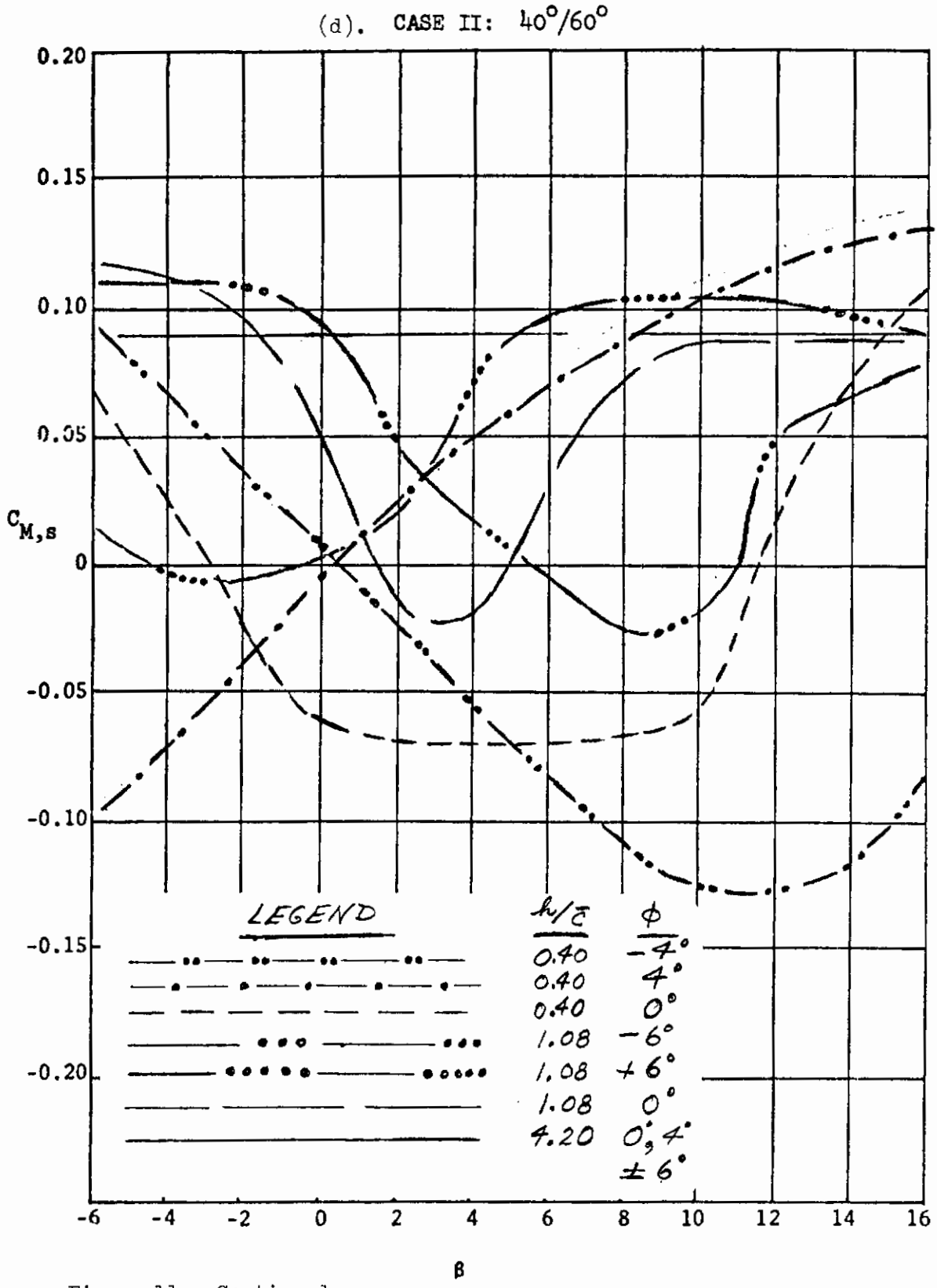

Figure 11. Continued.

Approved for Public Release

Contrails

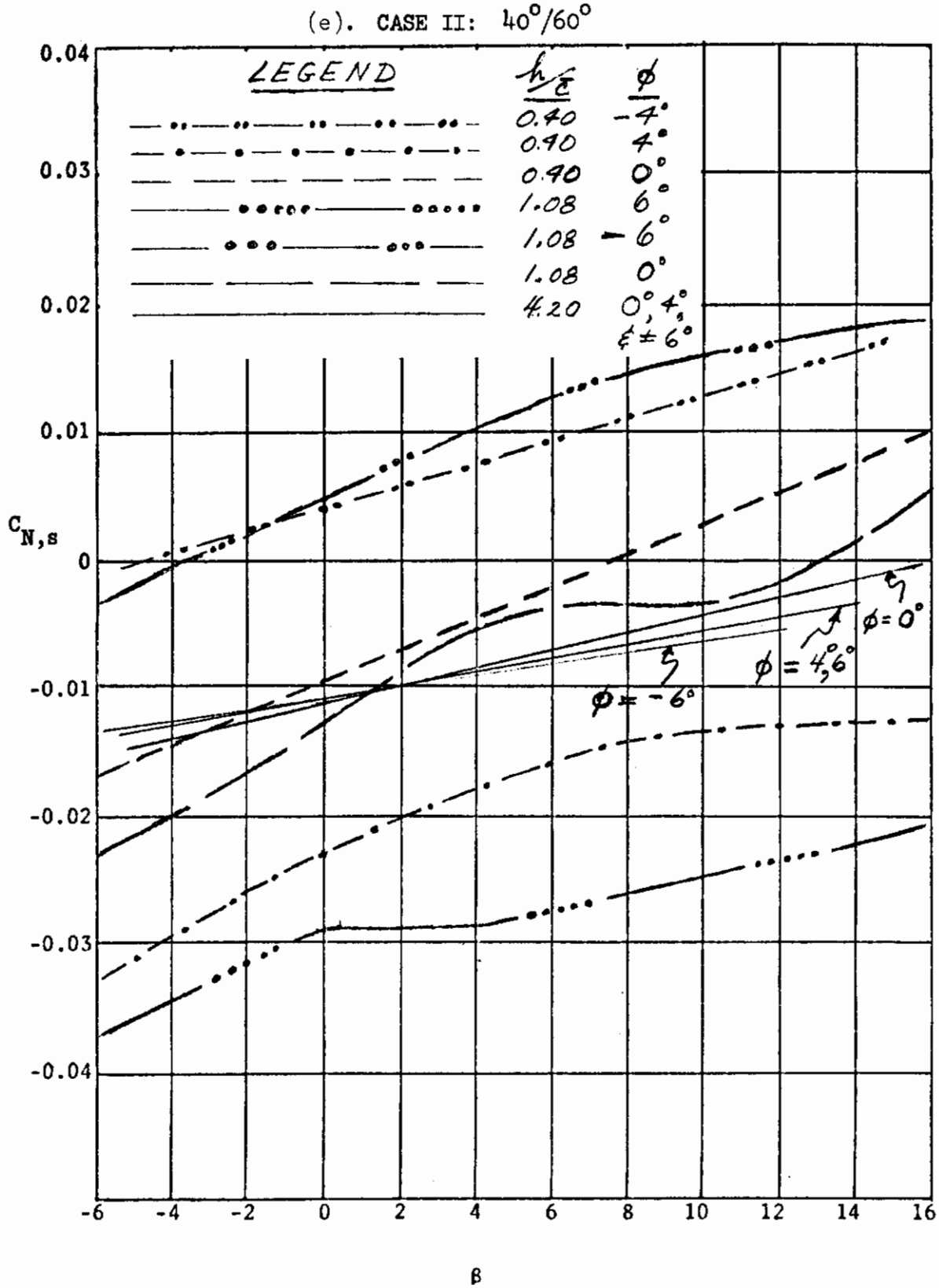

Figure 11. Concluded.

Approved for Public Release

Contrails

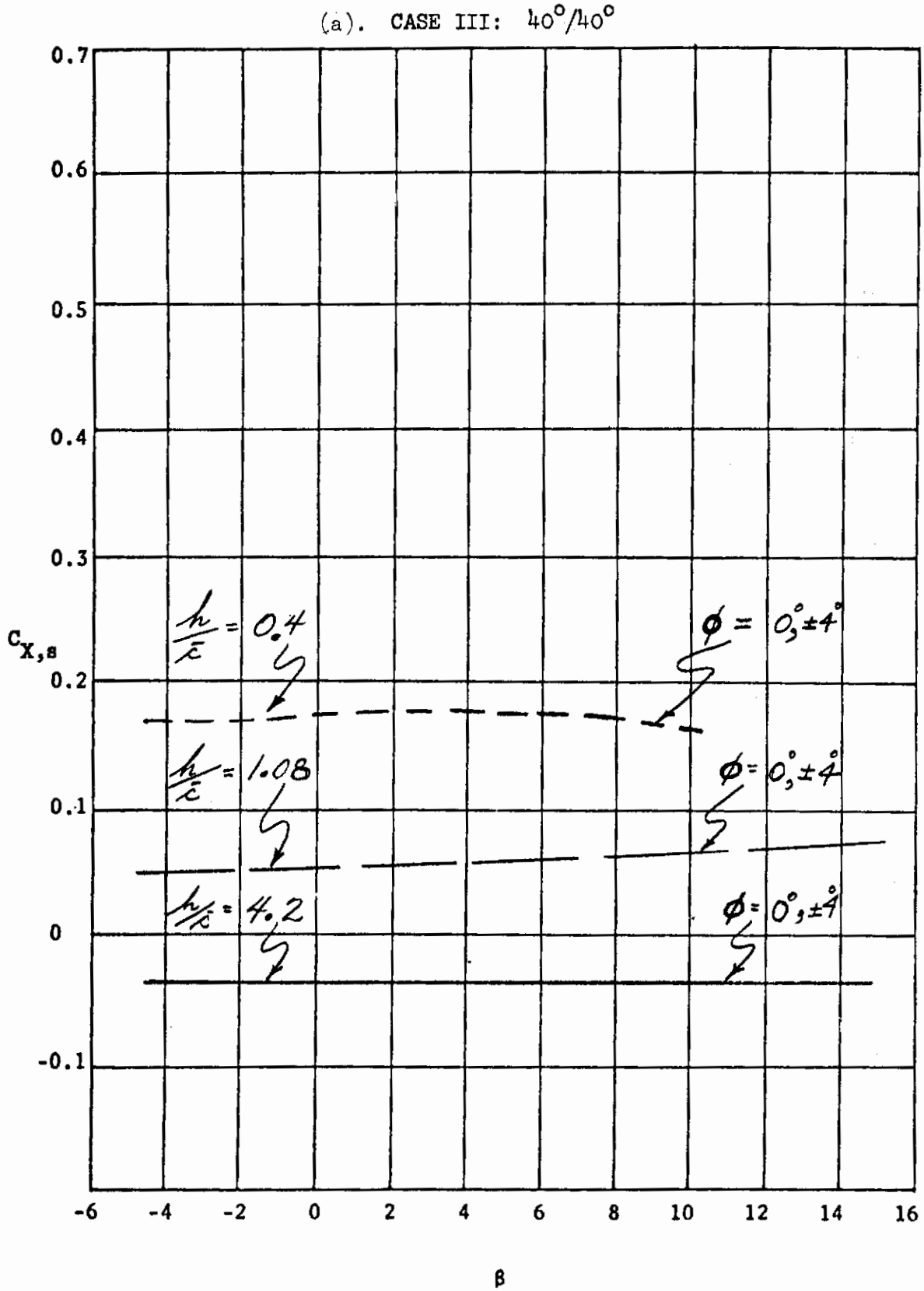

Figure 12. Longitudinal and lateral aerodynamic characteristics versus sideslip angle for various roll angles at three altitude ratios.

Approved for Public Release

Contrails

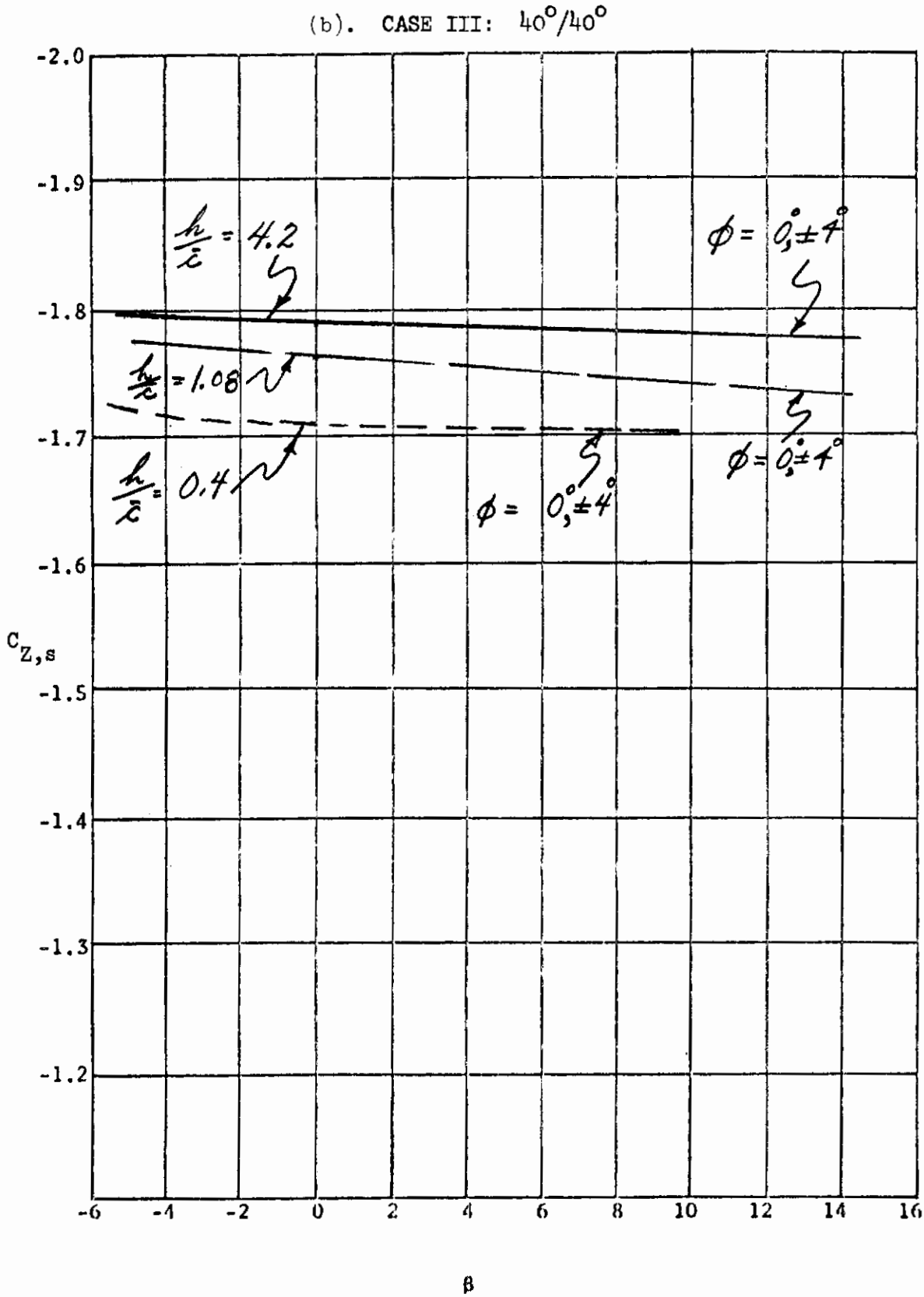

Figure 12. Continued.

Approved for Public Release

Contrails

(c). CASE III: 40°/40°

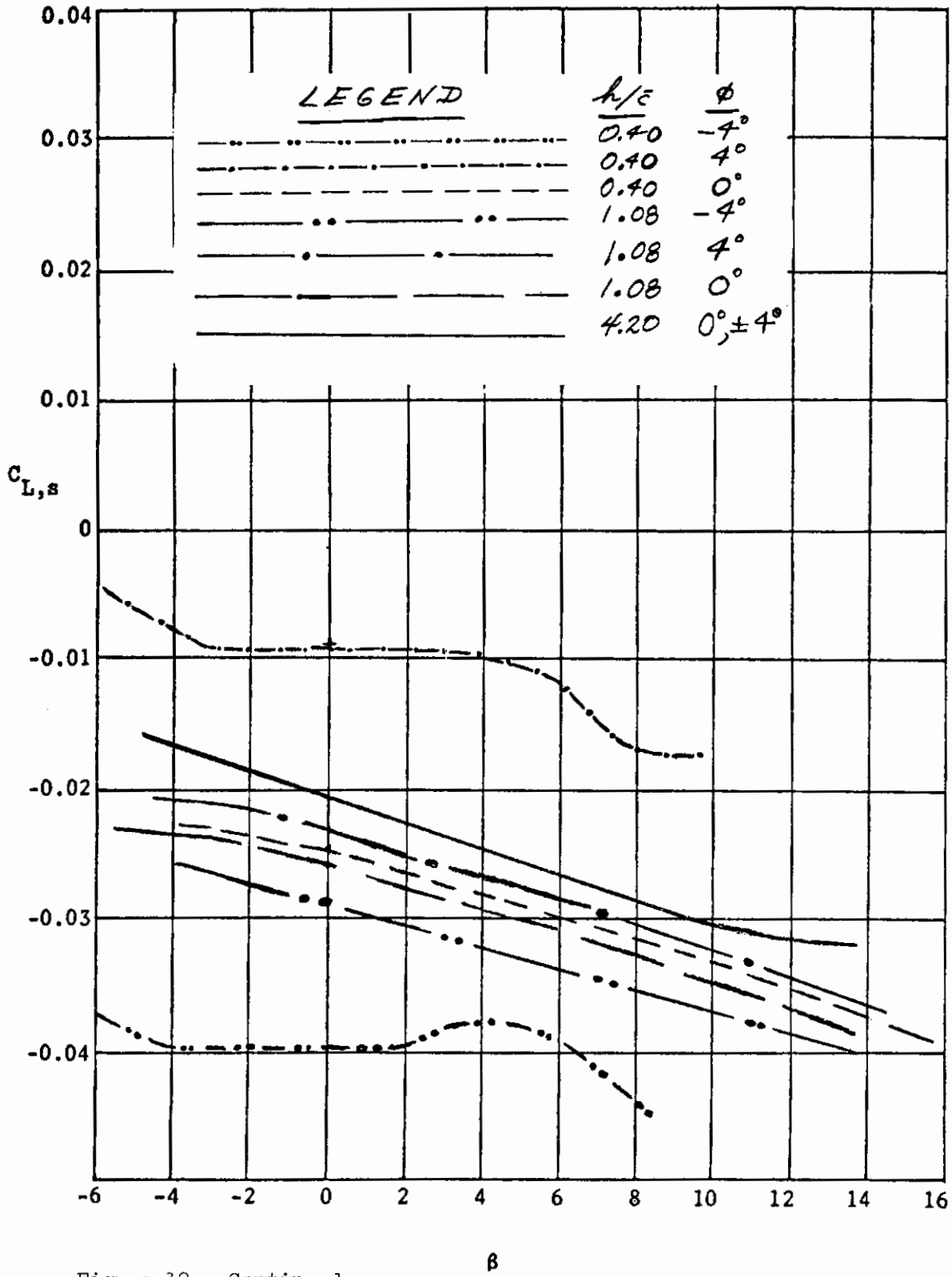

Figure 12. Continued.

Approved for Public Release

Contrails

(d). CASE III: 40°/40°

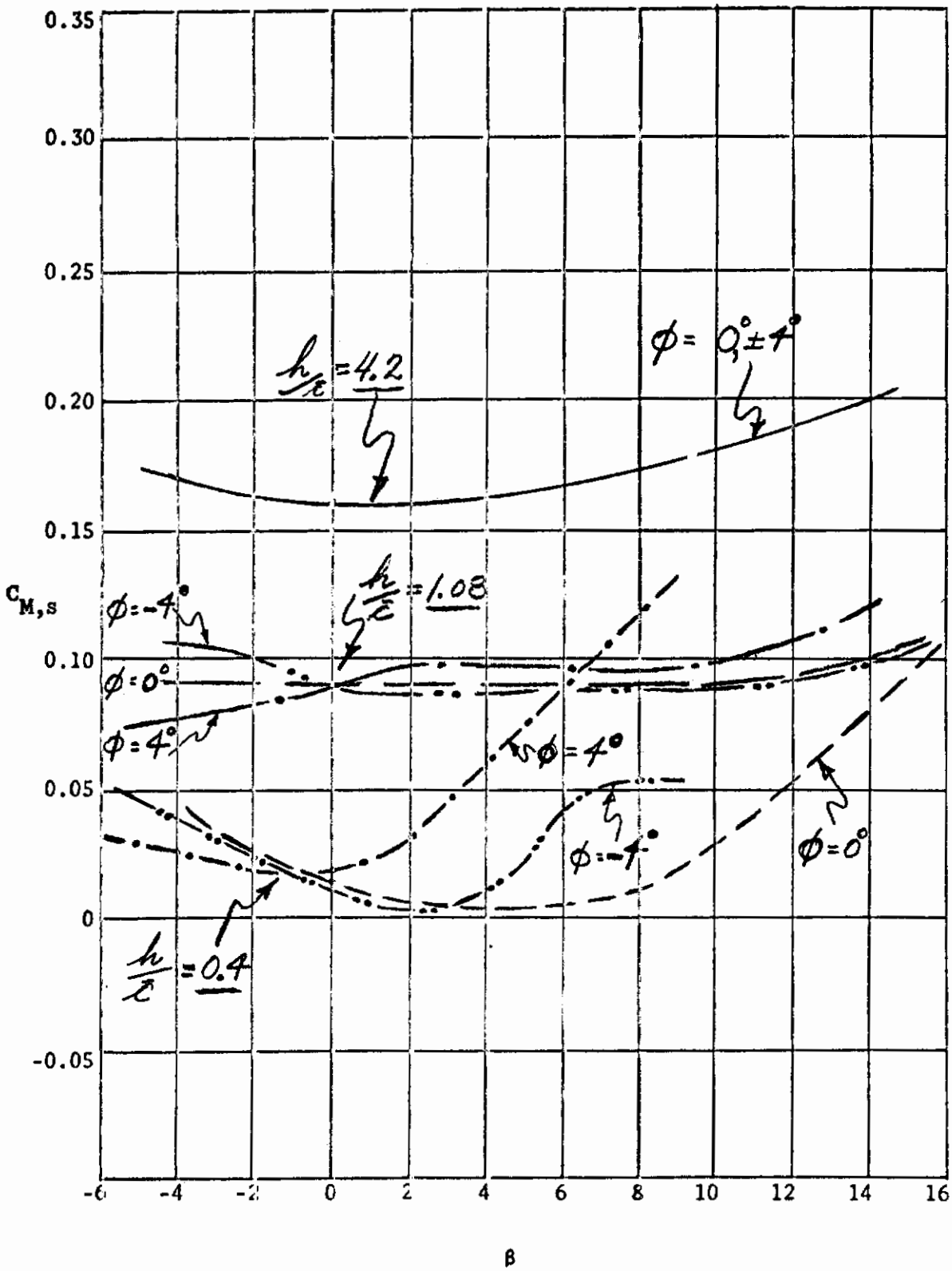

Figure 12. Continued.

Approved for Public Release

Contrails

(e). CASE III: 40°/40°

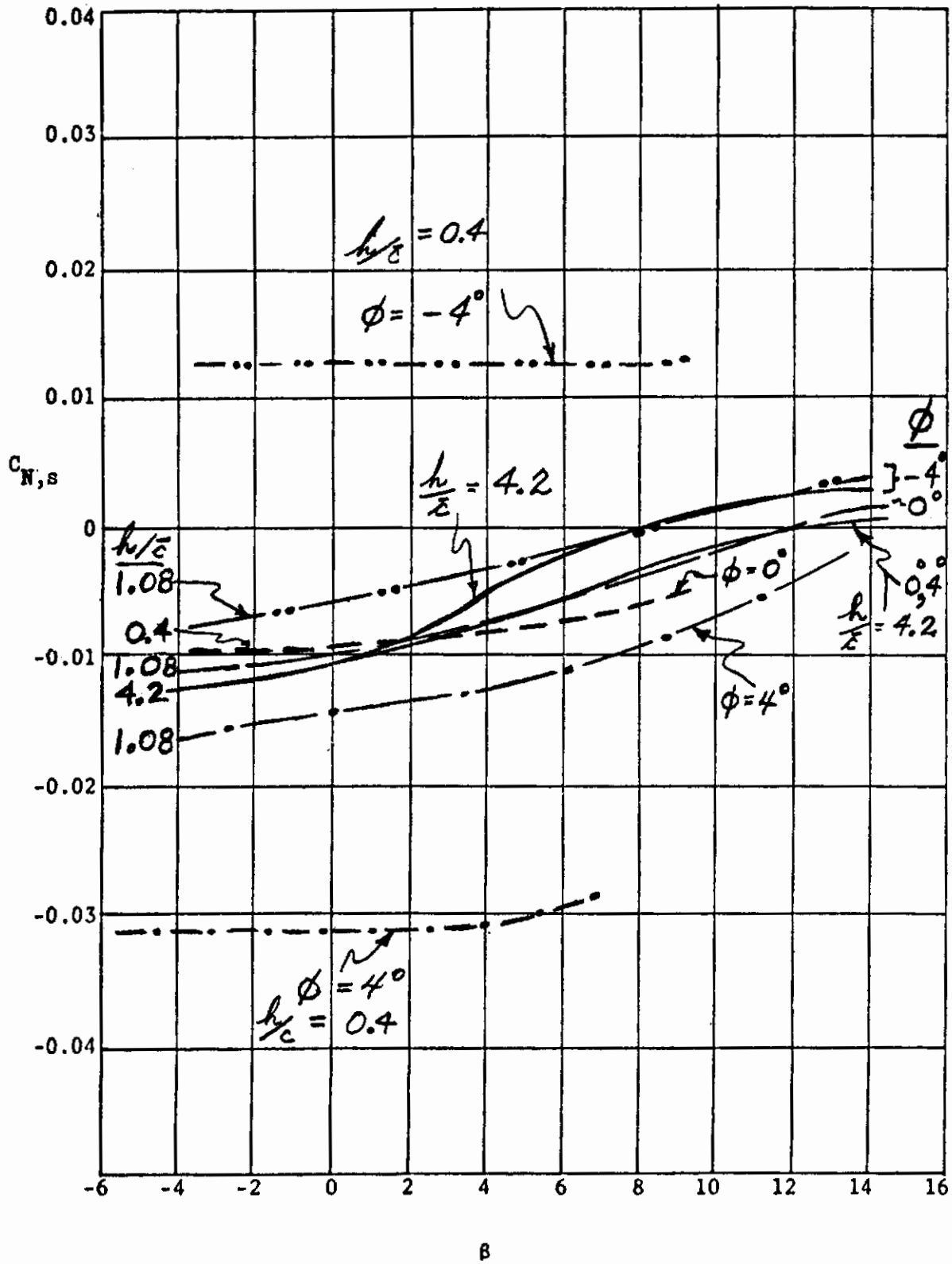

Figure 12. Concluded.

Approved for Public Release

Contrails

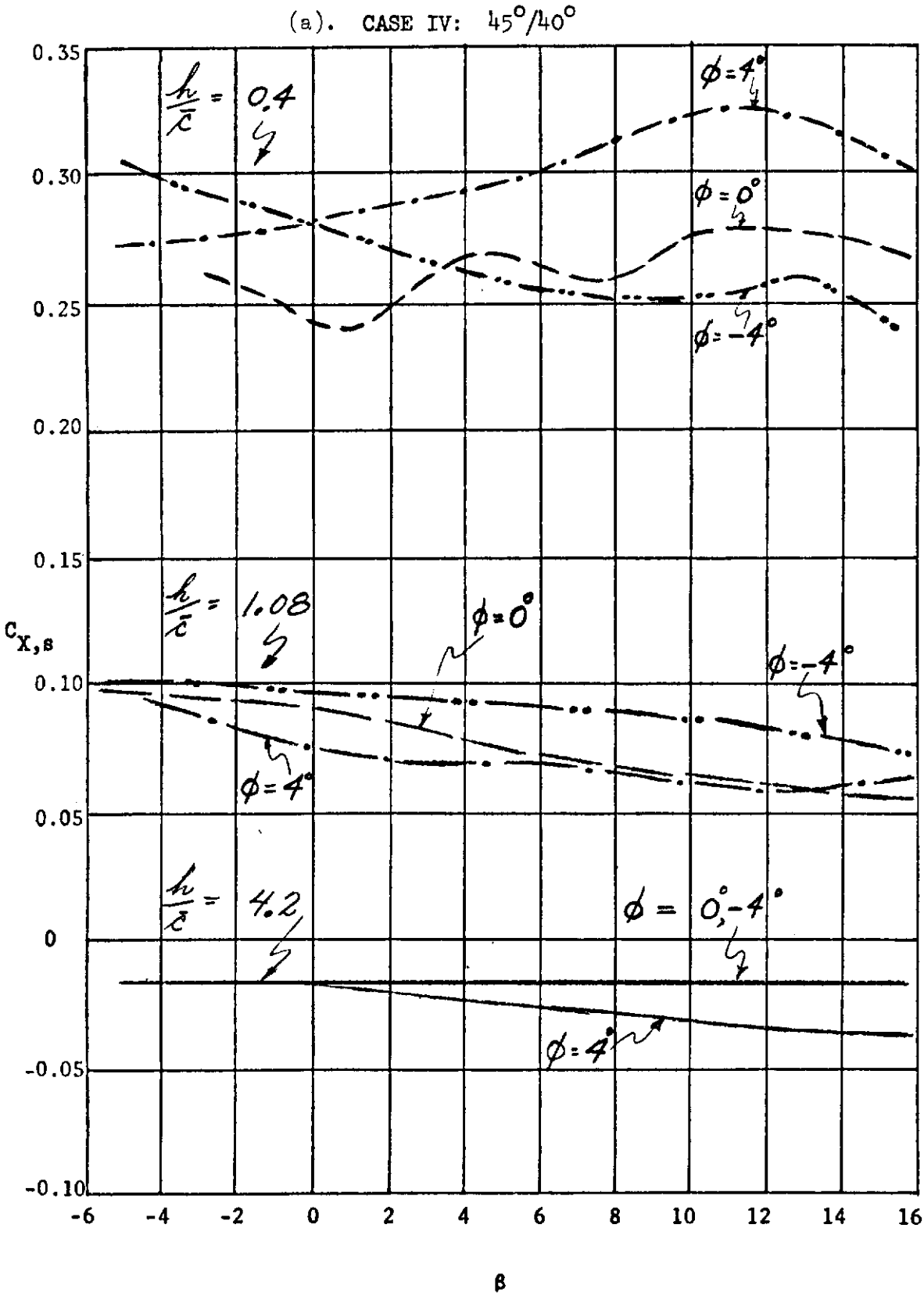

Figure 13. Longitudinal and lateral aerodynamic characteristics versus sideslip angle for various roll angles at three altitude ratios.

Approved for Public Release

Contrails

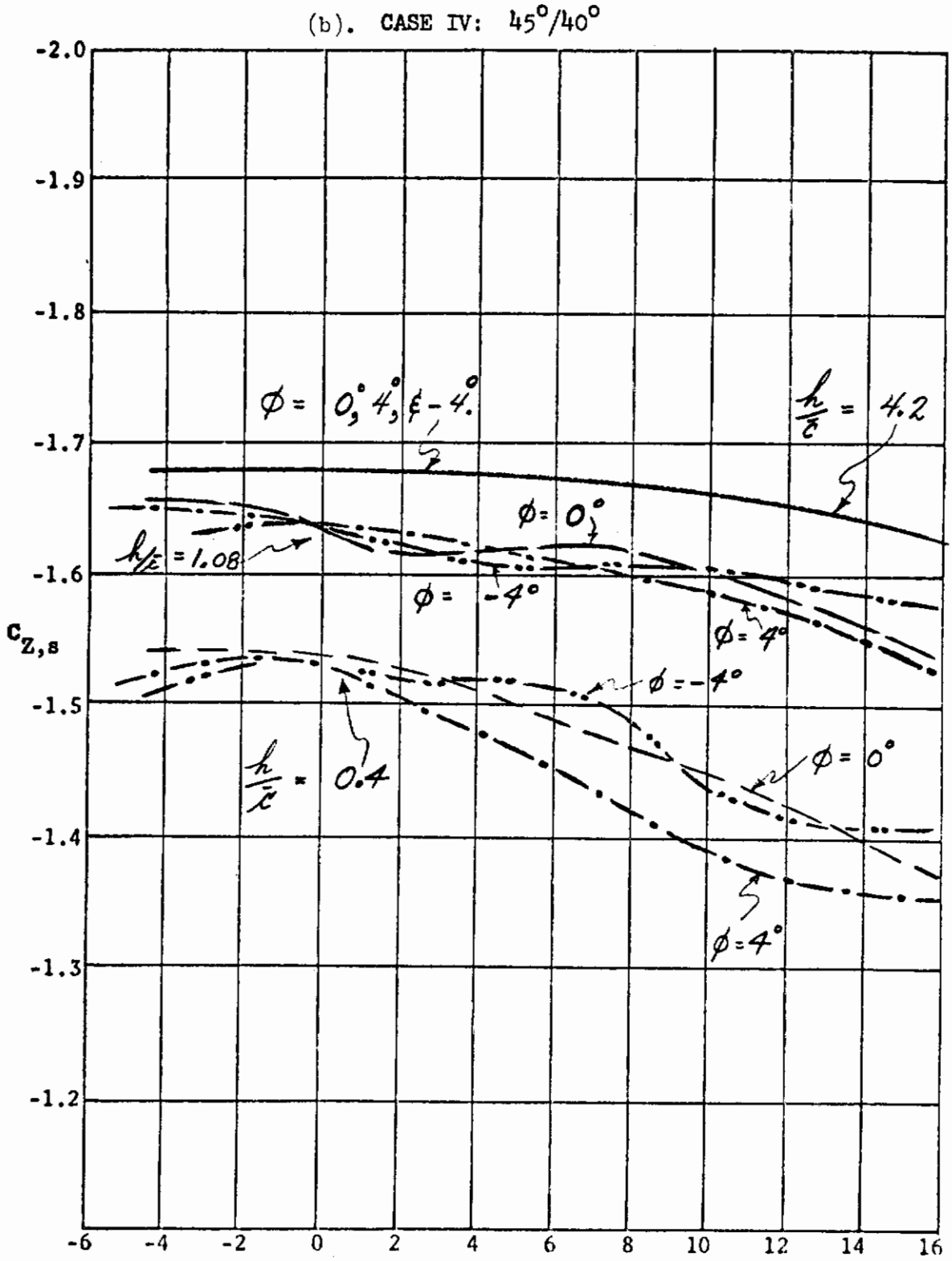

Figure 13. Continued.

Approved for Public Release

Contrails

(c). CASE IV: 45°/40°

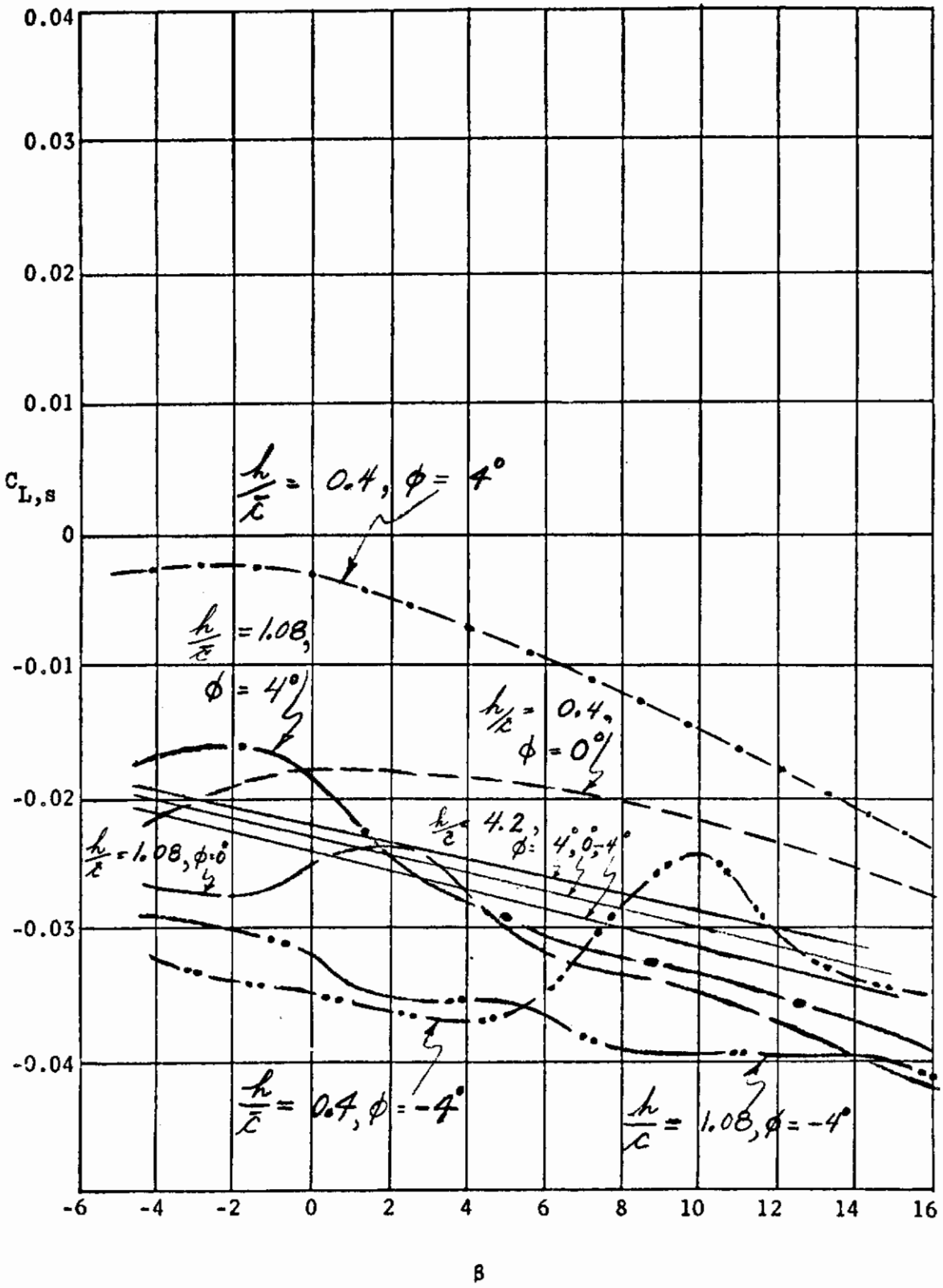

Figure 13. Continued.

Approved for Public Release

Contrails

(d). CASE IV: 45°/40°

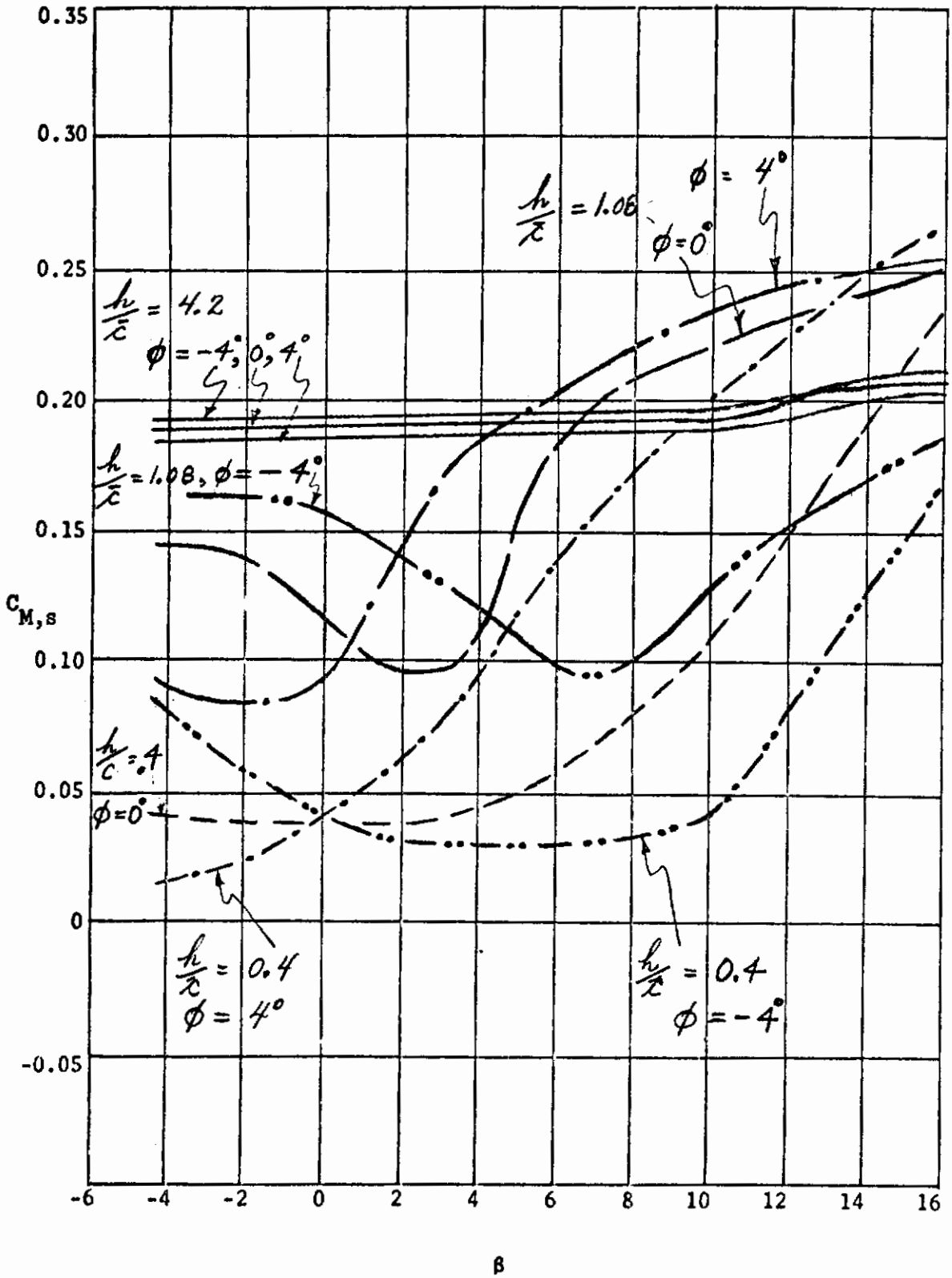

Figure 13. Continued.

Approved for Public Release

Contrails

(e). CASE IV: 45°/40°

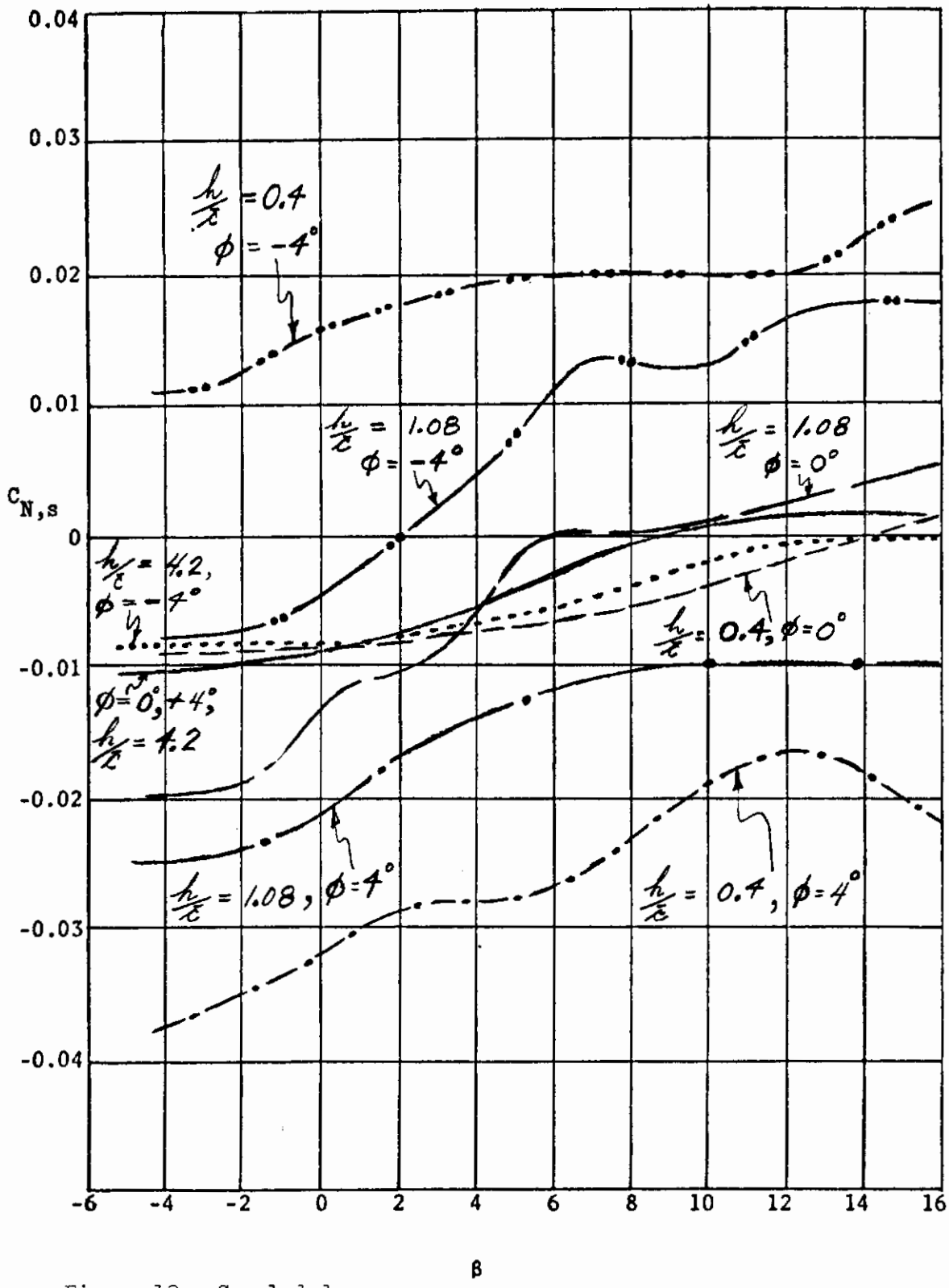

Figure 13. Concluded.

Approved for Public Release

Contrails

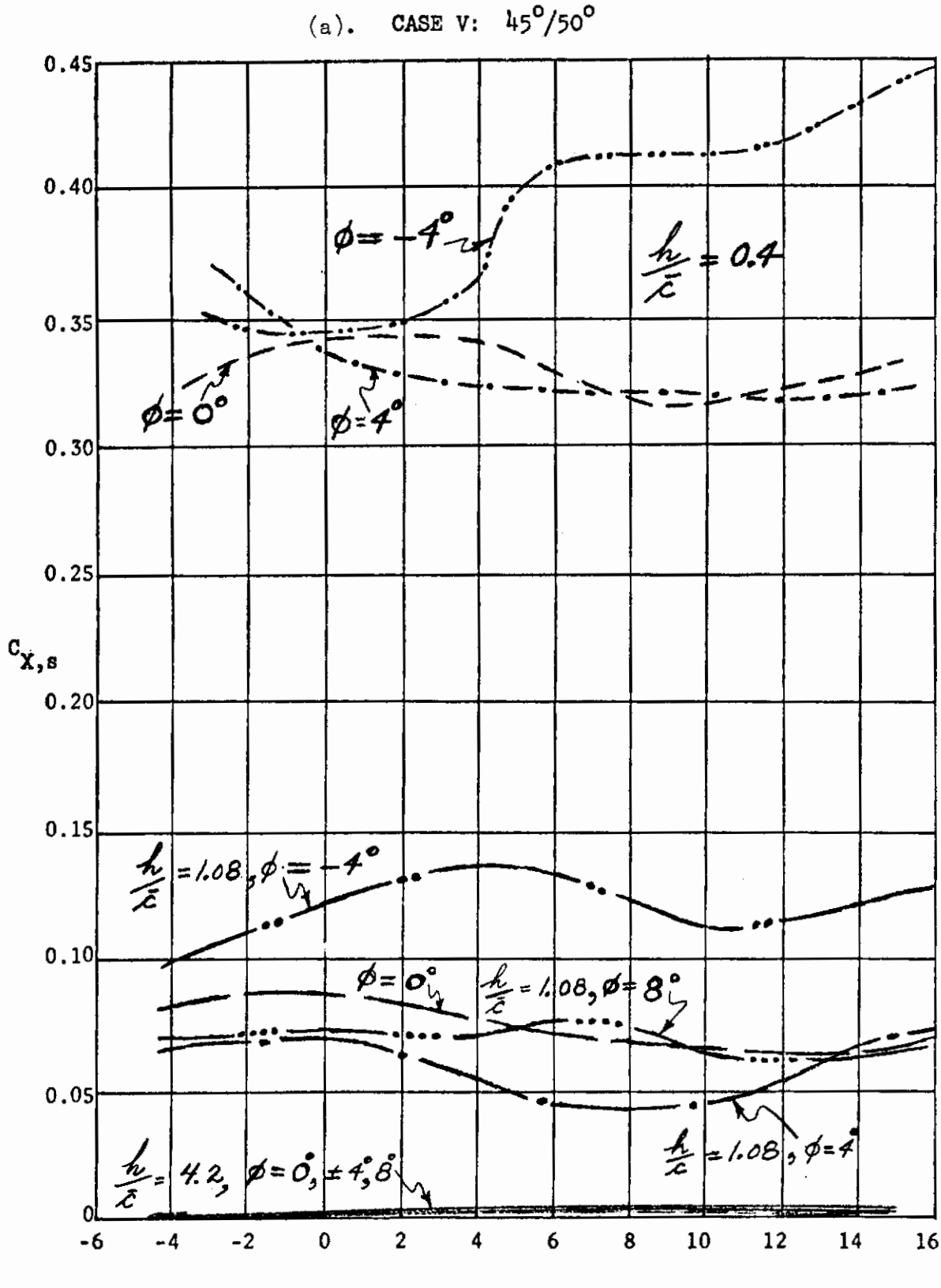

Figure 14. Longitudinal and lateral aerodynamic characteristics versus sideslip angle for various roll angles at three altitude ratios.

Approved for Public Release

Contrails

(b). CASE V: 45°/50°

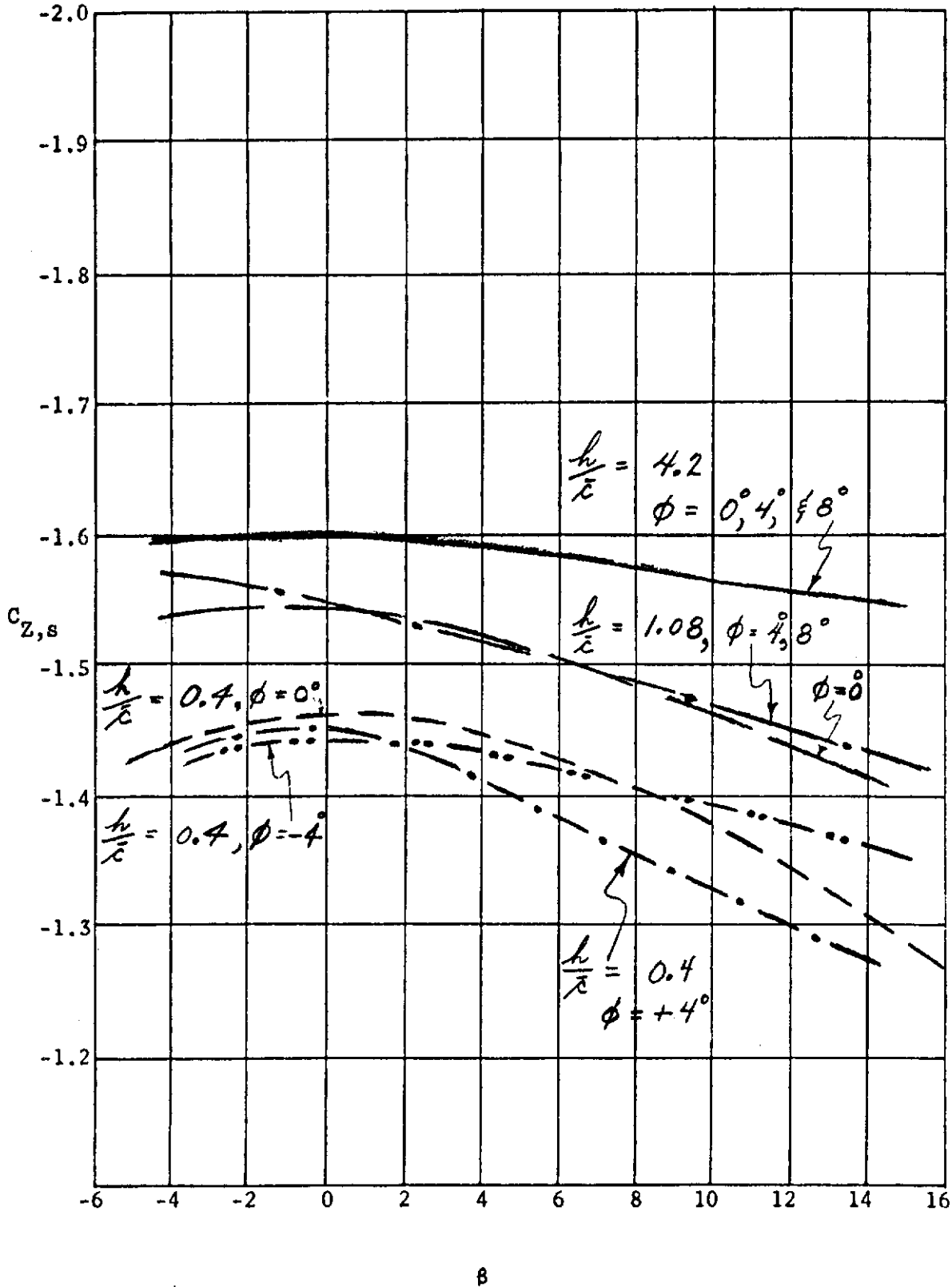

Figure 14. Continued.

Approved for Public Release

Contrails

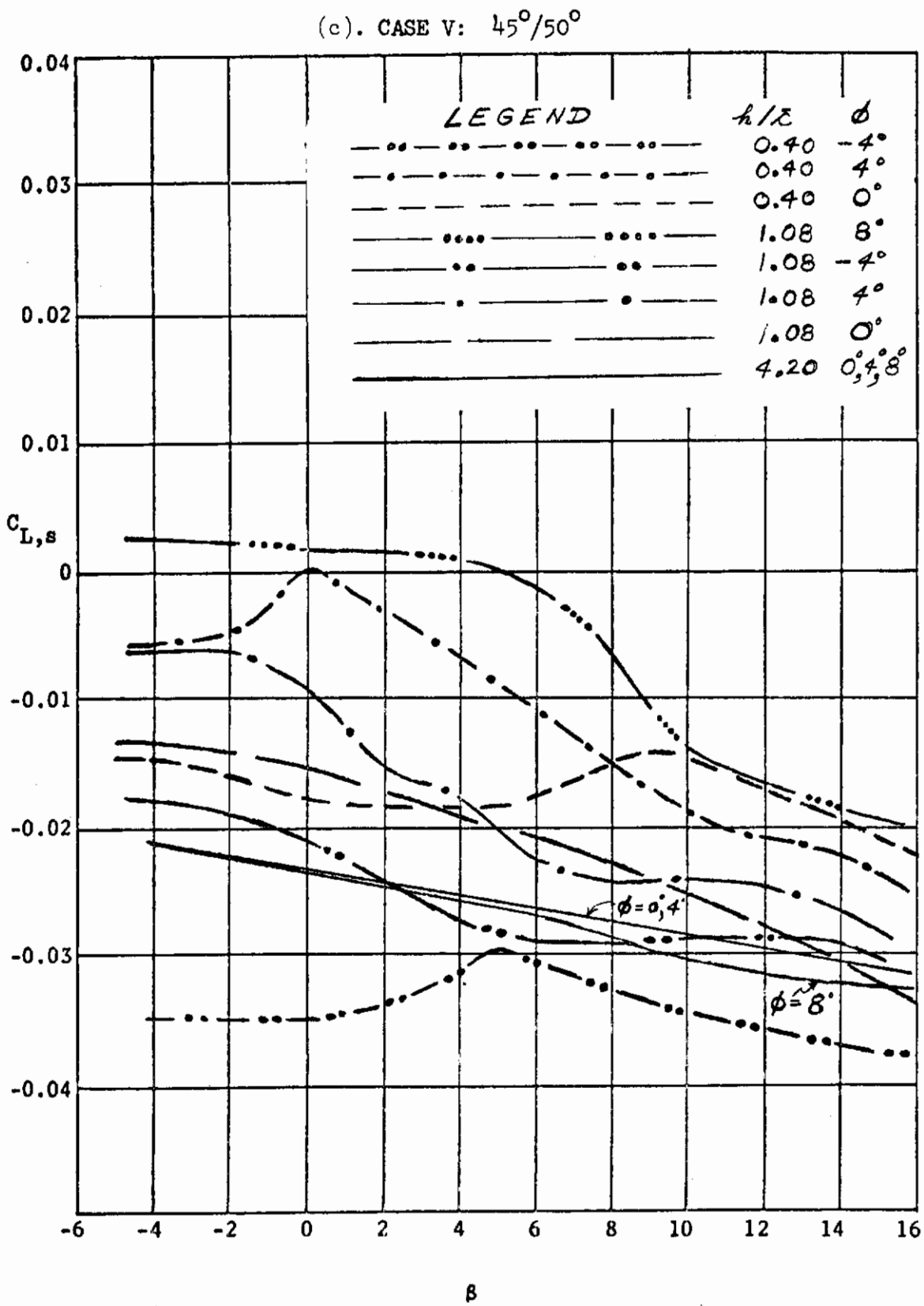

Figure 14. Continued.

Approved for Public Release

Contrails

(d). CASE V: 45°/50°

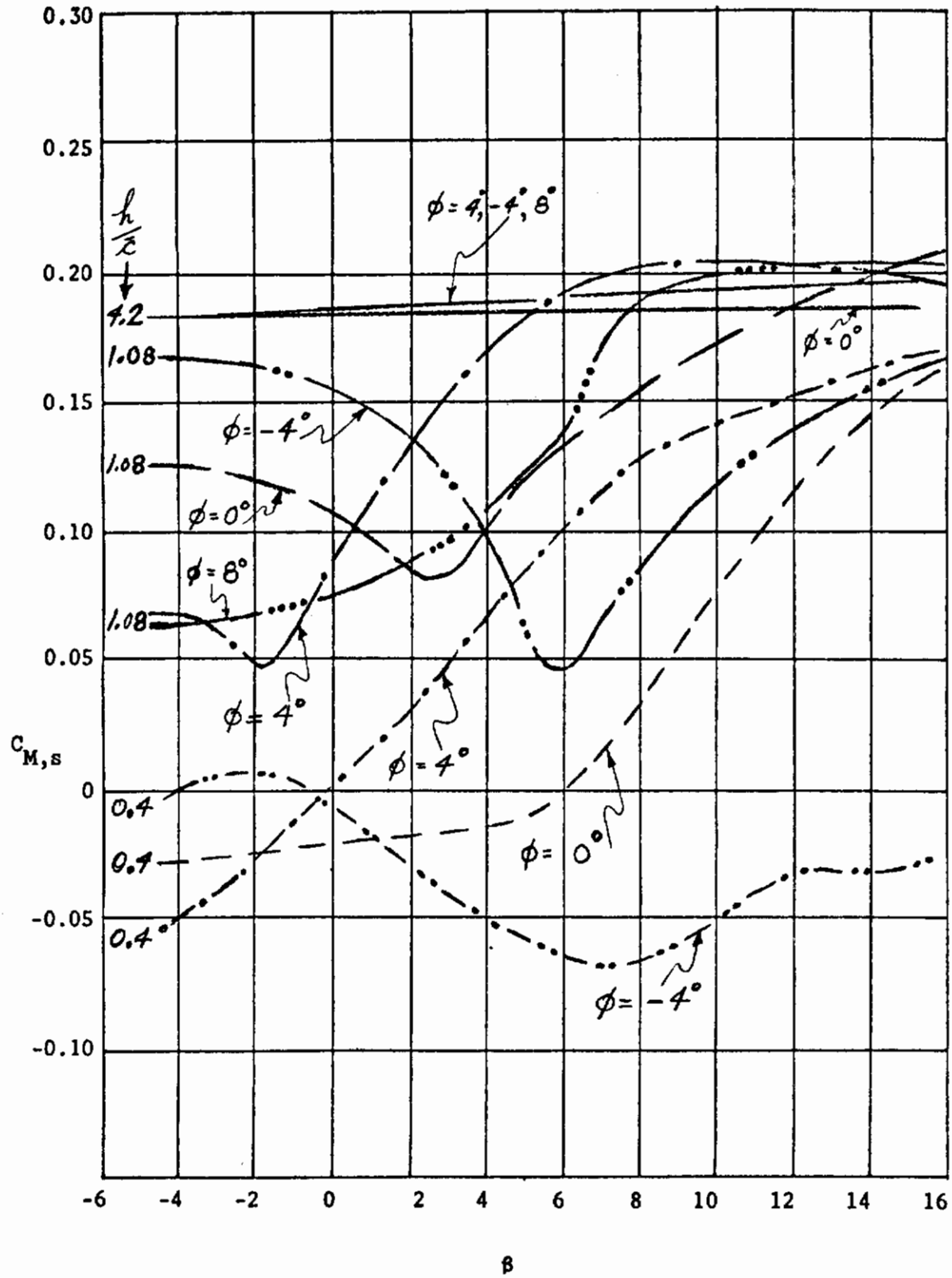

Figure 14. Continued.

Approved for Public Release

Contrails

(e). CASE V: 45°/50°

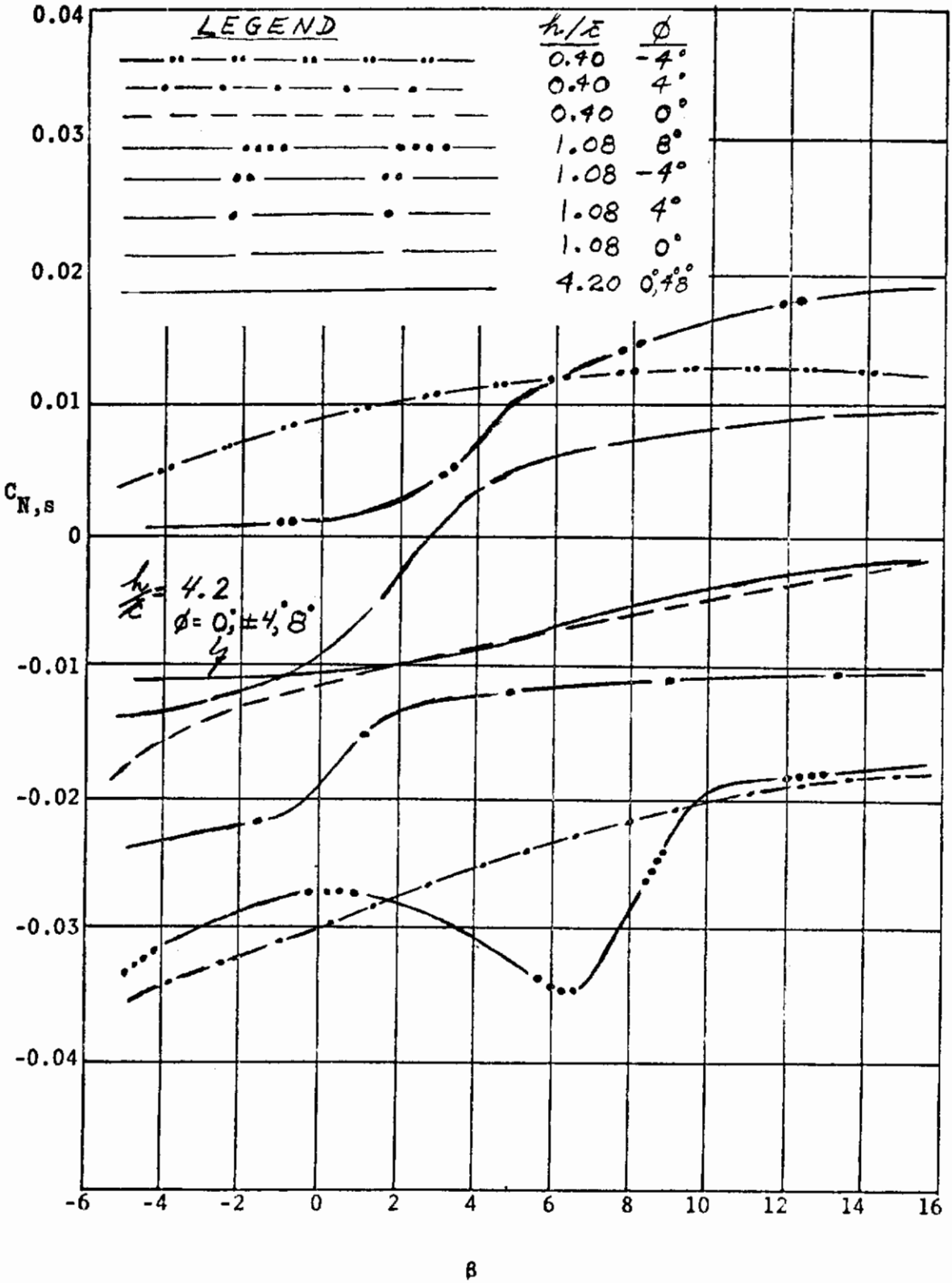

Figure 14. Concluded.

Approved for Public Release

Contrails

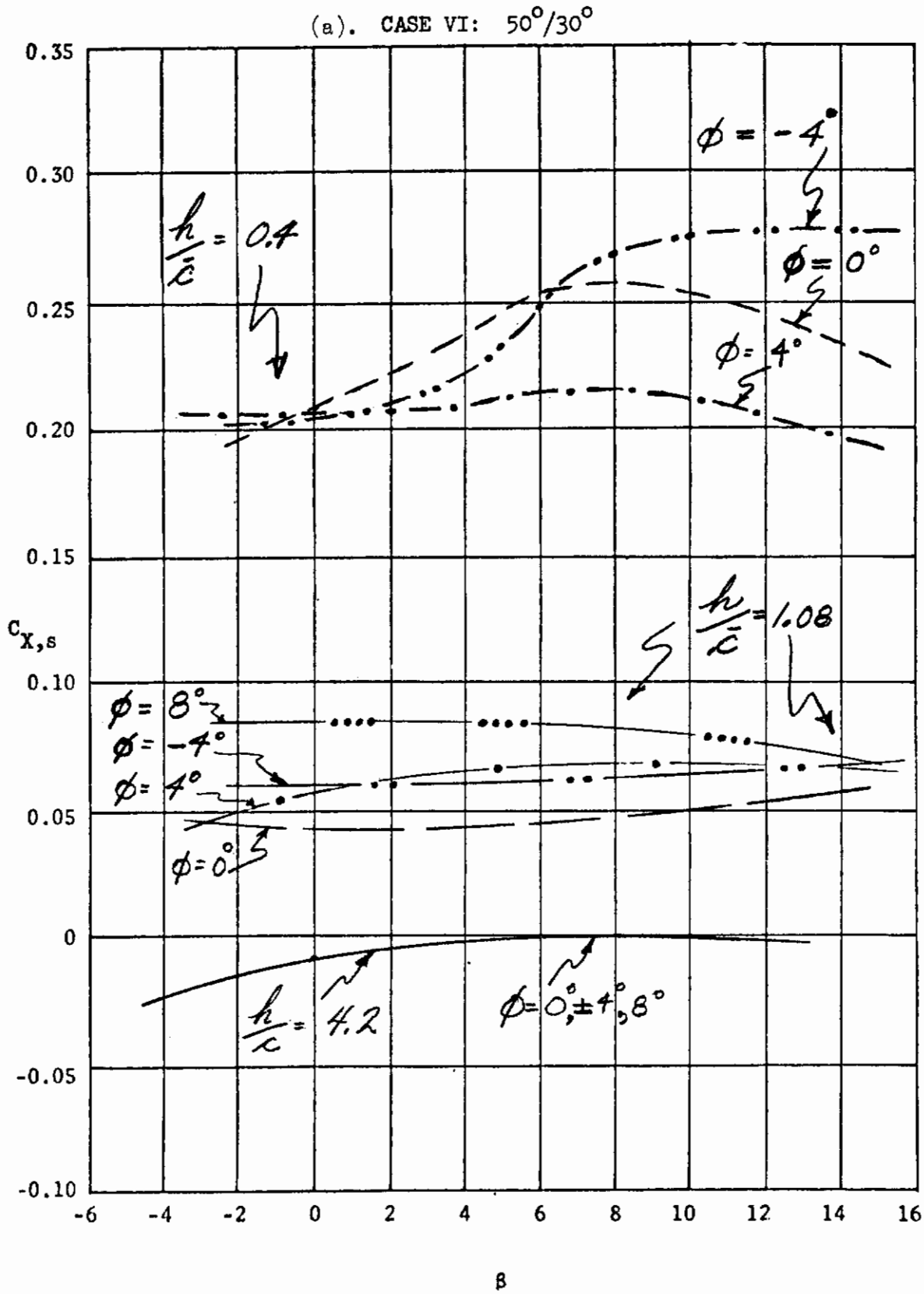

Figure 15. Longitudinal and lateral aerodynamic characteristics versus sideslip angle at various roll angles at three altitude ratios.

Approved for Public Release

Contrails

(b). CASE VI: 50°/30°

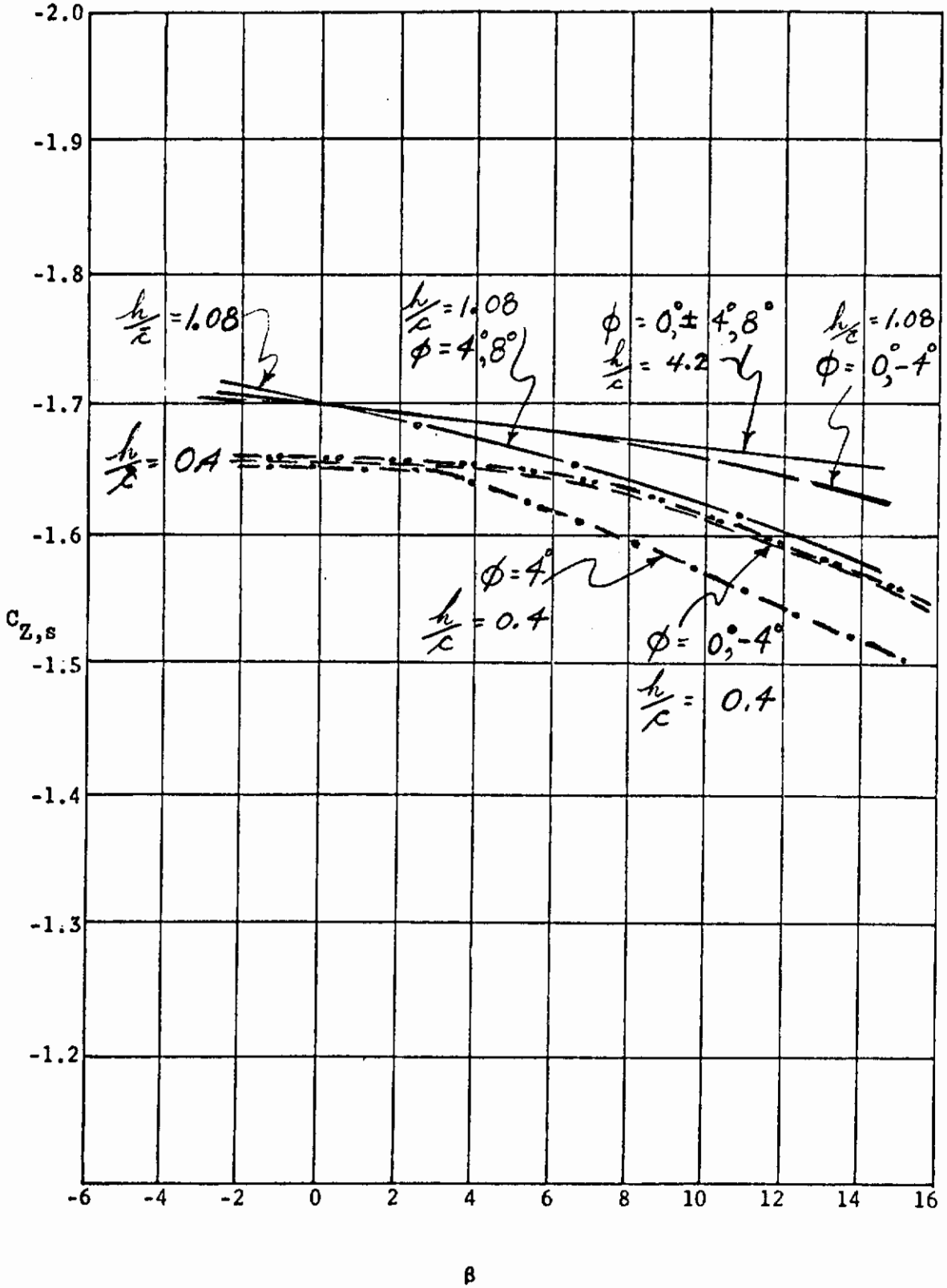

Figure 15. Continued.

Approved for Public Release

Contrails

(c). CASE VI: 50°/30°

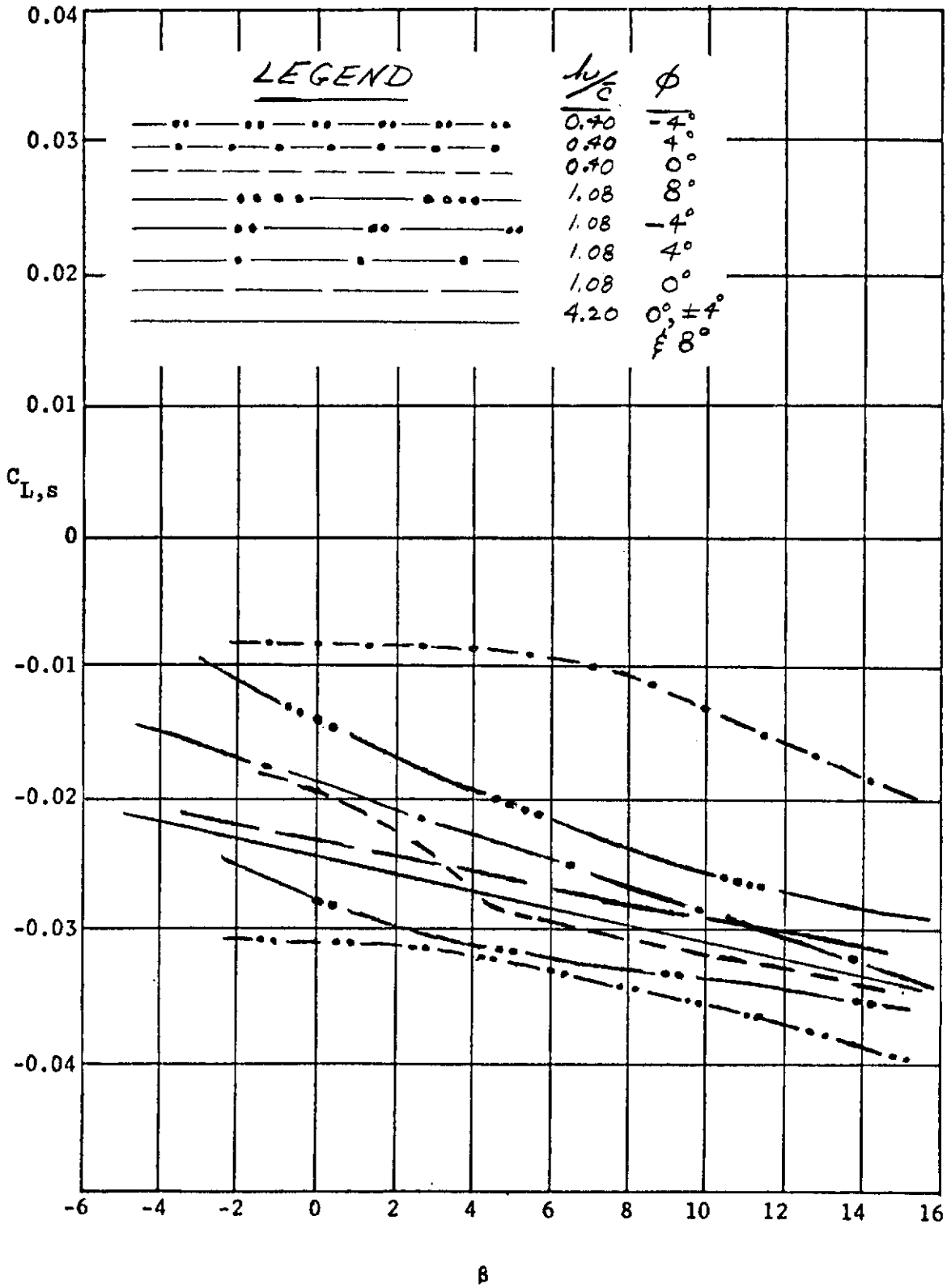

Figure 15. Continued.

Approved for Public Release

Contrails

(d). CASE VI: 50°/30°

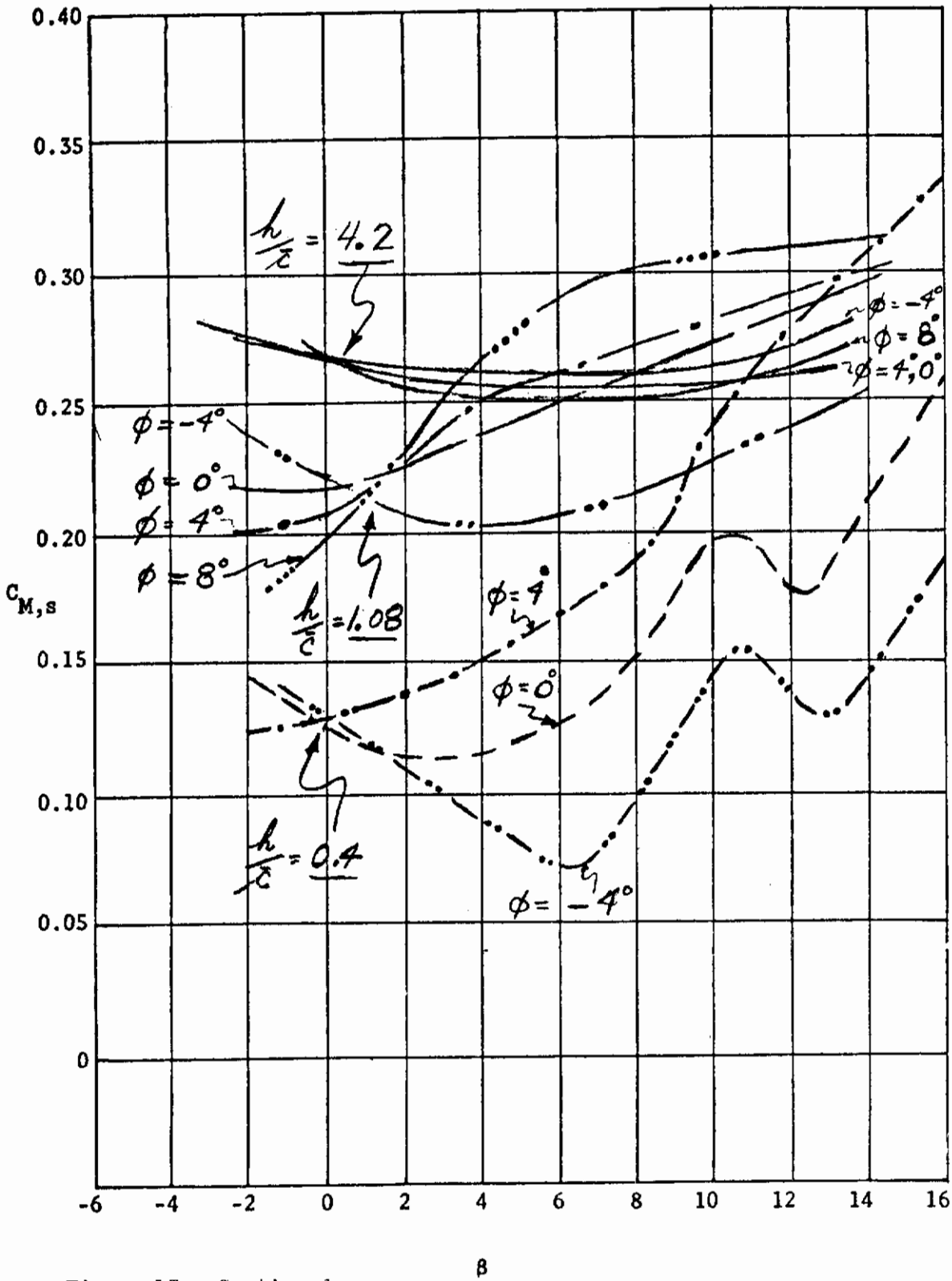

Figure 15. Continued.

Approved for Public Release

Contrails

(e). CASE VI: 50°/30°

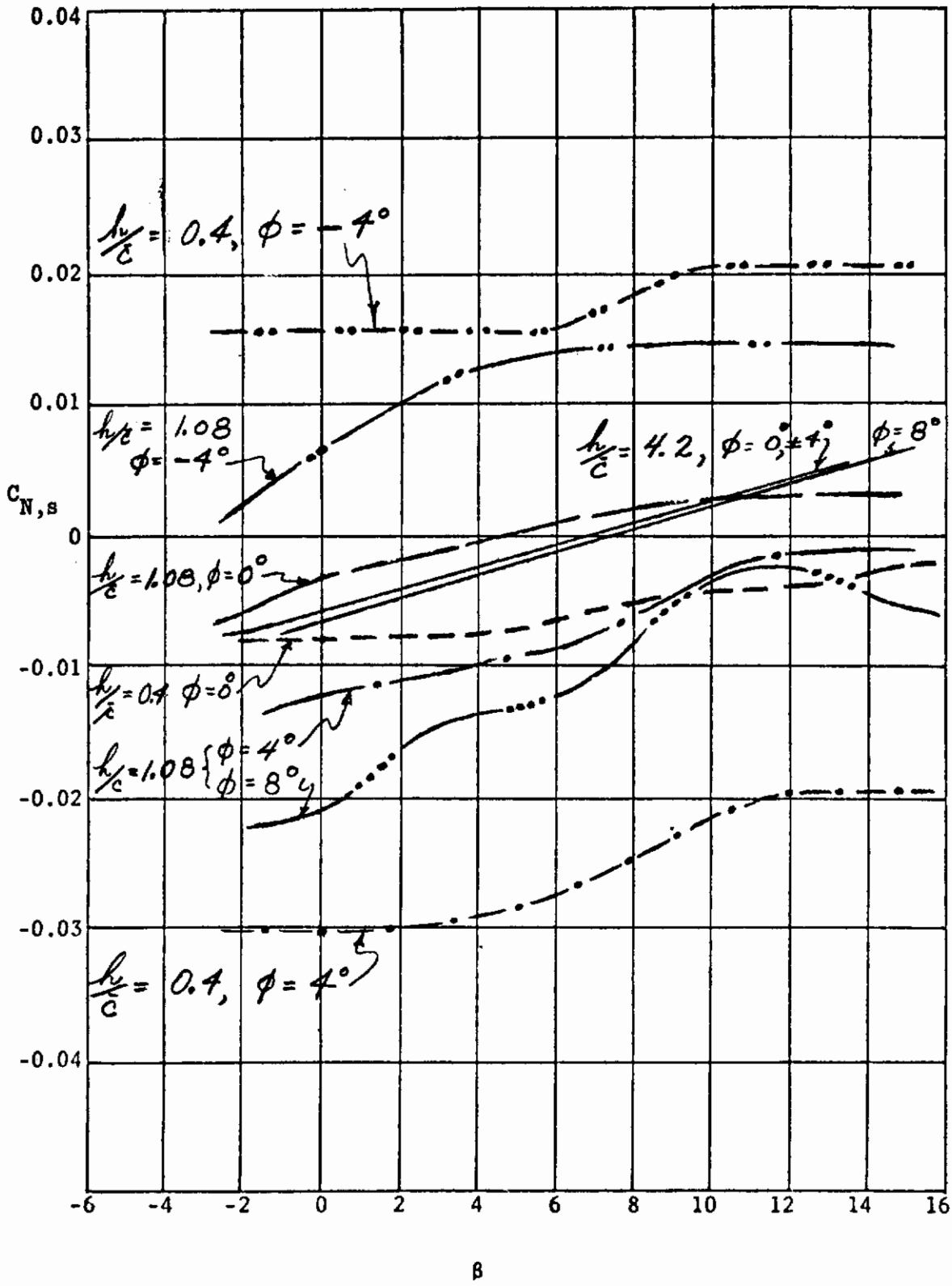

Figure 15. Concluded.

Approved for Public Release

Contrails

(a). CASE VII: 60°/20°

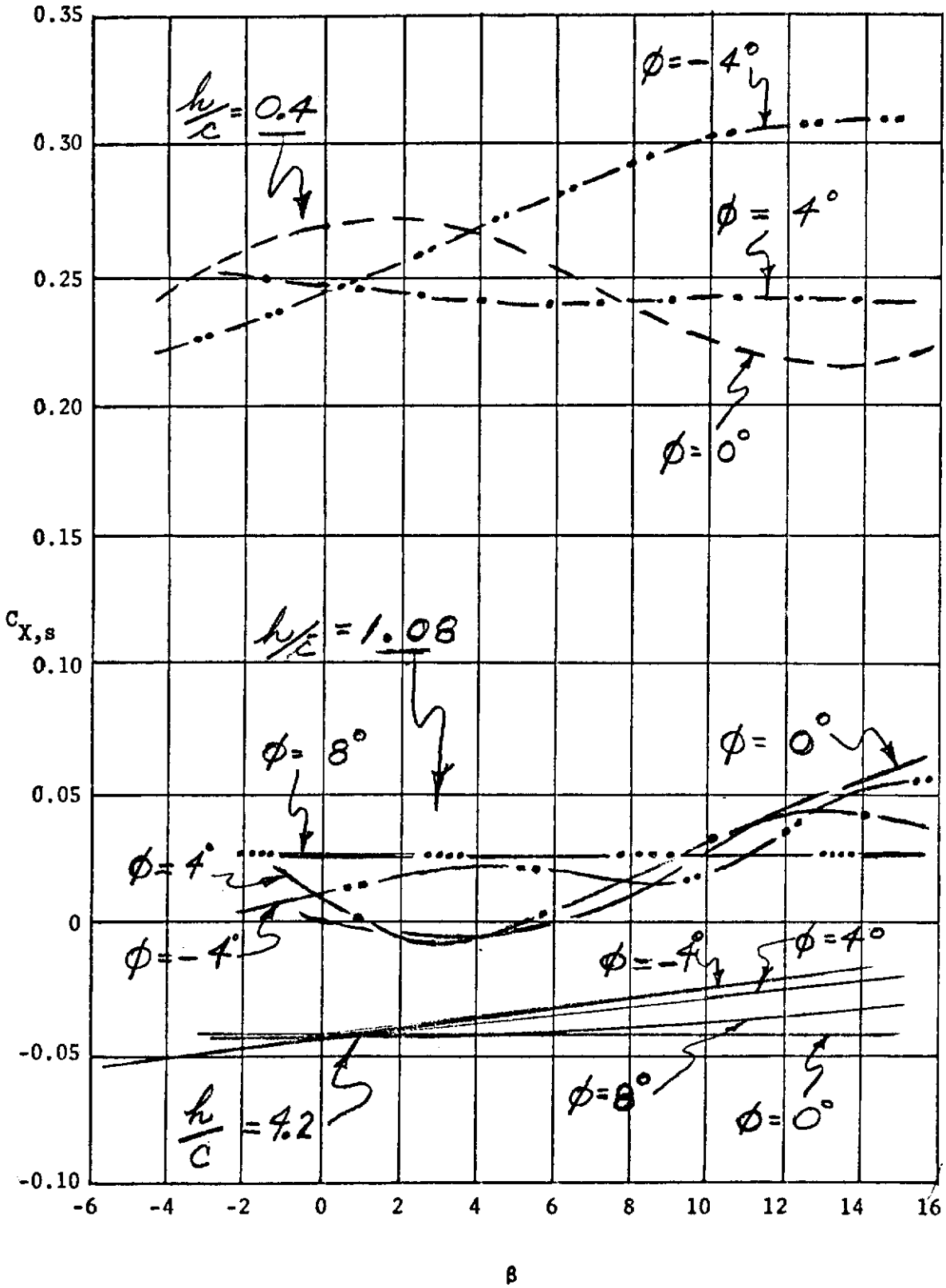

Figure 16. Longitudinal and lateral aerodynamic characteristics versus sideslip angle for various roll angles at three altitude ratios.

Approved for Public Release

Contrails

(b). CASE VII: 60°/20°

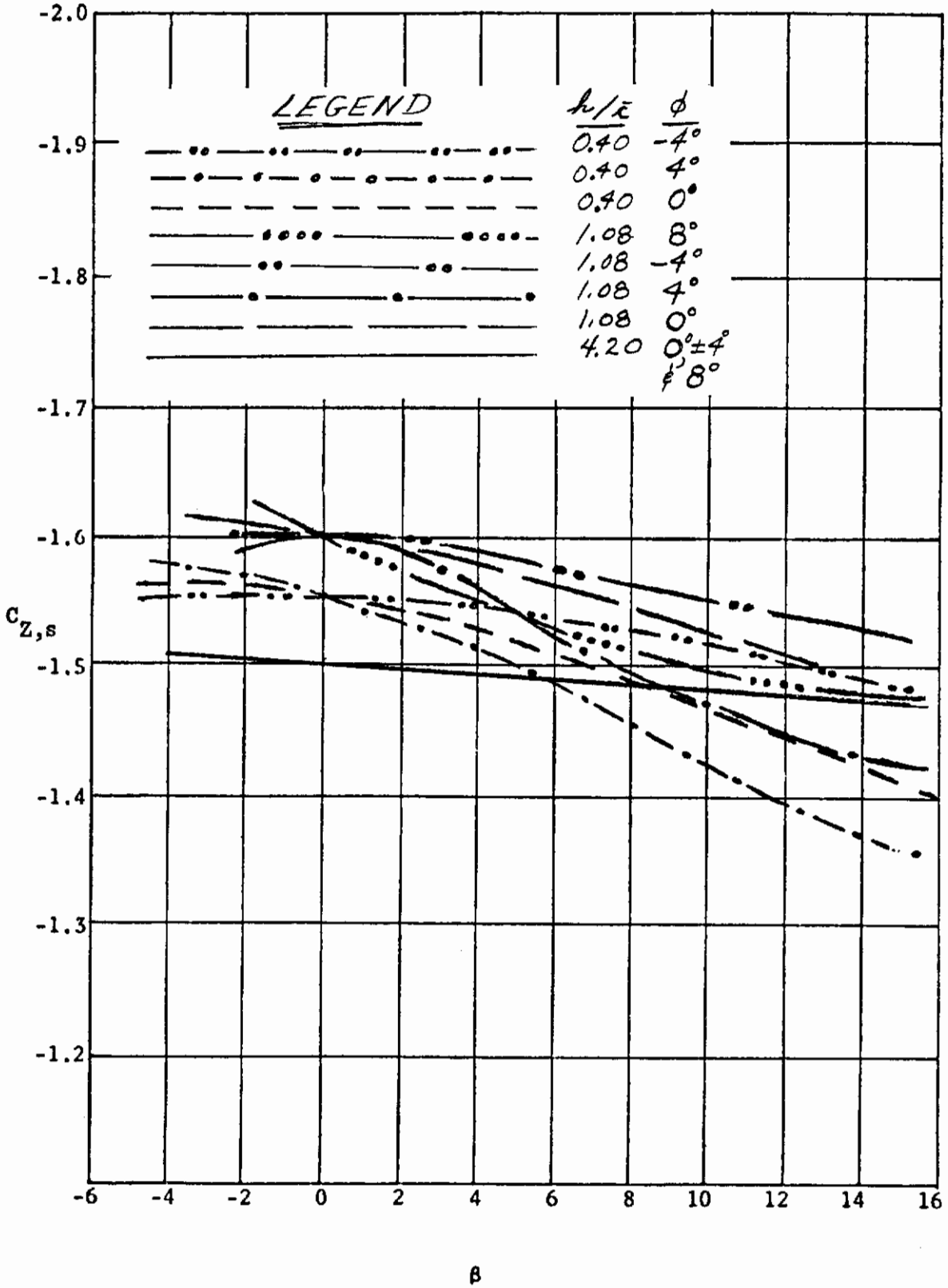

Figure 16. Continued.

Approved for Public Release

Contrails

(c). CASE VII: 60°/20°

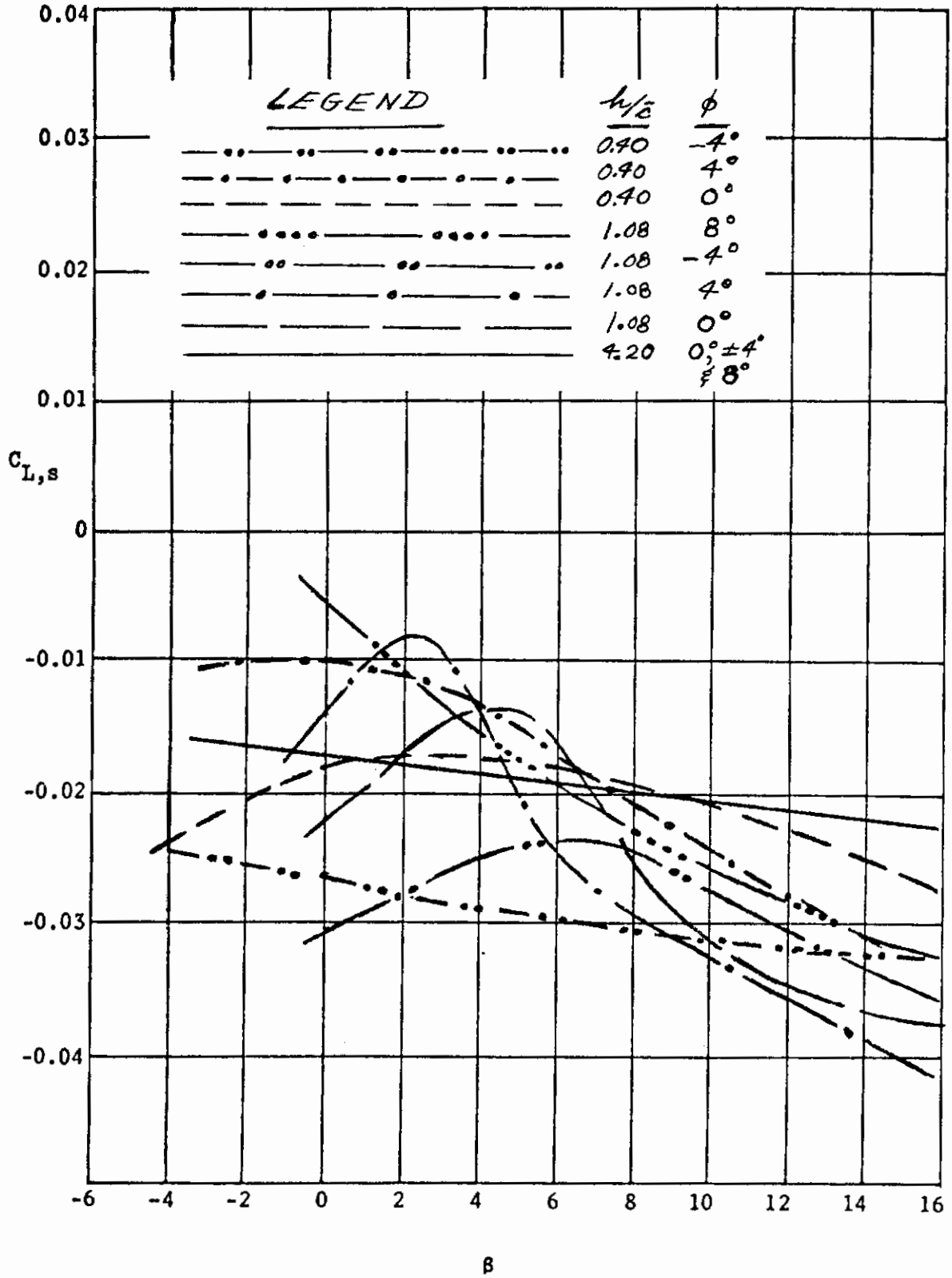

Figure 16. Continued.

Approved for Public Release

Contrails

(d). CASE VII: 60°/20°

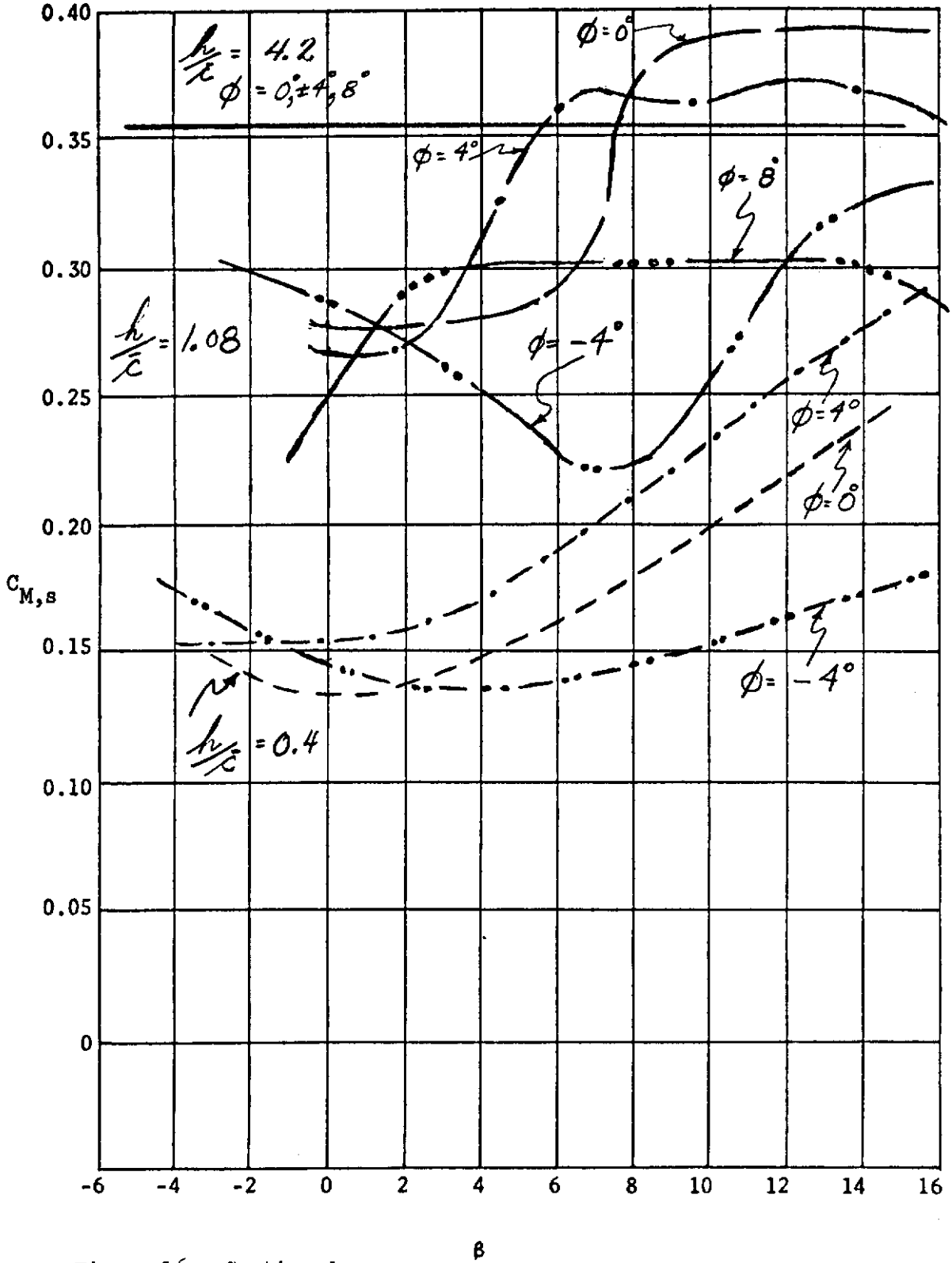

Figure 16. Continued.

Approved for Public Release

Contrails

(e). CASE VII: 60°/20°

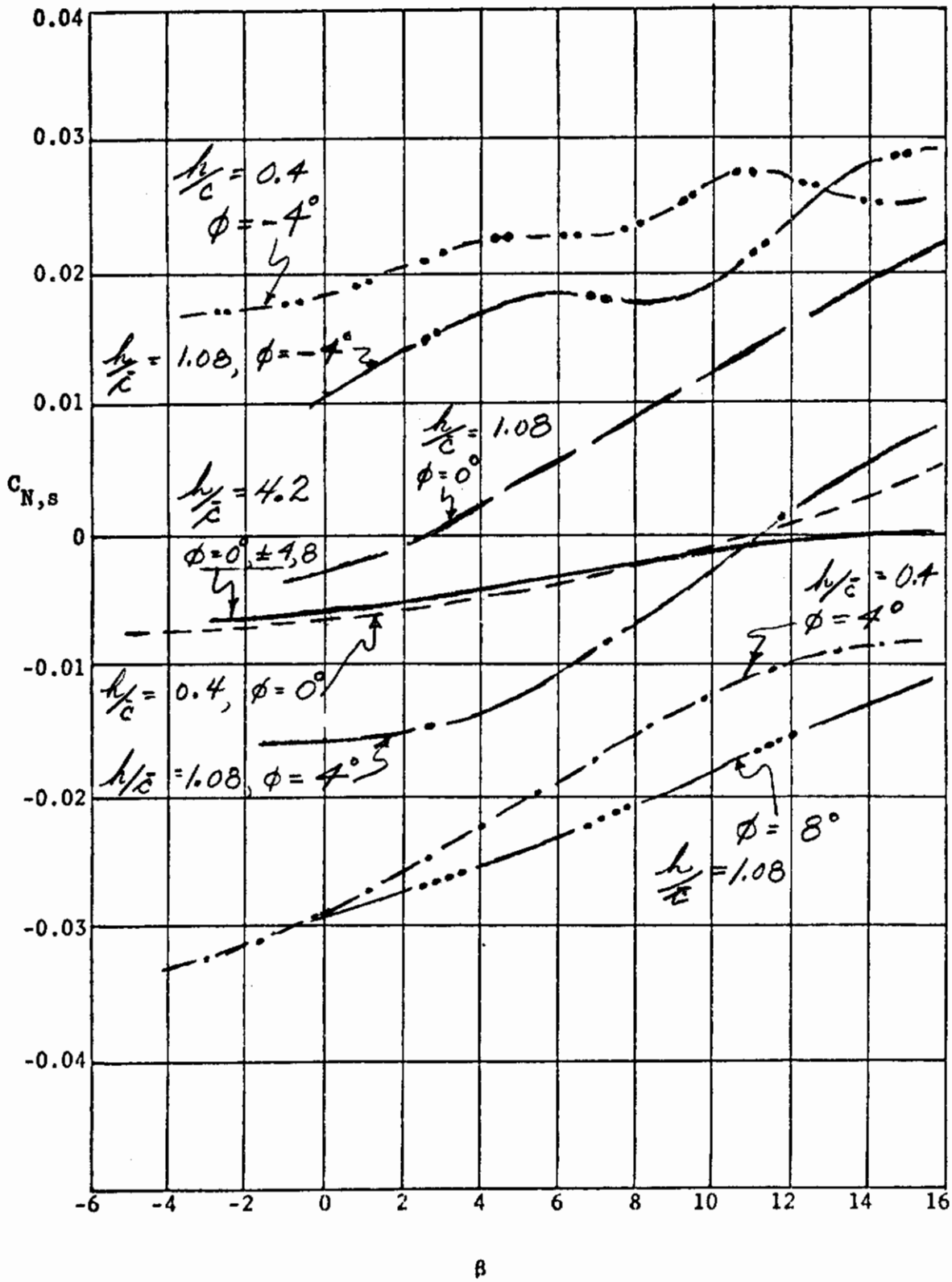

Figure 16. Concluded.

Approved for Public Release

Contrails

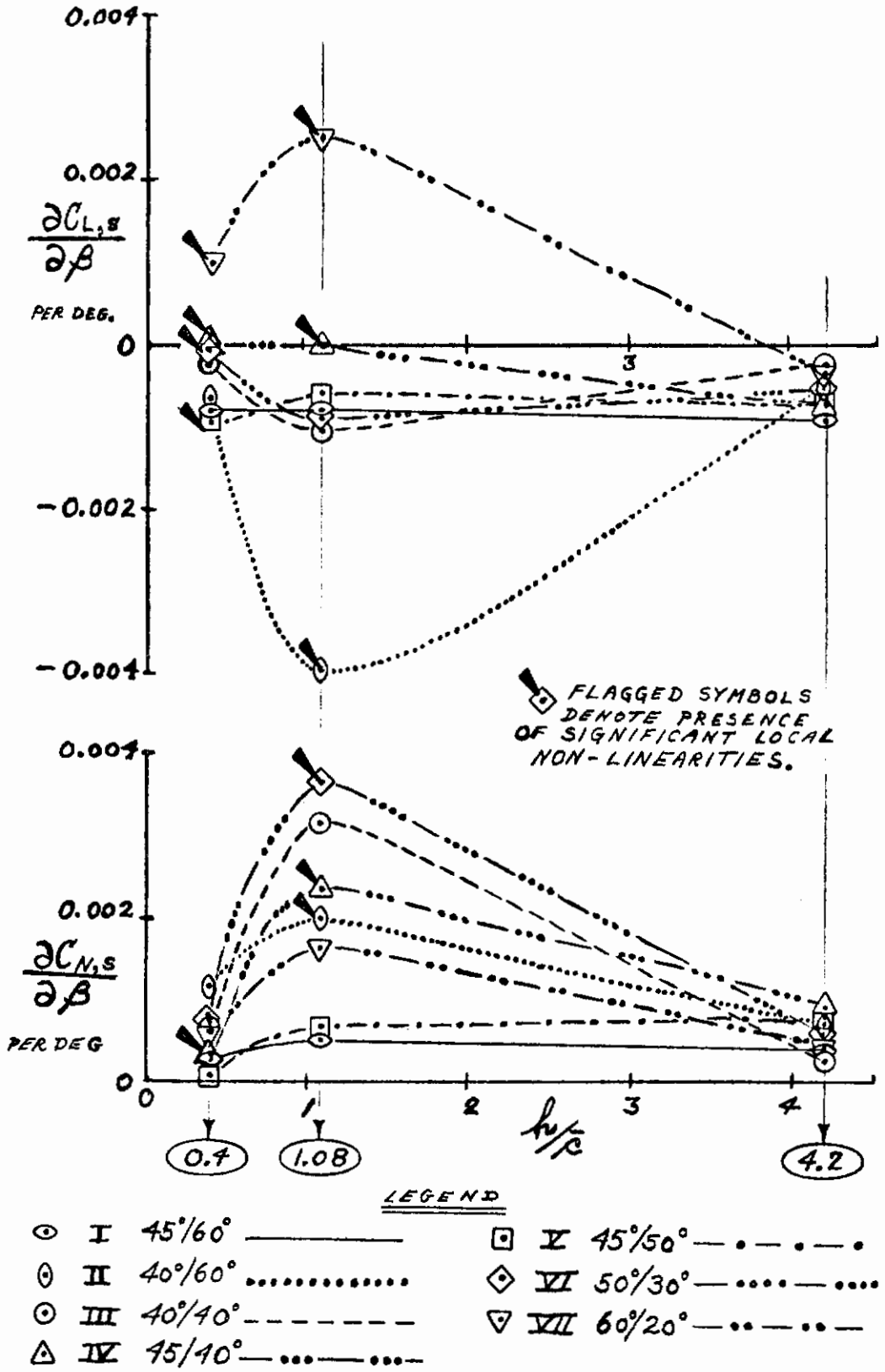

Figure 17. Dihedral effect and directional stability derivatives versus altitude ratio.

Approved for Public Release

Contrails

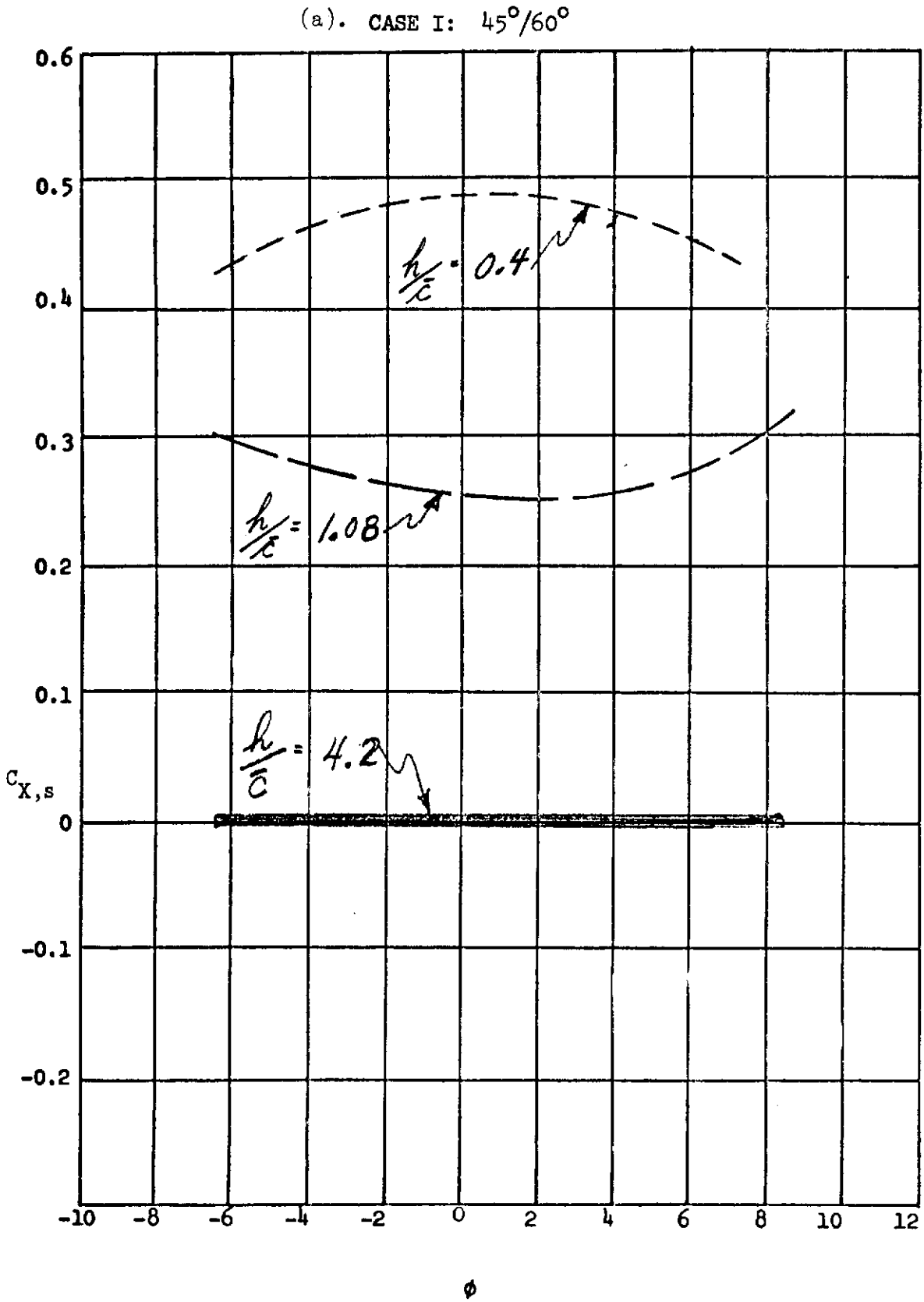

Figure 18. Longitudinal and lateral aerodynamic characteristics versus roll angle at three altitude ratios

Approved for Public Release

Contrails

(b). CASE I: 45°/60°

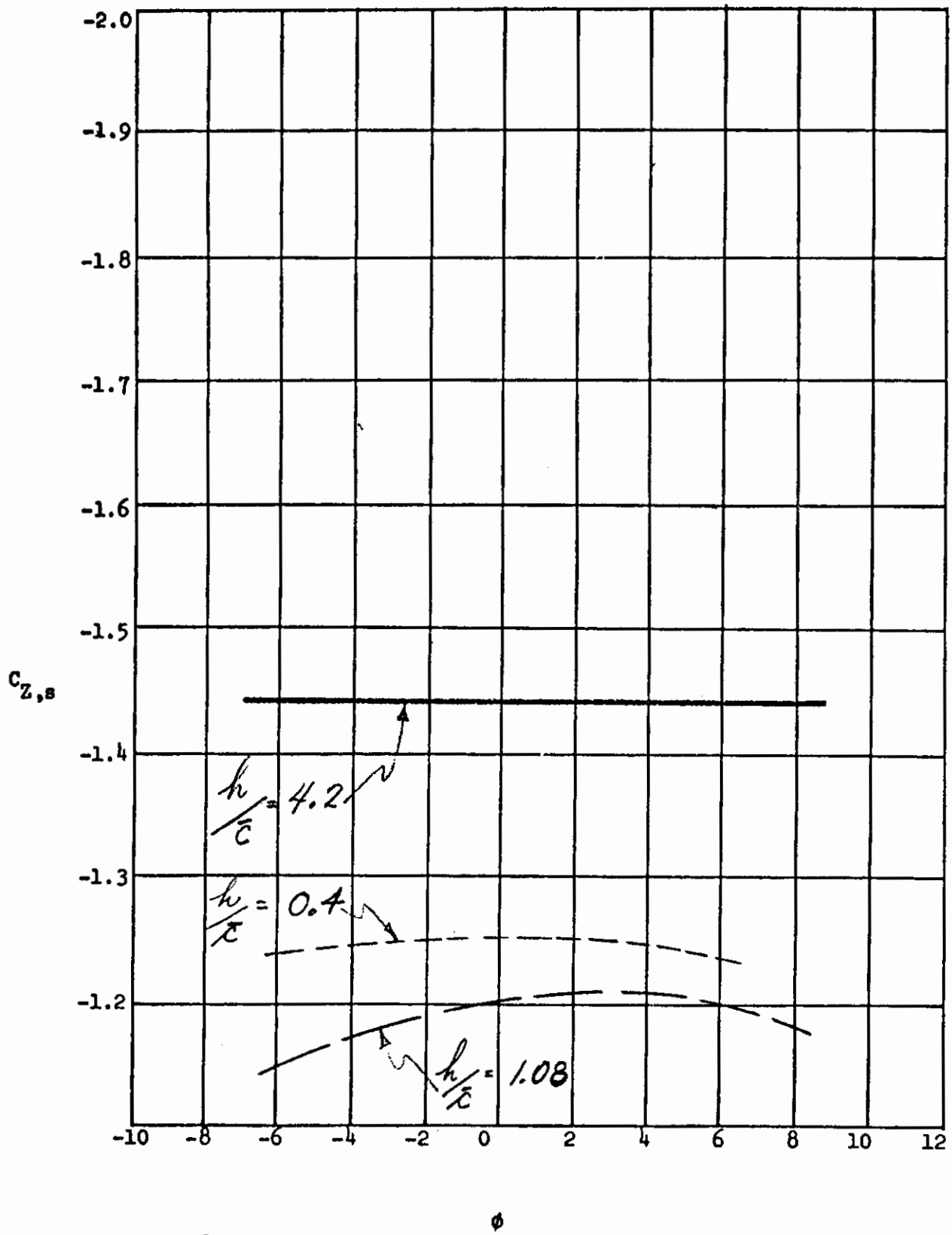

Figure 18. Continued.

Approved for Public Release

Contrails

(c). CASE I: 45°/60°

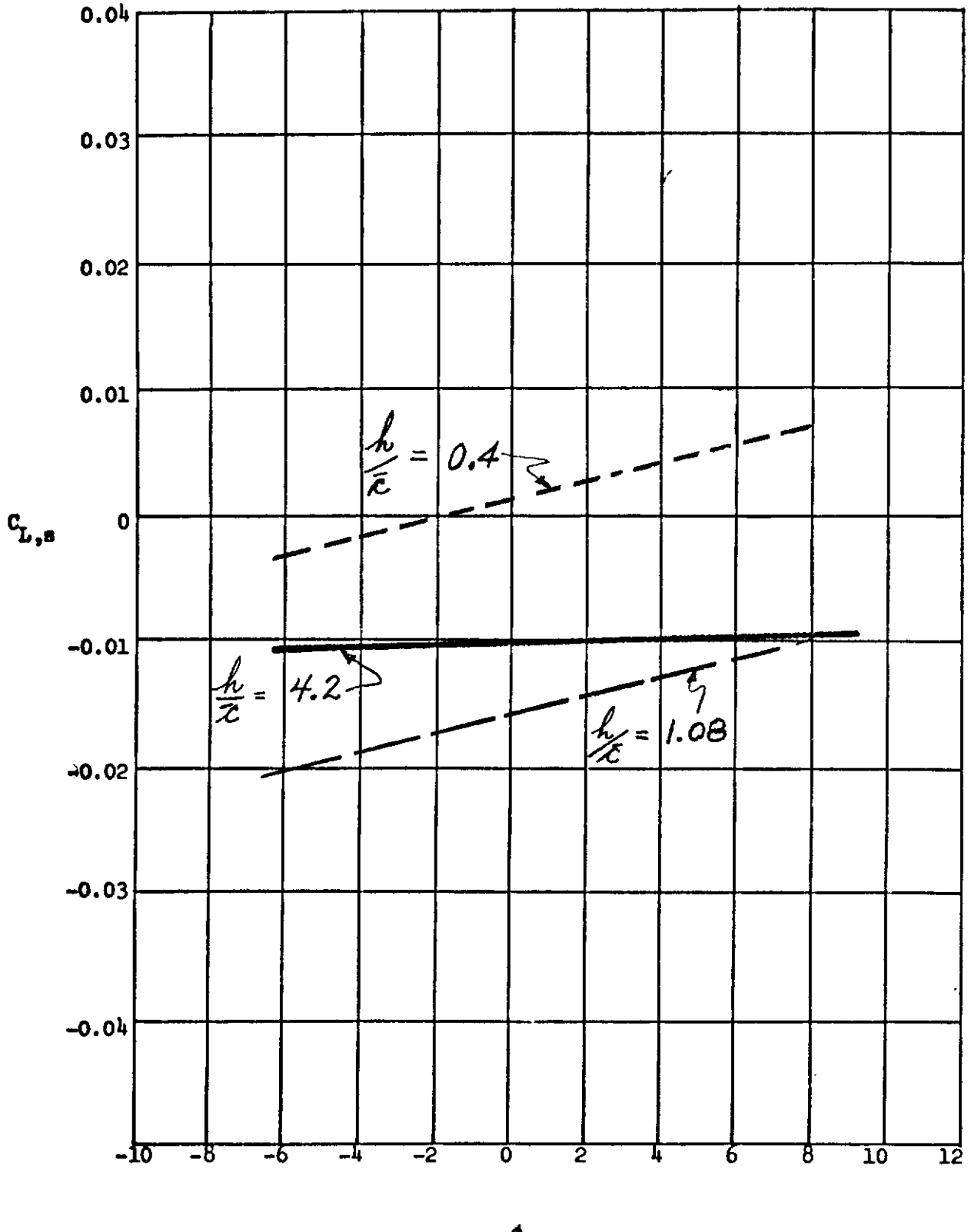

Figure 18. Continued.

Approved for Public Release

Contrails

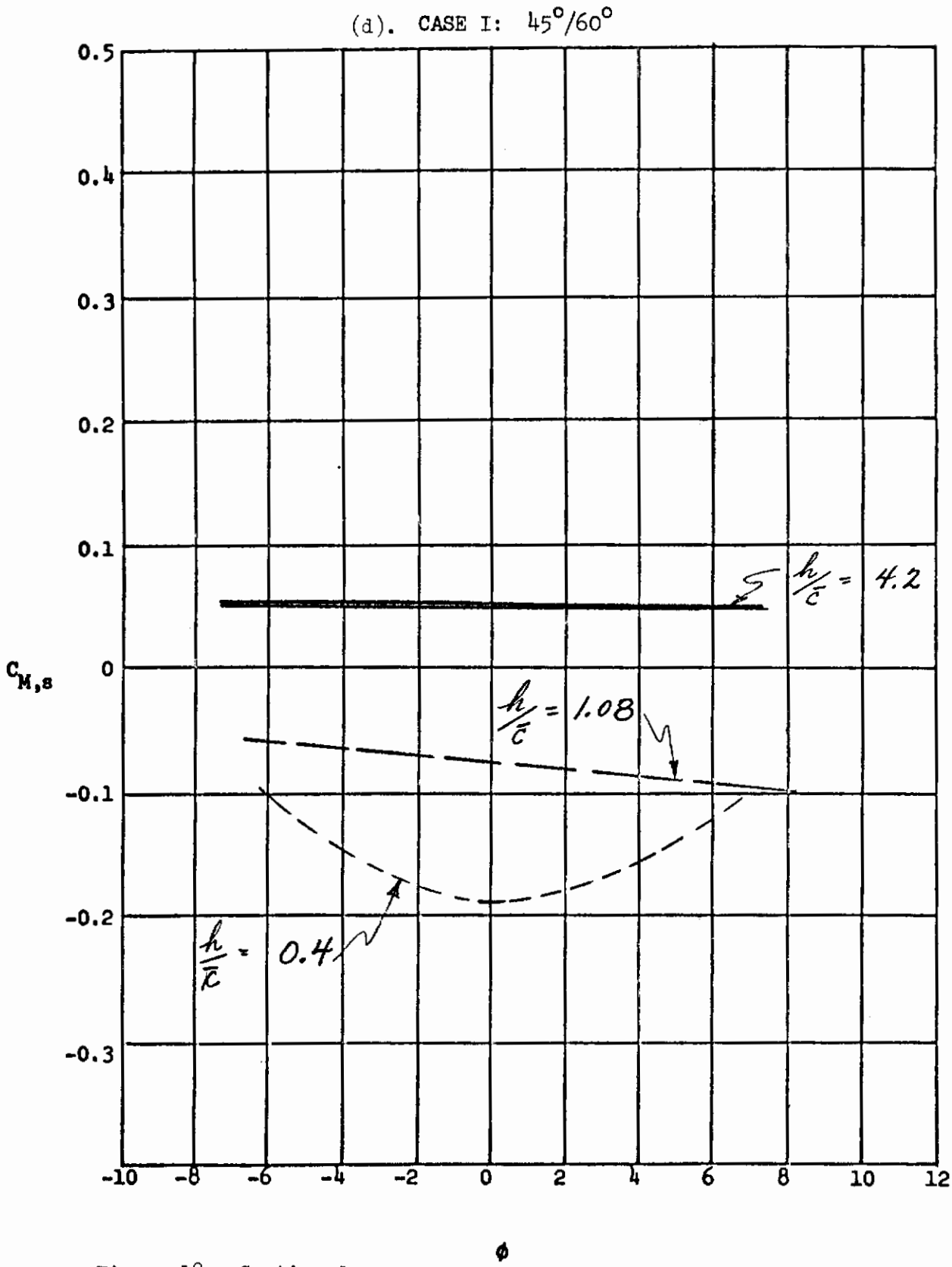

Figure 18. Continued.

Approved for Public Release

Contrails

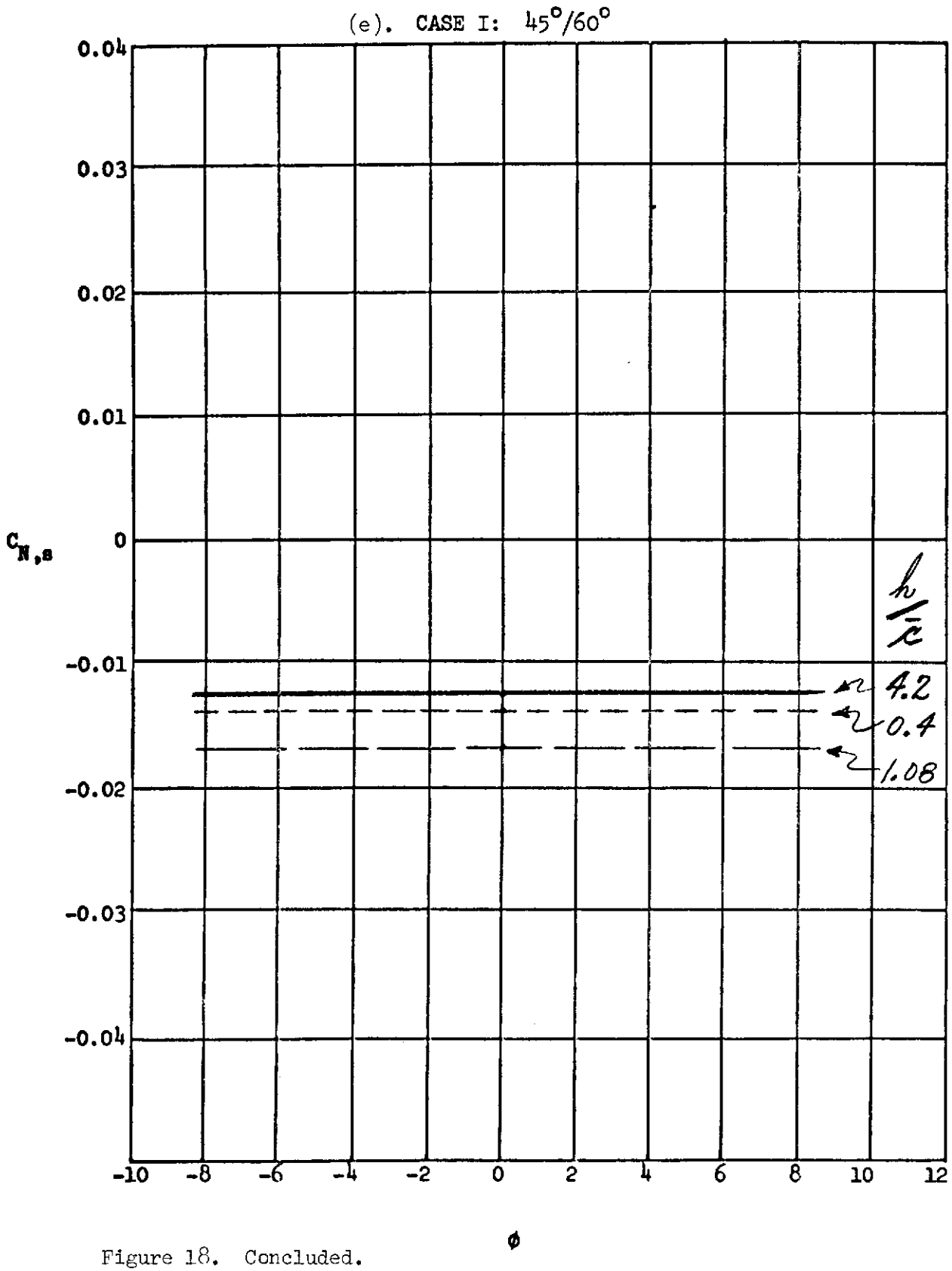

Figure 18. Concluded.

Approved for Public Release

Contrails

(a). CASE II: 40°/60°

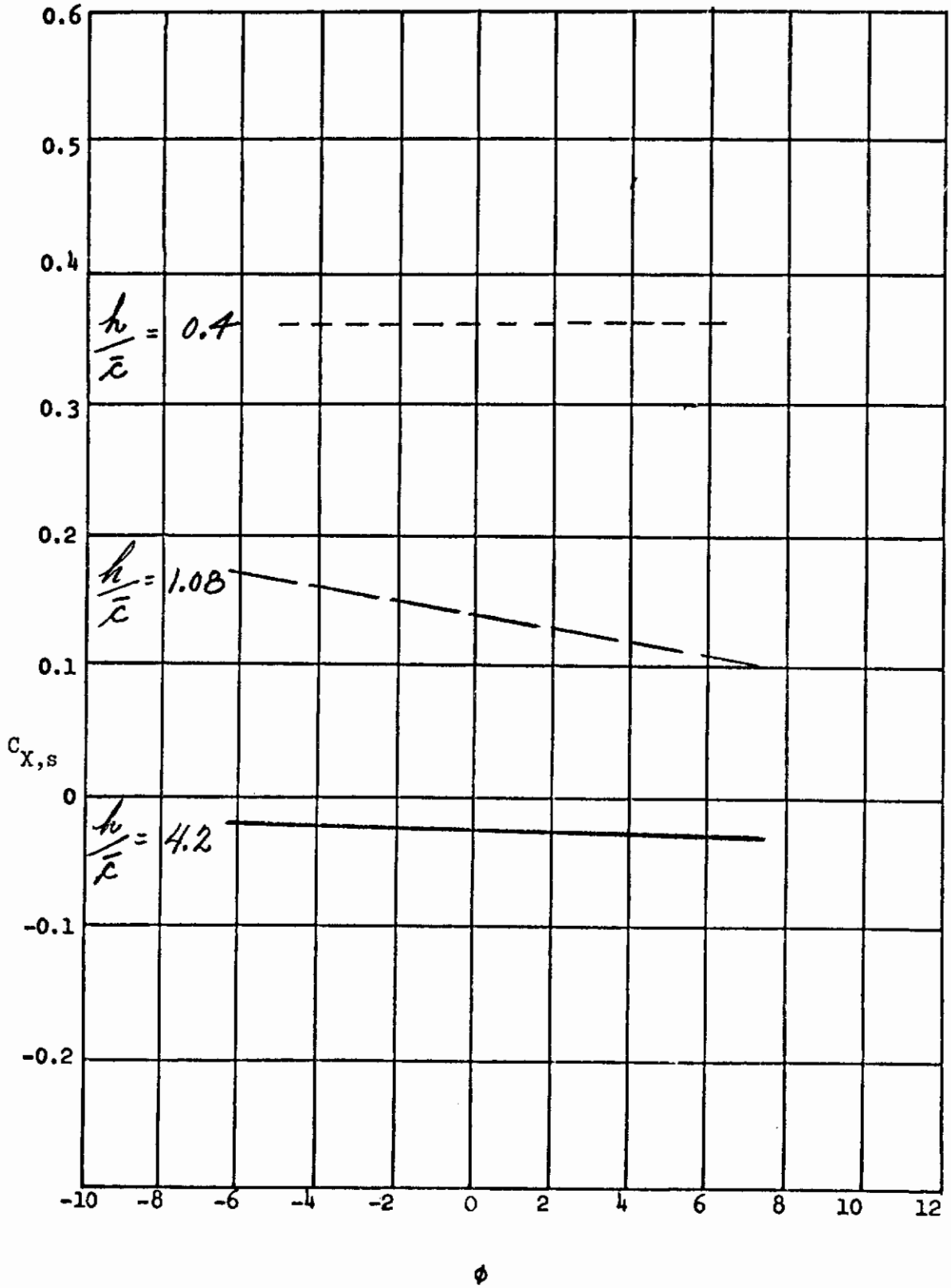

Figure 19. Longitudinal and lateral aerodynamic characteristics versus roll angle at three altitude ratios.

Approved for Public Release

Contrails

(b). CASE II: 40°/60°

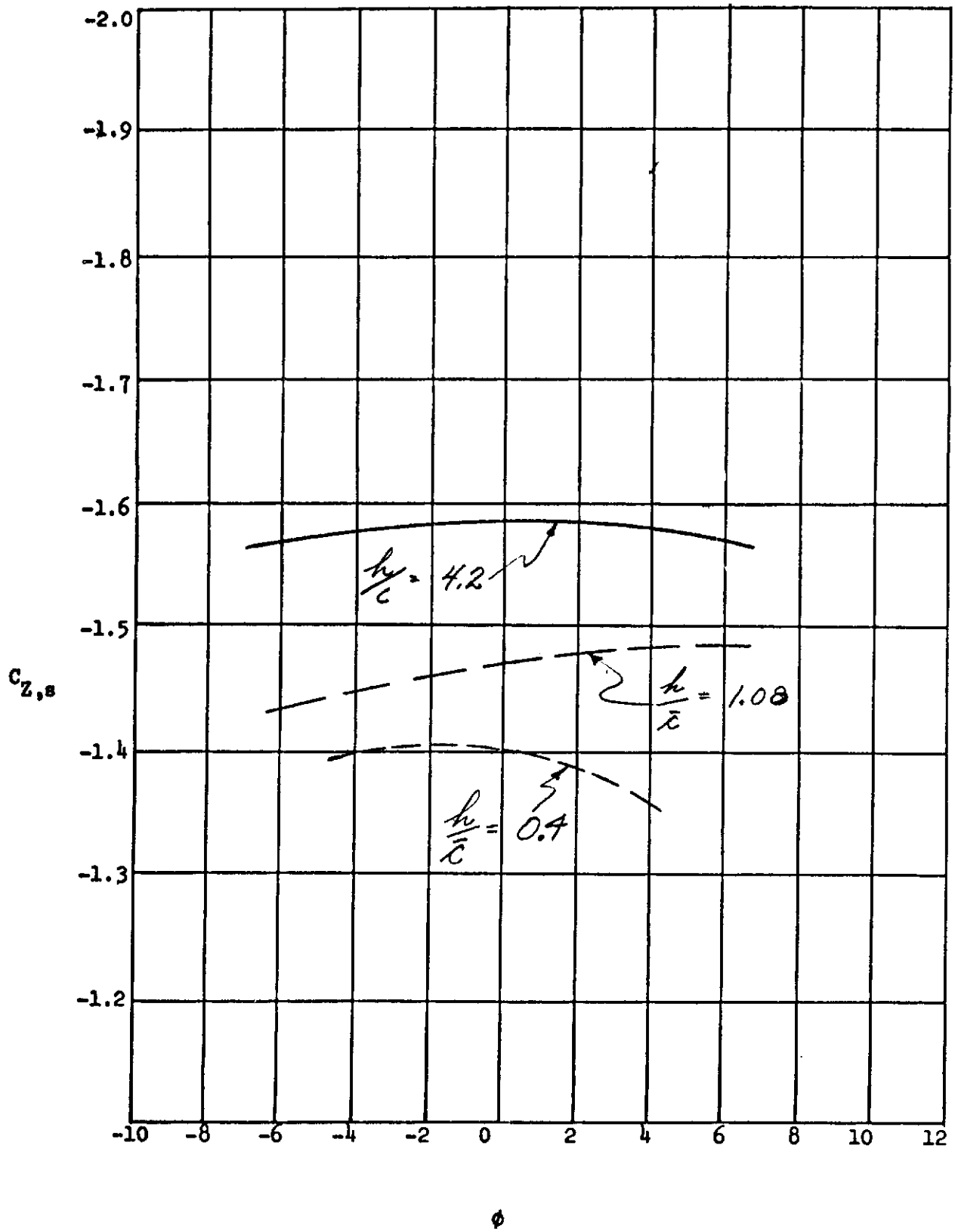

Figure 19. Continued.

Approved for Public Release

Contrails

(c). CASE II: 40°/60°

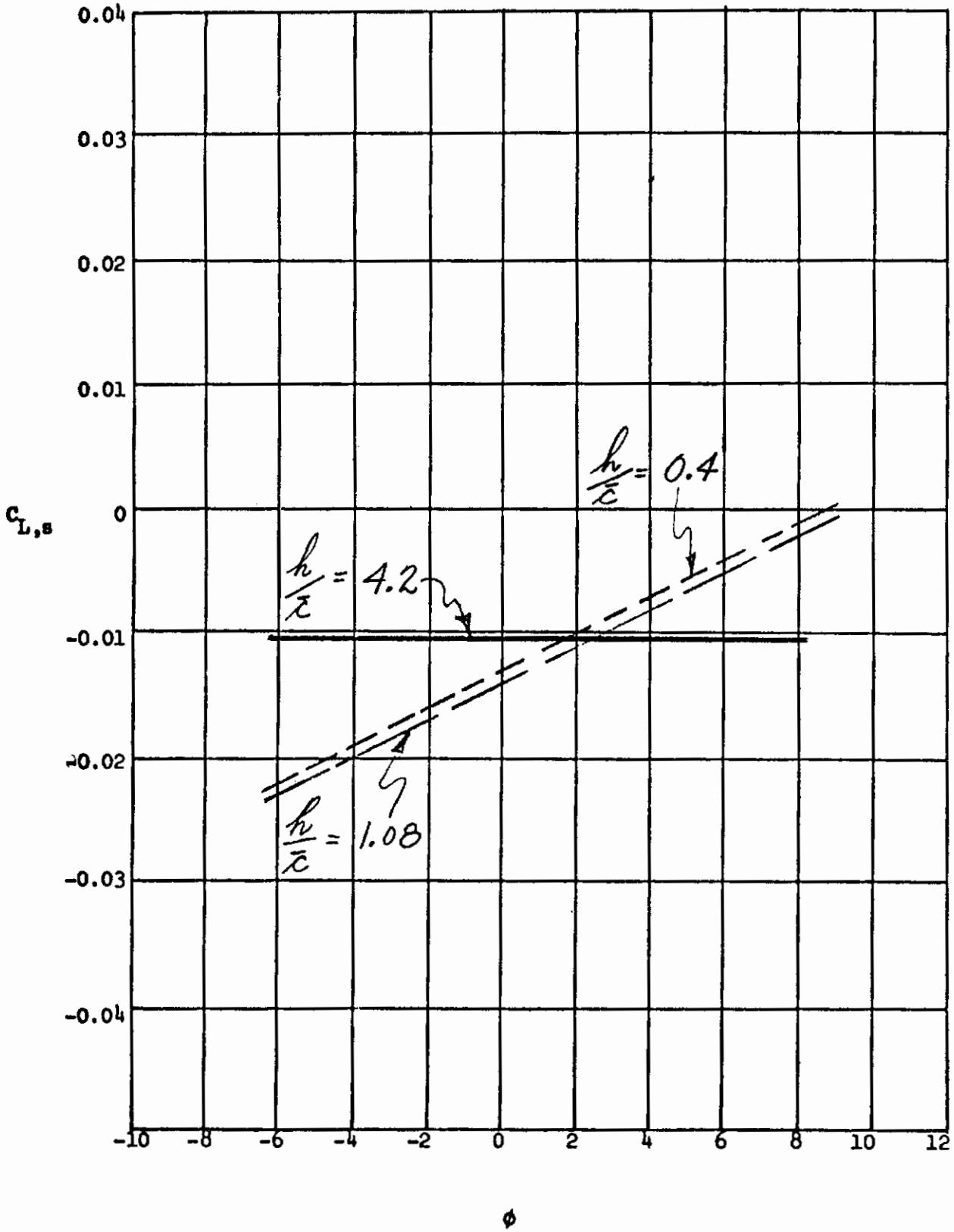

Figure 19. Continued.

Approved for Public Release

Contrails

(d). CASE II: 40°/60°

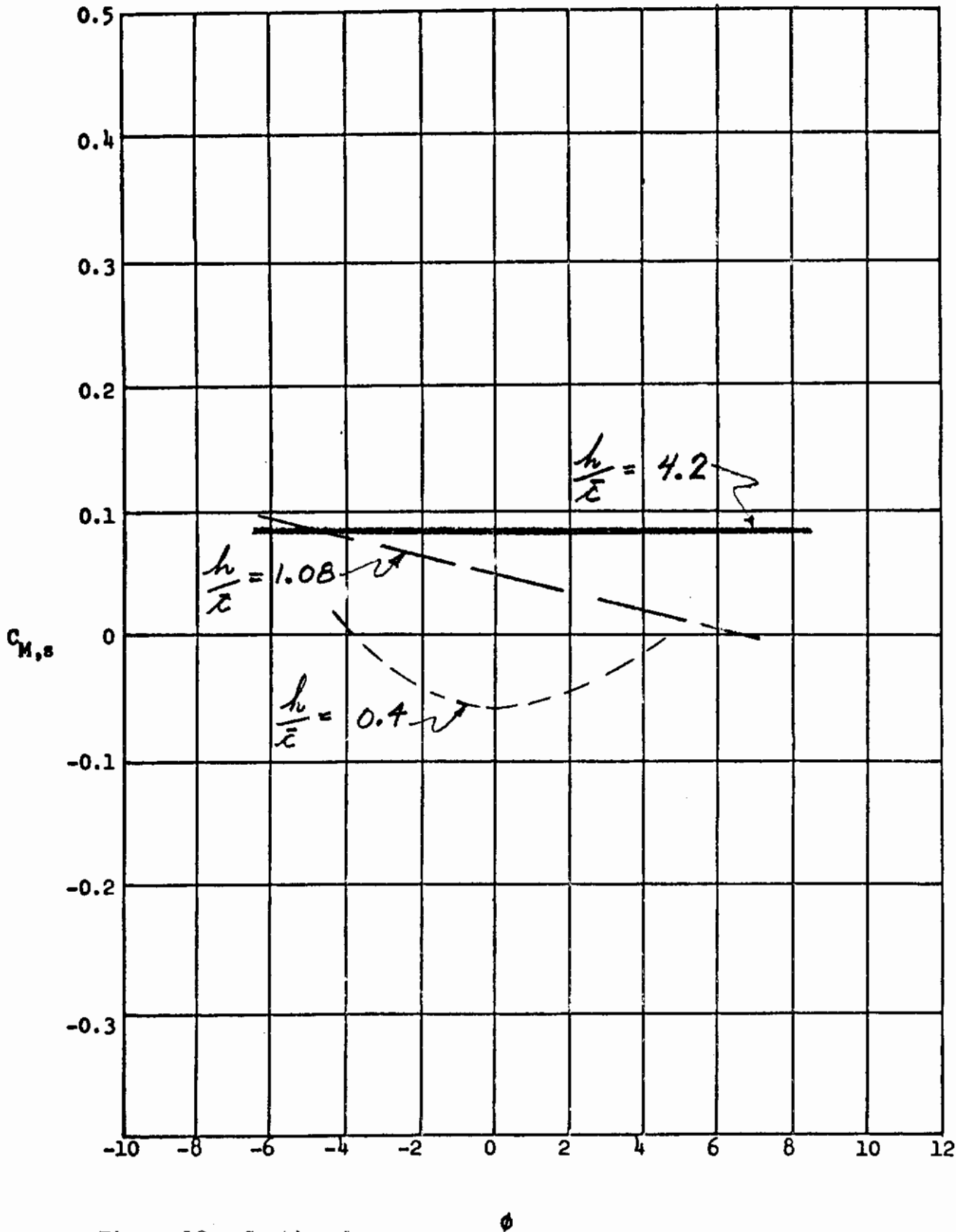

Figure 19. Continued.

Approved for Public Release

Contrails

(e). CASE II: 40°/60°

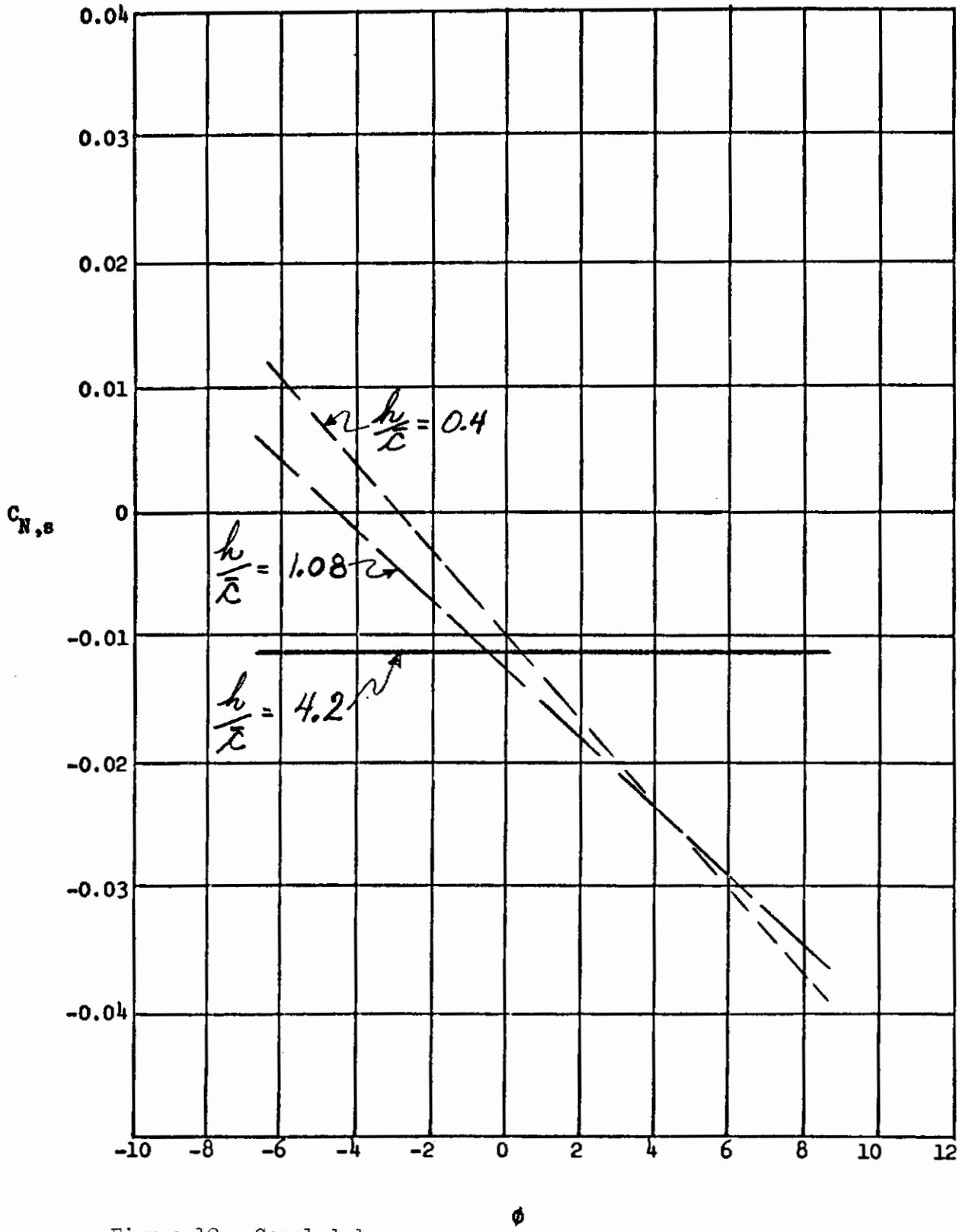

Figure 19. Concluded.

Approved for Public Release

Contrails

(a). CASE III: $40^{\circ}/40^{\circ}$

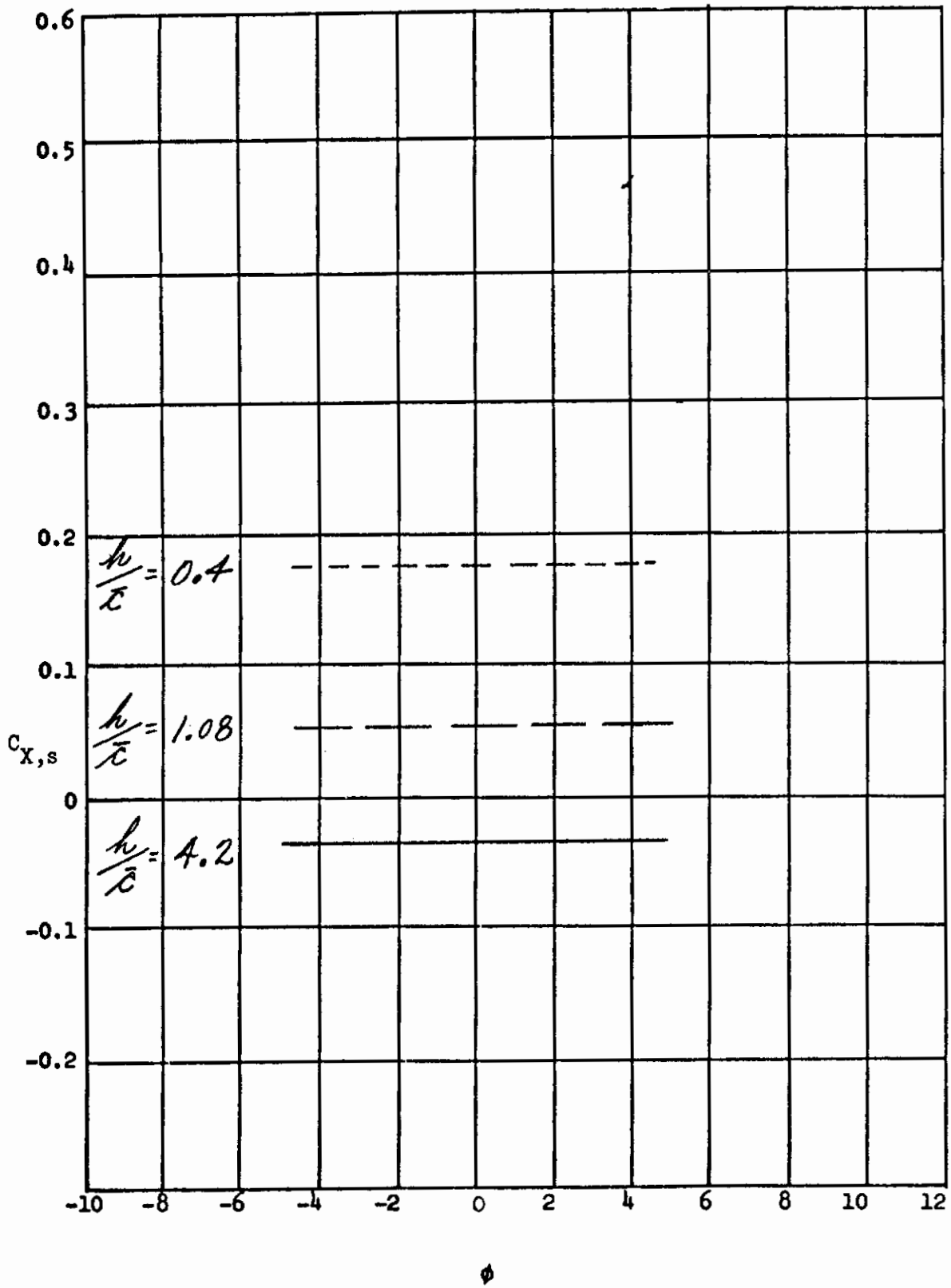

Figure 20. Longitudinal and lateral aerodynamic characteristics versus roll angle at three altitude ratios.

Approved for Public Release

Contrails

(b). CASE III: 40°/40°

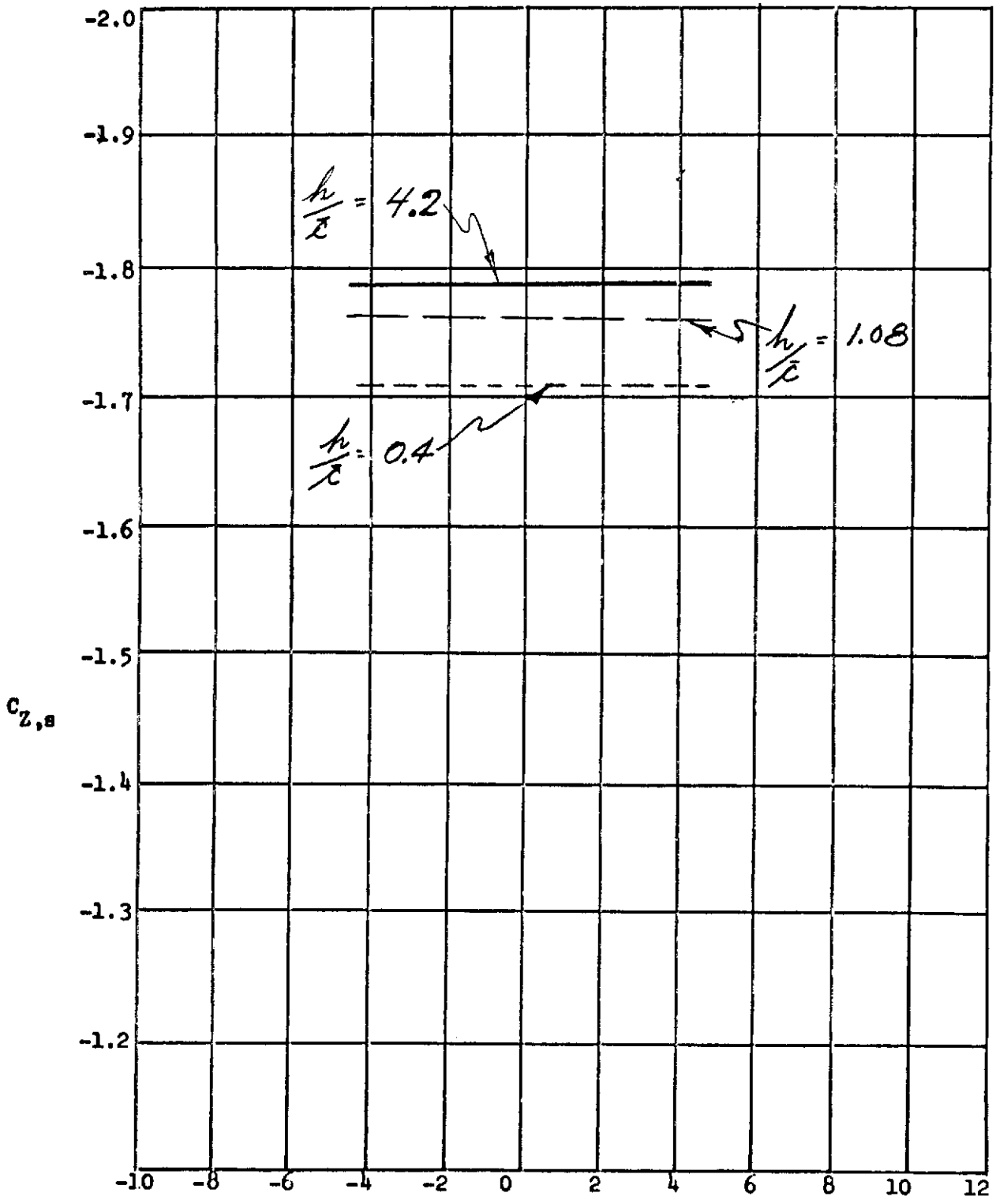

Figure 20. Continued.

Approved for Public Release

Contrails

(c). CASE III: 40°/40°

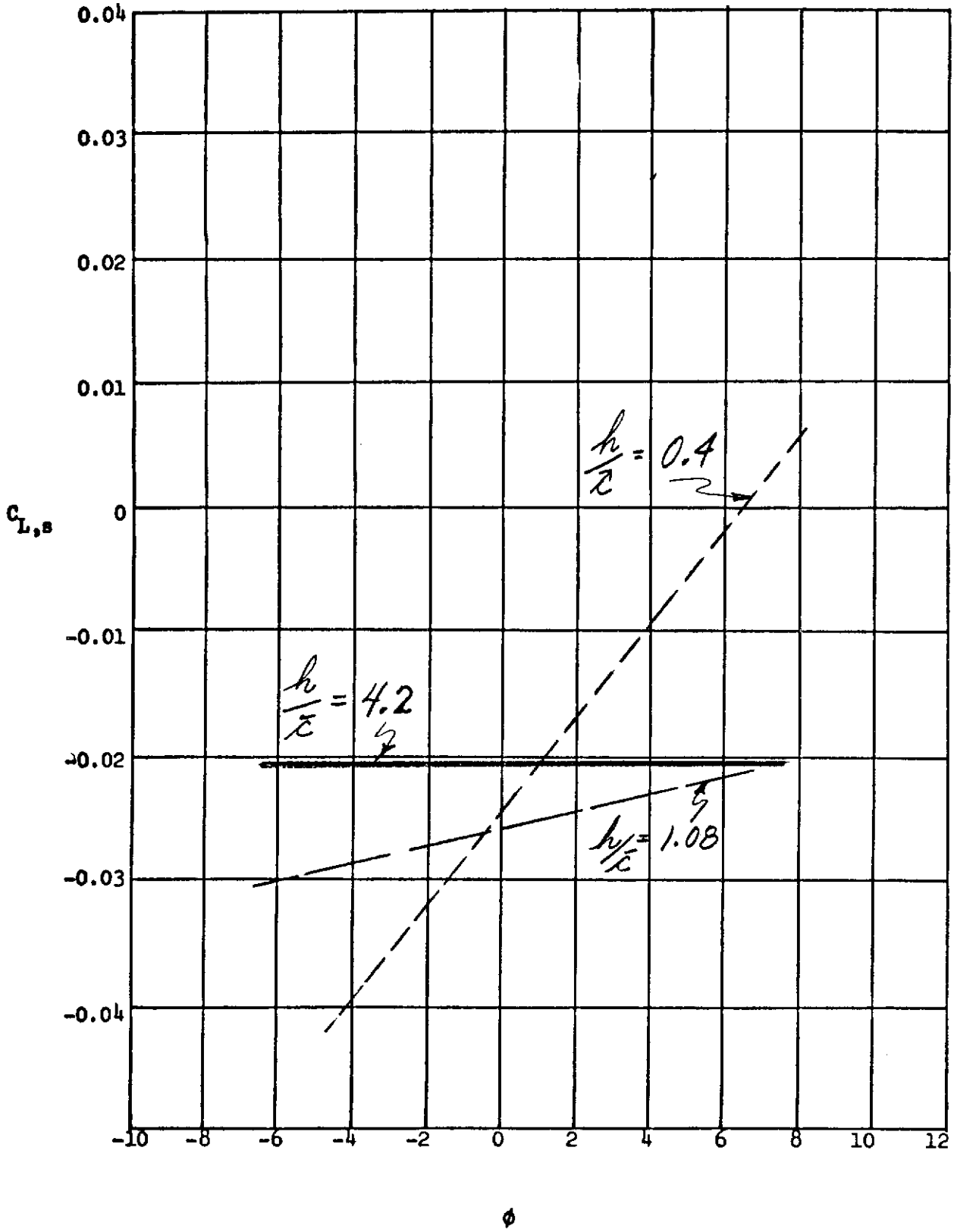

Figure 20. Continued.

Approved for Public Release

Contrails

(d). CASE III: 40°/40°

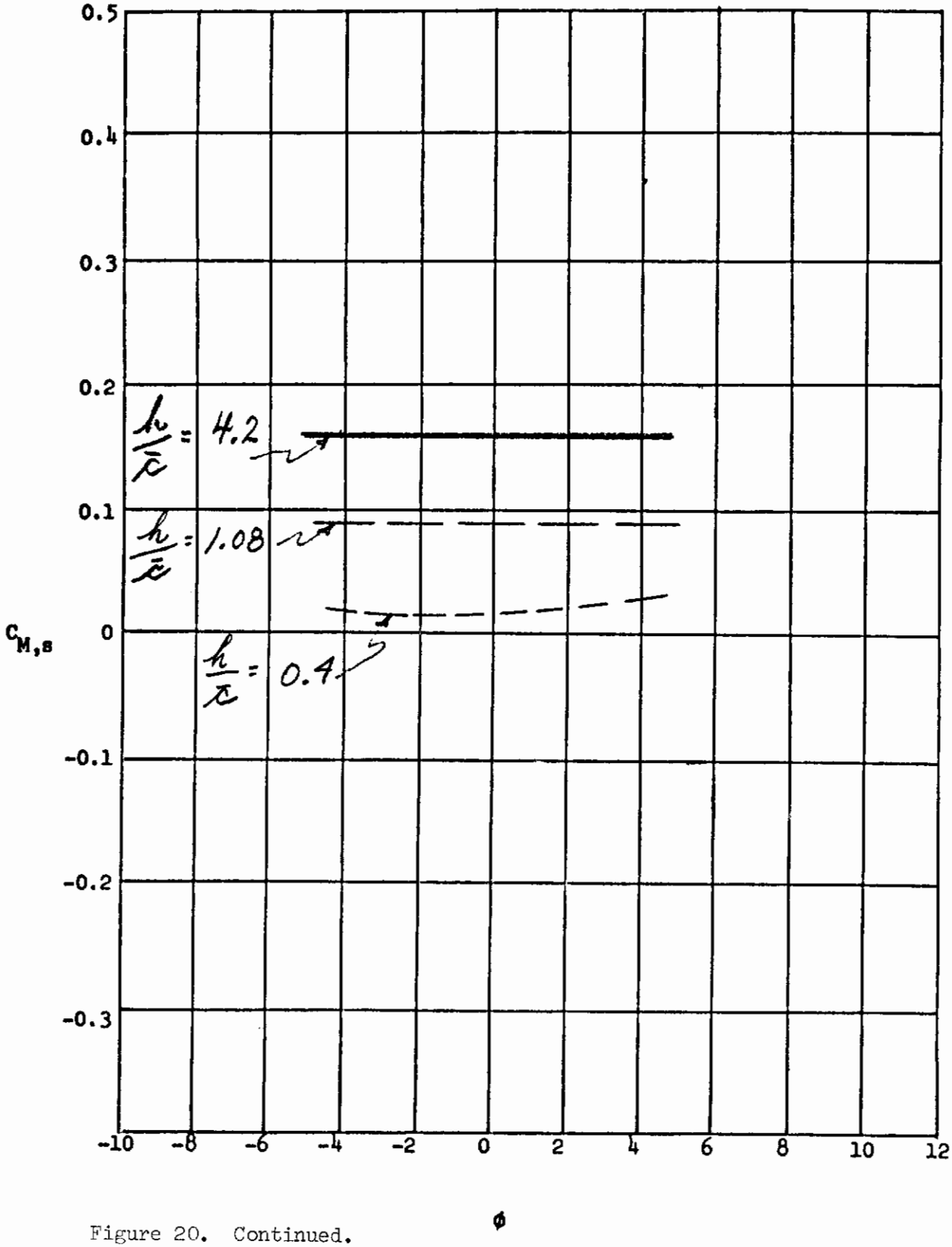

Figure 20. Continued.

Approved for Public Release

Contrails

(e). CASE III: 40°/40°

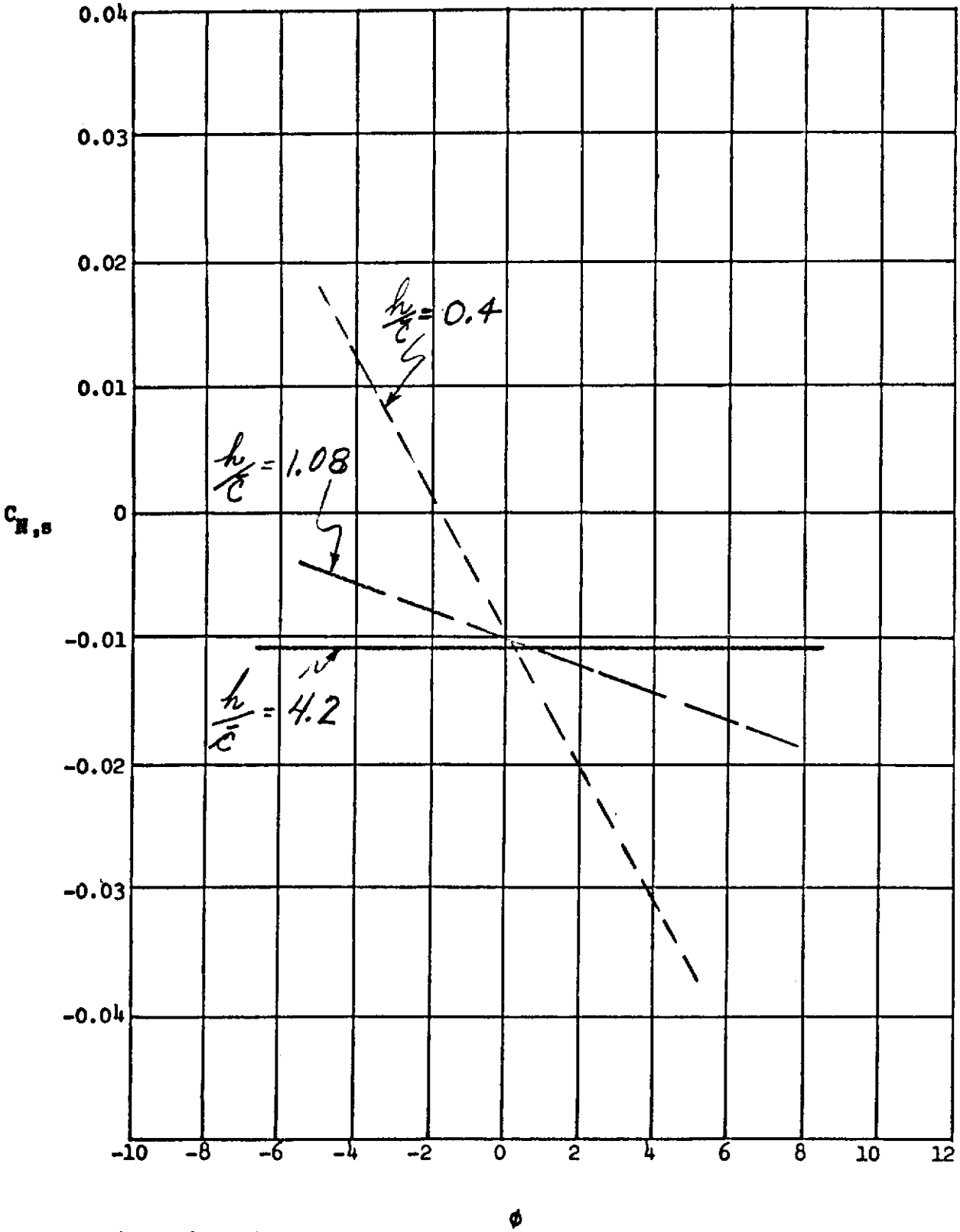

Figure 20. Concluded.

Approved for Public Release

Contrails

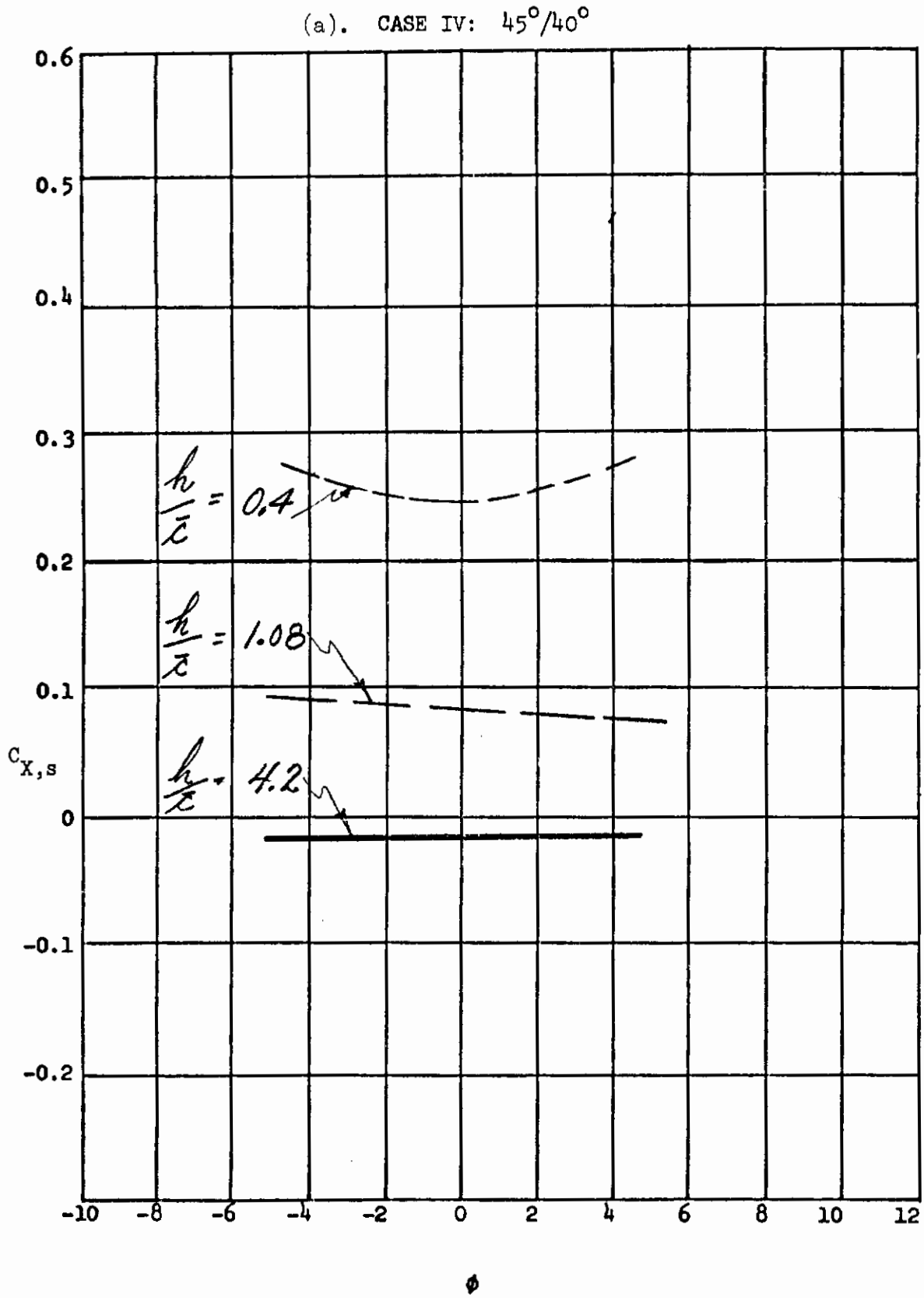

Figure 21. Longitudinal and lateral aerodynamic characteristics versus roll angle at three altitude ratios.

Approved for Public Release

Contrails

(b). CASE IV: 45°/40°

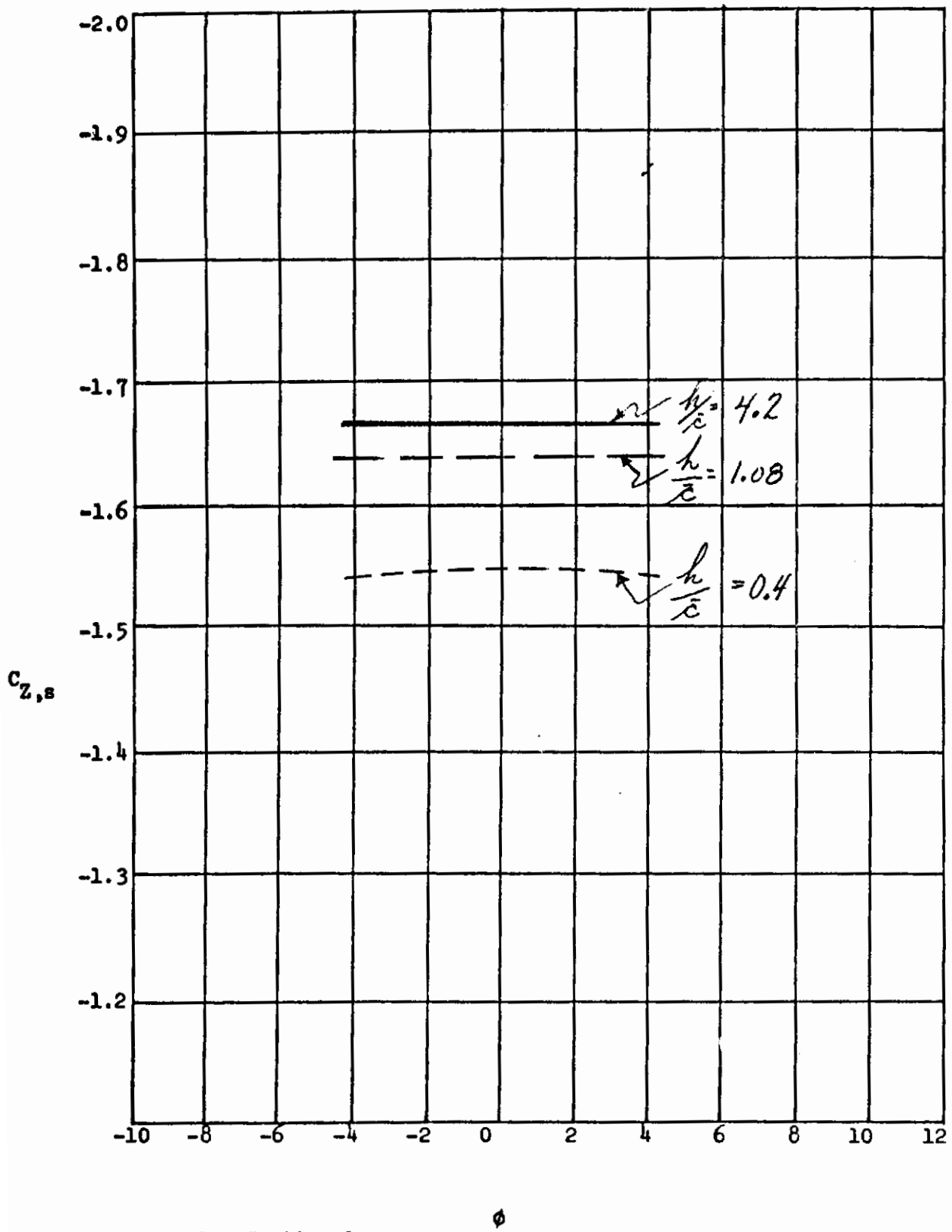

Figure 21. Continued.

Approved for Public Release

Contrails

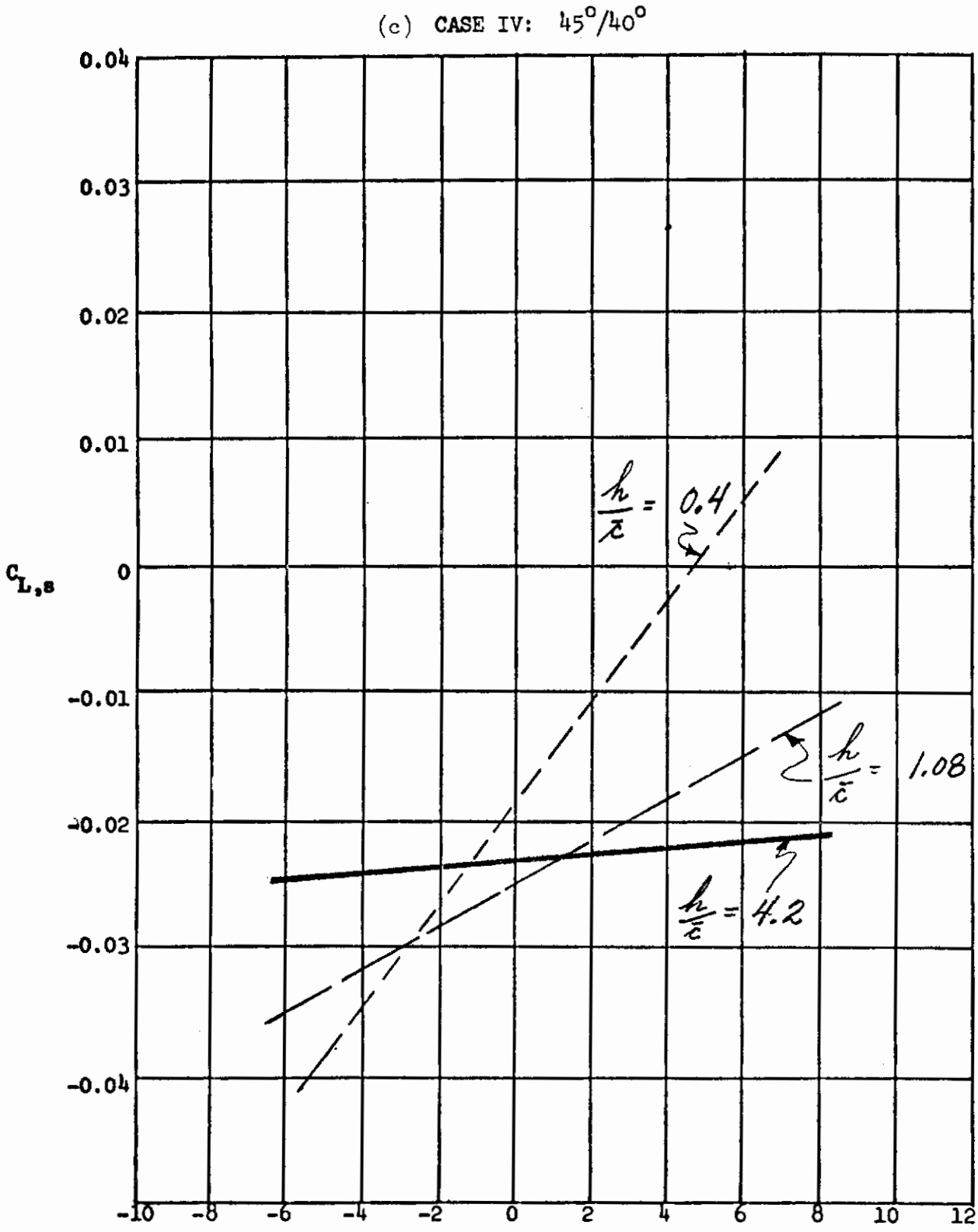

Figure 21. Continued.

Approved for Public Release

Contrails

(d). CASE IV: 45°/40°

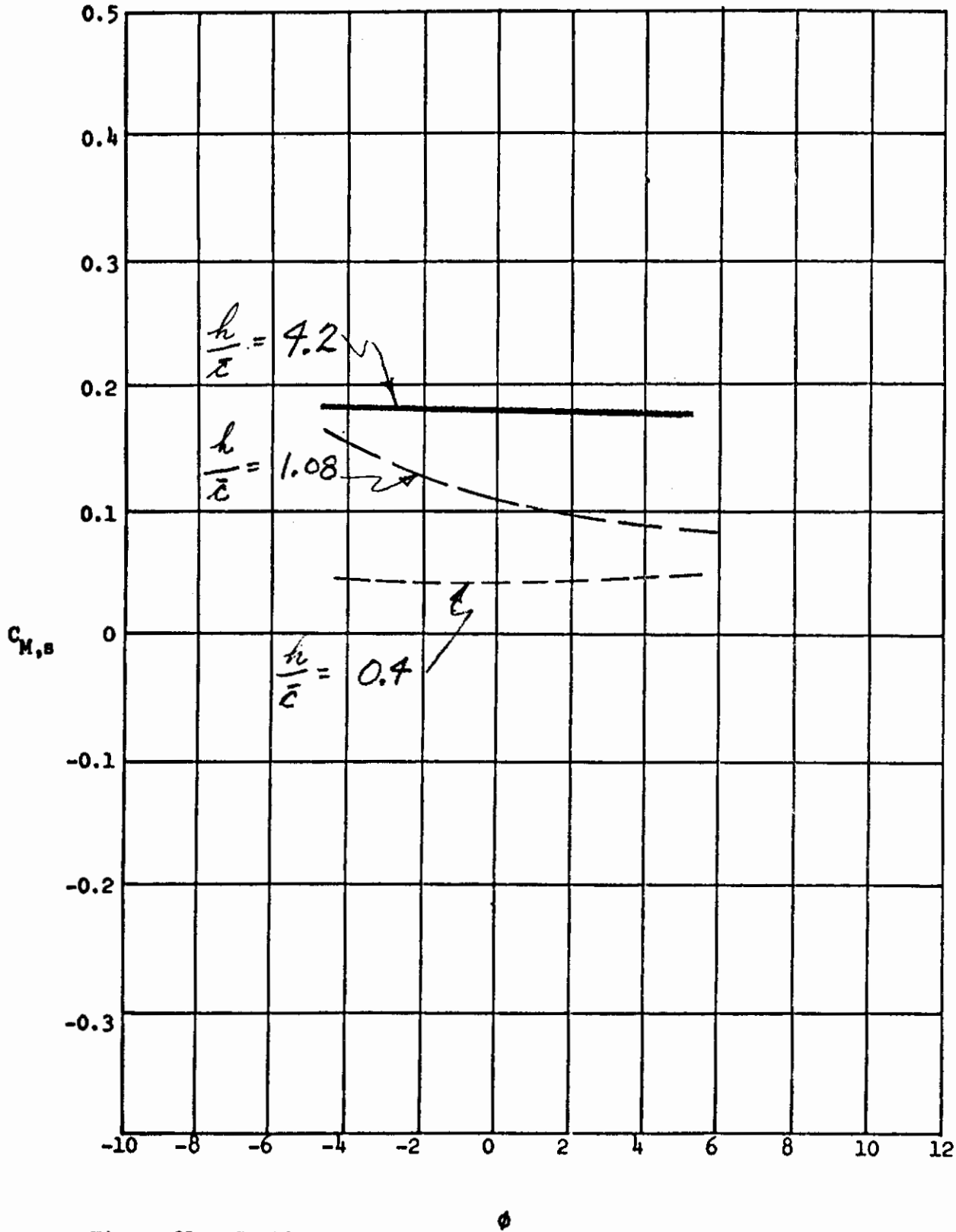

Figure 21. Continued.

Approved for Public Release

Contrails

(e). CASE IV: 45°/40°

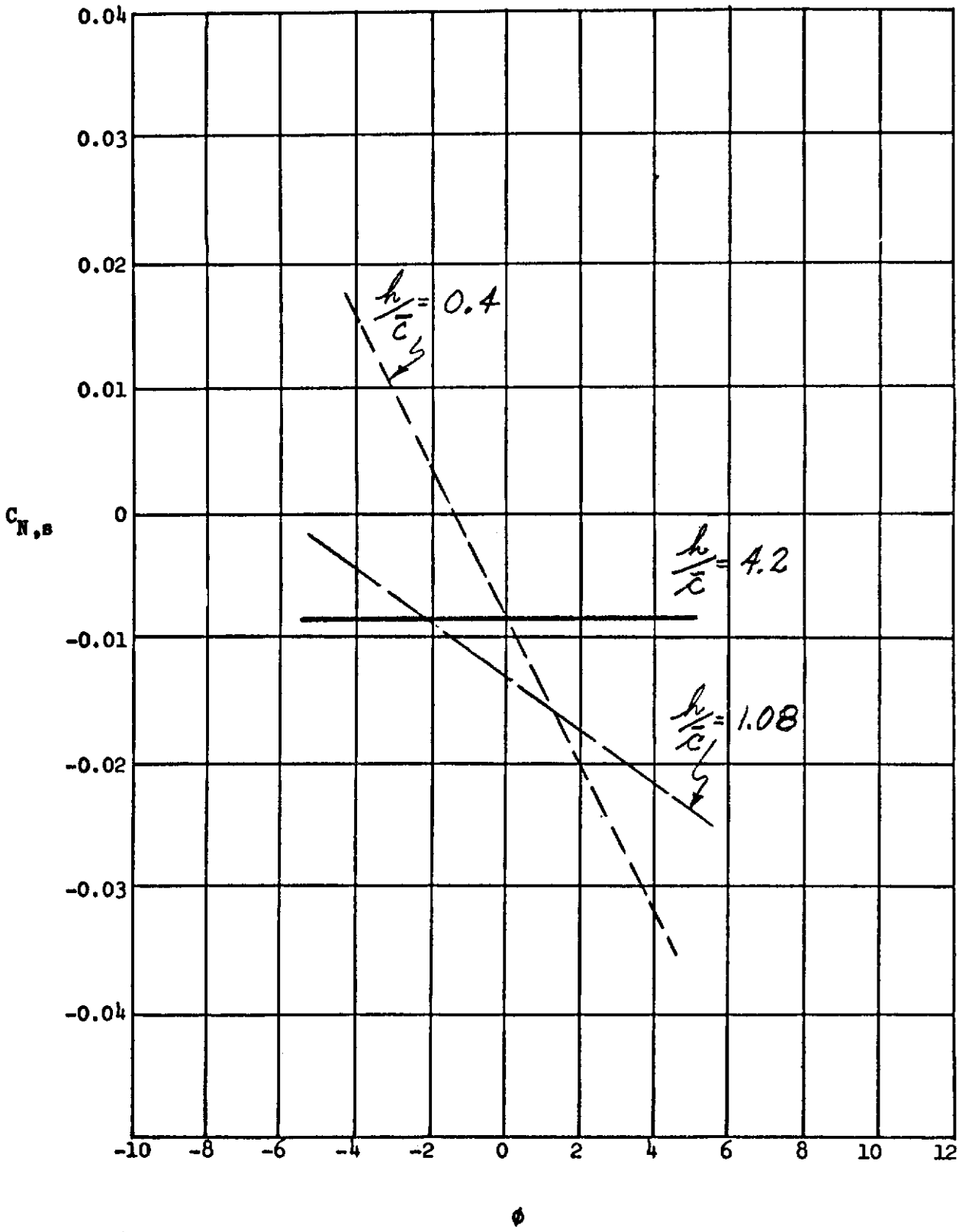

Figure 21. Concluded.

Approved for Public Release

Contrails

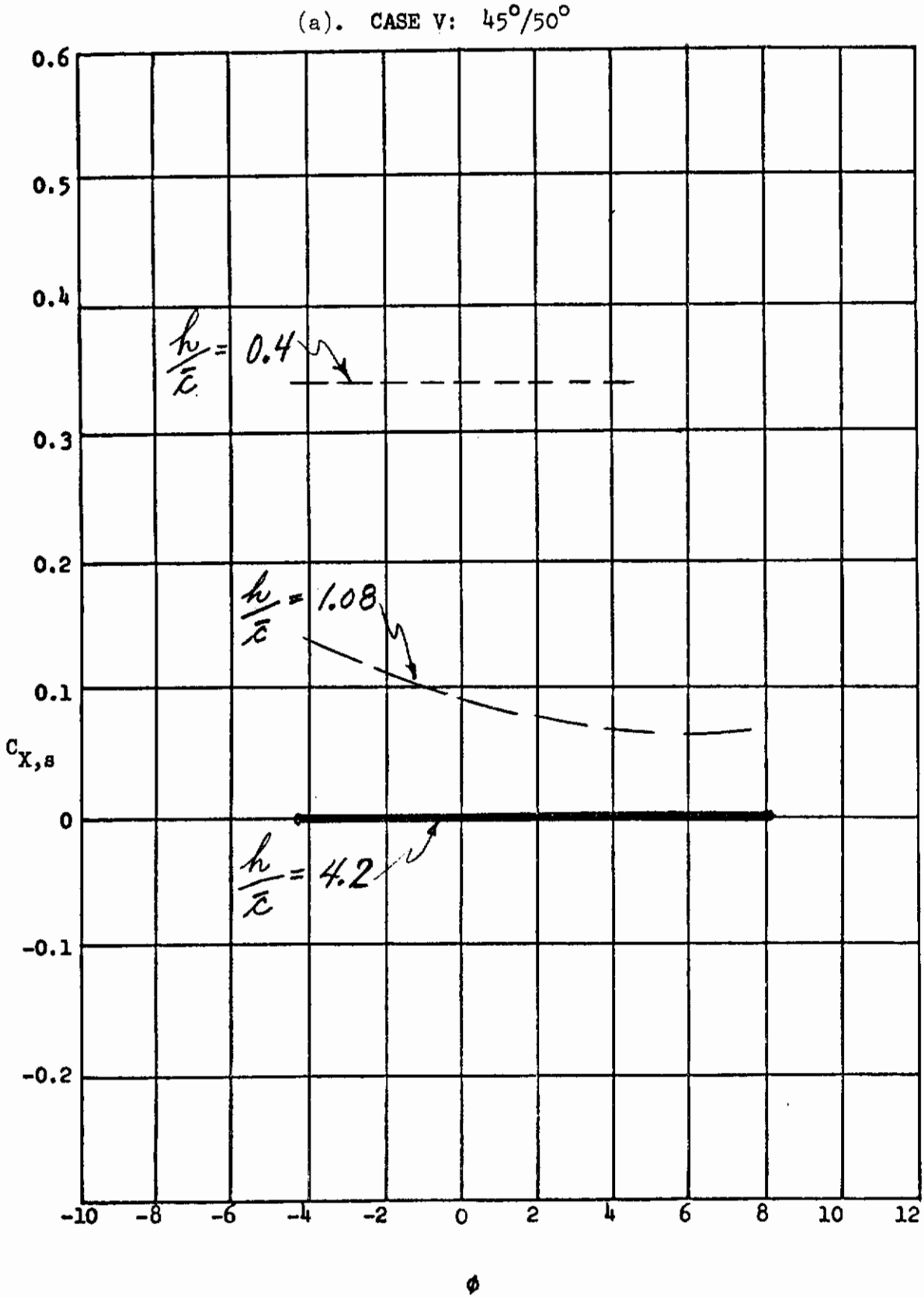

Figure 22. Longitudinal and lateral aerodynamic characteristics versus roll angle at three altitude ratios.

Approved for Public Release

Contrails

(b). CASE V: 45°/50°

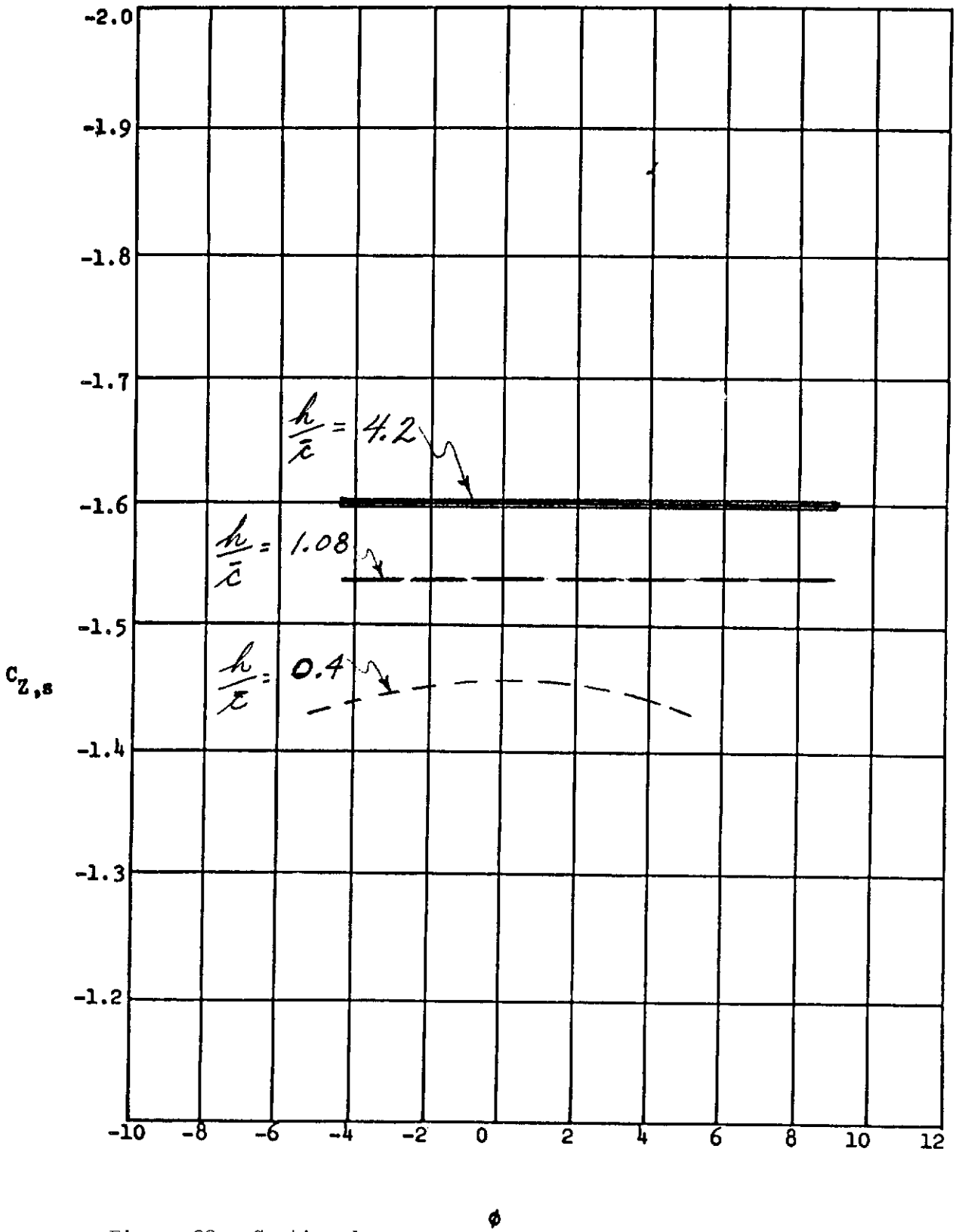

Figure 22. Continued.

Approved for Public Release

Contrails

(c). CASE V: 45°/50°

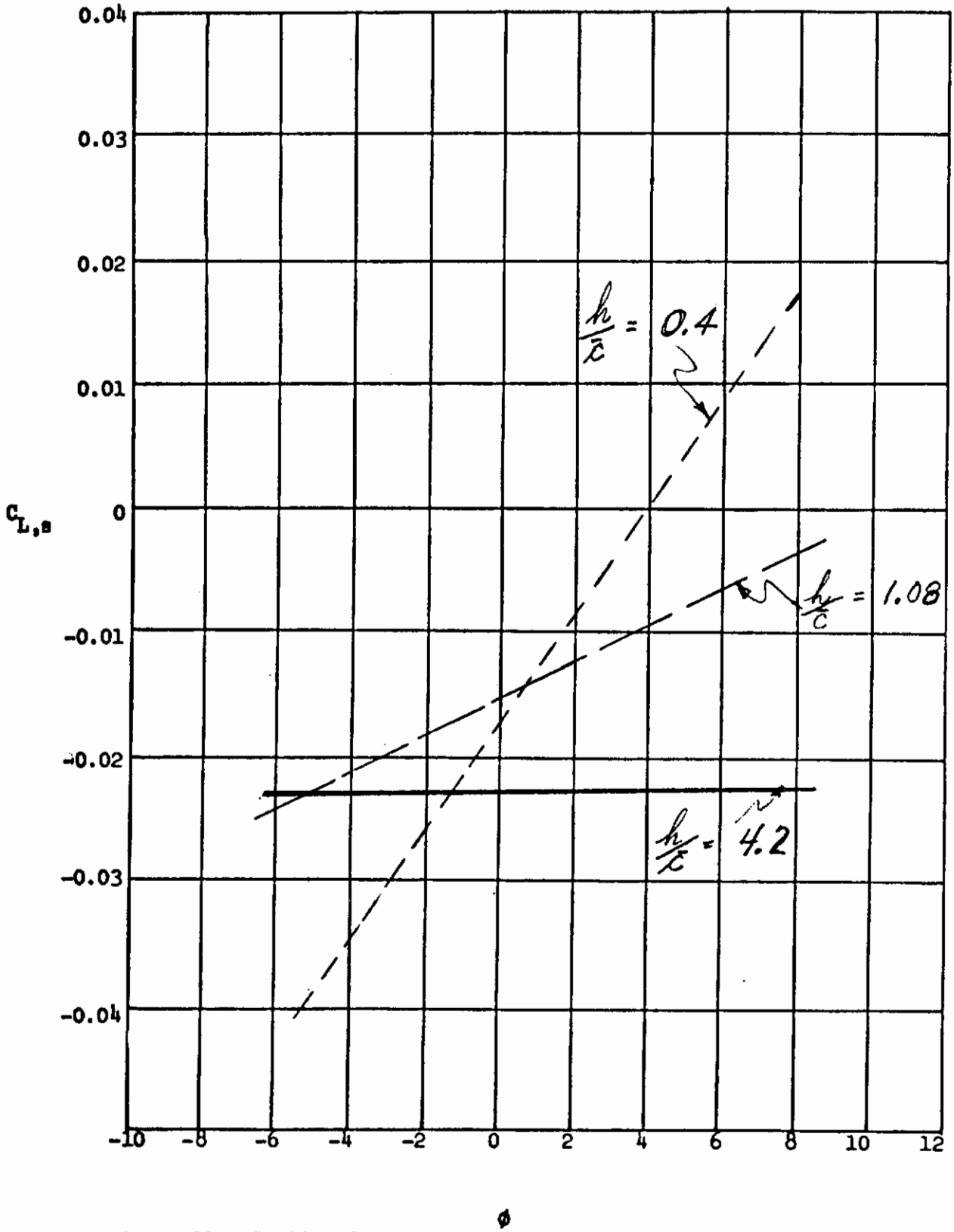

Figure 22. Continued.

Approved for Public Release

Contrails

(d). CASE V: 45°/50°

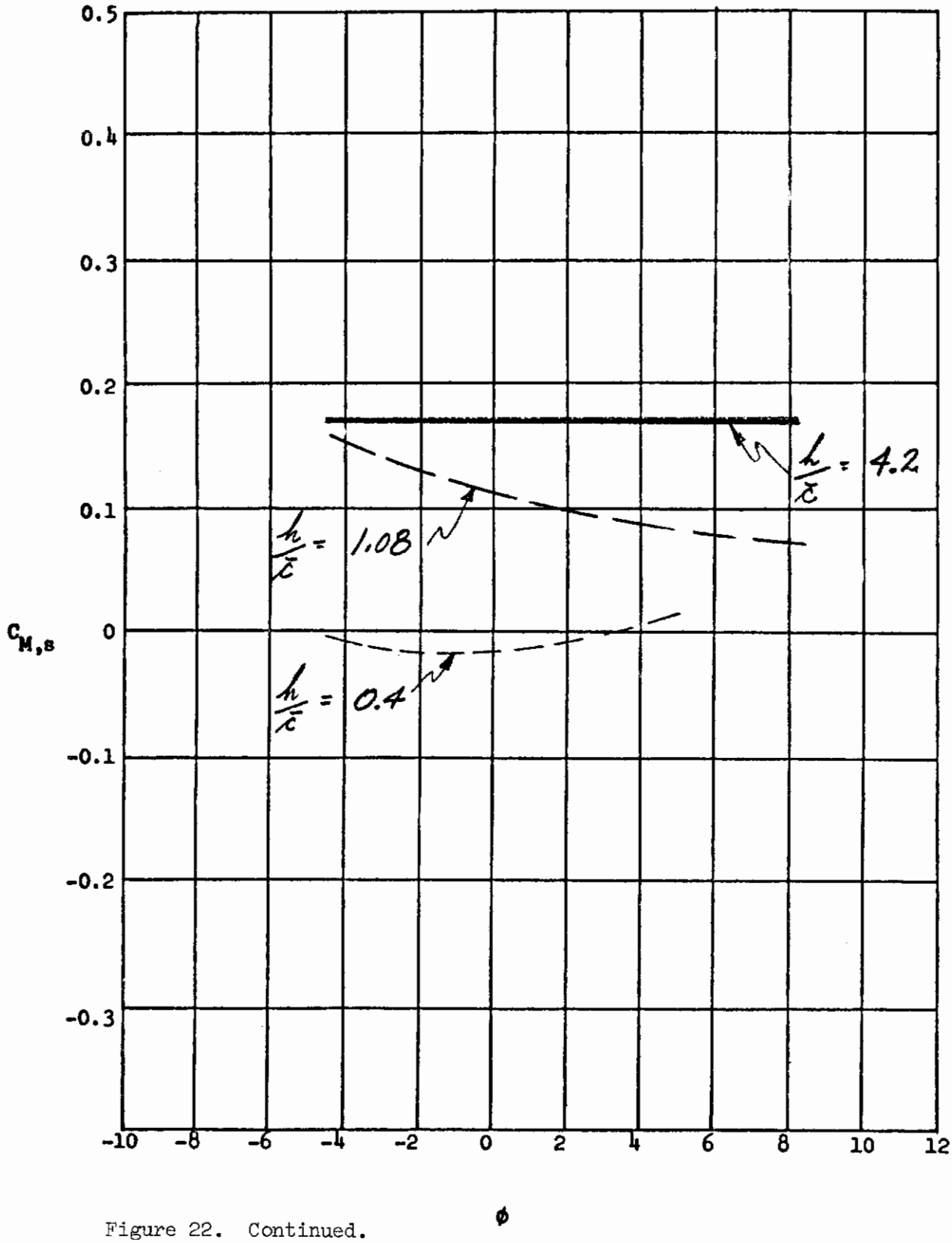

Figure 22. Continued.

Approved for Public Release

Contrails

(e). CASE V: 45°/50°

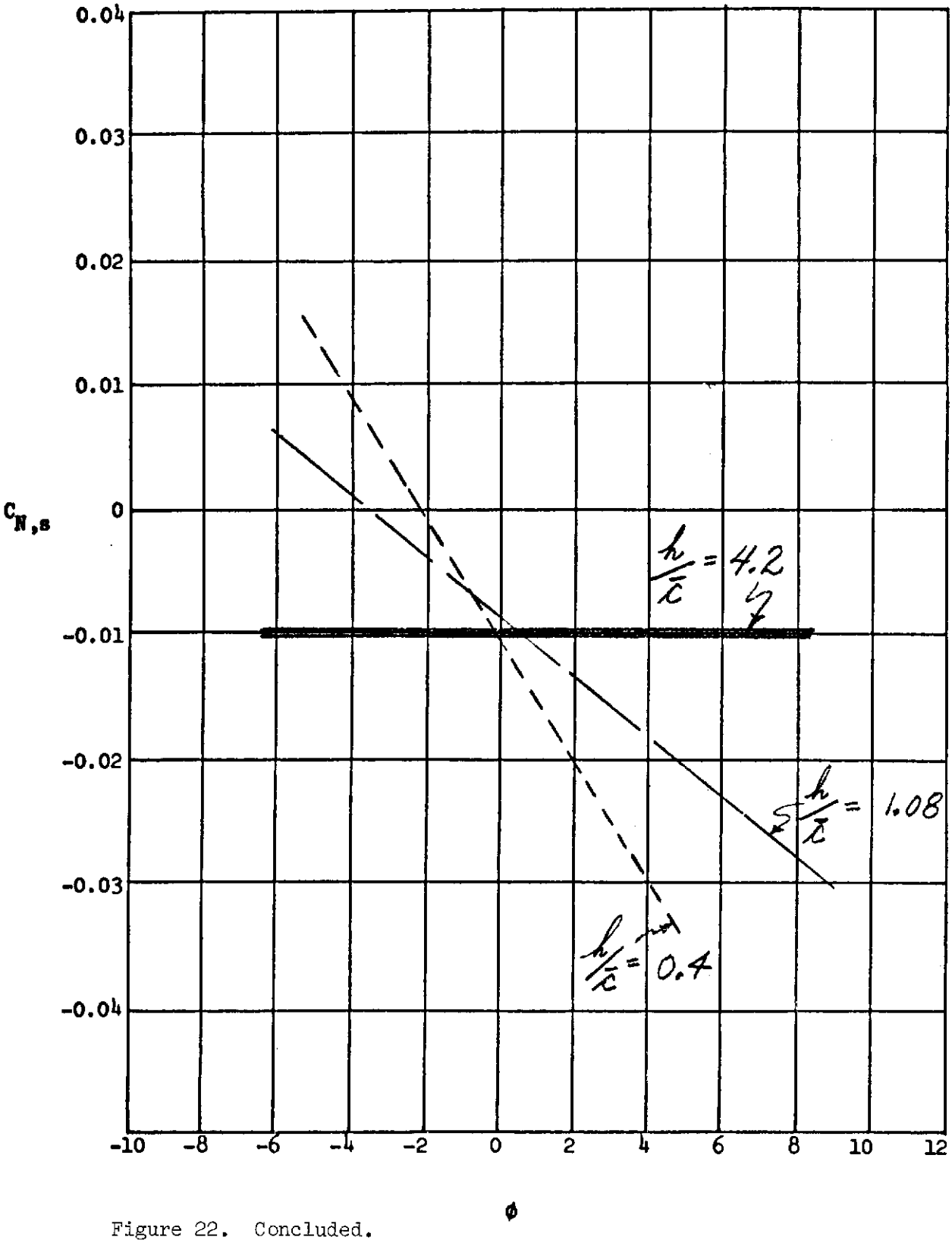

Figure 22. Concluded.

Approved for Public Release

Contrails

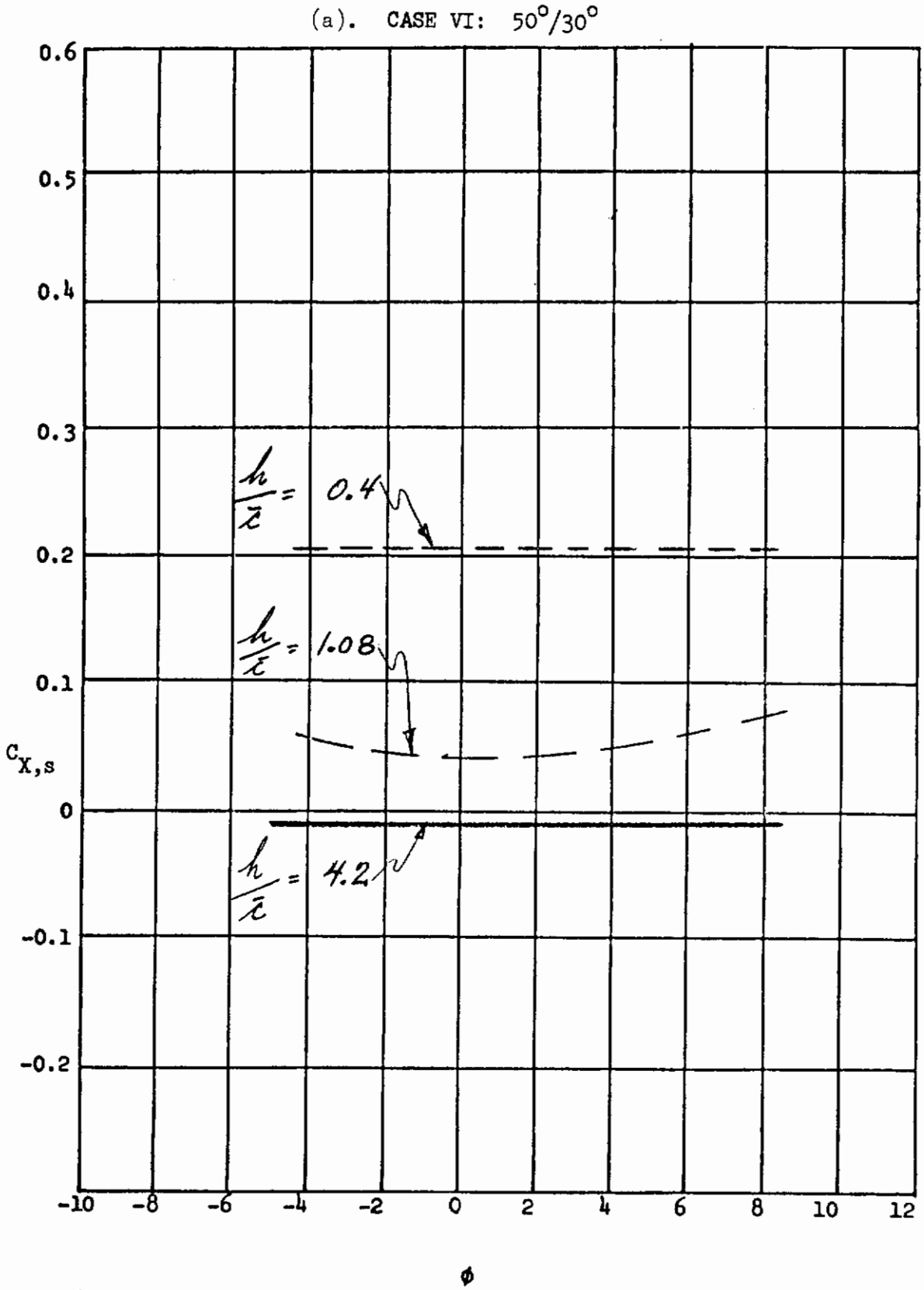

Figure 23. Longitudinal and lateral aerodynamic characteristics versus roll angle at three altitude ratios.

Approved for Public Release

Contrails

(b). CASE VI: 50°/30°

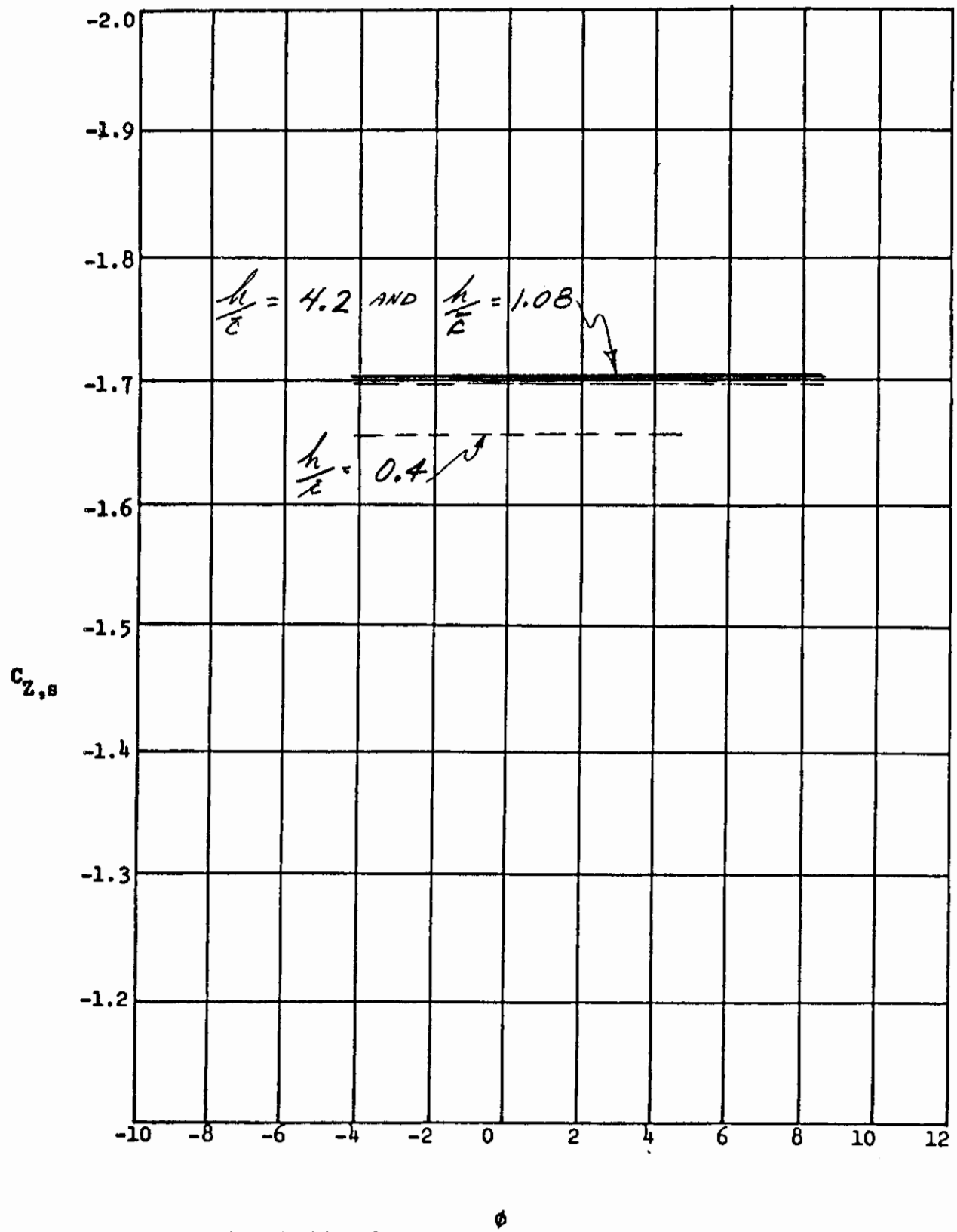

Figure 23. Continued.

Approved for Public Release

Contrails

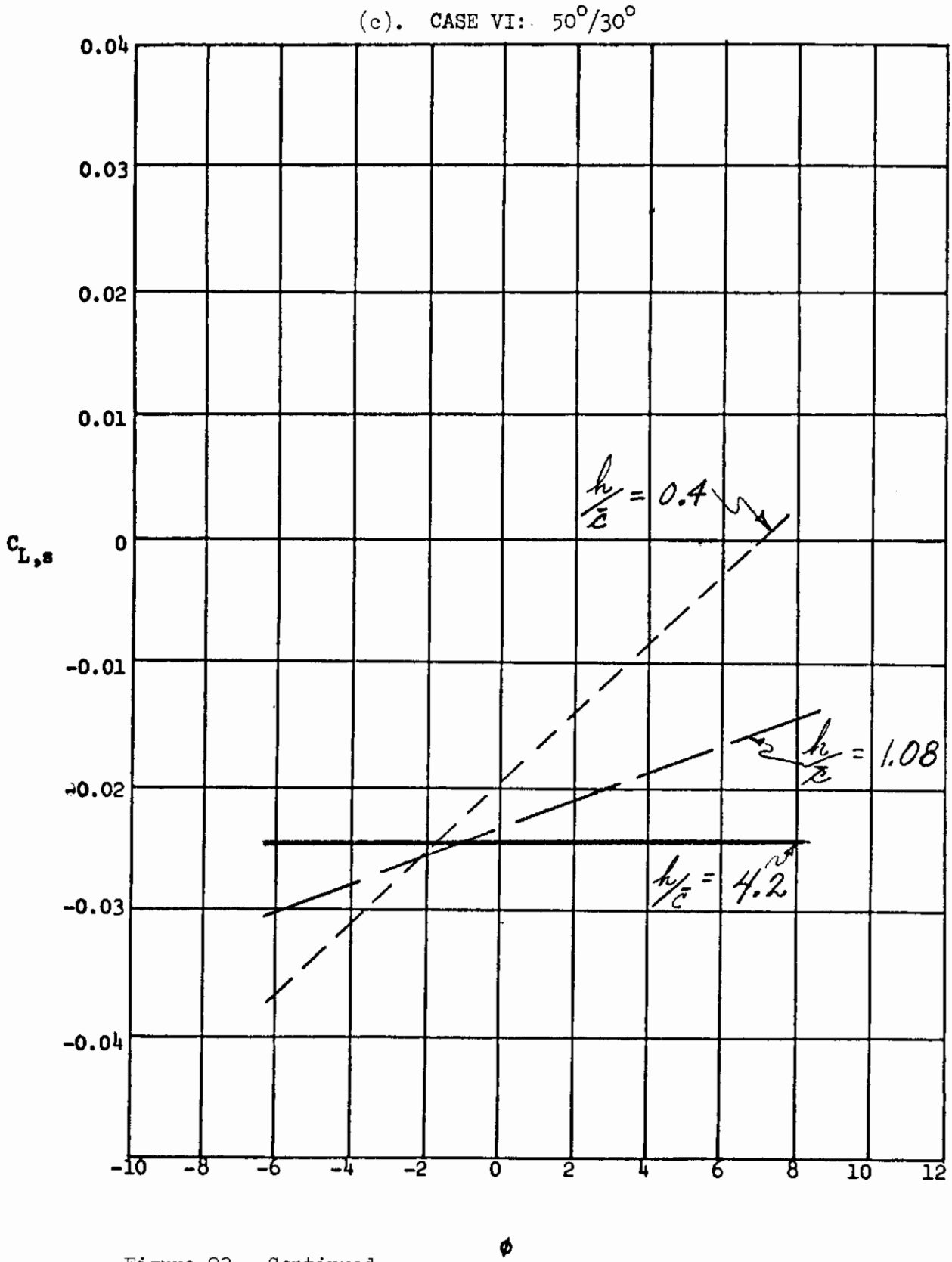

Figure 23. Continued.

Approved for Public Release

Contrails

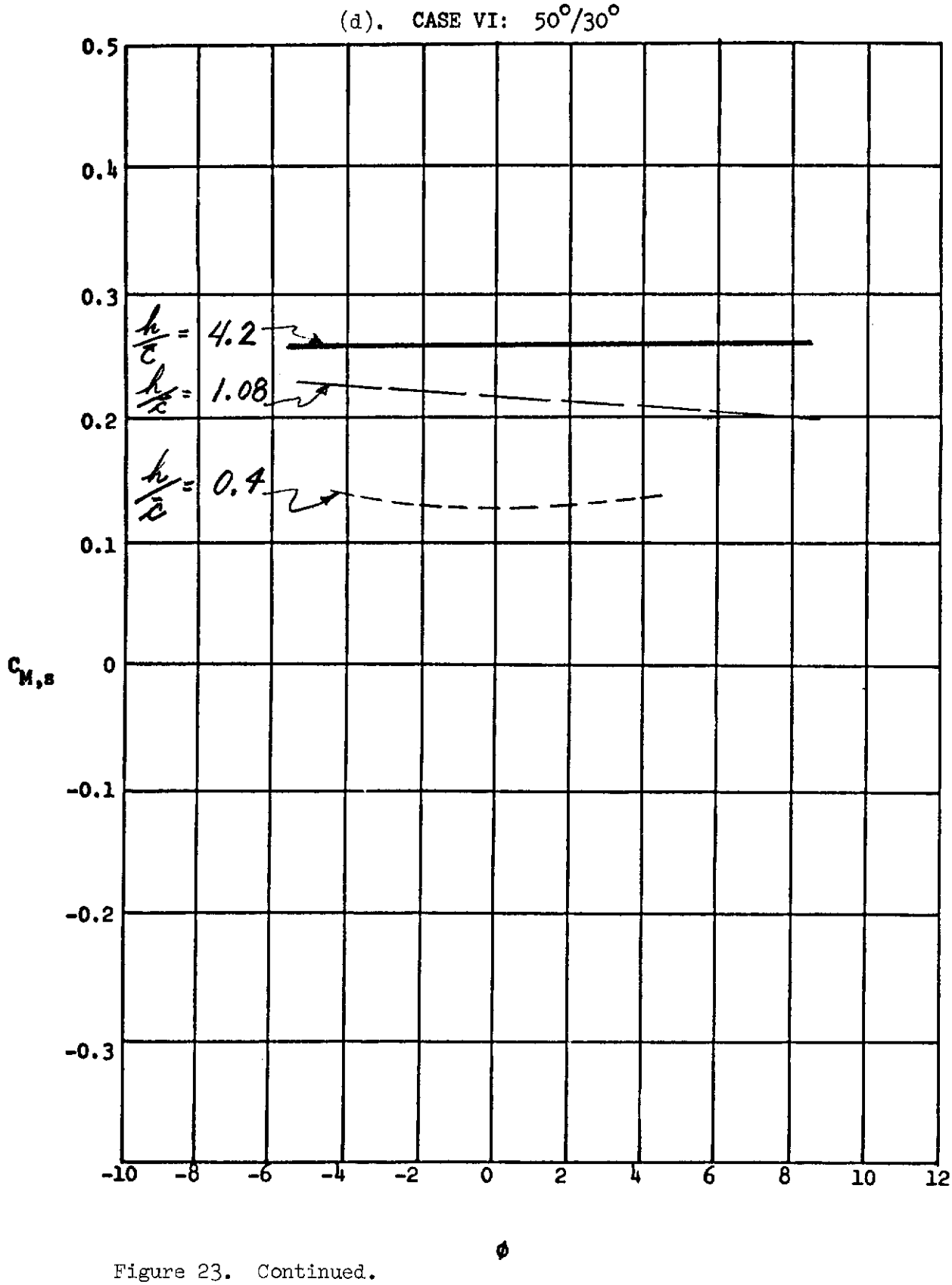

Figure 23. Continued.

Approved for Public Release

Contrails

(e). CASE VI: 50°/30°

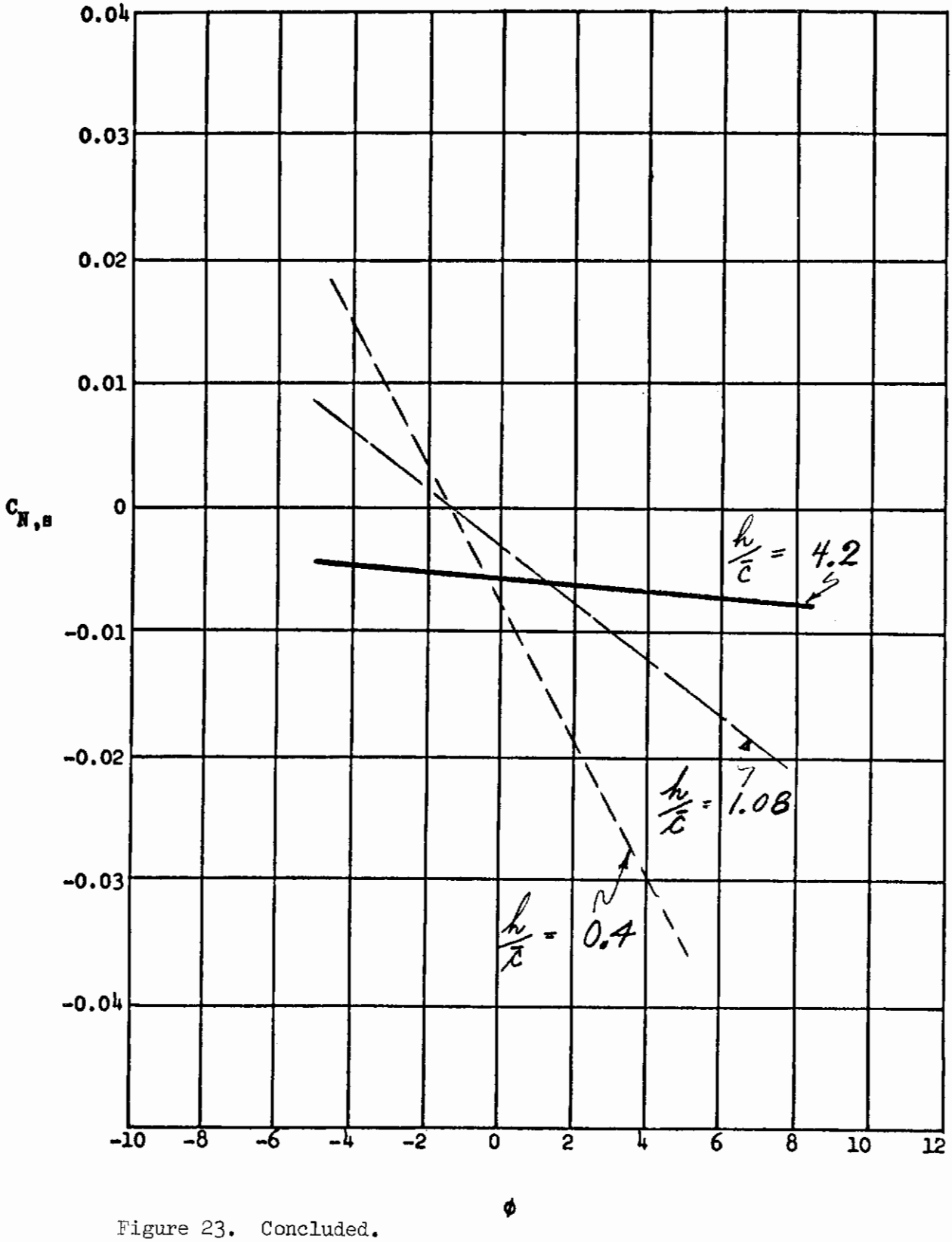

Figure 23. Concluded.

Approved for Public Release

Contrails

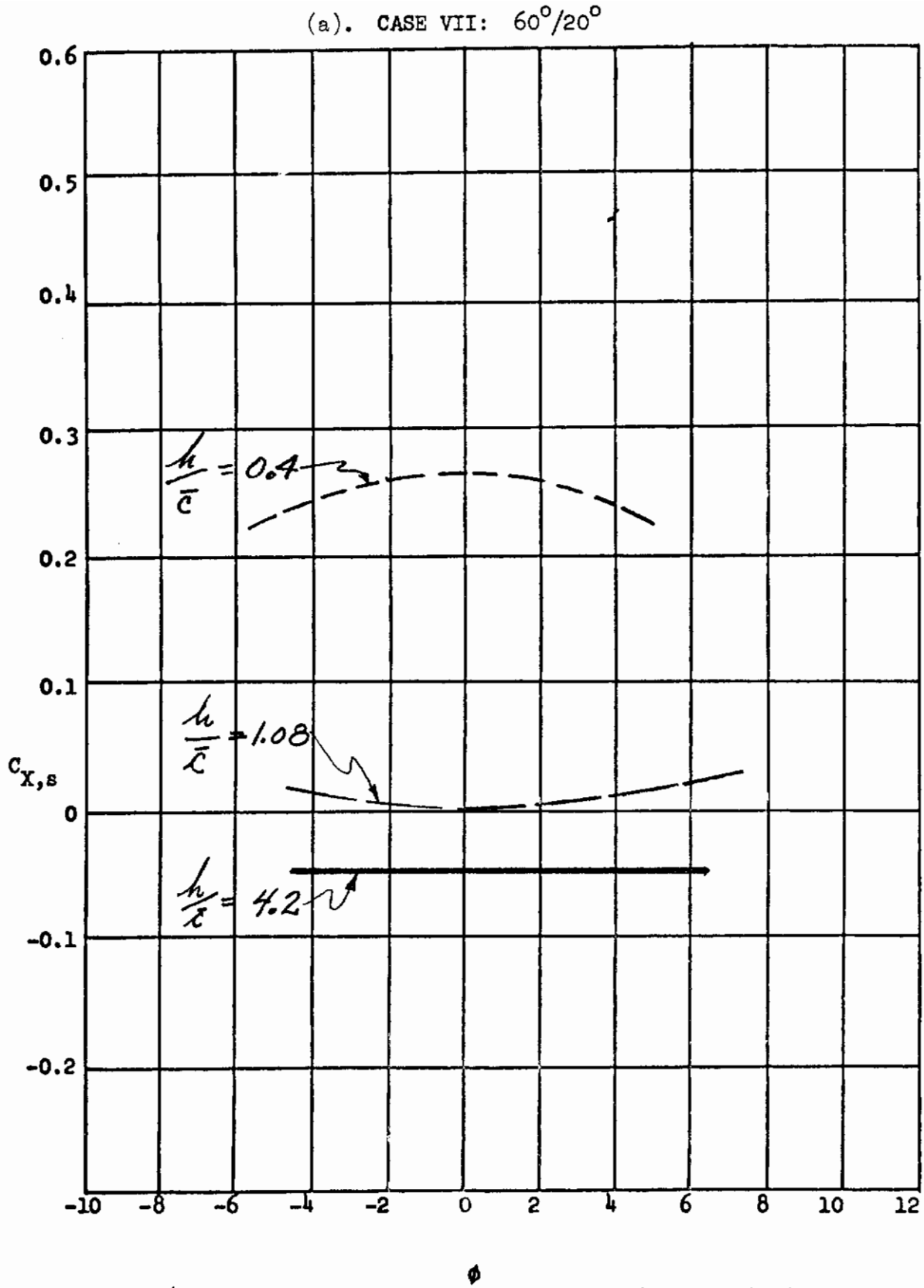

Figure 24. Longitudinal and lateral aerodynamic characteristics versus roll angle at three altitude ratios.

Approved for Public Release

Contrails

(b). CASE VII: 60°/20°

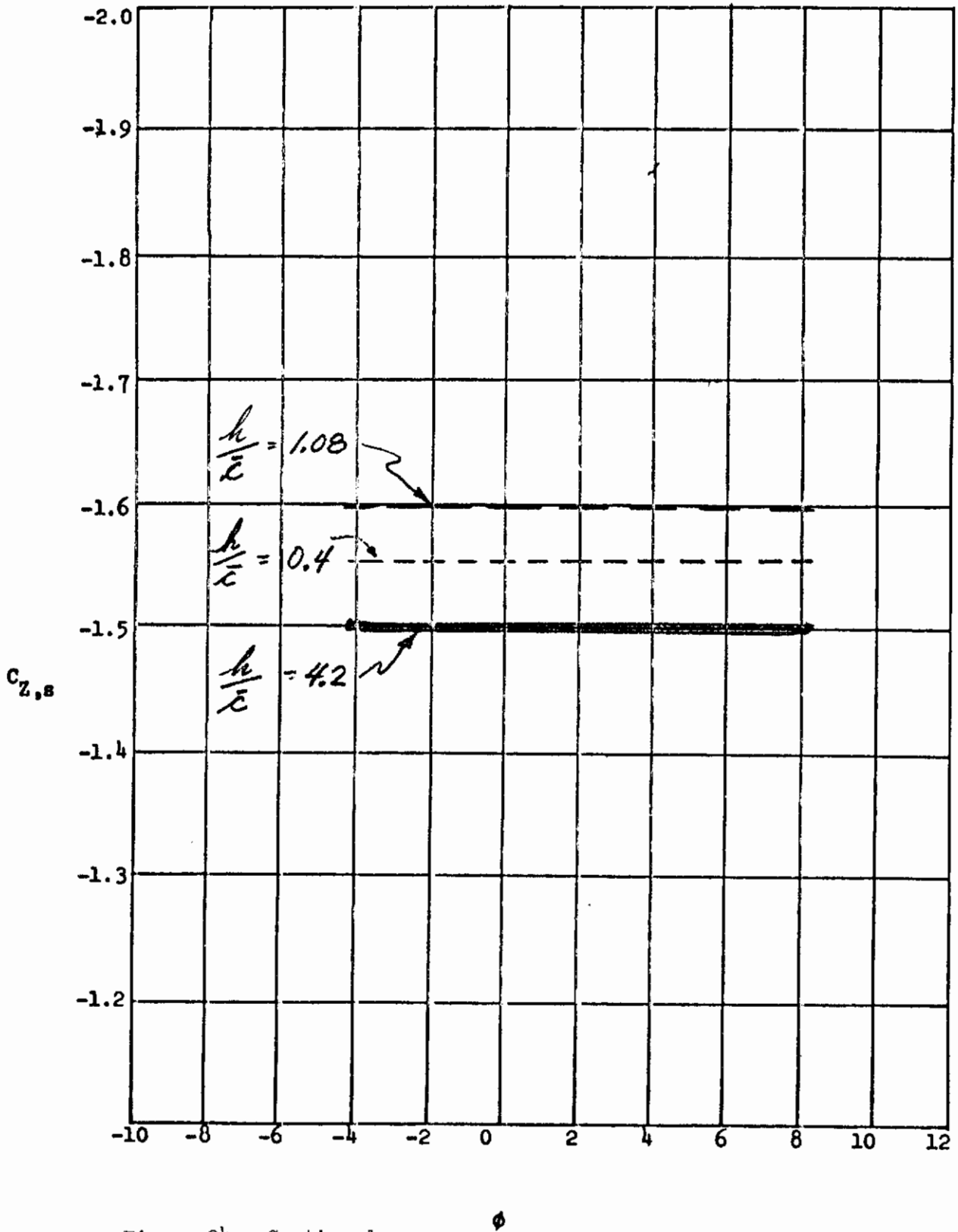

Figure 24. Continued.

Approved for Public Release

Contrails

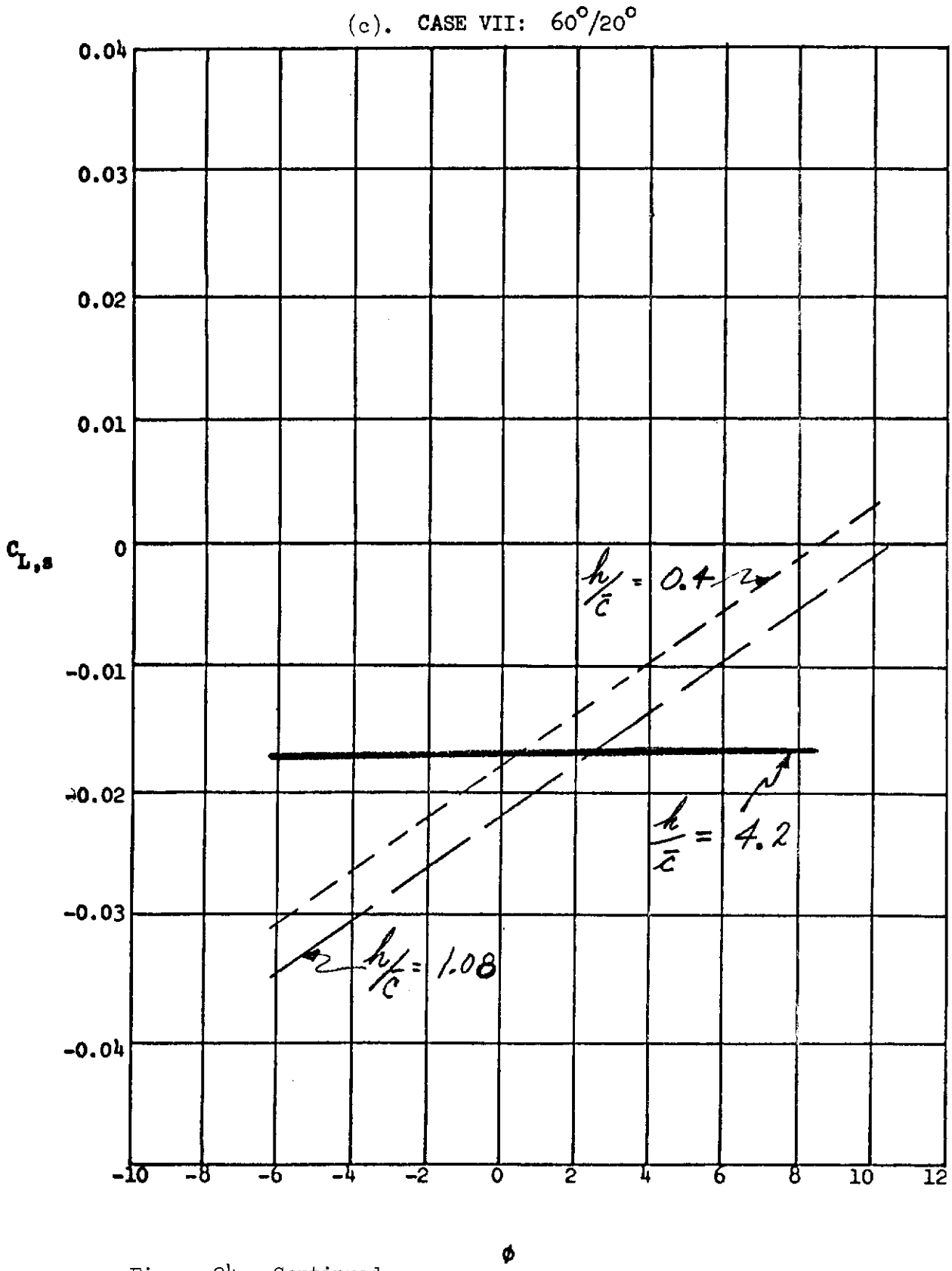

Figure 24. Continued.

Approved for Public Release

Contrails

(d). CASE VII: 60°/20°

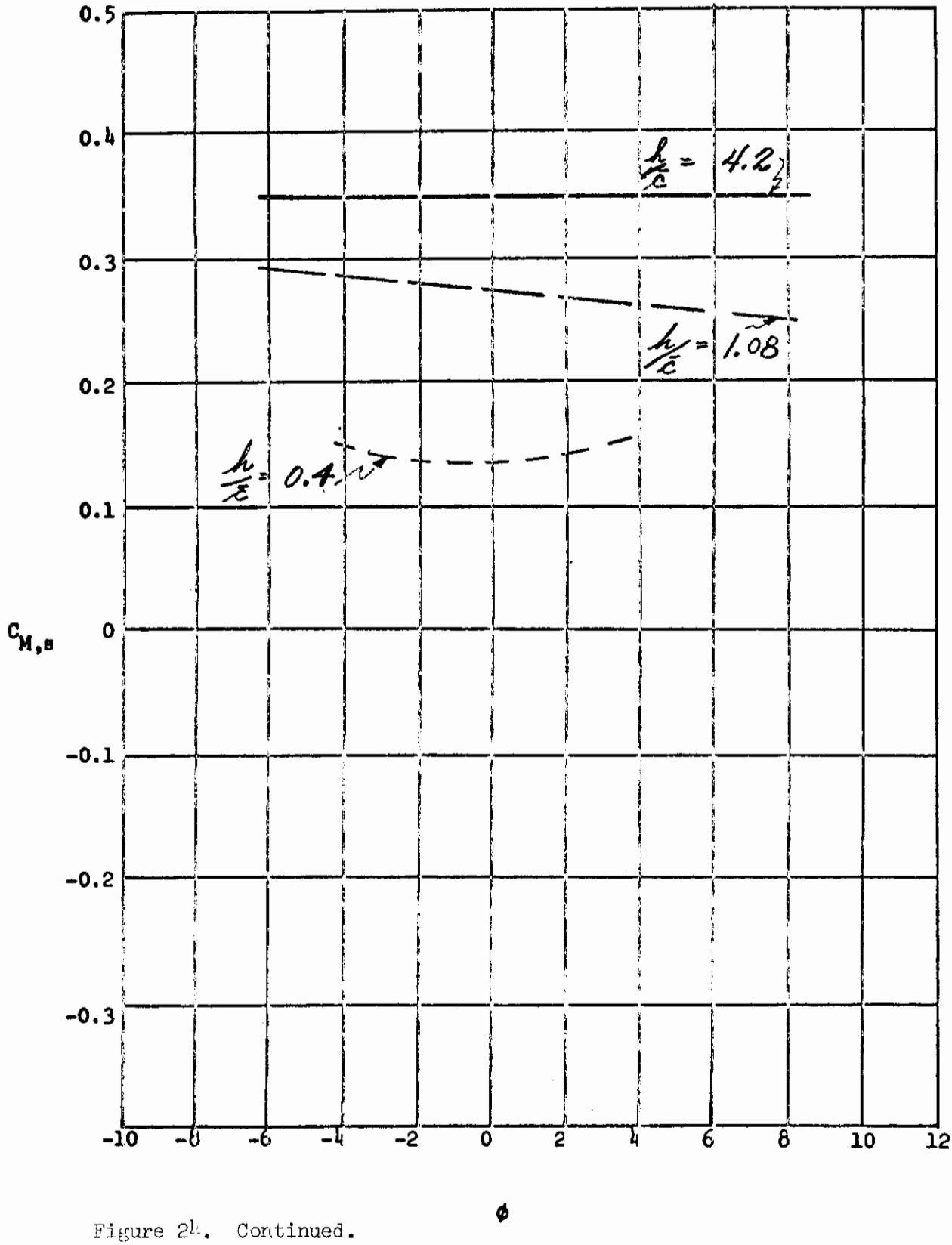

Figure 24. Continued.

Approved for Public Release

Contrails

(e). CASE VII: 60°/20°

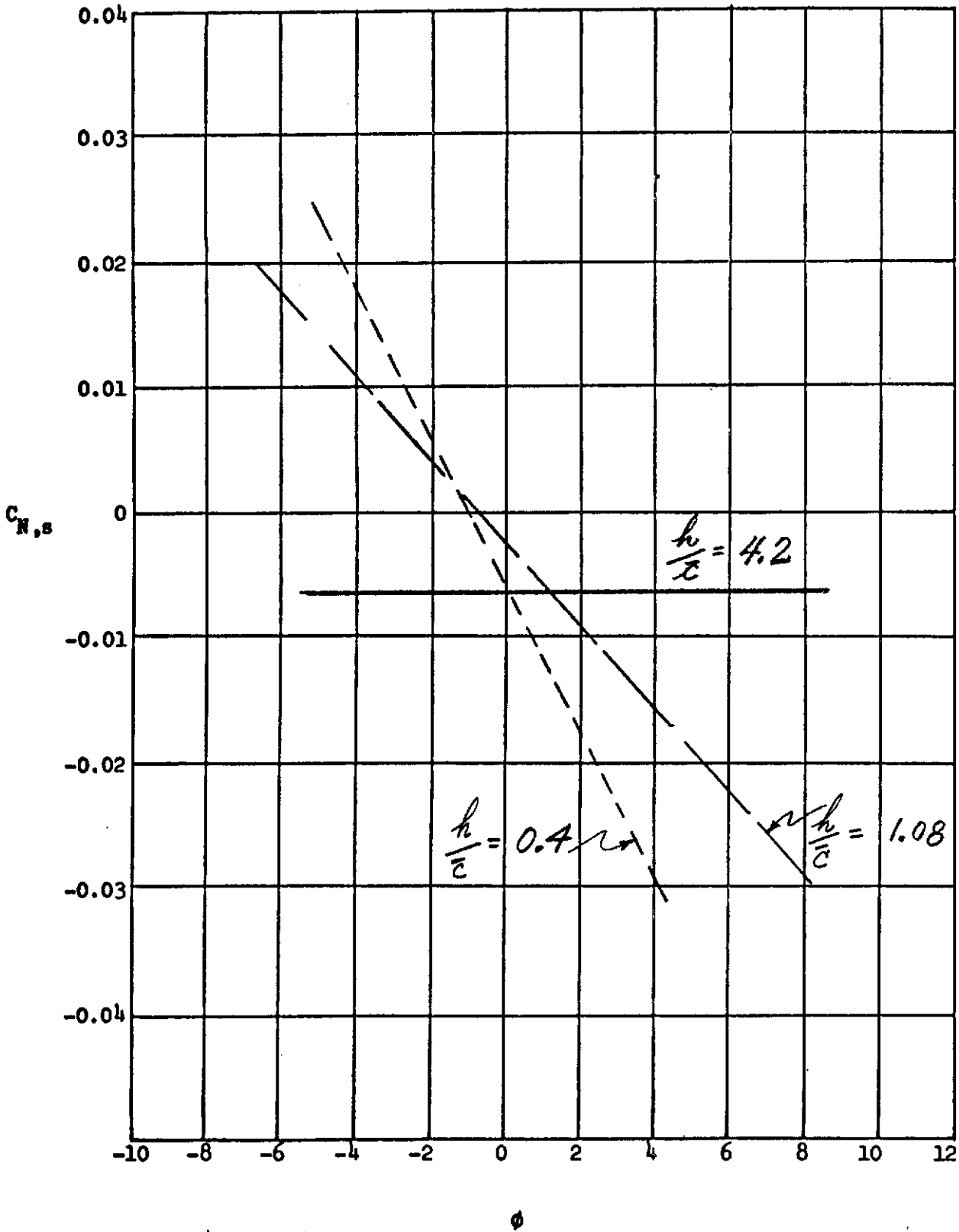

Figure 24. Concluded.

Approved for Public Release

Contrails

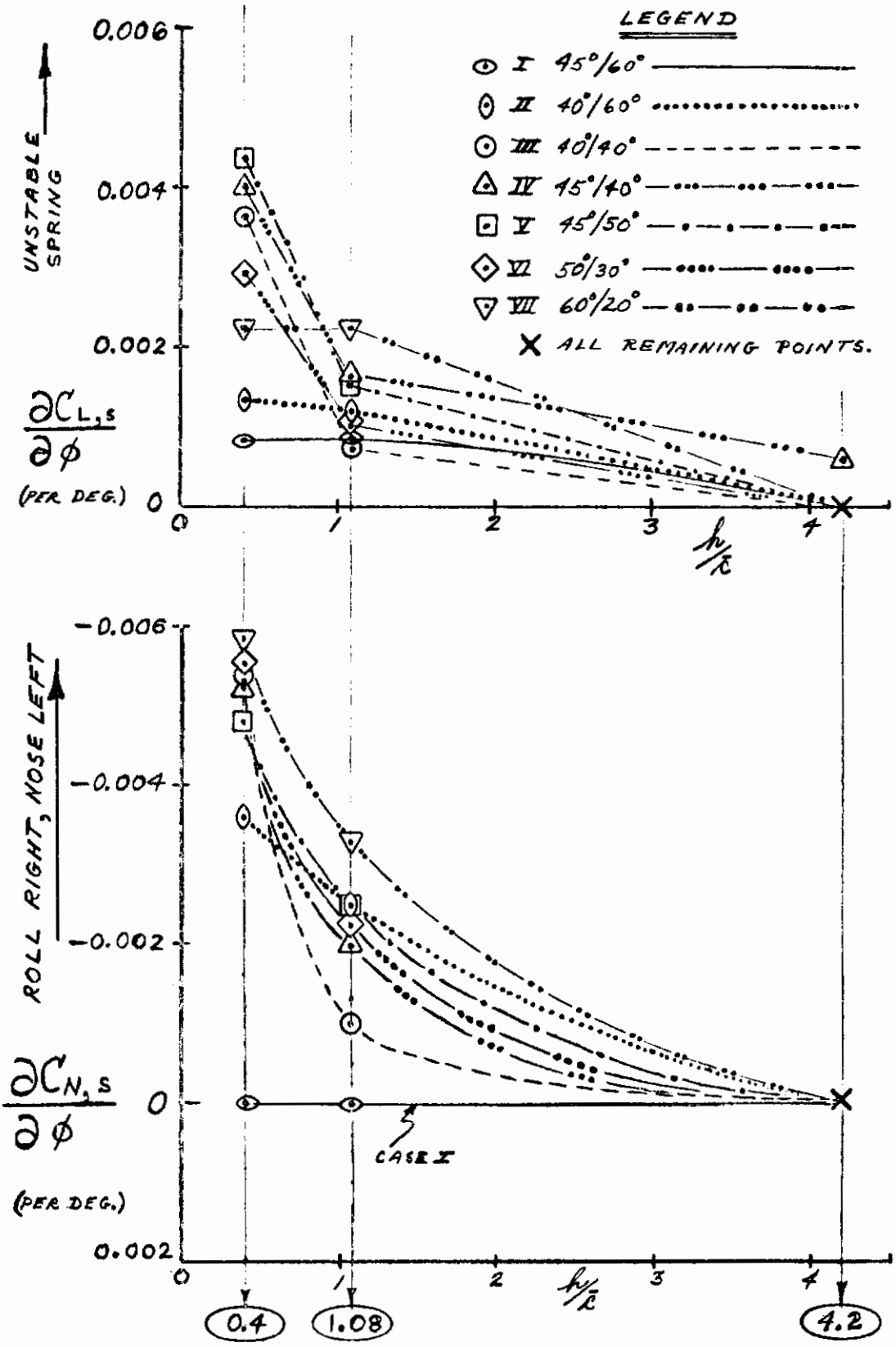

Figure 25. Rolling and yawing moment derivatives with roll angle versus altitude ratio.

Approved for Public Release

Contrails

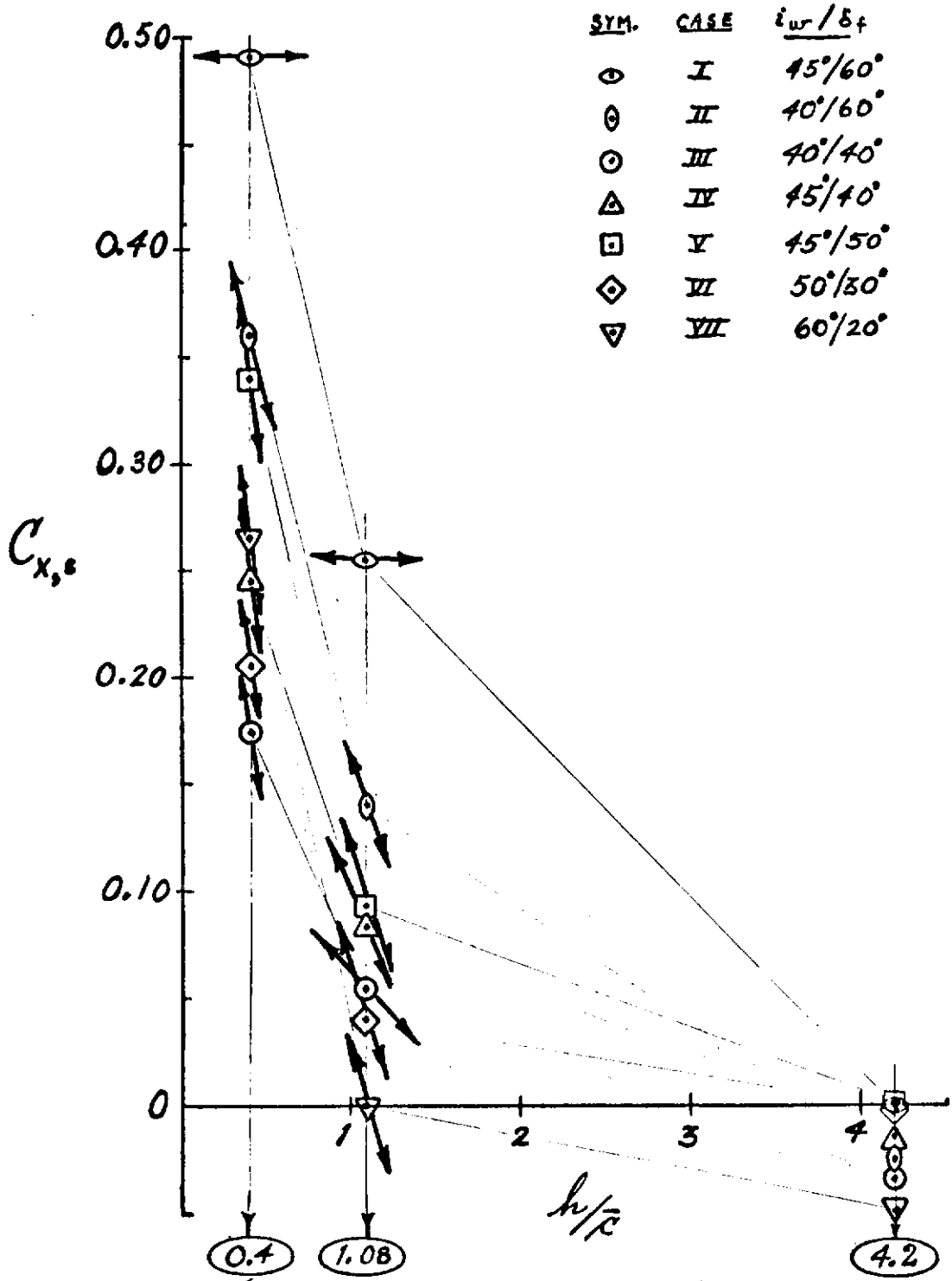

Figure 26. Local horizontal force variation with height predicted from yawing moment variation with roll angle.

Approved for Public Release

Contrails

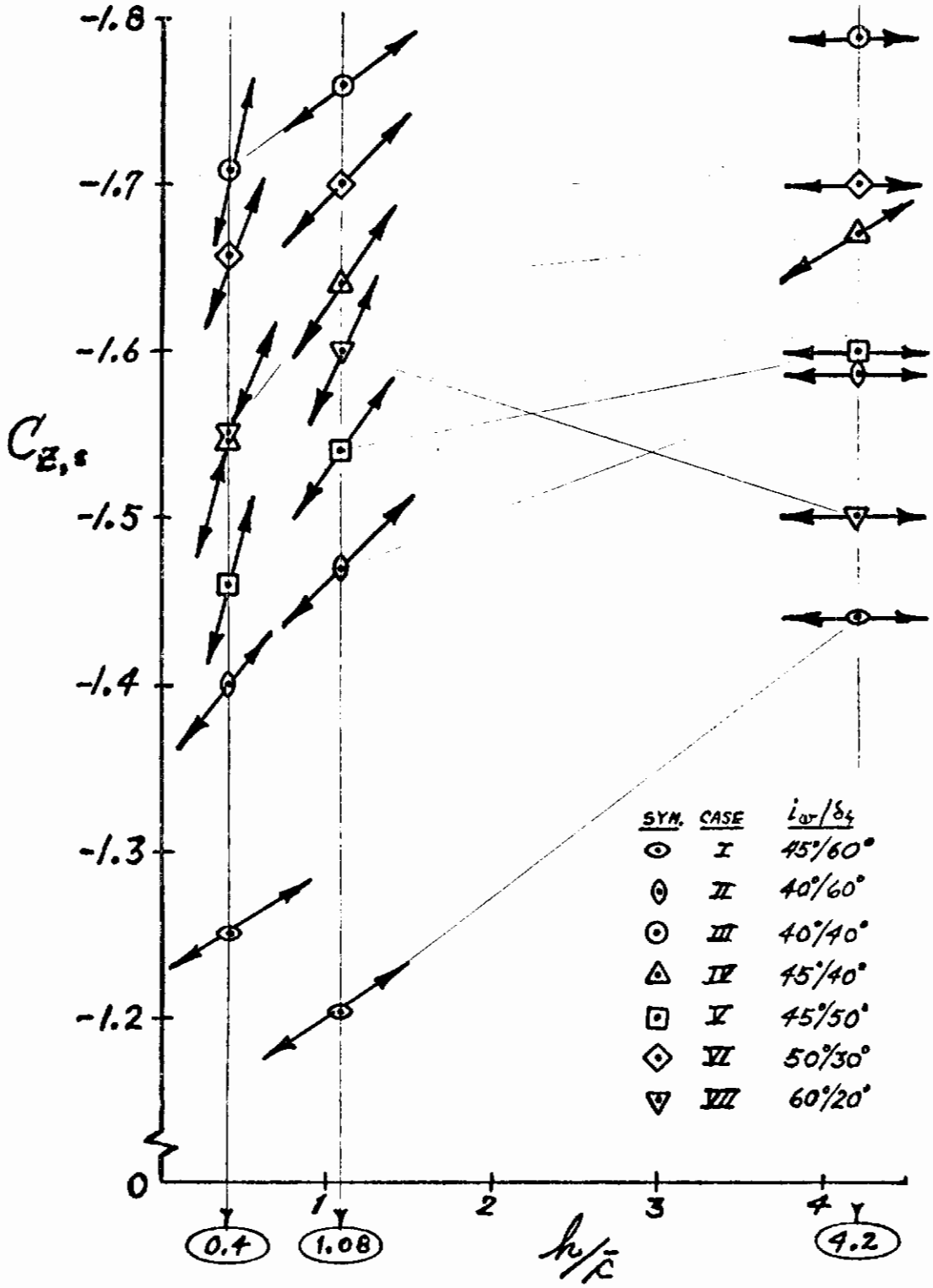

Figure 27. Local vertical force variation with height predicted from rolling moment variation with roll angle.

Approved for Public Release

Contrails

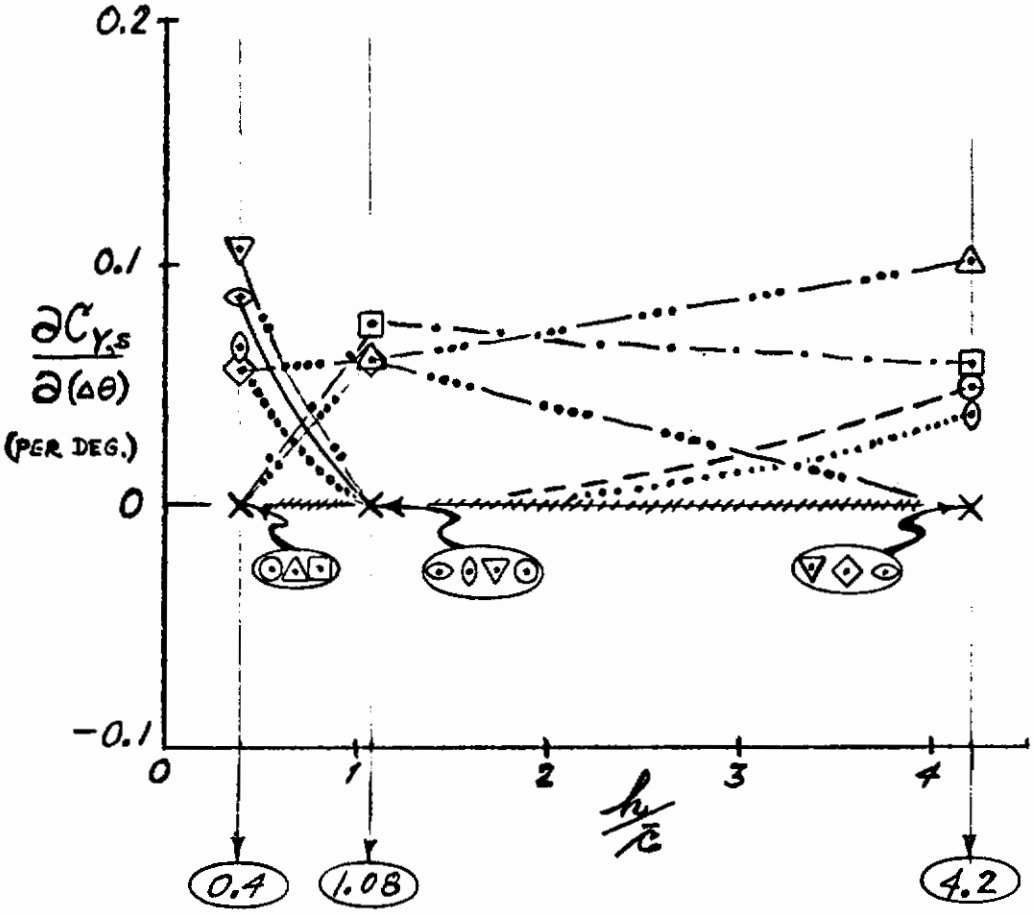

LEGEND

I	45°/60° ————	V	45°/50° — • — • —
II	40°/60°	VI	50°/30° — •••• — ••••
III	40°/40° - - - - - - - -	VII	60°/20° — •• — •• —
IV	45/40° — ••• — ••• — •••		ALL REMAINING POINTS

(a). Side force/differential pitch derivative

Figure 28. Lateral/directional control effectiveness derivatives versus altitude ratio.

Approved for Public Release

Contrails

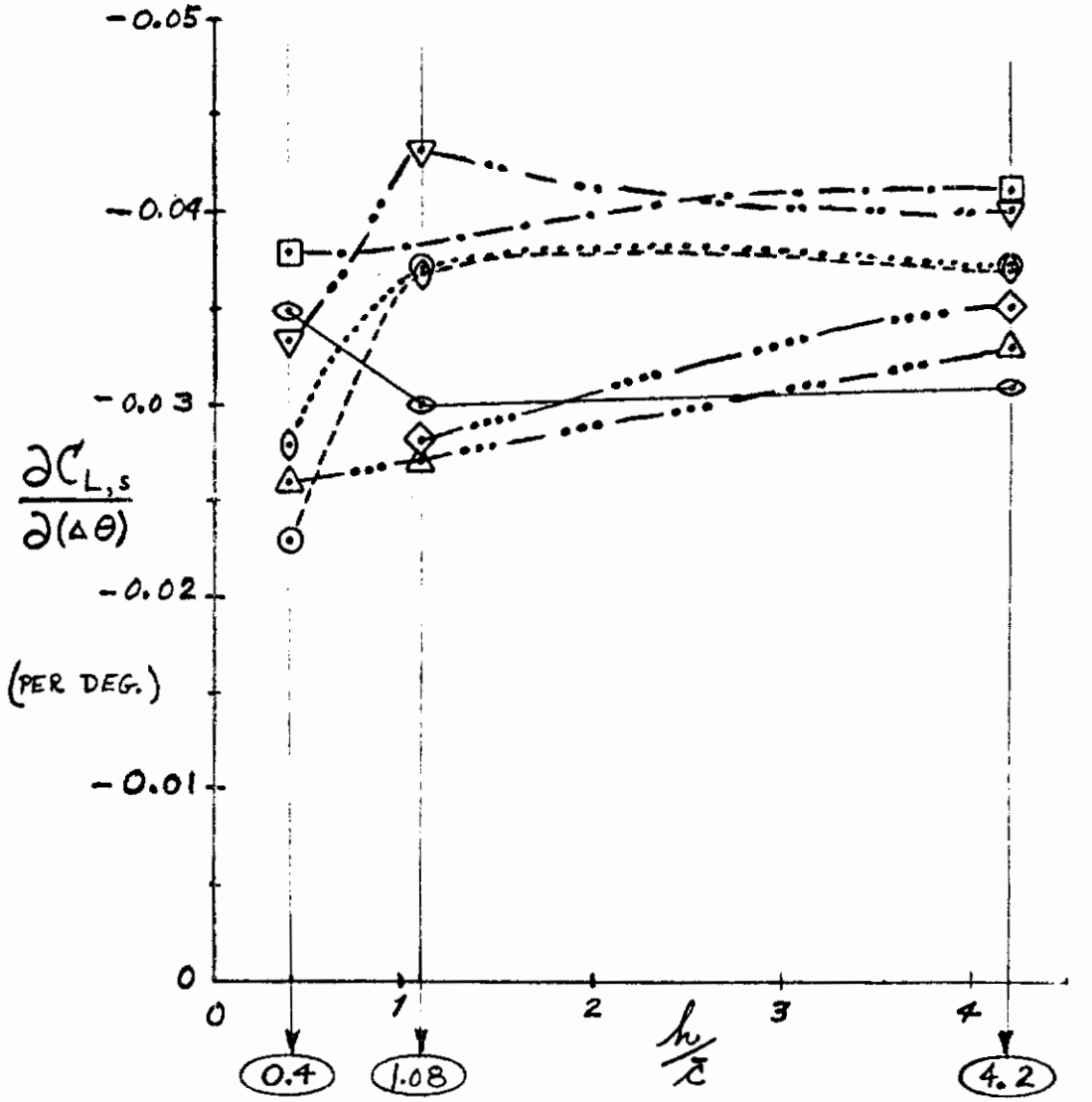

(b). Rolling moment/differential pitch derivative.

Figure 28. Continued.

Approved for Public Release

Contrails

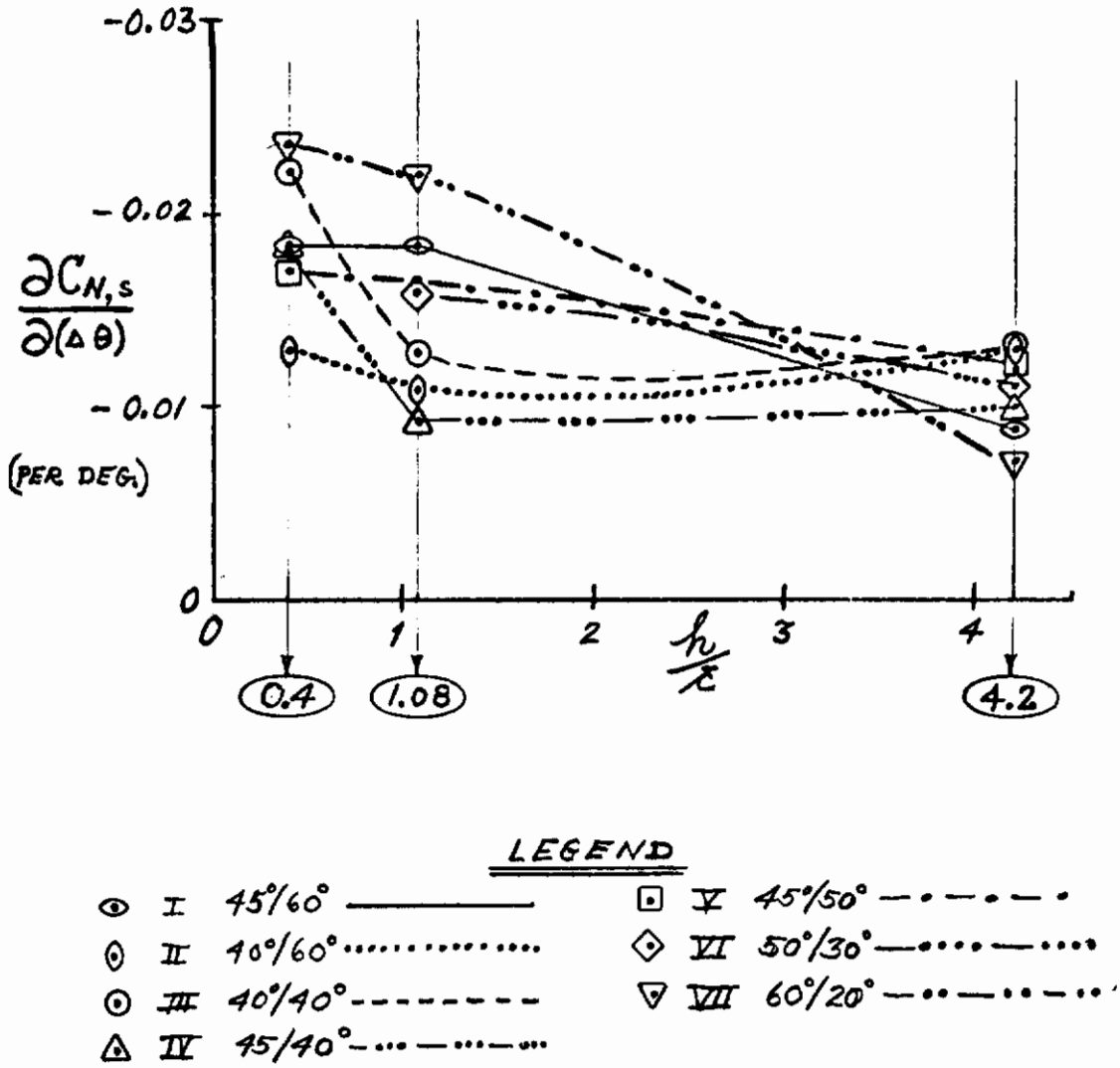

(c). Yawing moment/differential pitch derivative.

Figure 28. Concluded.

Approved for Public Release

Contrails

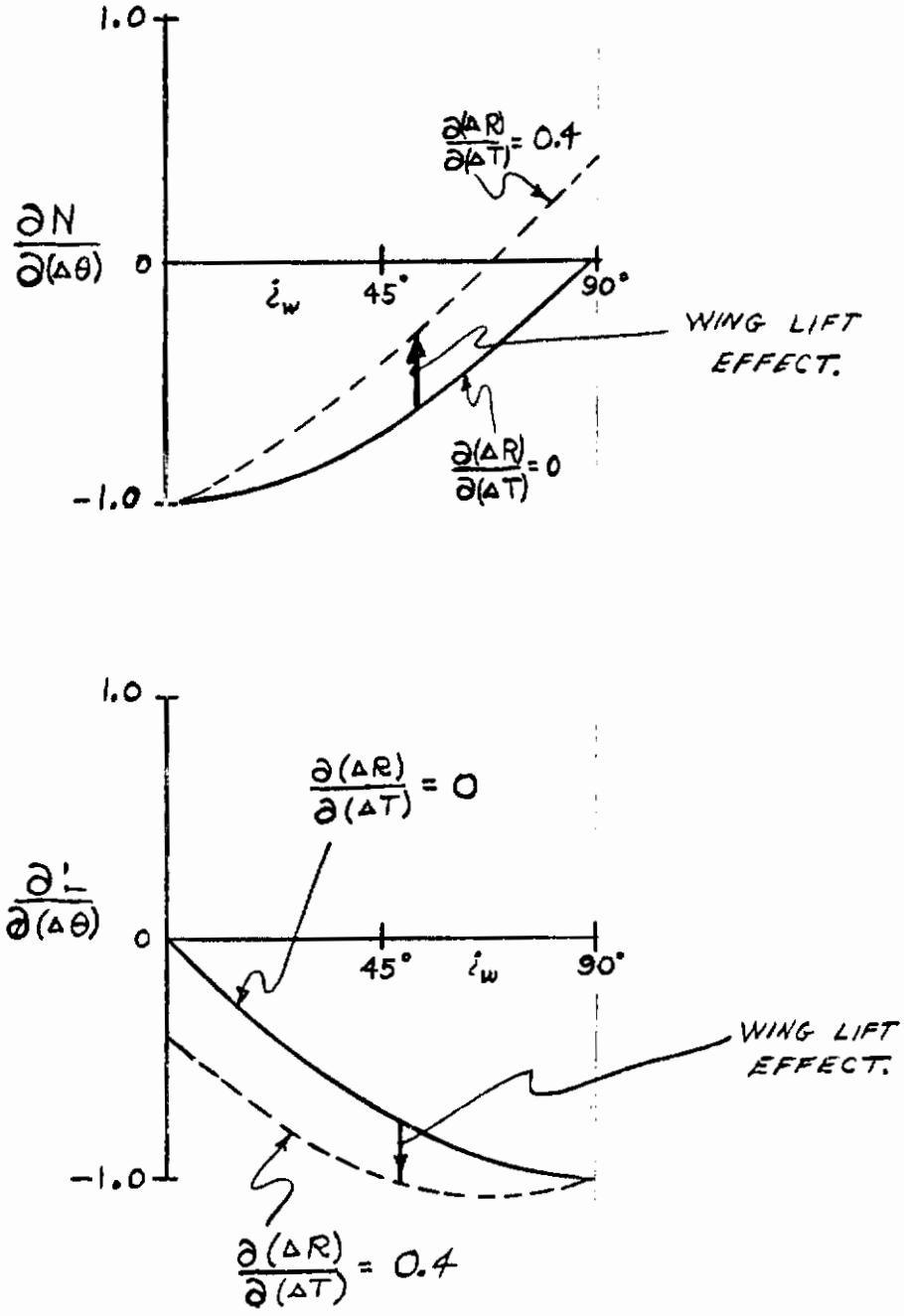

Figure 29. Results of simplified theory for differential pitch control effect.

Approved for Public Release

Contrails

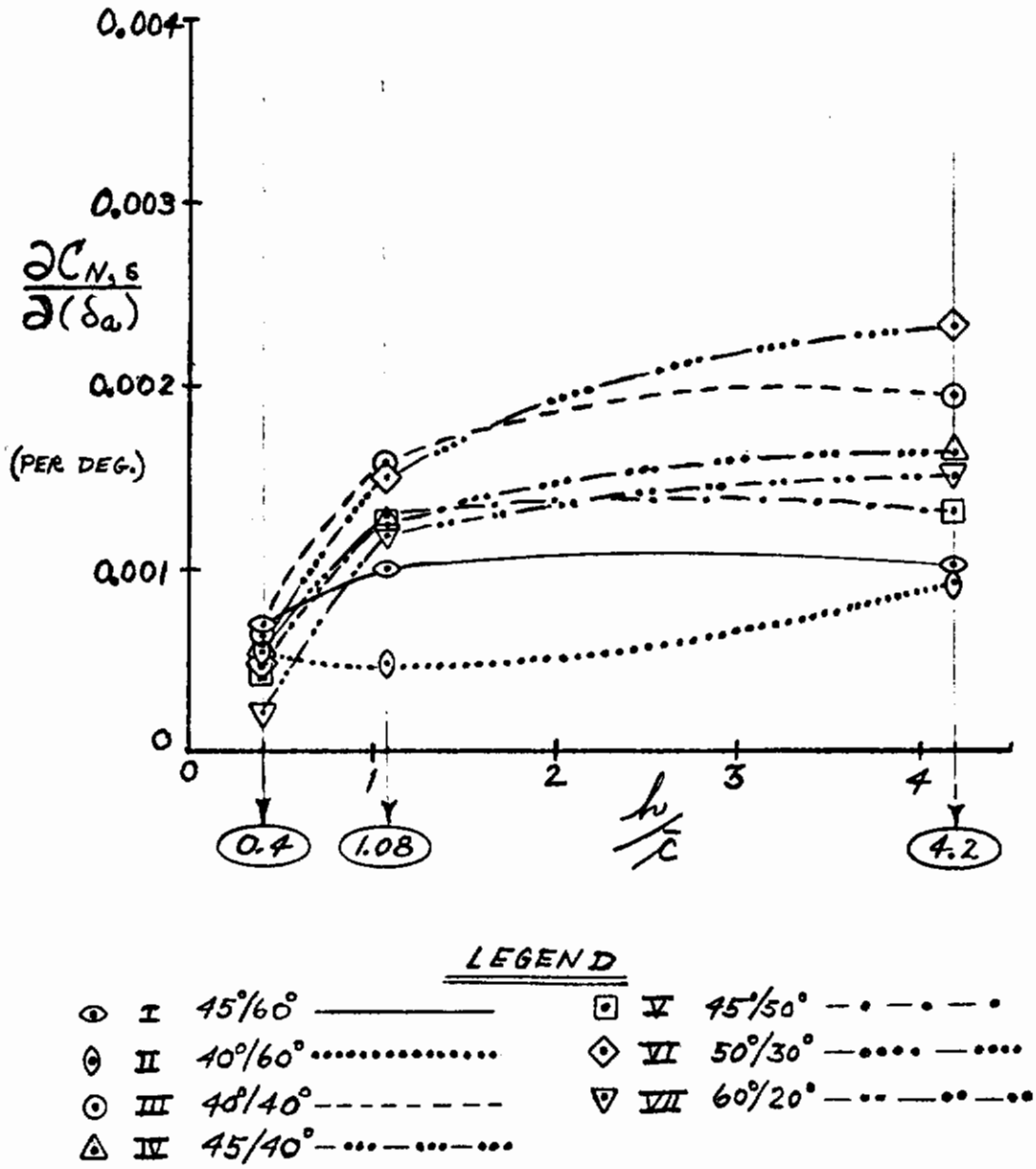

Figure 30. Yawing moment/aileron control effectiveness derivative versus altitude ratio.

Approved for Public Release

Contrails

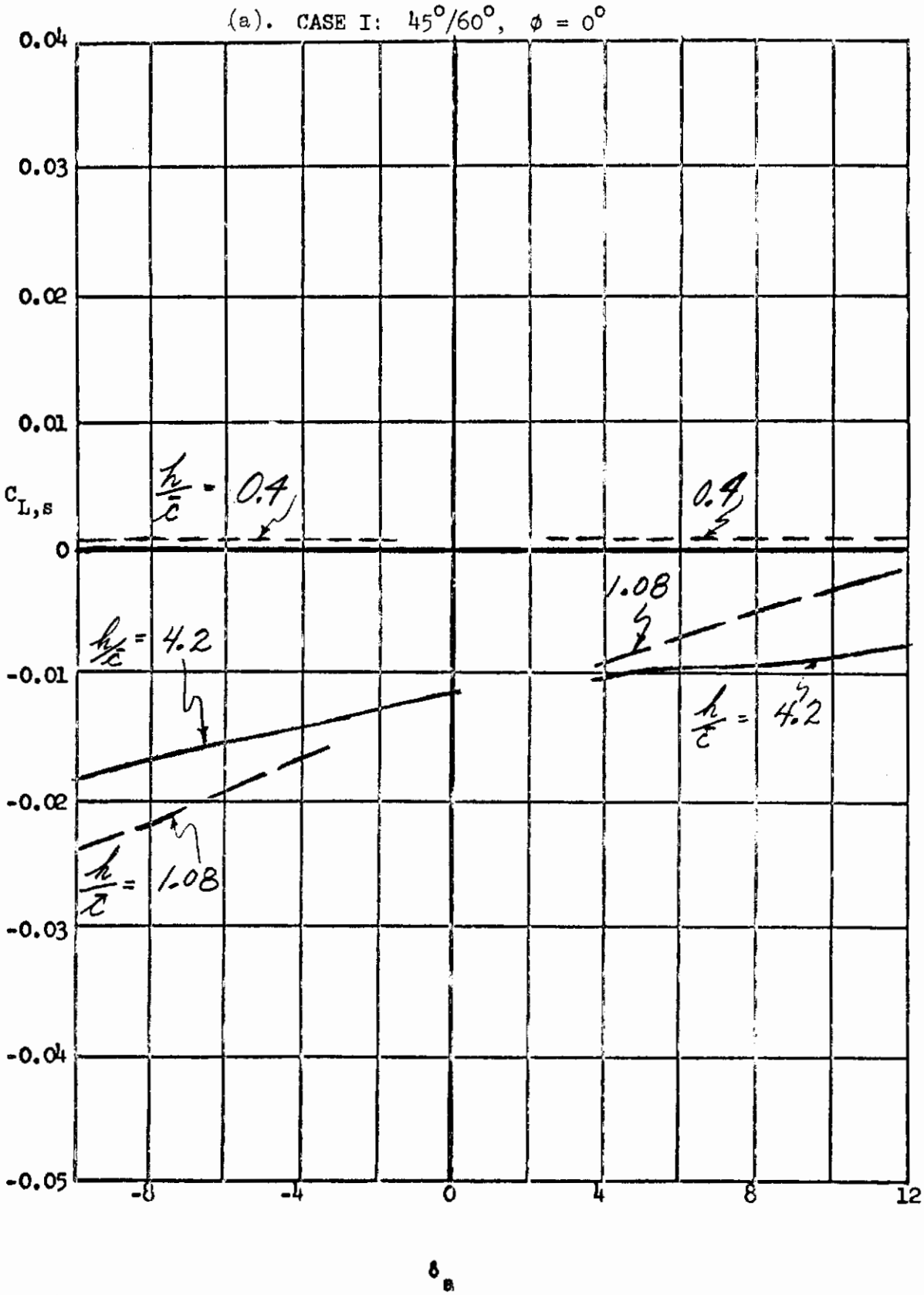

Figure 31. Rolling characteristic versus aileron deflection at three altitude ratios.

Approved for Public Release

Contrails

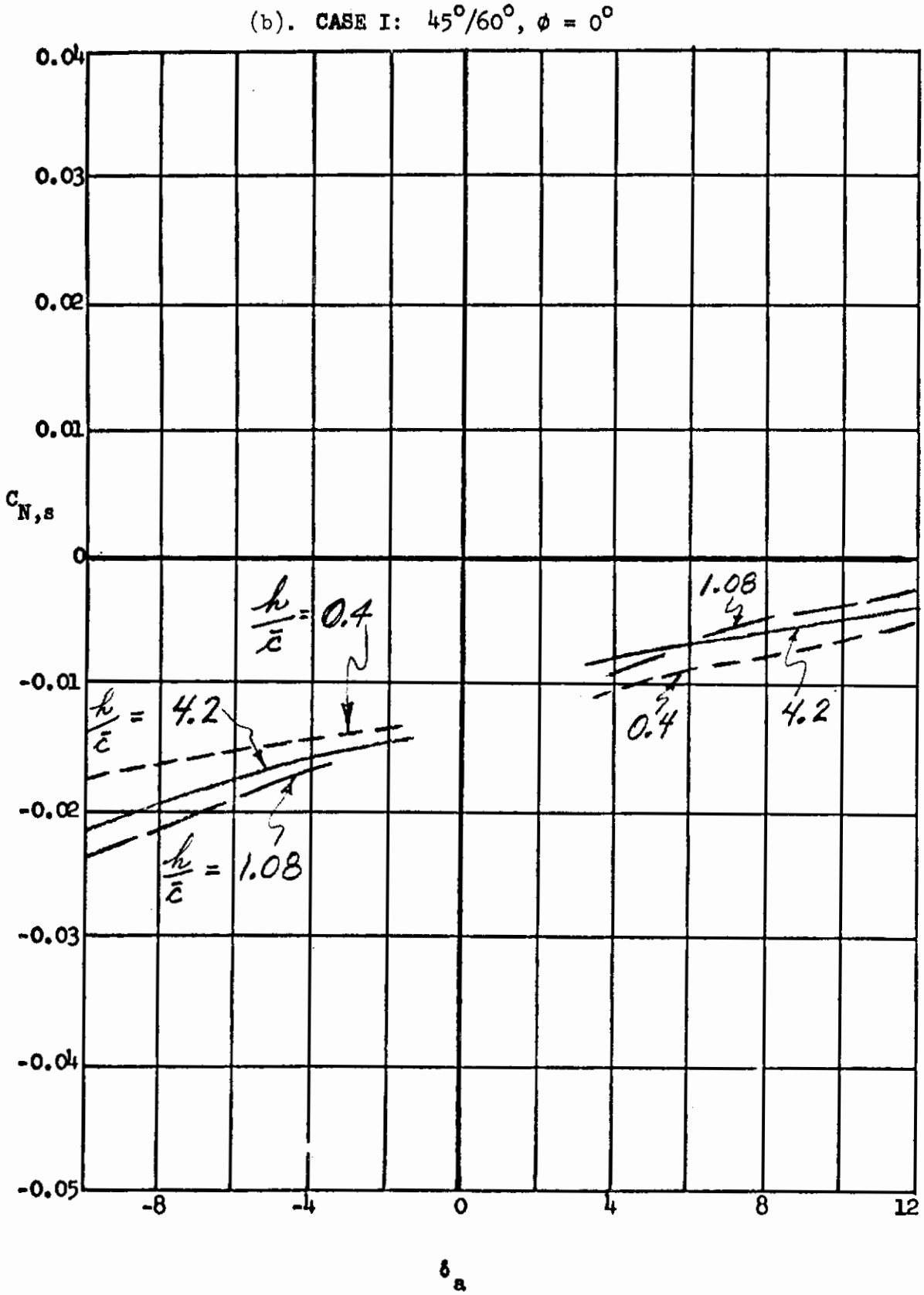

Figure 31. Yawing characteristic versus aileron deflection at three altitude ratios.

Approved for Public Release

Contrails

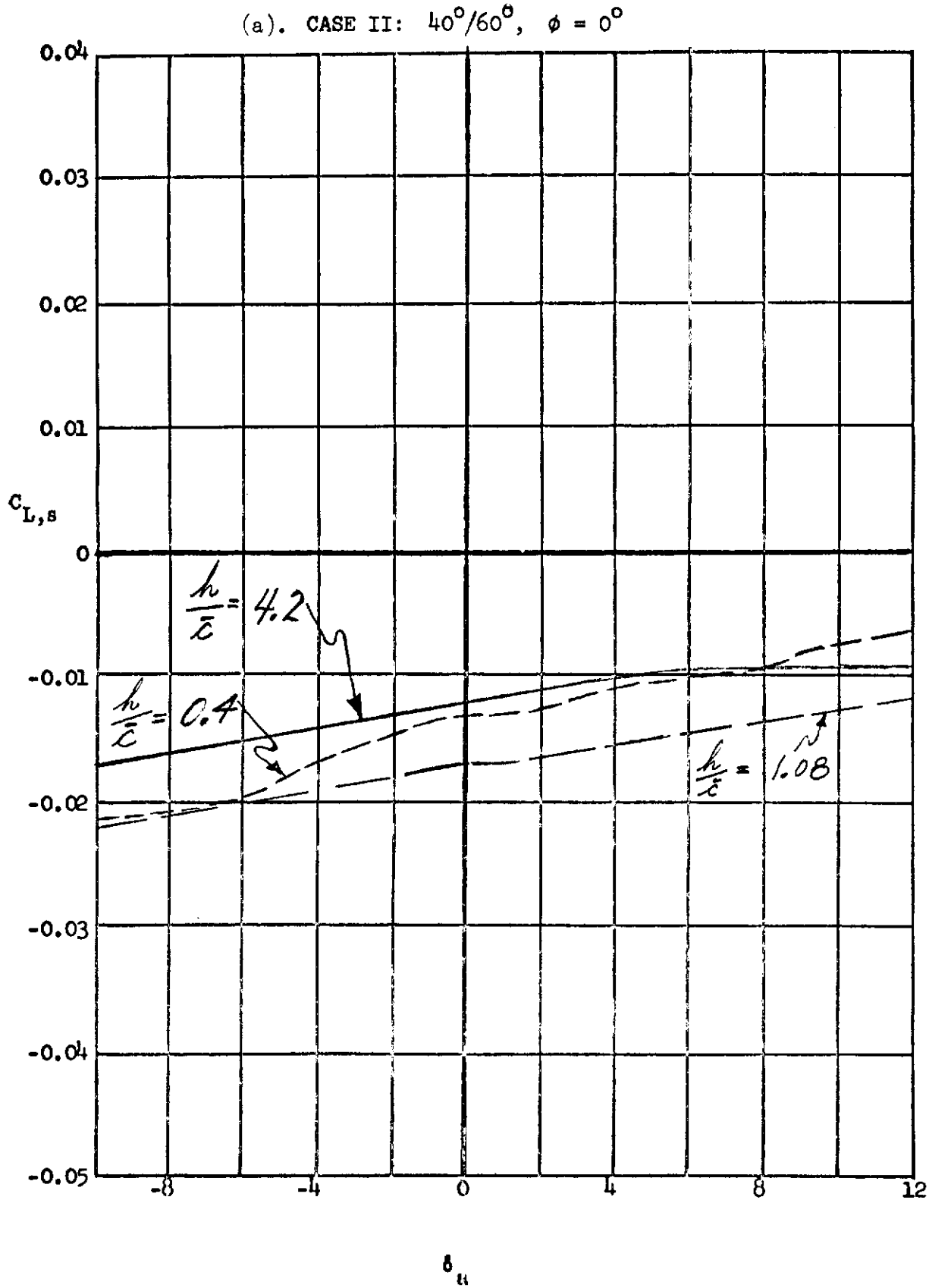

Figure 32. Rolling characteristic versus aileron deflection at three altitude ratios.

Approved for Public Release

Contrails

(b). CASE II: $40^\circ/60^\circ$, $\phi = 0^\circ$

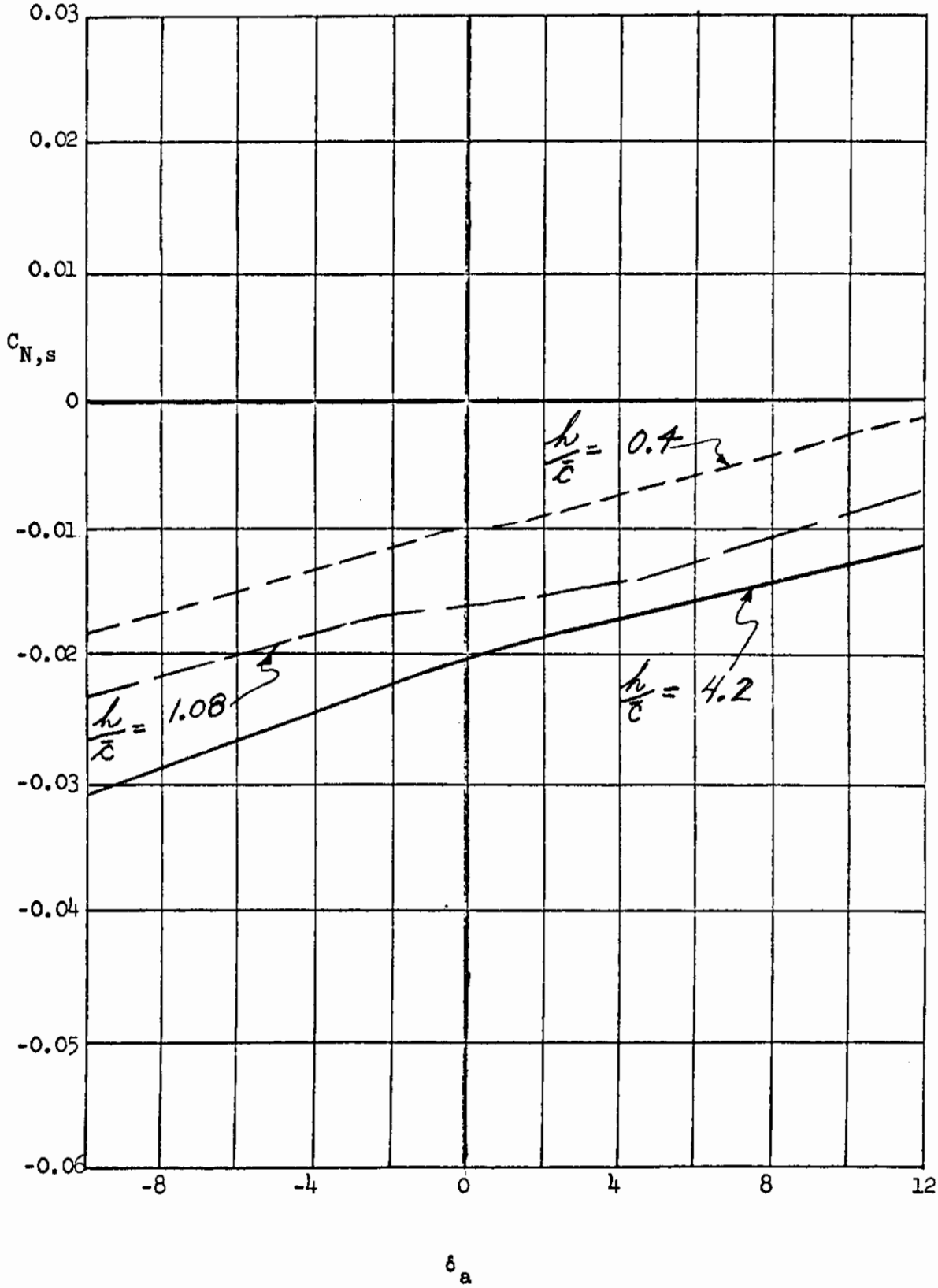

Figure 32. Yawing characteristic versus aileron deflection at three altitude ratios.

Approved for Public Release

Contrails

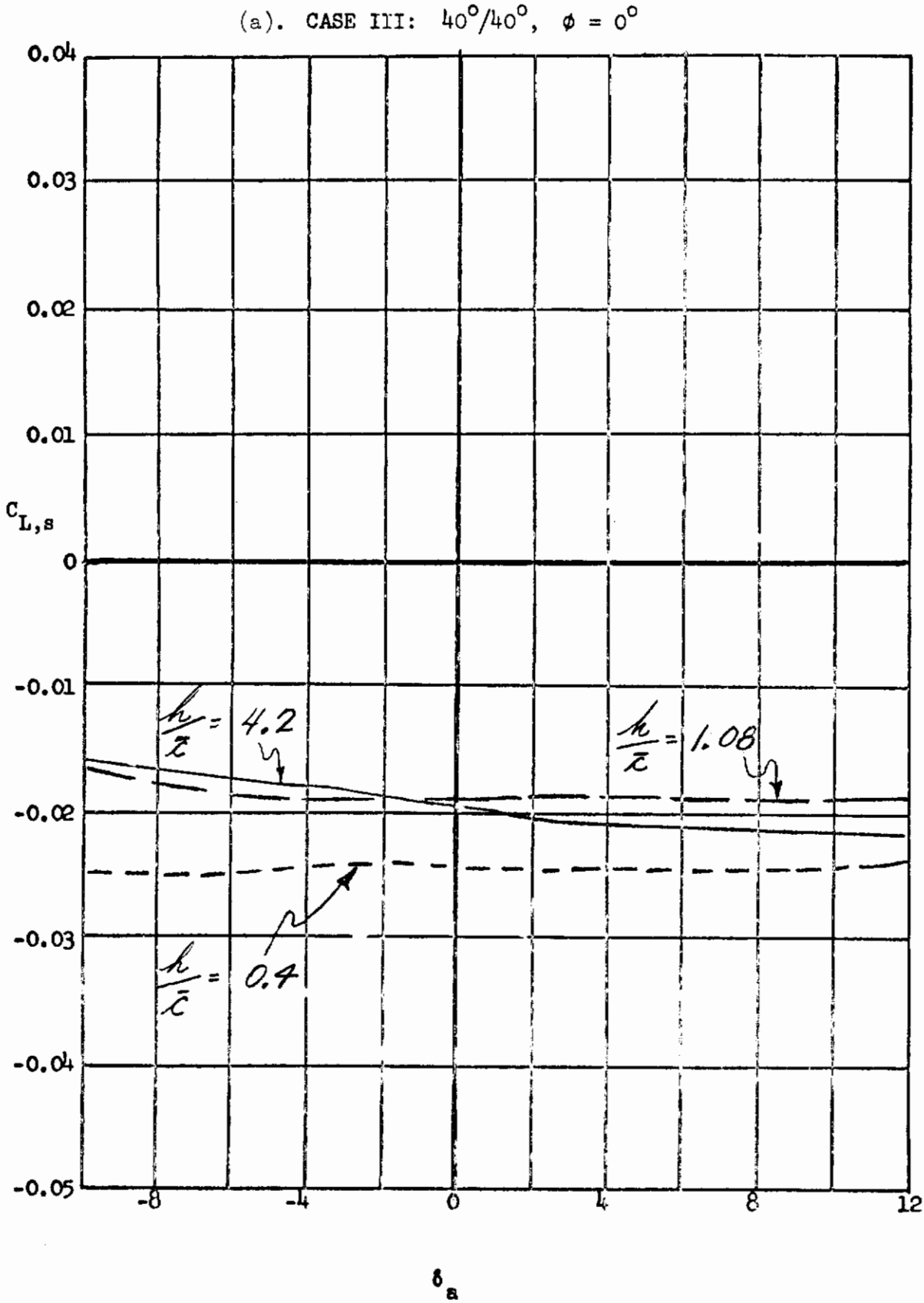

Figure 33. Rolling characteristic versus aileron deflection at three altitude ratios.

Approved for Public Release

Contrails

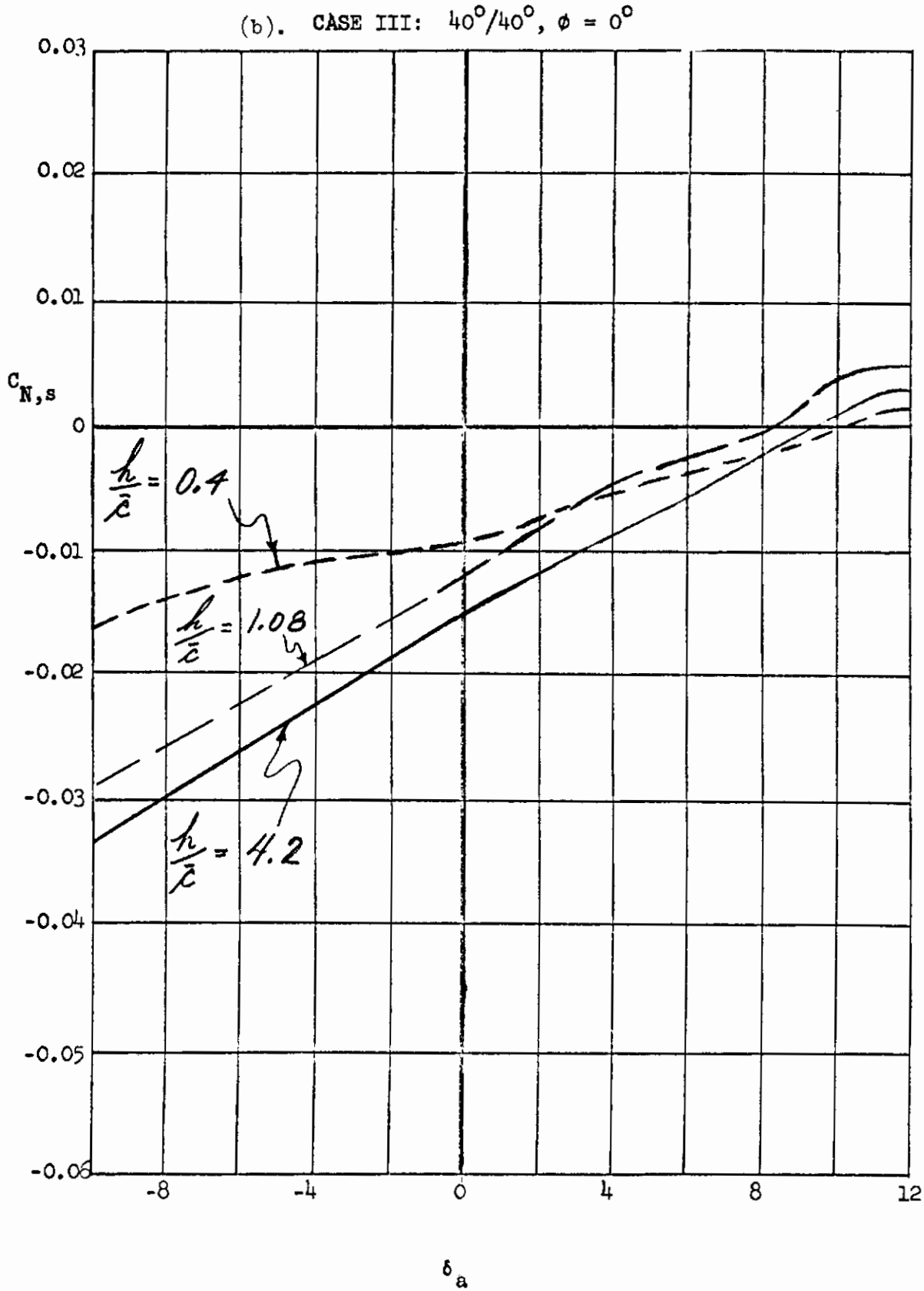

Figure 33. Yawing characteristic versus aileron deflection at three altitude ratios.

Approved for Public Release

Contrails

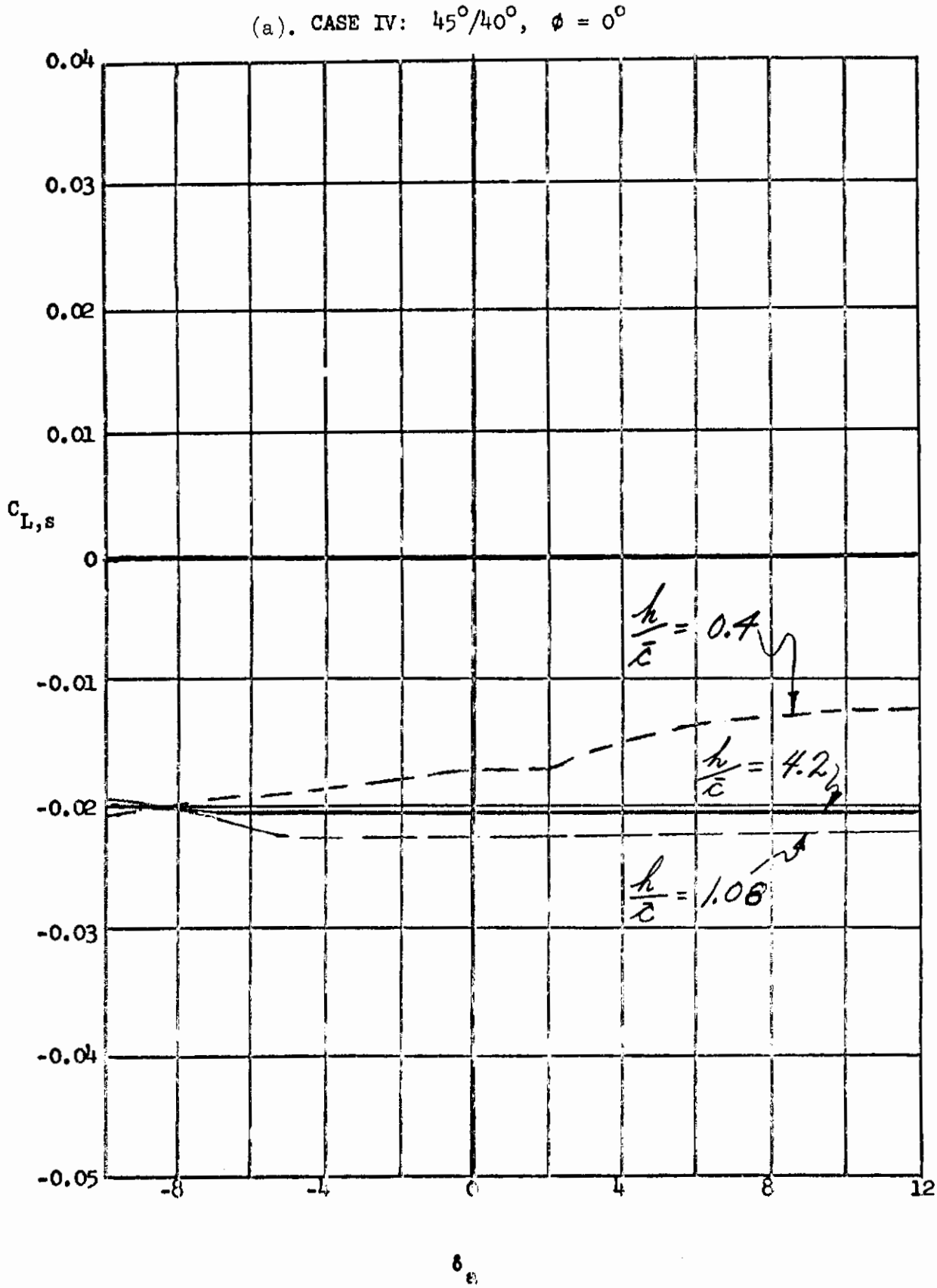

Figure 34. Rolling characteristic versus aileron deflection at three altitude ratios.

Approved for Public Release

Contrails

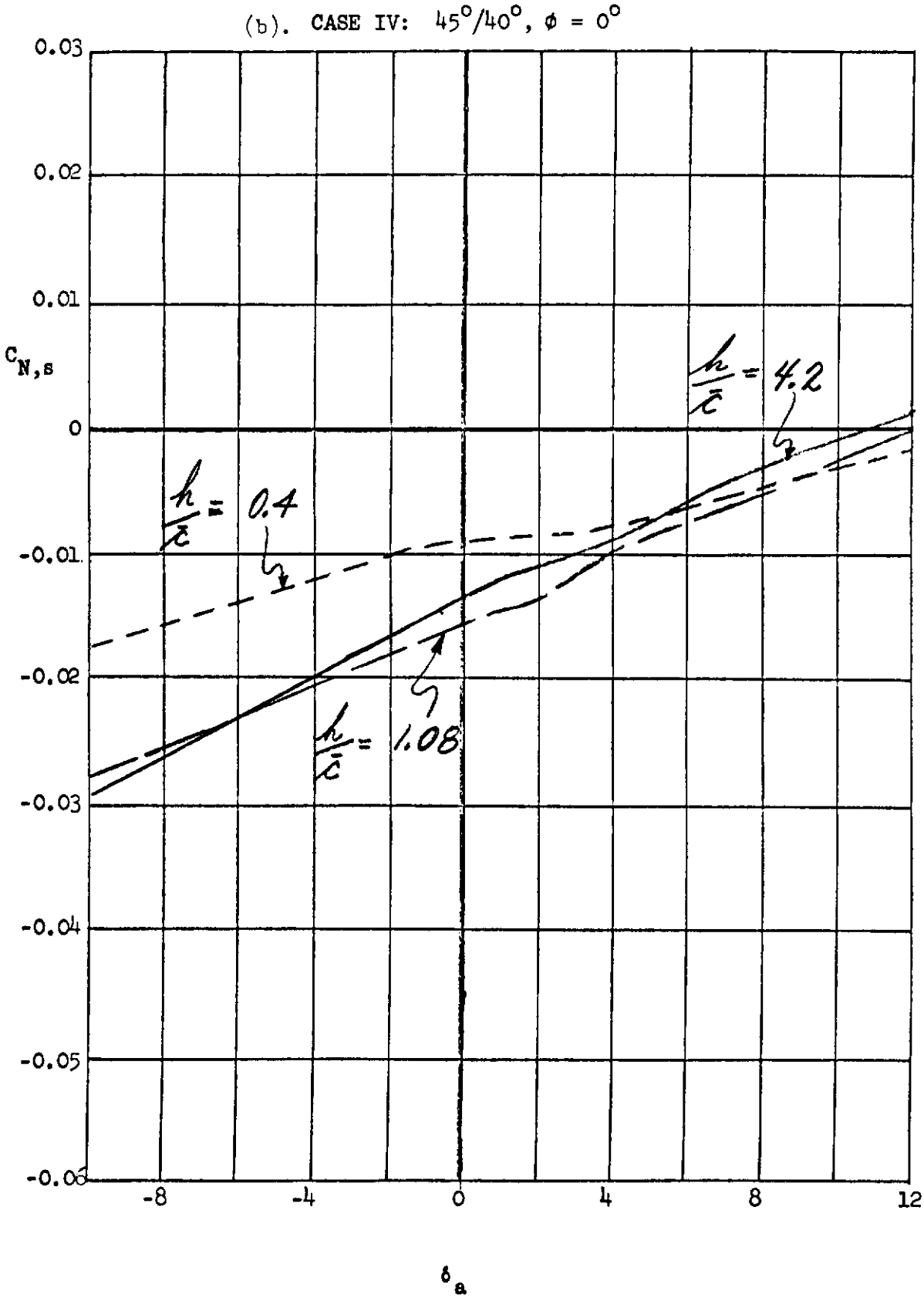

Figure 34. Yawing characteristic versus aileron deflection at three altitude ratios.

Approved for Public Release

Contrails

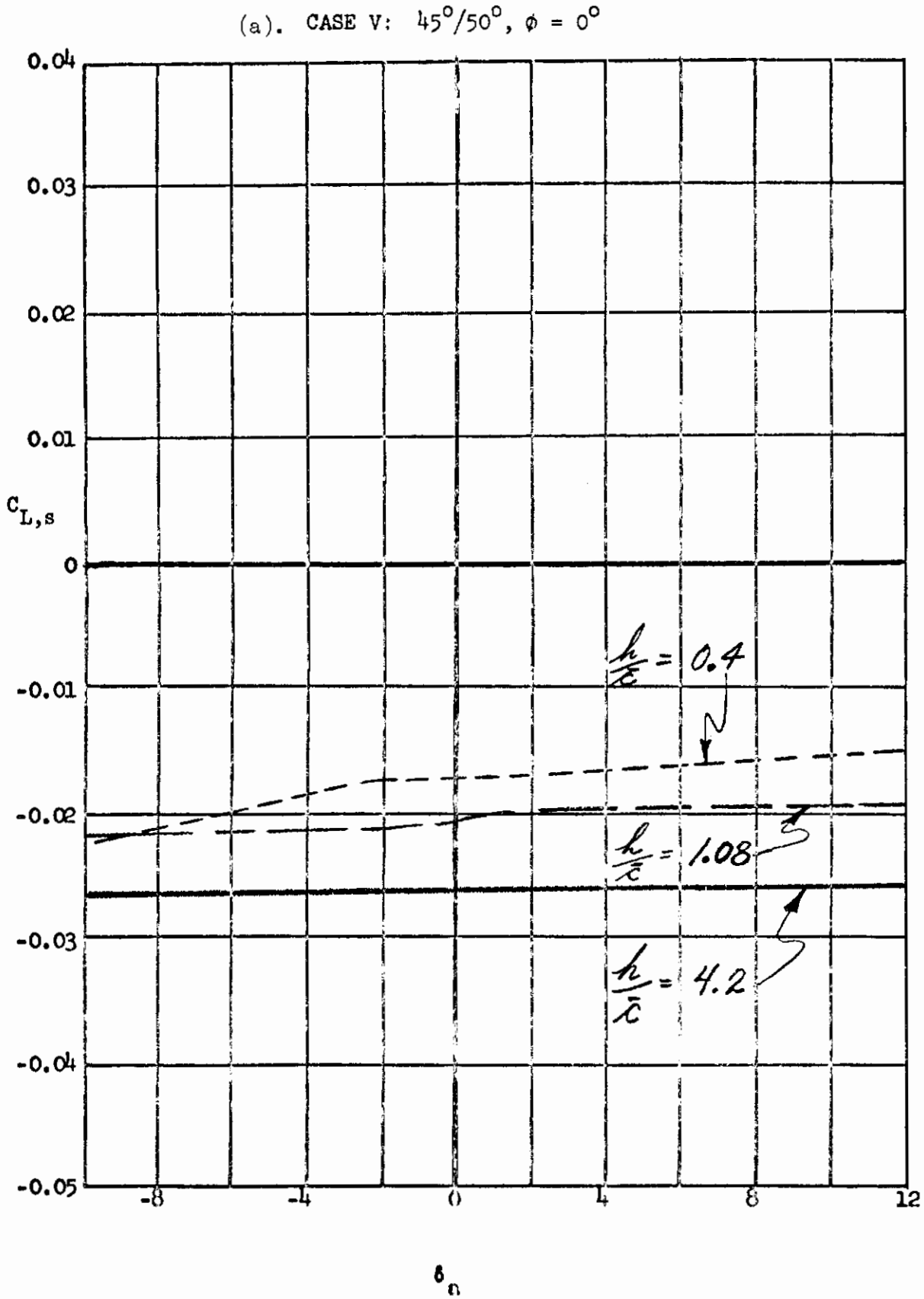

Figure 35. Rolling characteristic versus aileron deflection at three altitude ratios.

Approved for Public Release

Contrails

(b). CASE V: 45°/50°, ϕ = 0°

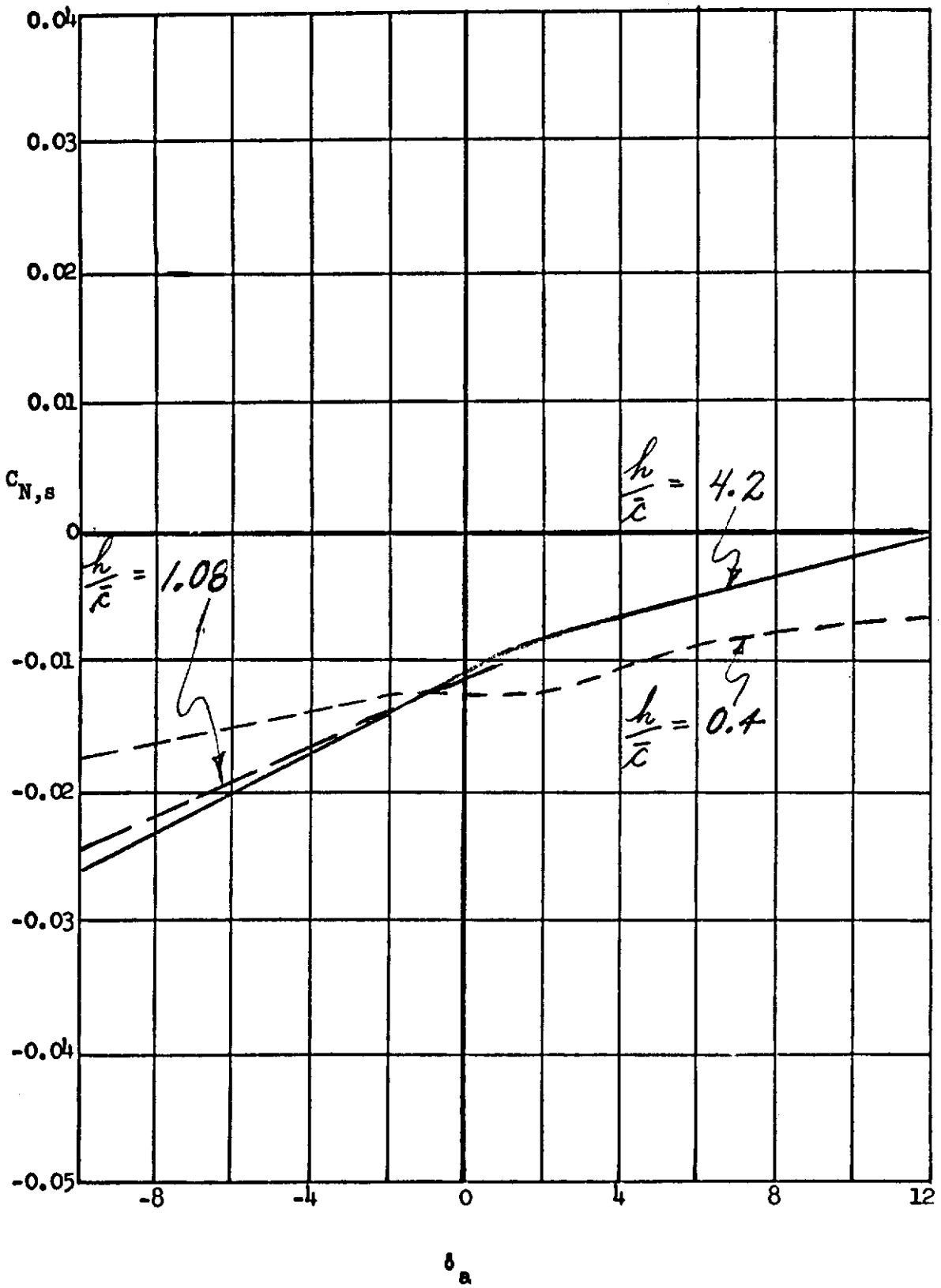

Figure 35. Yawing characteristic versus aileron deflection at three altitude ratios.

Approved for Public Release

Contrails

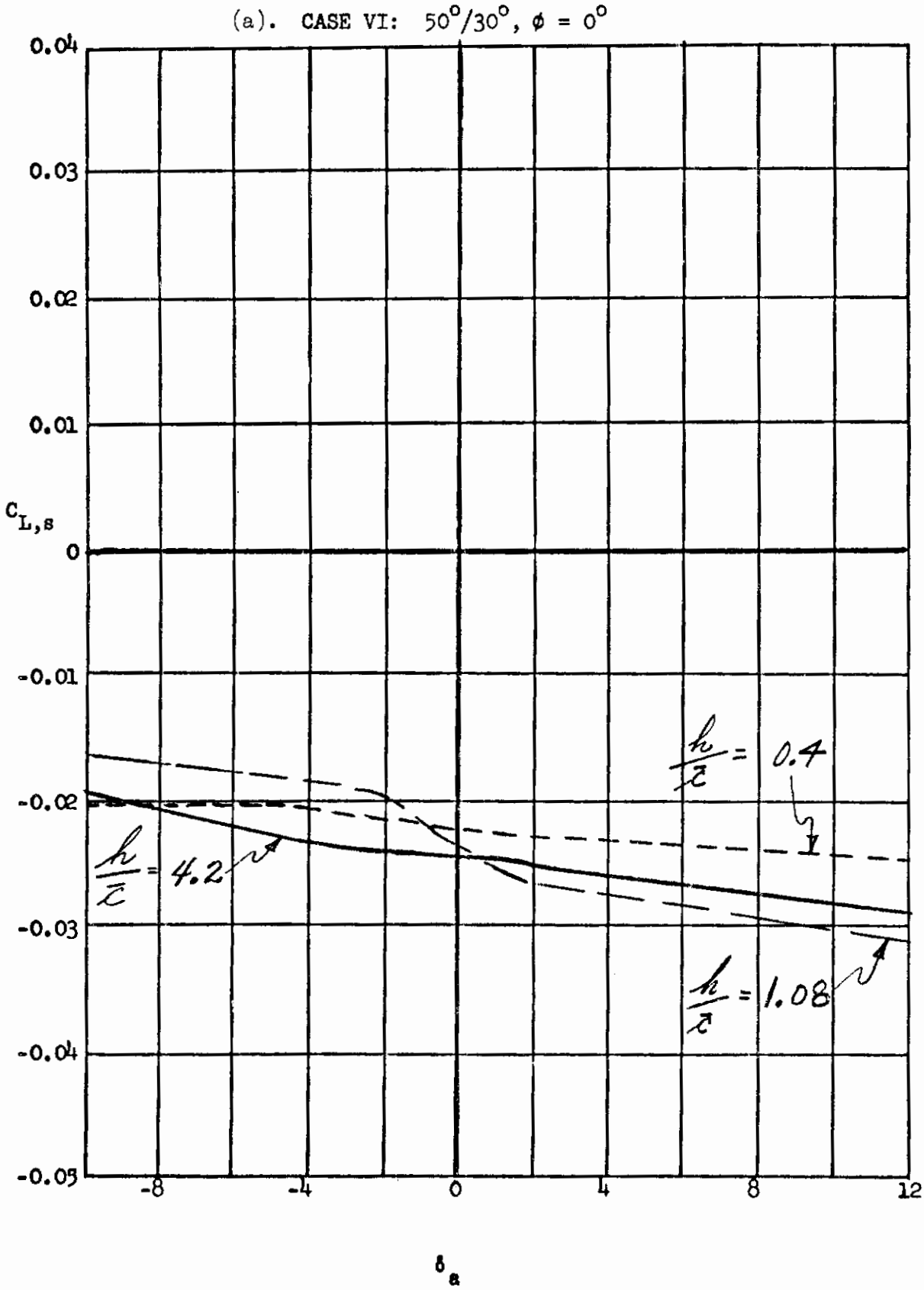

Figure 36. Rolling characteristic versus aileron deflection at three altitude ratios.

Approved for Public Release

Contrails

(b). CASE VI: $50^{\circ}/30^{\circ}$, $\phi = 0^{\circ}$

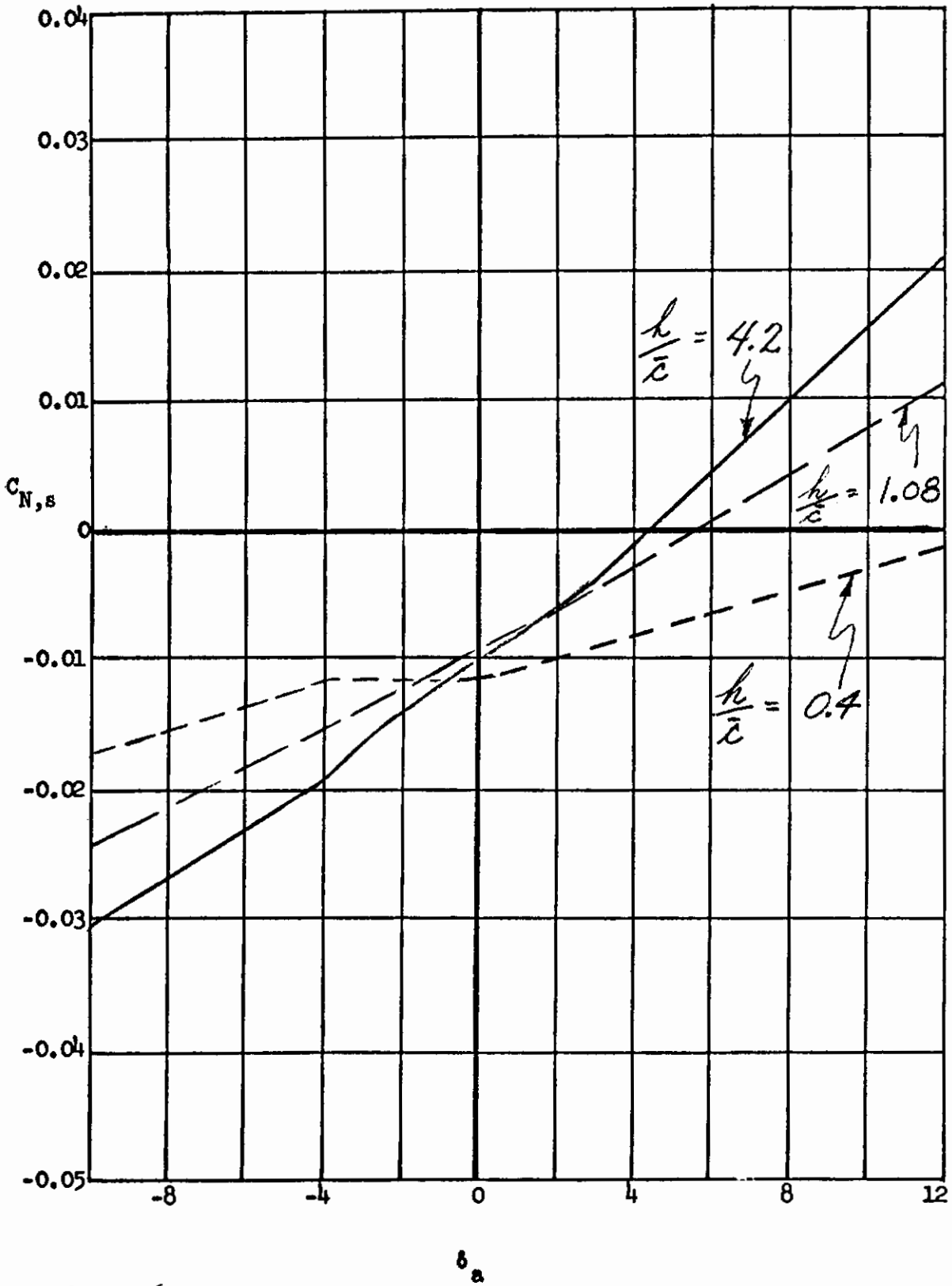

Figure 36. Yawing characteristic versus aileron deflection at three altitude ratios.

Approved for Public Release

Contrails

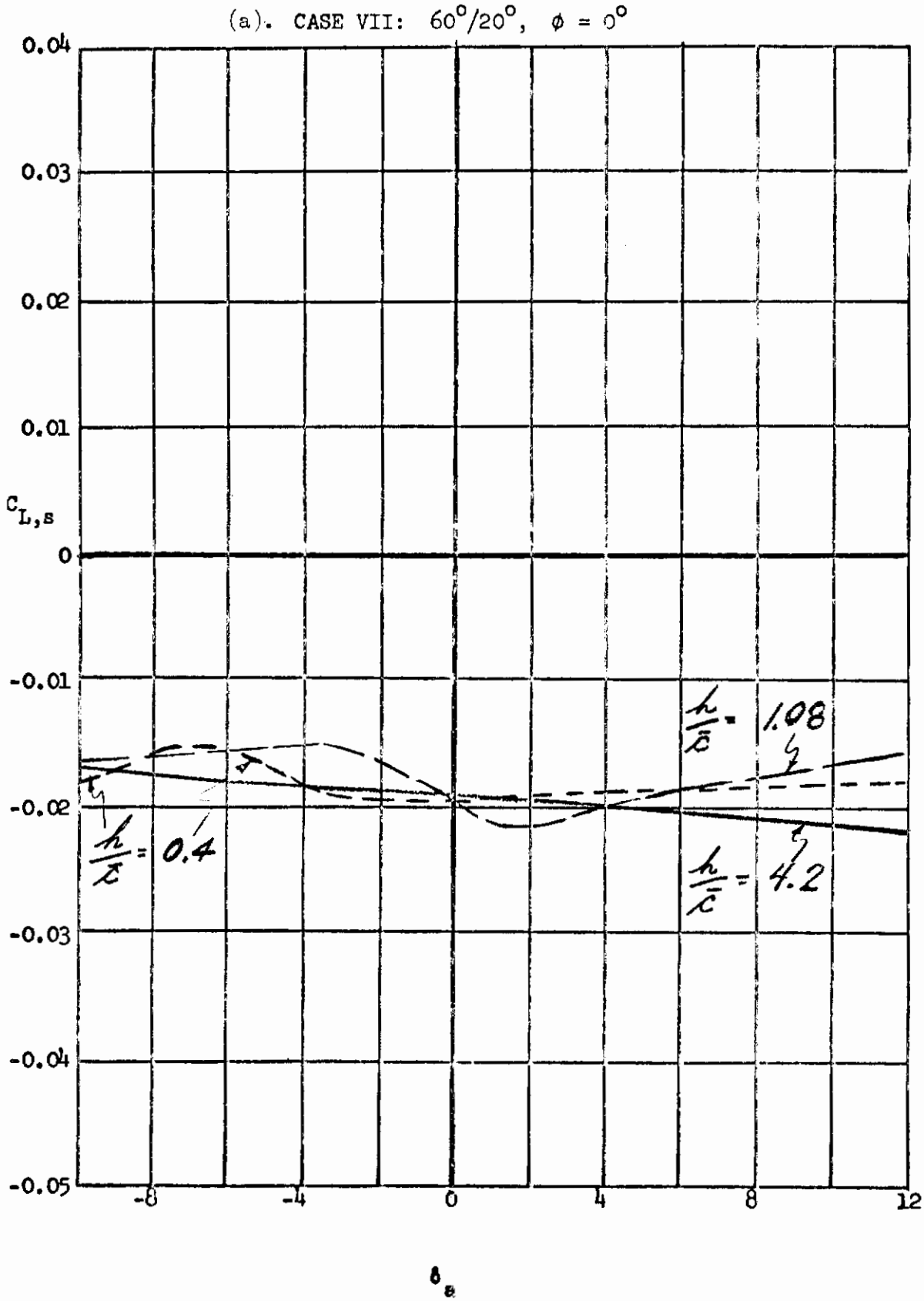

Figure 37. Rolling characteristic versus aileron deflection at three altitude ratios.

Approved for Public Release

Contrails

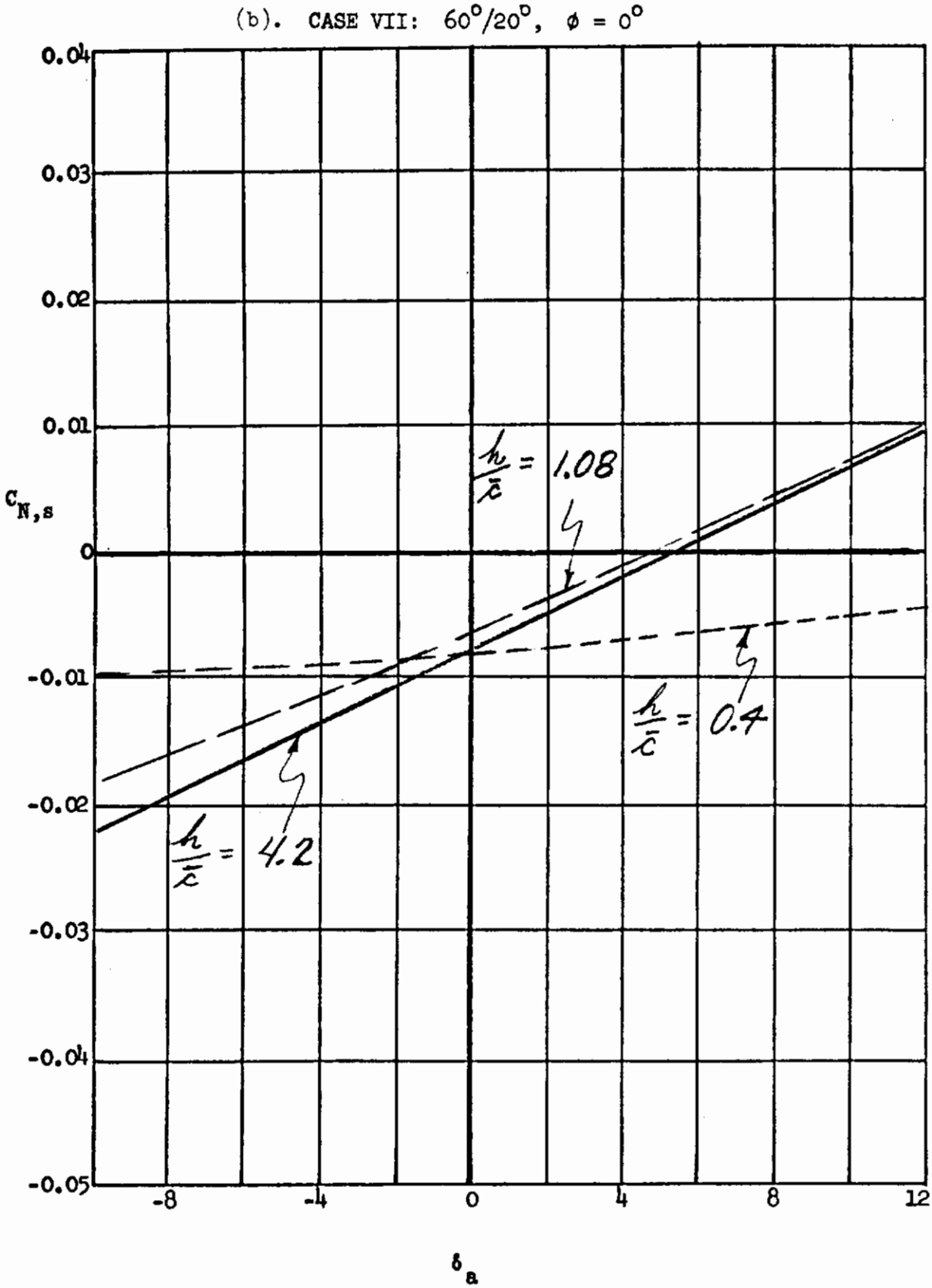

Figure 37. Yawing characteristic versus aileron deflection at three altitude ratios.

Approved for Public Release

Contrails

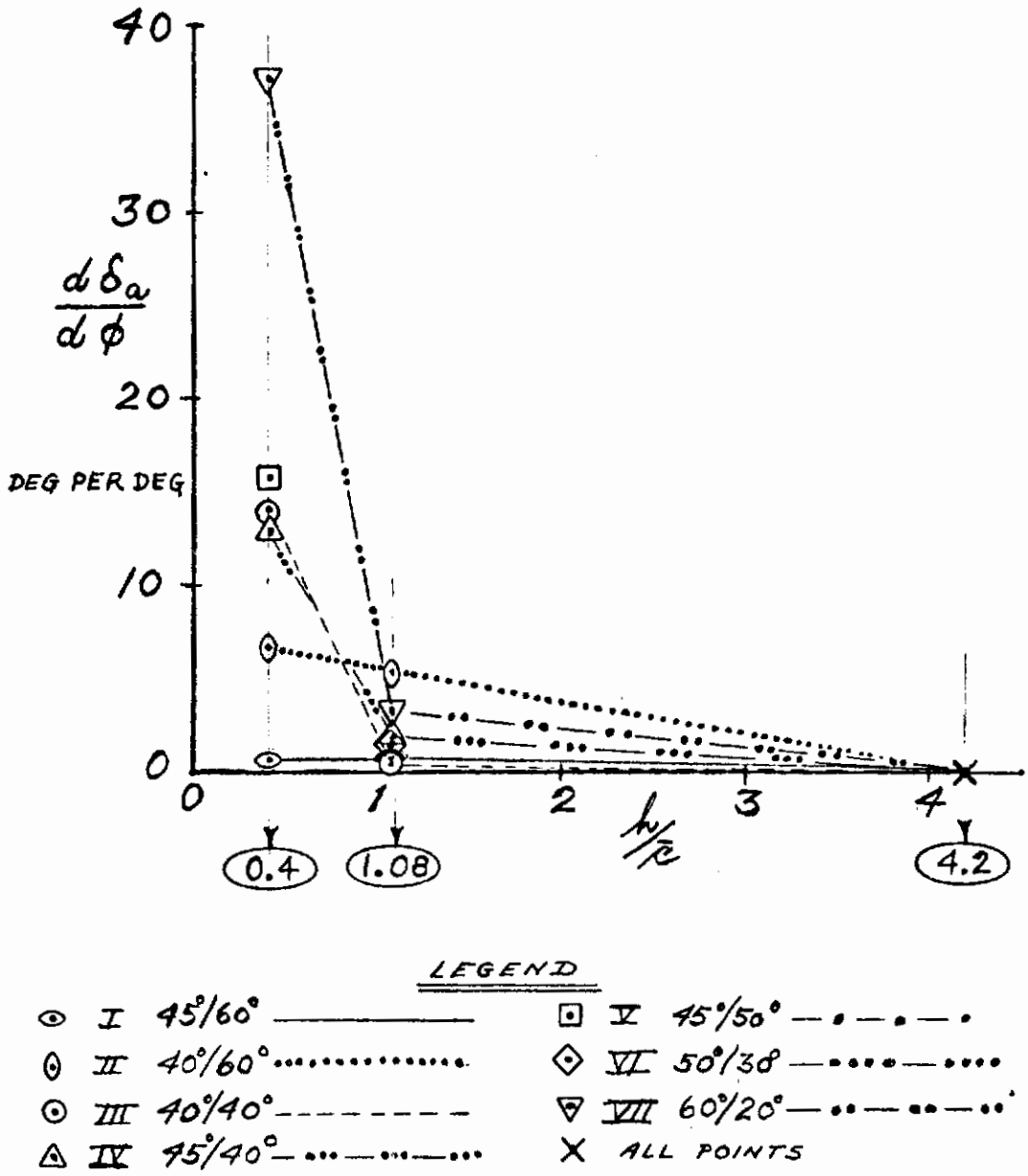

Figure 38. Aileron required per degree of bank angle based on linearized derivatives.

Approved for Public Release

Contrails

APPENDIX

Comparisons of Roll Angle Data with Predictions Based on Longitudinal Effects

The emphasis in this experimental investigation was on the determination of the effects of roll angle on the aerodynamics of a V/STOL aircraft in ground effect. In this flight regime, where the significant forces and moments acting on the aircraft are produced by the wing/propeller combinations, it might be expected that the changes in rolling moment and yawing moment with roll angle could be related to the vertical and horizontal force changes with height above the ground as indicated by Reference 6. That is, if the aircraft is banked near the ground one wing-half (or wing/propeller combination) is closer to the ground and the other wing-half is farther away. Assuming that one-half of the ground effect of the aircraft arises from each wing-half, it is possible to develop relationships for the roll moment and yaw moment as a function of aircraft roll angle as follows.

The interest here is in computing the changes in force that occur due to roll angle near the ground. For simplicity, it is assumed that the propeller forces do not change. Therefore x represents only the wing force. Denoting the local horizontal load in pounds per foot on the wing by x and using the subscripts $_p$ and $_s$ to refer to the port and starboard wings respectively, the total load on each wing panel is

$$X_p = \int_o^{b/2} x_p \quad dy \qquad\qquad X_s = \int_o^{b/2} x_s \quad dy$$

The total horizontal force acting on the aircraft is

$$X = X_p + X_s = \int_o^{b/2} x_p \quad dy + \int_o^{b/2} x_s \quad dy$$

x_p is a function of the height of the local spanwise station of the wing h_p and similarly x_s is a function of h_s. When the aircraft has a roll attitude, then at a spanwise station y

$$h_p = h_c + y\phi \qquad\qquad h_s = h_c - y\phi$$

where h_c is the height of the port or starboard wing at spanwise station zero.

Approved for Public Release

Contrails

The yawing moment acting on the aircraft is

$$N = \int_0^{b/2} x_p \; y \; dy - \int_0^{b/2} x_s \; y \; dy$$

and the rate of change of yawing moment with roll angle is

$$\frac{\partial N}{\partial \phi} = \int_0^{b/2} \frac{\partial x_p}{\partial h_p} \frac{\partial h_p}{\partial \phi} \; y \; dy - \int_0^{b/2} \frac{\partial x_s}{\partial h_s} \frac{\partial h_s}{\partial \phi} \; y \; dy$$

The rate of change of horizontal force with height, wings level is

$$\frac{\partial X}{\partial h} = \int_0^{b/2} \frac{\partial x_p}{\partial h_p} \; dy + \int_0^{b/2} \frac{\partial x_s}{\partial h_s} \; dy$$

It has been assumed that the change in sectional force with height can be linearized about an equilibrium height. This should be a satisfactory assumption for small roll angles.

Now the sectional force can be expressed in terms of a sectional force coefficient nondimensionalized by slipstream dynamic pressure and local chord. The height above ground is nondimensionalized by mean geometric chord to yield the following expressions:

$$\frac{\partial N}{\partial \phi} = q_s \left\{ \int_0^{b/2} \frac{\partial C_{X,p}}{\partial \bar{h}_p} \frac{c}{\bar{c}} \; y^2 \; dy + \int_0^{b/2} \frac{\partial C_{X,s}}{\partial \bar{h}_s} \frac{c}{\bar{c}} \; y^2 \; dy \right\}$$

and

$$\frac{\partial X}{\partial h} = q_s/\bar{c} \left\{ \int_0^{b/2} \frac{\partial C_{X,p}}{\partial \bar{h}_p} \; c \; dy + \int_0^{b/2} \frac{\partial C_{X,s}}{\partial \bar{h}_s} \; c \; dy \right\}$$

Now assuming symmetry of each wing panel

$$\frac{\partial C_X}{\partial \bar{h}} = \frac{\partial C_{X,p}}{\partial \bar{h}_p} = \frac{\partial C_{X,s}}{\partial \bar{h}_s}$$

Approved for Public Release

Contrails

and that the local load depends only on local height, the above equations become

$$\frac{\partial N}{\partial \phi} = q_s \frac{\partial C_x}{\partial \bar{h}} \left\{ 2 \int_o^{b/2} \frac{c}{\bar{c}} \, y^2 \, dy \right\}$$

$$\frac{\partial X}{\partial h} = \frac{q_s S}{\bar{c}} \frac{\partial C_X}{\partial \bar{h}}$$

Nondimensionalizing the rolling moment by span, and the spanwise distance, y, by the semispan, the yawing moment coefficient variation with roll angle can be expressed as

$$\frac{\partial C_{N,s}}{\partial \phi} = \left\{ \frac{b^2}{4S} \int_o^1 \frac{c}{\bar{c}} \, \tilde{y}^2 \, d\tilde{y} \right\} \frac{\partial C_X}{\partial \bar{h}}$$

Defining a lateral center of pressure, y_{cp} and nondimensionalizing this distance by the semispan,

$$\tilde{y}_{cp}^2 = \frac{\bar{c}b}{S} \int_o^1 \frac{c}{\bar{c}} \, \tilde{y}^2 \, d\tilde{y}$$

The yawing moment coefficient variation with roll angle becomes

$$\frac{\partial C_{N,s}}{\partial \phi} = \frac{b}{4\bar{c}} \, \tilde{y}_{cp}^2 \frac{\partial C_X}{\partial \bar{h}}$$

A similar development gives the following expressions for the rolling moment coefficient variation with roll angle in terms of the vertical force variation with height

$$\frac{\partial C_{L,s}}{\partial \phi} = - \frac{b}{4\bar{c}} \, \tilde{y}_{cp}^2 \frac{\partial C_Z}{\partial \bar{h}}$$

For a rectangular wing, the above expression gives a value of $\tilde{y}_{cp} = \frac{1}{\sqrt{3}}$ or approximately 58% of the semispan, for a wing with the characteristics of the XC-142 with a taper ratio of 0.61, $\tilde{y}_{cp}$ = 54% of the semispan.

Approved for Public Release

Contrails

These theoretical expressions show that a lift decrease with height giving a negative slope $\frac{\partial C_Z}{\partial \bar{h}}$ will result in an unstable roll spring ($\frac{\partial C_{L,s}}{\partial \phi} > 0$) owing to ground effect and a negative value of $\frac{\partial C_X}{\partial \bar{h}}$. That is, an increase in forward force with approach to the ground will produce an adverse yawing tendency ($\frac{\partial C_N}{\partial \phi} < 0$), a positive roll produces a moment tending to move the nose of the aircraft left. The terms agree with the data shown in Figures 18 → 24, where in all cases examined $\frac{\partial C_{L,s}}{\partial \phi}$ is positive and $\frac{\partial C_{N,s}}{\partial \phi}$ is negative.

Comparison of these experimentally measured slopes with this simple theory shows reasonable agreement with the yawing moment derivative but generally poor agreement with the rolling moment derivative. In all cases except one ($40^o/60^o$), the unstable roll spring is considerably larger than would be predicted based on the measured vertical force change with height. Some of this difference could arise due to linearization however, this does not appear to be of sufficient magnitude to explain the large differences. It is also difficult to determine slopes based on only three altitude points for the vertical and horizontal force variations. However, the nature of the data does not seem to indicate that this would contribute a large error in the case of vertical force variations.

Approved for Public Release

Contrails

LITERATURE CITED

1. Konrad, J. W. and Chubboy, R.: "Flight Report of XC-142A, Flight No. 37", LTV Vought Aeronautics Division, January 31, 1965.

2. Gratzer, L. B. and Mahal, A. S.: "Ground Effects in STOL Operation", Journal of Aircraft, Vol. 9, No. 3, March 1972.

3. Goodson, K. W.: "Effect of Ground Proximity on the Longitudinal, Lateral and Control Aerodynamic Characteristics of a Tilt-Wing Four-Propeller V/STOL Model", NASA TN D-4237, December 1967.

4. Goodson, K. W.: "Longitudinal Aerodynamic Characteristics of a Flapped Tilt-Wing Four-Propeller V/STOL Transport Model", NASA TN D-3217, February 1966.

5. Putman, W. F.: "An Experimental Investigation of Ground Effect on a Four-Propeller Tilt-Wing V/STOL Model", U. S. Army Aviation Material Laboratories, USAAVLABS Technical Report 68-45, Fort Eustis, Virginia, July 1968.

6. Jones, A. G.: "Analysis of XC-142A Yawing Moment Due to Ground Presence", AFFDL-TM-71-12, Air Force Flight Dynamics Laboratory, Wright-Patterson Air Force Base, November 1971.

7. Black, E. L. and Booth, G. C.: "Correlation of Aerodynamic Stability and Control Derivatives Obtained From Flight Tests and Wind Tunnel Tests on the XC-142A Airplane", AFDL-TR-68-167, June 1969.

8. Boyden, R. P. and Curtiss, H. C., Jr.: "Investigation of the Lateral/Directional Stability Characteristics of a Four-Propeller Tilt-Wing Model", U. S. Army Aviation Material Laboratories, USAAVLABS Technical Report 68-19, Fort Eustis, Virginia, July 1968.

9. Chambers, J. R. and Grafton, S. B.: "Investigation of Lateral/Directional Dynamic Stability of a Tilt-Wing V/STOL Transport", NASA TN D-5637, February 1970.

10. Chambers, J. R. and Grafton, S. B.: "Static and Dynamic Longitudinal Stability Derivatives of a Powered 1/9-Scale Model of a Tilt-Wing V/STOL Transport", NASA TN D-3591, September 1966.

11. Flinn, E. H. and Dr. Statler, I. C.: "V/STOL Aerodynamic Stability and Control", Proceedings of V/STOL Technology and Planning Conference, Las Vegas, Nevada, (Sponsored by AF Flight Dynamics Laboratory (FDV) Dayton, Ohio), September 1969.

12. Goodson, K. W.: "Ground Effects on a Four-Propeller Tilt-Wing Configuration Over a Fixed and a Moving Ground Plane", NASA TN D-3938, May 1967.

Approved for Public Release

Contrails

13. Heyson, H. H.: "Linearized Theory of Wind-Tunnel Jet-Boundary Corrections and Ground Effect for VTOL-STOL Aircraft", NASA TR R-124, Washington, D. C. 1962.

14. Holbrook, J. W., White, R. M. and Cooksey, J. M.: "A Low Speed Wind Tunnel Test of a .11 Scale XC-142A Powered Model in Ground Plane Proximity", Report No. 2-59730/7R-6113, LTV Vought Aeronautics Division, December 1965 to January 1966.

15. Kuhn, R. E.: "Ground Effects on V/STOL and STOL Aircraft", Conference on Aircraft Operating Problems, Langley Research Center, May 10 - 12, 1965.

16. Kuhn, R. E. and Hayes, W. C., Jr.: "Wind-Tunnel Investigation of Longitudinal Aerodynamic Characteristics of Three Propeller-Driven VTOL Configurations in the Transition Speed Range, Including Effects of Ground Proximity", NASA TN D-55, 1960.

17. Tapscott, R. J., Garren, J. F., Jr., Kelley, H. L. and Shanks, R.: "VTOL Instrument Flight Research Relating to Aircraft Requirements and Operating Characteristics for the Terminal Area", AIAA 7th Annual Meeting, Houston, Texas, October 1970.

18. Turner, T. R.: "A Moving-Belt Ground Plane for Wind-Tunnel Ground Simulation and Results for Two Jet-Flap Configurations", NASA TN D-4228, 1967.

19. Turner, T. R.: "Endless-Belt Technique for Ground Simulation", Presented at Conference on V/STOL and STOL Aircraft, Ames Research Center, Moffett Field, Calif. April 1966, pp. 435-446.

20. Vogler, R. D.: "Ground Effects on Single- and Multiple-Jet VTOL Models at Transition Speeds Over Stationary and Moving Ground Planes", NASA TN D-3213, 1966.

21. Ward, J. P. and LTC Jones, G. E.: "Lessons Learned From the XC-142 Program", Proceedings of V/STOL Technology and Planning Conference, Las Vegas, Nevada, (Sponsored by AF Flight Dynamics Laboratory (FDV)) September 1969.

22. Bairstow, L.: APPLIED AERODYNAMICS, Longmans, Green and Company, LTD. Second Edition 1939.

23. Perkins, C. D. and Hage, R. E.: AIRPLANE PERFORMANCE STABILITY AND CONTROL, John Wiley & Sons, Inc., 1949.

24. Curtiss, H. C., Jr., Putman, W. F. and Traybar, J. J.: "General Description of the Princeton Dynamic Model Track", U. S. Army Aviation Material Laboratories, USAAVLABS Technical Report 66-73, Fort Eustis, Virginia, November 1966.

Approved for Public Release

Contrails

25. Curtiss, H. C., Jr., Putman, W. F. and Lebacqz, J. V.: "An Experimental Investigation of the Longitudinal Dynamic Stability Characteristics of a Four-Propeller Tilt-Wing VTOL Model", USAAVLABS TR 66-80, February 1968.

26. Turner, T. R.: "Ground Influence on a Model Airfoil with A Jet-Augmented Flap as Determined by Two Techniques", NASA TN D-658, February 1961.

27. Champine, R. A., Kelley, H. L. Thibodeaux, and Tosti, L. P.: "A Flight Test Investigation of Terminal-Area Operations and Ground-Recirculation Effects Utilizing the XC-142 Tilt-Wing V/STOL Aircraft", National Aeronautics and Space Adminstration, LWP-927, January 1971.

Approved for Public Release

Contrails

Approved for Public Release

Contrails

UNCLASSIFIED

Security Classification

DOCUMENT CONTROL DATA - R & D

(Security classification of title, body of abstract and indexing annotation must be entered when the overall report is classified)

1. ORIGINATING ACTIVITY *(Corporate author)*
Trustees of Princeton University
Princeton, N. J. 08540

2a. REPORT SECURITY CLASSIFICATION
Unclassified

2b. GROUP

3. REPORT TITLE
THE EFFECT OF GROUND PROXIMITY ON THE LATERAL/DIRECTIONAL AERODYNAMIC AND CONTROL CHARACTERISTICS OF A TILT-WING V/STOL AIRCRAFT AT HIGH LIFT COEFFICIENCTS

4. DESCRIPTIVE NOTES *(Type of report and inclusive dates)*
Final Report

5. AUTHOR(S) *(First name, middle initial, last name)*
Howard C. Curtiss, Jr.
Joseph J. Traybar
William F. Putman

6. REPORT DATE
December 1973

7a. TOTAL NO. OF PAGES
149

7b. NO. OF REFS
27

8a. CONTRACT OR GRANT NO.
F33615-71-C-1206

b. PROJECT NO.
8219

c.

d.

9a. ORIGINATOR'S REPORT NUMBER(S)
Princeton University Aerospace and Mechanical Sciences Technical Report Number 1127

9b. OTHER REPORT NO(S) *(Any other numbers that may be assigned this report)*
AFFDL-TR-73-151

10. DISTRIBUTION STATEMENT

Approved for public release; distribution unlimited.

11. SUPPLEMENTARY NOTES
None

12. SPONSORING MILITARY ACTIVITY
U. S. Air Force Flight Dynamics Lab.
Wright-Patterson Air Force Base, Ohio

13. ABSTRACT

A series of experiments was performed in the Princeton Dynamic Model Track to determine the lateral/directional stability and control of a V/STOL type aircraft in ground proximity. Of primary interest were the characteristics associated with flight at high lift coefficients and utilizing high wing incidences with large flap deflections as may be encountered during STOL operations in landings and take-offs where the full or maximum effects of ground proximity are encountered. The configurations tested included combinations of wing incidence and flap deflection up to a maximum of 60 degrees.

Static force and moment measurements were made for seven different wing incidence/flap angle combinations using sideslip angle and roll angle as variables. Also, static measurements were made to determine the control effectiveness of ailerons and differential propeller pitch. All configurations were studied at three altitude ratios; one approximating a high altitude (or out-of-ground-effect height), another a low altitude (or in-ground-effect height), and the third an intermediate altitude case.

DD FORM 1 NOV 65 1473

UNCLASSIFIED
Security Classification

Approved for Public Release

Contrails

UNCLASSIFIED

Security Classification

14 KEY WORDS	LINK A		LINK B		LINK C	
	ROLE	WT	ROLE	WT	ROLE	WT
High-Lift System						
Tilt-Wing Aircraft						
Wing-In-Slipstream						
V/STOL Aircraft						
V/STOL Lateral/Directional Aerodynamics						
V/STOL Ground Effect						

UNCLASSIFIED

Security Classification

☆U.S.Government Printing Office: 1974 — 657-015/233

Approved for Public Release